C51.17/12:988/6

Tech Notes

JUNE 1988

PB88-925906

NTIS

U.S. DEPARTMENT OF COMMERCE
National Technical Information Service
Center for the Utilization of Federal Technology

ALSO DESCRIBES 90 FEDERAL TECHNICAL INFORMATION CENTERS

NOW! Work Directly with Government Labs and Engineering Facilities

"The Directory should be popular in research and business libraries"

—Reference Book Bulletin
American Libraries Association

Find them easily in the Directory of Federal Laboratory & Technology Resources. This valuable directory will guide you to hundreds of Federal agencies, laboratories, and engineering centers willing to share their expertise, equipment, facilities, and special services to aid your research and engineering efforts. Detailed summaries of these unique resources are arranged in 32 subject-oriented areas for easy reference. Descriptions of 90 Technical Information Centers are included.

These centers offer information services and expertise in areas such as fuels, cold regions, concrete, fisheries, toxicology, pesticides, plastics, and much more.

The NAME, ADDRESS, PHONE NUMBER OF A PERSONAL CONTACT IS LISTED FOR EACH RESOURCE!

Help is available in 32 technical areas including:

Aeronautics (31)* • Agriculture & Food (120) • Biological Sciences (68) • Building Technology (20) • Computer Technology (15) • Electrotechnology (43) • Energy (77) • Engineering (86) • Environmental Sciences (67) • Manufacturing (19) • Materials (61) • Medicine (112) • Nuclear (128) • Ocean Sciences & Technology (36) • Physical Sciences (110) • Transportation (14) • Plus others

*number of summaries

Four handy indexes make it easy to locate the resource you need.

1. Subject Term Index
Identifies resources in your technical interest areas.

2. State Index
Find all the resources in your State.

3. Resource Name Index
Look up any resource by name of laboratory or program.

4. Agency Index
Lists resources by agency and State.

All listed resources offer unique capabilities (not readily duplicated in the private sector) to encourage greater use of Federal technology.

To increase your awareness of hundreds of Federal Technology Resources available to work with you on your projects, order your DIRECTORY now!

ASK FOR:
PB88-100011/AAW

DIRECTORY OF FEDERAL LABORATORY AND TECHNOLOGY RESOURCES

CALL: (703) 487-4650

WRITE:

NTIS Springfield, VA 22161

Enclose check to NTIS for $36 plus $3 for shipping and handling or
Charge to: NTIS Deposit Account, American Express, VISA, or MasterCard.
Please furnish card number, expiration date, signature, and complete mailing address.

Tech Notes

Highlighting Selected U.S. Government Technology & Resources

JUNE 1988

Contents

Agriculture & Food 443

Computers 446

Electrotechnology 456

Energy 468

Engineering 474

Environmental Science & Technology 486

Manufacturing, Machinery & Tools 490

Materials 500

Medicine & Biology 516

Natural Resources Technology & Engineering 526

Physical Sciences 528

Transportation & Components 540

PENNSYLVANIA STATE UNIVERSITY 1988 DOCUMENTS COLLECTION

U S. Depository

Published monthly by the National Technical Information Service (NTIS), Tech Notes bring together individual one to two page fact sheets prepared by Federal agencies, their laboratories, or contractors. These fact sheets highlight current Federal technology determined to have commercial or practical application. Topics cover new processes, materials, techniques, software, instrumentation, and resources.

Some of the current sources are the Department of the Navy, Department of the Army, NASA, Department of Energy, Environmental Protection Agency, Department of the Interior, and the Department of Agriculture.

Special assistance is provided by the Federal Laboratory Consortium.

Change of address or questions concerning subscriptions should be sent to:
Subscriptions Department
National Technical Information Service
Springfield, VA 22161
(703) 487-4630

Suggestions, comments, or questions concerning Tech Notes should be directed to:
Tech Notes Editor
Room 300B F
National Technical Information Service
Springfield, VA 22161
(703) 487-4805

How to Use Tech Notes

Every Tech Notes fact sheet lists a source for additional information. The source of this information may be a special support package from the originating agency, a personal contact, a licensing opportunity, or a backup report available from NTIS.

Each fact sheet also is perforated to allow for easy removal for those subscribers who may wish to keep a special fact sheet file or route to others in their organization

Sources of Further Backup Information

Below are two representative examples of how each Tech Note fact sheet provides you with a source of further information. In most cases, this information is provided directly by the agency or its laboratory.

However, there are cases where NTIS is the source for backup documentation. In these cases, use the order form at the end.

Examples:

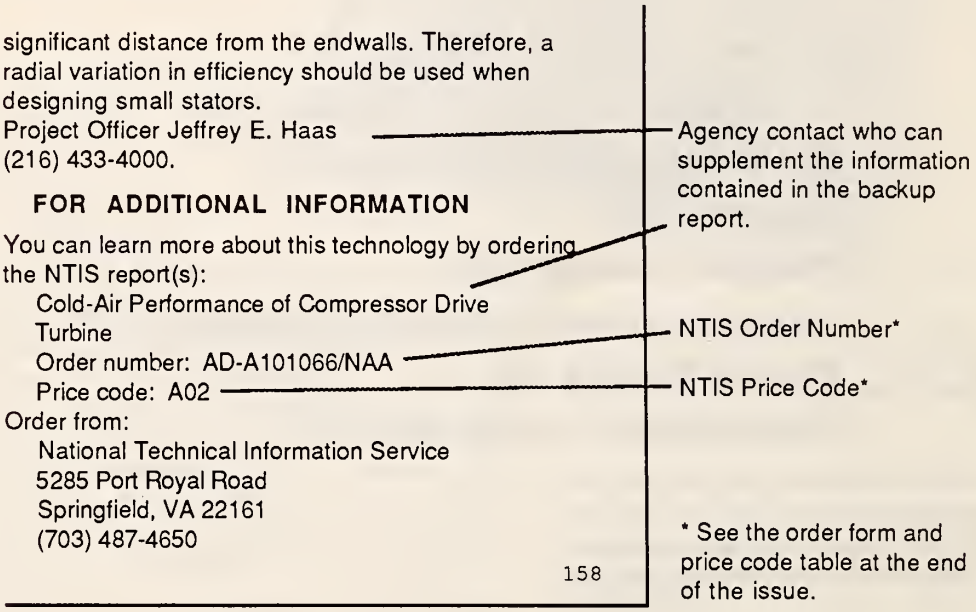
significant distance from the endwalls. Therefore, a radial variation in efficiency should be used when designing small stators.
Project Officer Jeffrey E. Haas
(216) 433-4000.
FOR ADDITIONAL INFORMATION
You can learn more about this technology by ordering the NTIS report(s):
Cold-Air Performance of Compressor Drive Turbine
Order number: AD-A101066/NAA
Price code: A02
Order from:
National Technical Information Service
5285 Port Royal Road
Springfield, VA 22161
(703) 487-4650
158
Agency contact who can supplement the information contained in the backup report.
NTIS Order Number*
NTIS Price Code*
* See the order form and price code table at the end of the issue.

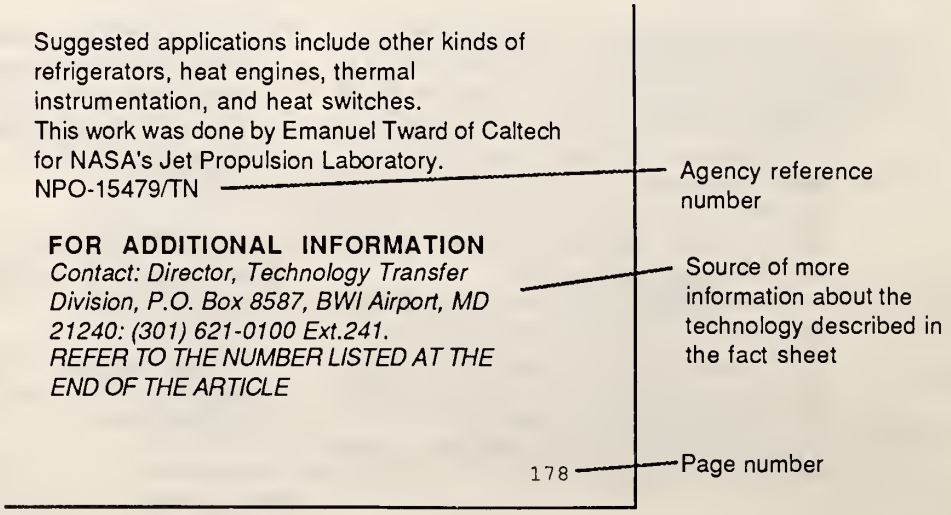
Suggested applications include other kinds of refrigerators, heat engines, thermal instrumentation, and heat switches.
This work was done by Emanuel Tward of Caltech for NASA's Jet Propulsion Laboratory.
NPO-15479/TN
FOR ADDITIONAL INFORMATION
Contact: Director, Technology Transfer Division, P.O. Box 8587, BWI Airport, MD 21240: (301) 621-0100 Ext.241.
REFER TO THE NUMBER LISTED AT THE END OF THE ARTICLE
178
Agency reference number
Source of more information about the technology described in the fact sheet
Page number

Tech Notes Title List for June 1988

Agriculture & Food

443 Vaccine for Swine Trichinosis (Licensing Opportunity)

444 Chemical in Wasp puts Caterpillars 'Under Arrest,' Could be new Insecticide

445 Soil Yields 72 New Varieties of a Natural Pest Control

Computers

446 Algorithm Sorts Groups of Data — Sets are sorted quickly according to weighted sums of elements. (Licensing Opportunity)

447 Integrated Circuit for Simulation of Neural Network — Ballast resistors are deposited on top of the circuit structure.

448 Electronic Neural Networks — memory based on neural network models is content-addressable and fault-tolerant. (Licensing Opportunity)

449 Electronic Neural-Network Simulator — Experimental circuits are faster than simulation programs fun on digital computers. (Licensing Opportunity)

450 Pitch-Learning Algorithm for Speech Encoders — Gross pitch errors are detected and corrected. (Licensing Opportunity)

451 The Mark III Hypercube-Ensemble Computers — Concurrent processors will operate at high speed. (Licensing Opportunity)

452 Unified Robot-Control System — Robot-joint motors are integrated with a control computer or computers. (Licensing Opportunity)

Software

453 Ada Linear-Algebra Program — Routines are provided for common scalar, vector, matrix, and quaternion operations.

454 Analyzing Commonality in a System — Cost can be decreased by use of fewer types of parts.

455 Simulation of Research and Development Projects — Measures of preference for alternative project plans can be calculated.

Other Items of Interest

460 Blanket Gate Would Address Blocks of Memory — Circuit-chip area would be used more efficiently. (Licensing Opportunity)

Electrotechnology

456 Million-Fold Improvement in Superconductor Resistance

457 High Gain Crossed Field Amplifiers Projects Completed

458 Tool Effectively Bends Pins on Printed Circuit Board Connectors

459 Dual-Bank Microstrip Antenna with Reactive Loading — An effective but bulky coaxial stub is replaced.

460 Blanket Gate Would Address Blocks of Memory — Circuit-chip area would be used more efficiently. (Licensing Opportunity)

461 Designing a Microwave Band-Stop Filter — Lumped-circuit design techniques are applied to iris-coupled cavities.

462 Lightweight Video-Camera Head — A separate optical assembly weighs only 80 grams.

463 Programmable Synaptic Arrays for Electronic Neural Networks — High resistances prevent hotspots in parallel input and output operation. (Licensing Opportunity)

464 Public-Facilities Locator for the Blind — An optoelectronic system would enable blind people to find key places without assistance.

465 Three-Waveguide Beam and Polarization Splitter — Different modes are guided to different output ports.

Testing & Instrumentation

466 Remote Sensor and Cable Identifier

467 Dual Pilot-Tone Calibration Technique — The signal-to-noise ratio would be increased.

Other Items of Interest

543 Variable-Reluctance Motor for Electric Vehicles — A scaled-down motor performed as expected.

Energy

468 Determination of Effects of Atmospheric Contamination on Photovoltaic Cells in Concentrating Systems

469 Monitoring of Residential Groundwater-Source Heat Pumps in the Northeast

470 Vortex Pyrolysis Reactor

471 Molybdenum Resistance Heater

472 Coatings Boost Solar-Cell Outputs — Efficiencies are increased by more-complete utilization of incident light.

473 Long-Life Electrolyte for Nickel/Hydrogen Cells — Decreased initial capacity is more than compensated by increased cycle life.

Engineering

474 Rototicon: Real-Time Control for an Autonomous Mobile Robot

475 Snail Cryopump

476 Advanced Numerical Methods for Ship Hydrodynamic Design

477 Lightweight Glass-Reinforced Plastic Deckhouse Panel Concept Developed

478 Computer-Aided Design of Turbine Blades and Vanes — Analysis and design procedures lead quickly to an efficient and strong final design.

479 Cover for Duct Expansion Joint — The size ad shape fo the cover reduces stress and increases strength. (Licensing Opportunity)

Engineering (cont.)

480 Estimating the Crack-Extension-Resistance Curve — The curve can not be obtained from residual strength data alone.

481 Failure-Time Distribution of an *m*-Out-of-*n* System — Formulas for reliability are extended to more general cases.

482 Stiffness Properties of Laminated Graphite/Epoxy Cylinders — The dominant constituent property is the longitudinal Young's Modulus of the fibers.

483 Wet-Atmosphere Generator — The water content in a gas is controlled. (Licensing Opportunity)

484 "Thumball" Auxiliary Data-Input Device — A track-ball-type device is mounted on a joystick operated by a thumb. (Licensing Opportunity)

Testing & Instrumentation

485 Sensor-Failure Simulator — Outputs of defective sensors are simulated or studies of reliability of control systems.

Other Items of Interest

470 Vortex Pyrolysis Reactor

Environmental Science & Technology

486 Design, Construction, and Maintenance of Cover Systems for Hazardous Waste: An Engineering Guidance Document

487 Guidance Manual for Selection and Use of Sorbents for liquid Hazardous Substance Releases

Testing & Instrumentation

488 Field Dispersant Effectiveness Test

489 Environmental "Frozen Assets" Described in Videotape

Other Items of Interest

468 Determination of Effects of Atmospheric Contamination on Photovoltaic Cells in Concentrating Systems

Manufacturing, Machinery, & Tools

490 Welding of Nickel Aluminide and Nickel-Iron Aluminides

491 Novel Vapor-Deposited Lubricants for Metal-Forming Processes

492 Fixture for Polishing Optical-Fiber Ends — Wedged and beveled ends are lapped with precision for laser applications. (Licensing Opportunity)

493 Grinding Inside a Toroidal Cavity — Weld lines can be ground smooth within about 0.001 in. (0.025 mm). (Licensing Opportunity)

494 Inflatable Probe Would Manipulate Delicate Parts — Delicate parts would be grasped gently. (Licensing Opportunity)

495 Locating Residual Wax in Coolant Channels — Neutron inspection finds deposits and defects invisible to x-rays.

496 Tool Protects Internal Threads During Rework — A simple device covers some areas but exposes other areas for grinding.

Software

497 COMMIX Code for Metal Casting — Teaching an old code new tricks.

498 Advanced Software for the Efficient Manufacture of Complex Industrial Castings

499 Allocating Spare Parts in Complicated Systems — Assortments are analyzed for cost effectiveness and effects on system functionality.

Materials

500 Cellulose III Cotton Fiber Resists Abrasive Wear (Licensing Opportunity)

501 Superplasticity in Aluminum-Base Alloys

502 Data Management System for Materials Sciences

503 Corrosion Data on Cable Shielding Published

504 Testing Long-Term Exposure to Vacuum — A laboratory facility enables storage of materials under controlled vacuum conditions.

505 Numerical Simulation of Silicon-Ribbon Growth — A mathematical model includes nonlinear effects.

506 Determination of Grain-Size Distributions — Images of microstructures are analyzed by transform methods.

507 Effects of Radiation on Insulators — Data have been compiled on a variety of thermosetting and thermoplastic polymers.

508 Temperature, Humidity, and Polymer Aging — A theoretical basis is found for an empirical equation.

509 Galvanic Corrosion in (Graphite/Epoxy)/Alloy Couples — Some alloys need protection against corrosion in salt water.

510 Optimization of Processing of Si_3N_4 — Process changes are iterated under the guidance of x-radiography.

511 Lubrication Handbook for the Space Industry — Properties and application data are given for over 500 solid and liquid lubricants.

512 Microstructure and Weld Cracking in Inconel 718* — Theories on the relationship between metallurgy and microfissuring are confirmed.

513 Polyarylene Ethers with Improved Properties — Ease of processability and mechanical properties generally exceed those of commercial materials. (Licensing Opportunity)

514 Stronger Fire-Resistant Epoxies — A new curing agent improves mechanical properties and works at a lower temperature. (Licensing Opportunity)

Testing & Instrumentation

515 Laser Sensors Used to Detect Material Vibration — Vibrations of Less Than One Micron are Measured

Other Items of Interest

491 Novel Vapor-Deposited Lubricants for Metal-Forming Processes

528 Alternative Refrigerants

542 Field Repair of Thermoplastic Windows and Canopies — A hand-held induction heater makes quick and easy repairs.

Medicine & Biology

516 Three-Dimensional Electron Microscopy of Biologically Active Macromolecules

517 Arm-Powered Bicycle for the Disabled

518 Automatic Decomposition of the Electromyogram

519 Human Movement Monitoring System to Study Posture, Walking, and Jumping

520 Handbook on Animal Models Available

521 Powered Lift for Paraplegics — People with paralyzed legs ca transfer themselves to and from wheelchairs. (Licensing Opportunity)

Testing & Instrumentation

522 Fiber-Optics Flouroimmuno-Sensor

523 Biomolecular Interaction Analysis System (BIAS) — Using a microcomputer to extend chromatography techniques.

524 Holter Monitoring Predicts Effectiveness of Anti-arrhythmia Treatment

525 Low Voltage Scanning Electron Microscope

Other Items of Interest

464 Public-Facilities Locator for the Blind — An optoelectronic system would enable blind people to find key places without assistance.

Natural Resources Technology & Engineering

526 Diffusion of Contaminants in the Atmosphere Studied

527 Calculating Atmospheric Effects in Satellite Imagery: Part 2 — Practical computational techniques are developed.

Physical Sciences

528 Alternative Refrigerants

529 New Diffraction and Crystal Databases Available

530 Thermodynamic Refrigerant Mixture Charts now Available

531 New Use for High-Transition (HT) Superconductors Demonstrated

532 Hybrid Electrostatic/Acoustic Levitator — Particles and drops can be rotated and vibrated.

Software

533 Computer Program for Linear Algebra — A collection of routines is provided for basic vector operations.

534 Fast-Polynomial-Transform Program — A modular approach saves computational resources.

535 Mathematical Routines for Engineers and Scientists — Programs for frequently-used mathematical procedures save time.

Testing & Instrumentation

536 'Signatures' Help Researchers Trace Artifact Origins

537 Modulated-Voltage Metastable-Ionization Detector — The range of measurable gas concentrations is extended. (Licensing Opportunity)

538 Ultrasonic Scanner Evaluated

539 Three-Axis Superconducting Gravity Gradiometer — Gravity Gradients can be measured even on accelerating platforms. (Licensing Opportunity)

Other Items of Interest

456 Million-Fold Improvement in Superconductor Resistance

Transportation & Components

540 Airplane Wings for Faster Climbing and Slower Landing — Reshaped airfoils improve performance. (Licensing Opportunity)

541 Computer Scheduling of Airplane Arrivals — Controllers would be assisted in the coordination of many simultaneous flights. (Licensing Opportunity)

542 Field Repair of Thermoplastic Windows and Canopies — A hand-held induction heater makes quick and easy repairs.

543 Variable-Reluctance Motor for Electric Vehicles — A scaled-down motor performed as expected.

Other Items of Interest

484 'Thumball' Auxiliary Data-Input Device — A trackball-type device is mounted on a joystick operated by a thumb. (Licensing Opportunity)

Agriculture & Food

443 Vaccine for Swine Trichinosis (Licensing Opportunity)

444 Chemical in Wasp puts Caterpillars "Under Arrest," Could be New Insecticide

445 Soil Yields 72 New Varieties of a Natural Pest Control

United States Department of Agriculture

Research Technology
Agricultural Research Service

Vaccine for Swine Trichinosis

The nematode worm *Trichinella spiralis* costs the pork industry more than $400 million per year in lost sales and control measures. Now a vaccine has been developed to prevent pigs from picking up this muscle-invading parasite that causes trichinosis.

Several vaccines against trichinosis have been produced in recent years, but the immunity rate they afforded was low. The new vaccine developed by Agricultural Research Service scientists promises a higher degree of immunity than has ever before been possible.

Previous vaccines were derived from extracts of adult Trichinella; the new vaccine comes from killed larvae. It induces up to 88 percent immunity.

This new treatment offers farmers a practical, effective measure to prevent transmission of trichinosis.

For technical information, contact Kenneth D. Murrell, USDA-ARS Beltsville Agricultural Research Center, Bldg. 003, Room 227, BARC-West, Beltsville, MD 20705. Patent Application Serial No. 07/068,499, *"Vaccine for Swine Trichinosis."*

For Additional Information:

To discuss this effort further, contact:

Dr. Kenneth Murrell
Beltsville Agricultural Research Center,
Bldg. 003, Room 227, BARC West,
Beltsville, MD 20705: (301) 344-2195

For inquiries concerning rights for the commercial use of this invention should be addressed to

Office of Federal Patent Licensing
Center for the Utilization of Federal Technology
Room 13R, NTIS
Springfield, VA 22161; (703) 487-4738

Refer to Patent Application 7-068,499/TN

United States Department of Agriculture

Research Technology
Agricultural Research Service

Chemical in Wasp puts Caterpillars "Under Arrest," Could be New Insecticide

A tiny parasitic wasp injects its caterpillar victims with lethal crystals that could be the source of a new insecticide, U.S. Department of Agriculture scientists said.

"The crystals contain a 'chemical arrestant' that stops an insect in its caterpillar, or larval, stage from molting--shedding its skin. It can't develop into an adult," said chemist Thomas A. Coudron of the Agricultural Research Service.

In nature, Coudron said, the female Euplectrus plathypenae wasp stings its host and injects the arrestant into the insect's bloodstream. "The host insect stops growing and, unable to shed its skin, dies," he said.

In the laboratory, he injected the crystals into insects of many species, stopping growth in bollworm, armyworm, cabbage looper, asparagus beetle and common green lacewing. His next step is to isolate and identify the chemical arrestant in the crystals, which he found in the wasp's reproductive tract.

"New sources of pesticides are needed," he said, "because insects have become resistant to old ones. We are also concerned about the fate of many chemicals that may pollute the environment."

Coudron worked with entomologist Benjamin Puttler at the agency's Biological Control of Insects Laboratory, Columbia, Mo. Insect larvae develop through six stages called "instars," Puttler said. "The chemical arrestant affects larvae before the fifth and sixth instars, when they do 90 percent of their feeding damage to crop plants."

Coudron is conducting studies to determine if the chemical arrestant is potent when insects eat it--as opposed to having it injected into their blood.

If so, it could be sprayed on crops, like many conventional insecticides and biological control microbes.

FOR ADDITIONAL INFORMATION: To discuss this effort further, contact Thomas A. Coudron, Biological Control of Insects Laboratory, Agricultural Research Service, USDA, Columbia, Mo. 65205; (314) 875-5361.

NIH
Research & Technology

U.S. Department of Health and Human Services Public Health Service National Institutes of Health

Soil Yields 72 New Varieties of a Natural Pest Control

Soil from the Himalayan mountains, from a car bumper in Iceland, or even from the bottom of a cat's foot could mean death to insect pests.

In soil from these and other places—almost always brought by vacationing friends—U.S. Department of Agriculture scientists have found 72 new varieties of a soil bacterium, *Bacillus thuringiensis* (Bt)—a natural control for insect pests.

Three varieties, two from beside an airport in Baltimore, Maryland, and one from the Snake River in Jackson, Wyoming, await patents. In a field trial, they were as effective as the best available chemicals at killing cabbage loopers and worms, says Phyllis A.W. Martin, a geneticist with USDA's Agricultural Research Service in Beltsville, Maryland.

Bt kills insects by rupturing their stomach cells, making them unable to feed and digest food. "There might still be live caterpillars on a crop, but they can't do much damage if they can't feed," Martin says. And eventually, the insect larvae will die.

"Scientists have been hunting for this kind of control from Bt for about 25 years," says Russell S. Travers, formerly an ARS researcher working with Martin and now with Novo Laboratories, Wilton, Connecticut. He believes that the new varieties are 10 times as effective as present commercial Bt strains and could replace them in an industry worth about $40 million a year worldwide.

The fact that Martin and Travers derived all of their new Bt from soil may change Bt history. "Previously, scientists thought that to get the bacterium you had to find a dead insect; we just assumed it was an insect disease," Travers says. "But our studies indicate that Bt is really a normal component of many soils."

TIM McCABE

ARS geneticist Phyllis Martin and entomologist Russell Travers expose a variety of new Bt strains to sunlight to weigh the effects of sunlight on the strain's toxicity under outdoor conditions. (0787X768-23)

The scientists aren't ready to test most of the new varieties in the field. For now, Martin says, "we're trying to find out exactly what makes a Bt 'hot' and from those indicators, we'll know which of the new varieties warrant field tests."

For Additional Information:

To discuss this effort further, contact:

Phyllis Martin
USDA Insect Pathology Laboratory
Bldg. 011A
Beltsville, MD 20705; (301) 344-1723

For inquiries concerning rights for the commercial use of this invention should be addressed to

Office of Federal Patent Licensing
Center for the Utilization of Federal Technology
Room 13R, NTIS
Springfield, VA 22161; (703) 487-4738

Refer to Patent Application 7-050,450/TN

Computers

446 Algorithm Sorts Groups of Data — Sets are sorted quickly according to weighted sums of elements. (Licensing Opportunity)

447 Integrated Circuit for Simulation of Neural Network — Ballast resistors are deposited on top of the circuit structure.

448 Electronic Neural Networks — memory based on neural network models is content-addressable and fault-tolerant. (Licensing Opportunity)

449 Electronic Neural-Network Simulator — Experimental circuits are faster than simulation programs fun on digital computers. (Licensing Opportunity)

450 Pitch-Learning Algorithm for Speech Encoders — Gross pitch errors are detected and corrected. (Licensing Opportunity)

451 The Mark III Hypercube-Ensemble Computers — Concurrent processors will operate at high speed. (Licensing Opportunity)

452 Unified Robot-Control System — Robot-joint motors are integrated with a control computer or computers. (Licensing Opportunity)

Software

453 Ada Linear-Algebra Program — Routines are provided for common scalar, vector, matrix, and quaternion operations.

454 Analyzing Commonality in a System — Cost can be decreased by use of fewer types of parts.

455 Simulation of Research and Development Projects — Measures of preference for alternative project plans can be calculated.

Other Items of Interest

460 Blanket Gate Would Address Blocks of Memory — Circuit-chip area would be used more efficiently. (Licensing Opportunity)

NASA Tech Brief
National Aeronautics and Space Administration

Licensing Opportunity

Algorithm Sorts Groups of Data

Sets are sorted quickly according to weighted sums of elements.

An algorithm sorts sets of data into an ascending or descending order. Such sorting can become difficult for grouped data; i.e., multiple sets of data, where each set of data involves several measurements or related elements. The sorting becomes increasingly cumbersome as more elements are added to each set.

For efficient sorting, the algorithm finds the set that contains the minimum or maximum most significant data. The sets of data are then sorted as desired. The algorithm has been implemented in a computer program that handles the daily temperature readings of the Voyager spacecraft; in particular, those related to the special telecommunications-tracking requirements of Voyager 2.

The sorting process is simplified by the reduction of each multielement set of data to a single representative number. First, each set of data is expressed as a polynomial with a suitably chosen base, using the elements of the set as coefficients. The most significant element would be placed in the term containing the largest exponent. The base is selected by examining the range in value of the data elements. The resulting series is then summed to yield a single representative number. These numbers are then easily sorted, and each such number is converted back to its original set of data by successive division.

The computer program includes a sample data file containing 500 sets of data. Each set contains five elements. The program sorts the sets in ascending order in 3 to 5 seconds on an IBM PC-AT (or equivalent) computer equipped with a hard disk; on a similarly equipped PC-XT (or equivalent), the time is still less than 10 seconds. Operating instructions are included.

This program is written in BASIC (specifically the Microsoft QuickBASIC compiler) for interactive execution and has been implemented on the IBM PC computer series operating under PC-DOS with a central-memory requirement of approximately 40K of 8-bit bytes. (Note: The bulk of this memory space is occupied by the run-time support modules; the program is executable directly from DOS.) A hard disk is desirable for speed, but is not required. The program was developed in 1986.

This program was written by J. D. Evans of Caltech for **NASA's Jet Propulsion Laboratory**.

Inquiries concerning rights for the commercial use of this invention should be addressed to the Patent Counsel, NASA Resident Office-JPL Refer to NPO-17077/TN

Jet Propulsion Lab.
4800 Oak Grove Drive
Pasadena CA 91109

Technology Utilization Mgr.: Norman L. Chaffin
Mail Stop 156-211
(818) 354-2240

NASA Resident Technology Utilization Officer: Gordon S. Chapman
Mail Stop 180-801
(818) 354-4849

Patent Counsel: Paul F. McCaul
Mail Code 180-801
(818) 354-2734

FOR ADDITIONAL INFORMATION: *Contact: Director, Technology Transfer Division, P.O. Box 8757, BWI Airport, MD 21240; (301) 621-0100 Ext. 241*

REFER TO THE NUMBER LISTED AT THE END OF THIS ARTICLE

NASA Tech Brief
National Aeronautics and Space Administration
NASA's Jet Propulsion Laboratory, Pasadena, California

Integrated Circuit for Simulation of Neural Network

Ballast resistors are deposited on top of the circuit structure.

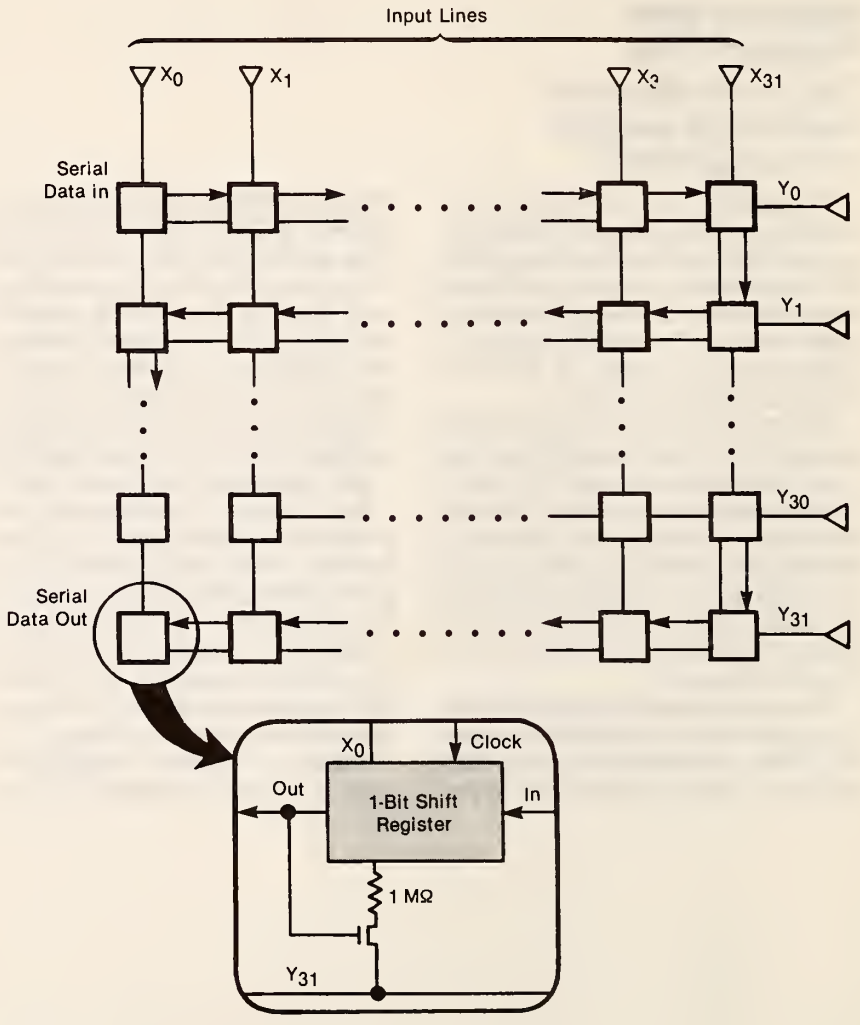

A Cascadable, Programmable, VLSI(32 × 32) Synaptic Chip based on the neural network architecture provides a basic building block for larger (e.g., 512 × 512) neural network embodiments.

A cascadable, programmable binary connection matrix is fabricated in VLSI form as a basic building block for assembly of like units into content-addressable electronic memory matrices that operate somewhat like networks of neurons. In such a matrix, connections are formed during the storage of data, and the data are recalled from memory by prompting the matrix with approximate or partly erroneous signals. In many cases, redundancy in the pattern of connections causes the matrix to respond with the correct stored data.

The matrix is an integrated circuit, the active elements of which are complementary metal-oxide/semiconductor (CMOS) devices. Each circuit chip includes 32 input ("X") lines and 32 output ("Y") lines (see figure). Each node of the matrix includes an analog switch that is turned on or off according to the output of the associated stage of a 1-bit serial shift register connected in cascade. The shift register is controlled by its input line; the binary connection data is serially shifted into the matrix along the input line at the rate of 1 bit per clock cycle.

To keep the static and dynamic power consumption below a maximum acceptable level, a 1-MΩ ballast resistor is connected in series with each analog switch. The active circuit elements are formed by conventional CMOS fabrication processes. Contact windows are opened in the metalization layer of the CMOS chip to enable the deposition of a patterned layer of suitable resistive material. In comparison with conventional CMOS processes for very-large-scale integrated circuits, this process lends itself more readily to the attainment of the required 5-percent precision in the ballast resistances.

A representative 512- by 512-node matrix would be made by assembling a 16-by-16 array of such chips. At a practical clock rate of 1 MHz, the connection pattern could be shifted into this matrix in a time of 0.262 s.

This work was done by Anilkumar P. Thakoor, Alexander W. Moopenn, and Satish K. Khanna of Caltech for **NASA's Jet Propulsion Laboratory**.
NPO-17059 /TN

FOR ADDITIONAL INFORMATION: *Contact: Director, Technology Transfer Division, P.O. Box 8757, BWI Airport, MD 21240; (301) 621-0100 Ext. 241*
REFER TO THE NUMBER LISTED AT THE END OF THIS ARTICLE

NASA Tech Brief
National Aeronautics and Space Administration
NASA's Jet Propulsion Laboratory, Pasadena, California

Licensing Opportunity

Electronic Neural Networks

A memory based on neural network models is content-addressable and fault-tolerant.

An experimental memory system behaves like a biological memory in several respects: It retrieves data when stimulated by imperfect input, it is redundant enough to continue functioning when a memory cell fails and the stored data are addressed by the form of the data themselves, rather than by location as in conventional electronic memories.

The system (see Figure 1) includes an electronic equivalent of a synaptic network; in particular, a matrix of programmable binary switching elements over which the data are distributed. The switches are programmed in parallel by the outputs of serial-input/parallel-output shift registers (not shown). The input and output terminals of a bank of high-gain nonlinear amplifiers (representing neurons) are connected in a nonlinear-feedback configuration by the switches and by memory-prompting shift registers.

An input-data vector is encoded by a microprocessor or other small computer, then fed to the serial-input/parallel-output shift registers. To recall stored data, the prompting shift registers interrogate the matrix with a pattern of ones and zeros that approximates the information sought. If the recalling approximation is sufficiently close, the electronic neurons turn on and present the exact stored data.

The circuits based on discrete electronic components and architectures derived from the neural net concepts display several unique features, including fast associative recall of information, parallel input/output, and intrinsic fault-tolerance. Development of thin-film-based, nonvolatile, programmable, binary synaptic arrays (matrices of resistive microswitches) for high-density associative memory systems is currently in progress.

The example of Figure 2 illustrates the writing and reading of information in a 4-by-4 matrix of switched resistors. To insure that the reading of a memory does not cause spurious writing, the writing voltage must be double the reading voltage. In this

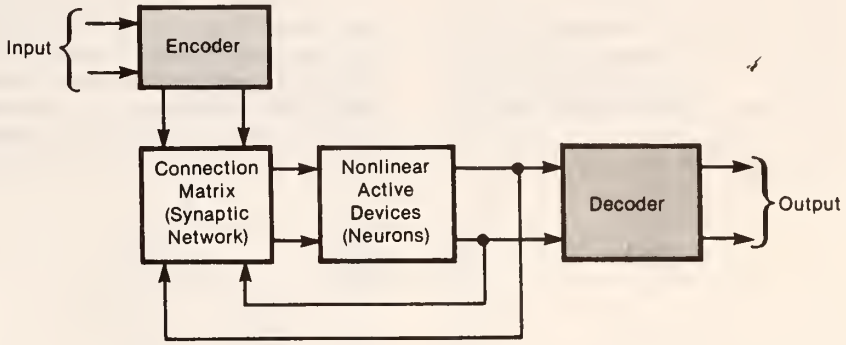

Figure 1. The **Memory System** includes a connection matrix of switching elements (representing a synaptic network) and a bank of nonlinear feedback amplifiers that mimic somewhat the behavior of neurons.

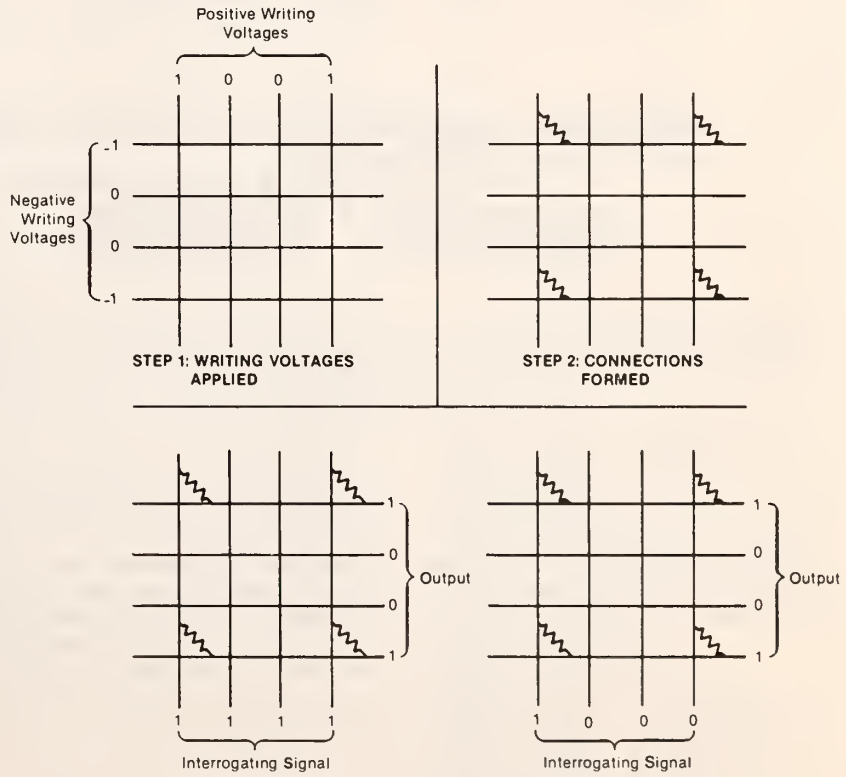

Figure 2. A **Small Switching Matrix** illustrates the approximate-input/exact-output and fault tolerance of the simulated neuron network.

example, the binary number 1001 is to be stored. A unit positive voltage is therefore impressed on the first and fourth vertical lines and a unit negative voltage on the first and fourth horizontal lines. The ancillary switching circuitry detects the double-unit voltage difference at the intersections of the lines with the + 1 and − 1 voltages and responds by switching in the resistors at these four intersections. The resistors remain after the writing voltage is turned off.

The data can be read out, for instance, by interrogating with signals on the vertical lines and detecting currents on the horizontal lines. In this example, if the interrogating signal is 1111, it causes currents representing 1001 to flow out of the horizontal lines. The 1111 reading signal is only an approximation of the data; yet it causes the precise 1001 value to be read out. A reading signal of 1000, 0001, 1101, 1011, or 1001 would also produce the correct result.

Since the number 1001 is effectively recorded in two places in the matrix, the correct readout can be obtained with one or two resistors missing, depending on the interrogating signal. If two diagonally located resistors are missing, an interrogation by 1111, 1001, 1101, or 1011 still gives an output of 1001. If only the upper right resistor is missing, a correct output will still be obtained as long as the interrogating signal includes a 1 on the leftmost vertical line.

The fault-tolerant, content-addressable memory concept has great potential for use in large interactive memories. Applications may include the next generation of computers, expert systems, and artificial intelligence. If constructed as very-large-scale integrated circuits, these memories may be denser and more reliable than those now in use.

This work was done by John Lambe, Alexander Moopen, and Anilkumar P. Thakoor of Caltech for **NASA's Jet Propulsion Laboratory**.

Title to this invention has been waived under the provisions of the National Aeronautics and Space Act [42 U.S.C. 2457(f)], to the Caltech/JPL. Inquiries concerning licenses for its commercial development should be addressed to

Edward Ansell,
Director of Patents and Licensing
Mail Stop 301-6
California Institute of Technology
1207 East California Boulevard
Pasadena, CA 91125.

Refer to NPO-16680, /TN

Jet Propulsion Lab.
4800 Oak Grove Drive
Pasadena CA 91109

Technology Utilization Mgr.: Norman L. Chaffin
Mail Stop 156-211
(818) 354-2240

NASA Resident Technology Utilization Officer: Gordon S. Chapman
Mail Stop 180-801
(818) 354-4849

Patent Counsel: Paul F. McCaul
Mail Code 180-801
(818) 354-2734

FOR ADDITIONAL INFORMATION: *Contact: Director, Technology Transfer Division, P.O. Box 8757, BWI Airport, MD. 21240; (301) 621-0100 Ext. 241*

REFER TO THE NUMBER LISTED AT THE END OF THE ARTICLE

NASA Tech Brief
National Aeronautics and Space Administration
NASA's Jet Propulsion Laboratory, Pasadena, California

Licensing Opportunity

Electronic Neural-Network Simulator

Experimental circuits are faster than simulation programs run on digital computers.

A hybrid analog/digital neurocomputer made of standard components aids research in neural-network computing. It is used to study such neural-network concepts as those described in the following article.

The computer contains a digital random-access memory that stores binary synaptic information and an array of analog threshold amplifiers with input and output sample-and-hold circuits that simulate neurons. The computer is faster than the software simulations previously used to experiment with electronic neural networks.

The computer is controlled by two clock signals, C_1 and C_2. The rate of clock C_2 is N times that of C_1, where N is the number of neurons. In the figure, there are 16 neurons, so that in this case, C_2 is 16 times as fast as C_1.

On each cycle of C_1, a serial shift register selects a neuron input for updating and sampling by one of the sample-and-hold circuits in group SH_1. The neuron input signal is determined by two factors: the current neuron output state at the outputs of the sample-and-hold circuits in group SH_2 and the synaptic information at the memory outputs that control pass-transistor array SW_2.

The updating process is repeated at each cycle of C_1, each neuron being checked in turn as directed by the serial shift registers. On each cycle of C_2, the neuron outputs — as determined by the updated inputs and the inhibiting signal — are sampled by the circuits in group SH_2, completing one system cycle. Thus, the system throughput and cycle time are set by the update-clock rate and the number of neurons. To prevent an update from being interrupted, the two clocks are not permitted to overlap.

The neurocomputer offers a significant reduction in hardware complexity over a fully-parallel electronic neural network. It is easily expandable and can be configured to simulate neural networks with either a feedback or feed-forward architecture. Furthermore, synapses with multiple quantized gray levels can be implemented with the incorporation of additional digital random-access memories.

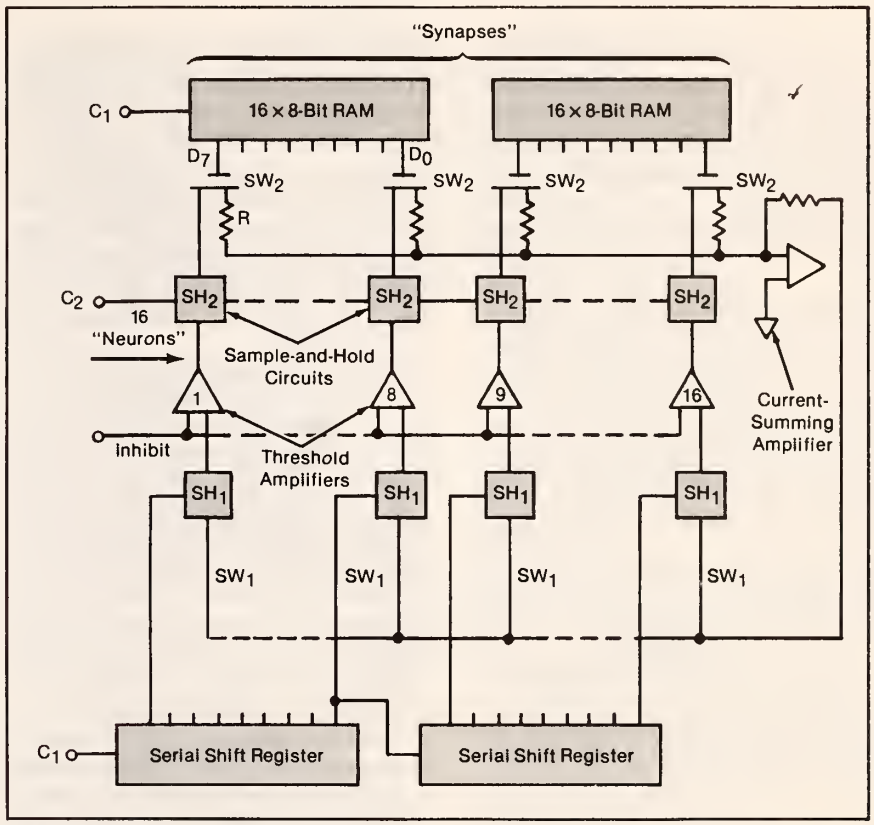

A Serial Shift Register Routes Clock Pulses C_1 to neurons in sequence. Clock pulses C_2 interrogate the neurons. The neuron interconnection information is stored in the simulated synapses (the memory chips). The system shown here contains 16 neurons and 256 binary synaptic nodes. It can readily be expanded to greater complexity.

This work was done by Alex W. Moopenn, Anilkumar P. Thakoor, and John J. Lambe of Caltech for **NASA's Jet Propulsion Laboratory**.

This invention is owned by NASA, and a patent application has been filed. Inquiries concerning nonexclusive or exclusive license for its commercial development should be addressed to the Patent Counsel, NASA Resident Office-JPL

Refer to NPO-17058 /TN

Jet Propulsion Lab.
4800 Oak Grove Drive
Pasadena CA 91109

Technology Utilization Mgr.: Norman L. Chalfin
Mail Stop 156-211
(818) 354-2240

NASA Resident Technology Utilization Officer: Gordon S Chapman
Mail Stop 180-801
(818) 354-4849

Patent Counsel:
Paul F. McCaul
Mail Code 180-801
(818) 354-2734

FOR ADDITIONAL INFORMATION: *Contact: Director, Technology Transfer Division, P.O. Box 8757, BWI Airport, MD 21240; (301) 621-0100 Ext. 241*
REFER TO THE NUMBER LISTED AT THE END OF THIS ARTICLE

NASA Tech Brief
National Aeronautics and Space Administration
NASA's Jet Propulsion Laboratory, Pasadena, California

Licensing Opportunity

Pitch-Learning Algorithm for Speech Encoders

Gross pitch errors are detected and corrected.

An adaptive algorithm detects and corrects errors in a sequence of estimates of the pitch period of speech. The algorithm operates in conjunction with the techniques used to estimate the pitch period. The algorithm can be used in such parametric and hybrid speech coders as linear predictive coders and adaptive predictive coders.

The estimation of the pitch period is susceptible to gross errors, which are large in magnitude, typically because of pitch-period doubling or background noise. The estimation is also subject to fine pitch errors, which are due to the limited resolution of the pitch-estimation technique or to the variation of the pitch period with time. Gross errors result in distorted encoded speech spurts that are subjectively very objectionable. Fine pitch errors are more tolerable but reduce the natural-sounding quality of the encoded speech.

The algorithm is based on the observation that the range of pitch periods for a given speaker is narrower than that for all speakers: in the general speaker population, pitch periods range between 2 ms and 20 ms, whereas the pitch period of a single speaker has a range typically less than 5 ms wide. Most gross errors fall outside this relatively narrow range and hence can be easily detected.

The pitch-period range of an incoming speech signal depends heavily on the speaker and can change significantly when someone else begins to speak. When the algorithm detects such a change, the learning is initialized, and the new pitch-period range is estimated.

The algorithm can be described as a three-stage procedure, which is repeated for each pitch-period estimate. In the first stage, each new pitch-period estimate is included in a progressive average of all of the pitch-period estimates made since the most recent reset of the learning algorithm. Pitch-period samples taken during moments of silence are arbitrarily assigned pitch periods of zero and excluded from the average.

According to experiments, there is a high probability that the instantaneous pitch-period estimate will lie between 0.75 and 1.25 times the average. In the second stage, the algorithm tests each subsequent pitch-period estimate to determine whether, in fact, it lies within this range. If it does, the estimate is assumed correct and the averaging continues. If the estimate falls outside the range, a gross error is assumed: in this case, a new estimate for the present pitch period is made from the previous and next pitch-period estimates.

If the new estimate lies within the range, a correction counter is set to zero. If it lies outside the range, the correction counter is incremented. The third stage of the algorithm is based on the assumption that a reliable pitch-period estimate has a small number of gross errors; in this case, the allowable number of consecutive errors is arbitrarily set at three. When the correction counter indicates a higher number, the pitch-period range estimate is deemed to be in error. (This is most likely to occur when a new person begins to speak.)

When an error is detected, the pitch-period average is discarded, the averaging counters are reset, and the system begins to relearn the pitch range. Error detection and correction are suspended during the first eight nonzero pitch-period estimates, when the new average is established.

This work was done by B. R. Udaya Bhaskar of Comsat Laboratories for **NASA's Jet Propulsion Laboratory**.

Title to this invention has been waived under the provisions of the National Aeronautics and Space Act [42 U.S.C. 2457(f)], to the COMSAT Laboratories. Inquiries concerning licenses for its commercial development should be addressed to

COMSAT Laboratories
22300 COMSAT Drive
Clarksburg, MD 20871

NPO-17045, /TN

Jet Propulsion Lab.
NASA Resident Office
Technology Utilization Officer: Gordon S. Chapman
Mail Stop 180-801
4800 Oak Grove Drive
Pasadena, CA 91109
(818) 354-4849
Patent Counsel: Paul F. McCaul
Mail Code 180-801
4800 Oak Grove Drive
Pasadena, CA 91109
(818) 354-2734
Technology Utilization Mgr. for JPL: Norman L. Chalfin
Mail Stop 156-211
4800 Oak Grove Drive
Pasadena, CA 91109
(818) 354-2240

FOR ADDITIONAL INFORMATION: *Contact: Director, Technology Transfer Division, P.O. Box 8757, BWI Airport, MD 21240; (301) 621-0100 Ext. 241*
REFER TO THE NUMBER LISTED AT THE END OF THIS ARTICLE

NASA Tech Brief
National Aeronautics and Space Administration
NASA's Jet Propulsion Laboratory, Pasadena, California

Licensing Opportunity

The Mark III Hypercube-Ensemble Computers

Concurrent processors will operate at high speed.

The Mark III Hypercube concept is being applied in the development of a series of increasingly powerful computers. When fully developed, the Mark III computers will be especially useful for the solution of physical problems with spatially and temporally varying quantities. Disciplines that will benefit from the speed and memory capacity of the Mark III Hypercube include astrophysics, geophysics, chemistry, weather, high-energy physics, applied mechanics, image processing, oil exploration, aircraft design, and microcircuit design.

As in previous hypercube networks, each of $N = 2^k$ identical concurrent processors is located at a node that corresponds to a corner of a k-dimensional cube. Each processor is connected to its k nearest neighbors along the topological equivalents of the k edges that meet at that corner. The prototype contained 4 nodes; two additional 32-node models were built and are operational. A subsequent 1 gigaflop 128-node model is now under construction and will be operational by the end of 1988.

The Mark III concept includes very powerful nodes connected by high-speed communication links. The processor at each node is composed of three subprocessors that are tightly coupled through a 4-Mbyte main node memory on a common bus (see figure). The peak rate of data transfer between the main memory and each subprocessor is 12 Mbytes/s. To minimize the degradation of performance caused by simultaneous attempts of the subprocessors to gain access to the main node memory, each subprocessor is also provided with a high-speed local memory. The main subprocessor arbitrates the memory contentions.

The input/output control subprocessor includes an MC68020 microprocessor, 64 Kbytes of high-speed local memory, and a direct-memory-access channel-support module. This subprocessor is capable of an input/output-channel transfer rate up to 68 Mbits/s.

The main subprocessor is also based on the MC68020 and operates at over 2 million instructions per second. It includes a 32-bit arithmetic and logic unit and a full 32-bit address generator. The local memory of 128 Kbytes has faster access than does the shared main memory; this allows the microprocessor to reach its full execution speed.

The high-speed floating-point subprocessor is a peripheral unit attached to the node board by a daughter-board connector. This subprocessor is responsible for heavy floating-point arithmetic: it can increase the speed of such computations to as much as 50 times that achievable with the floating-point coprocessor that is part of the main subprocessor.

The shared main memory is partitioned into four address-interleaved dynamic memory modules, each having its own dynamic memory controller. Circuitry is included to correct one-bit data errors in memory and to signal (but not to correct) two-bit errors; in the latter case, the main subprocessor is interrupted. The read/write memory cycle is 200 ns from a valid address strobe.

The success of the Mark III Hypercube concept will depend on the development of software to tap the high-speed potential of concurrent processing. In particular, it will be necessary to spread the computational work load as evenly as possible among all the nodes and to reduce the need for data transfers among the nodes.

The lack of good software — both at the operating system and application level — is the main issue holding back the development of parallel computers. Work is also being applied to the development of useful "parallel supercomputer software tools" on the basis of the experience in using "real parallel machines" to solve "real problems."

This work was done by John C. Peterson, Jesus O. Tuazon, Don Lieberman, and Moshe Pniel of Caltech for **NASA's Jet Propulsion Laboratory**.

In accordance with Public Law 96-517, the contractor has elected to retain title to this invention. Inquiries concerning rights for its commercial use should be addressed to

Edward Ansell,
Director of Patents and Licensing
Mail Stop 301-6
California Institute of Technology
1207 East California Boulevard
Pasadena, CA 91125
Refer to NPO-16772, /TN

Jet Propulsion Lab.
4800 Oak Grove Drive
Pasadena CA 91109

Technology Utilization Mgr.: Norman L. Chalfin
Mail Stop 156-211
(818) 354-2240

NASA Resident Technology Utilization Officer: Gordon S. Chapman
Mail Stop 180-801
(818) 354-4849

Patent Counsel: Paul F. McCaul
Mail Code 180-801
(818) 354-2734

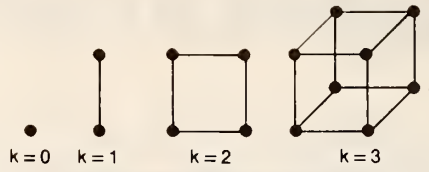

HYPERCUBE NODE STRUCTURE

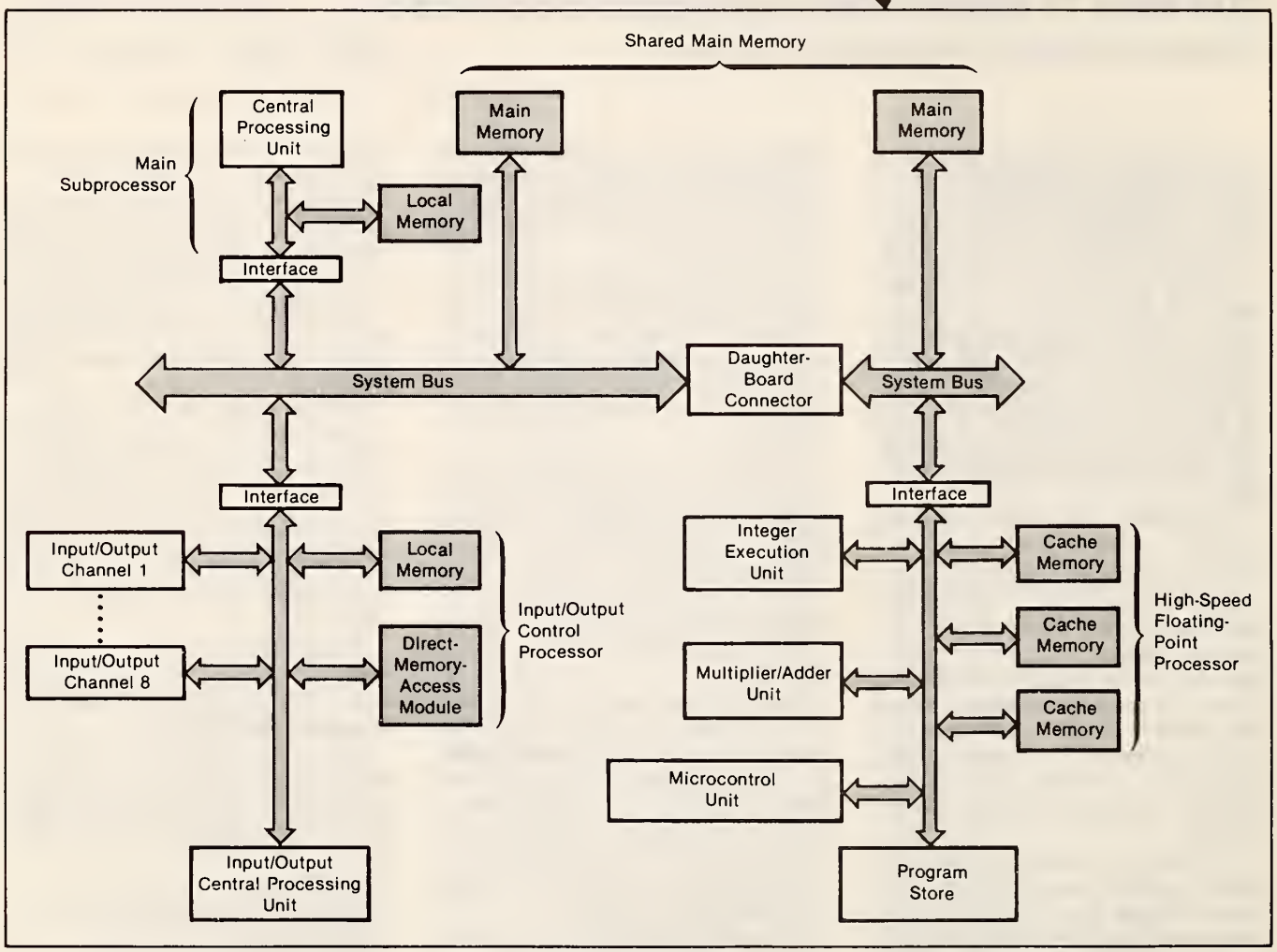

NODE PROCESSOR

The **Processor of Each Node** of Mark III Hypercube ensemble is a specialized computer that contains three subprocessors and a shared main memory. The hypercube ensemble solves a problem quickly by simultaneousiy processing a part of the problem at each such node and passing the combined results to a host computer.

FOR ADDITIONAL INFORMATION: *Contact: Director, Technology Transfer Division, P.O. Box 8757, BWI Airport, MD. 21240; (301) 621-0100 Ext. 241*

REFER TO THE NUMBER LISTED AT THE END OF THE ARTICLE

NASA Tech Brief
National Aeronautics and Space Administration
NASA's Jet Propulsion Laboratory, Pasadena, California

Licensing Opportunity

Unified Robot-Control System

Robot-joint motors are integrated with a control computer or computers.

A robot controller uses only 1 microprocessor to control as many as 16 joint-actuating motors. The control system uses a high-speed bus to communicate with the joint-interface circuits, an addressing scheme that makes it possible to write commands to several motors simultaneously, and an efficient assembly-language servo code. These features enable the control of the 16 joints at a 1-kHz servo rate. In contrast, commercial robot controllers include separate microprocessors for each joint to achieve the same rate. The new system is suitable for the control of motors in numerically-controlled manufacturing systems.

The use of a single joint-control processor results in fewer components, lower cost, and simpler architecture than are required in existing systems of comparable performance. Moreover, the single processor can correlate events on different joints — an impossible feat if a separate processor is assigned to each joint.

The joint-control microprocessor is the NS32016 (or equivalent), a 32-bit linear-address-space microprocessor. It is mounted on the joint-level processor circuit card, which also contains a floating-point arithmetic unit; an interruption-controlling unit; a 32K read-only memory; a 128K random-access memory; two serial ports; a parallel data interface; an interface between the fast, direct data bus and the joint interface cards; and an interface with the multibus (a standard data bus) that links the controller to an external controller (see figure). The controller card supplies control signals to the joint interface cards and accepts feedback signals from them. The card contains about 100 integrated circuits and costs about $400 (at 1986 prices).

Each of the joint interface cards (one card for four joints) contains an interface with the fast, direct data bus; pulse-width modulation (PWM) generators; interfaces with the quadrature angle encoders on the motors; digital tachometers; analog-to-digital converters; and an electronically-erasable, programmable read-only memory. A joint interface card applies digital control signals from the controller card to the PWM generators that in turn provide motor-drive pulses to the power amplifiers.

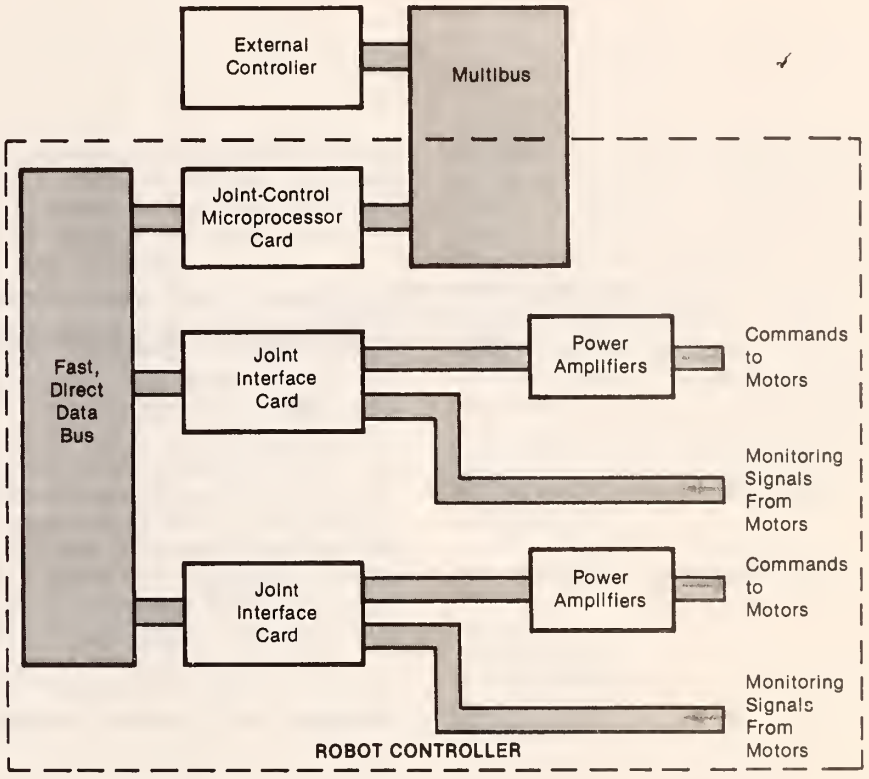

A **Fast, Direct Data Bus** carries digital signals between the controller card and the joint interface cards. The joint interface cards supply digital motor-control signals to the motors through power amplifiers and provide digital monitoring signals to the controller card.

Direct digital control of the PWM generators, instead of the usual analog control, eliminates digital-to-analog conversion and its nonlinearity and drift with temperature. With a loss of energy of only 5 percent, as compared with up to 50 percent for analog control, direct digital control is also more efficient.

Each power amplifier contains power transistors, driver circuits, a short-circuit detector, and current-feedback resistors. The cost of the components of the power amplifiers is less than $100 per motor (1986 prices).

The analog-to-digital converters accept signals that represent shaft positions, motor currents, inductive freewheeling currents, and power-supply voltages. They furnish this information to the controller card in digital form. Acting in concert with the quadrature encoder interfaces, the digital tachometers measure the angular velocities of the motor shafts so accurately and quickly that instantaneous motor accelerations can be calculated reliably from any two consecutive velocity measurements — impossible with analog tachometers. Moreover, because the digital tachometers use the outputs of the angle encoders, they do not require the installation of additional equipment on the motors.

The controller determines the torques, back-electromotive-force constants, electrical resistances, and winding temperatures of the motors; the loads upon the motors; and the status of the power supply. The controller can also identify and act on the following problems:

- Open or short motor circuits,
- Broken encoder wires or constant volt-

ages in encoder inputs,
- Malfunctions of potentiometers,
- Insufficient power to drive the motors, and
- Failures of components on the joint interface cards.

In response, the controller can apply the proper voltages to the motors, open the motor circuits where necessary, provide regenerative damping through any motor in either direction, and apply or release electromagnetic brakes.

The controller contains a code-generator software so that it can adapt to the particular motors and sensors used. After robot hookup, the motor, encoder, potentiometer polarities can be changed from software. The control method used can be different on every motor. The code generator writes highly optimized assembly code.

This work was done by Zoltan F. Szakaly of Caltech for **NASA's Jet Propulsion Laboratory**.

This invention is owned by NASA, and a patent application has been filed. Inquiries concerning nonexclusive or exclusive license for its commercial development should be addressed to the Patent Counsel, NASA Resident Office-JPL Refer to NPO-17134./TN

Jet Propulsion Lab.
4800 Oak Grove Drive
Pasadena CA 91109

Technology Utilization Mgr.: Norman L. Chalfin
Mail Stop 156-211
(818) 354-2240

NASA Resident Technology Utilization Officer: Gordon S. Chapman
Mail Stop 180-801
(818) 354-4849

Patent Counsel: Paul F. McCaul
Mail Code 180-801
(818) 354-2734

FOR ADDITIONAL INFORMATION: *Contact: Director, Technology Transfer Division, P.O. Box 8757, BWI Airport, MD. 21240; (301) 621-0100 Ext. 241*
REFER TO THE NUMBER LISTED AT THE END OF THE ARTICLE

NASA Tech Brief
National Aeronautics and Space Administration

Computer Software

Ada Linear-Algebra Program

Routines are provided for common scalar, vector, matrix, and quaternion operations.

A computer program extends the Ada programming language to include linear-algebra capabilities similar to those of the HAL/S programming language. The package is designed for such avionics applications as software for the Space Station.

In addition to the HAL/S built-in functions, the package incorporates the quaternion functions used in the Shuttle and Galileo projects and routines from LINPACK that solve systems of equations involving general square matrices. Language conventions in this package follow those of HAL/S to the maximum extent practical and minimize the effort required for writing new avionics software in Ada and translating existing software to Ada.

Valid numeric types are scalar, vector, matrix, and quaternion. (Quaternions are four-component vectors used here to represent motion between coordinate frames.) Infix operators are used instead of function calls to define dot products, cross products, quaternion products, and mixed scalar·vector, scalar·matrix, and vector·matrix products.

There are two generic packages: one for floating-point components and one for integer components. The actual component types are selectable by the user and are passed as formal parameters to the generic packages. The floating-point package is instantiated for double- and single-precision components, the integer package is instantiated for double-precision integer components, and the three instantiations are collected in a single package. Each floating-point instantiation offers 71 subprograms, and the integer instantiation offers 56.

All the common vector, matrix, and quaternion arithmetic and input/output operations are provided. HAL/S functions include ABVAL, UNIT, TRACE, DET, INVERSE, TRANSPOSE, and IDENTITY. Quaternion functions include INVERSE, CONJUGATE, and functions that convert between quaternion and matrix representations of coordinate rotations. LINPACK procedures include GEFA, GECO, GESL, and GEDI and are represented by eight procedures in each floating-point package.

This program was written by A. R. Klumpp and C. L. Lawson of Caltech for **NASA's Jet Propulsion Laboratory**. *NPO-17119 /TN*

FOR ADDITIONAL INFORMATION *CONTACT:*

COSMIC®
112 Barrow Hall
University of Georgia
Athens, GA 30602
(404) 542-3265

Analyzing Commonality in a System

Cost can be decreased by use of fewer types of parts.

The System Commonality Analysis Tool (SCAT) computer program was designed to aid managers and engineers in identifying common, potentially common, and unique components of a system. Commonality lowers the overall cost of a system through the use of the smallest variety of items or types of subsystems in the greatest number of applications. SCAT, through utilization of a comprehensive data base on parts, determines cost effectiveness by comparing the life-cycle costs of unique and standard configurations of parts. The SCAT data base reflects both engineering and financial data. SCAT was instituted for the analysis of commonality in the Space Station but is easily applicable to such other projects as commonality in software, which is used as an example in the detailed documentation.

SCAT incorporates three major functions: (1) a program for the creation and maintenance of a data base, (2) the analysis of commonality, and (3) such system utilities as host-operating-system commands and loading and unloading of the data base. The data base on parts contains "generic" attributes needed to calculate life-cycle costs, and "discriminating" attributes for engineering design data. SCAT selects parts that are similar, based on selection criteria defined by the user.

One can choose either of two algorithms for analysis. The direct algorithm uses supplied cost figures for design, development, testing, and first-product calculations. The relational algorithm estimates these costs based on a complexity factor (simple, medium, complex); the type of item (electrical, mechanical, and the like); and the percent of new development needed. SCAT also contains a software-commonality algorithm that requires the size of the package, the expected number of years of use, and whether the programs are critical to a mission, developed in-house, or dependent on equipment that is not yet available.

SCAT produces reports that tabulate maintenance, initial configurations, and expected total costs. By examining systems made of unique parts and systems made of parts having comparable functions, SCAT can help determine which parts are good candidates for commonality. SCAT is menu-driven and includes an online help facility.

SCAT is written in FORTRAN 77 for interactive execution. SCAT is available in two machine versions. The IBM PC version has been implemented on an IBM PC/XT-compatible computer operating under MS-DOS (V.2.0 and 3.0) with a central-memory requirement of approximately 640K of 8-bit bytes. The SCAT PC version requires a 10-MB hard disk, the commercial R:base 5000 (V1.0 or 1.01) data base, and the Micro-RIM data-base interface package, which is compatible with MicroSoft FORTRAN V.3.2 or 3.31. The VAX version of SCAT has been implemented on a VAX 11/780 and a VAX 8600 under VMS 4.X with a VT100 or VT220 terminal. The SCAT VAX version requires the commercial RIM-7 (UD 12) data base and the RIM-7 FORTRAN interface library. The program was developed in 1987.

This program was written by Alfred Pacheco and Kevin Pool of The Boeing Co. for **Marshall Space Flight Center.**
MFS-28271 /TN

FOR ADDITIONAL INFORMATION
CONTACT:

COSMIC®
112 Barrow Hall
University of Georgia
Athens, GA 30602
(404) 542-3265

Simulation of Research and Development Projects

Measures of preference for alternative project plans can be calculated.

The Simulation of Research and Development Projects (SIMRAND) program aids in the optimal allocation of research and development resources needed to achieve project goals. SIMRAND models the system subsets or project tasks as various network paths to a final goal. Each path is described in terms of such task variables as the cost per hour, the cost per unit, and the availability of resources. Uncertainty is incorporated by treating task variables as probabilistic random variables.

SIMRAND calculates the measure of preference for each alternative network. The networks yielding the highest utility function (or certainty equivalence) are then ranked as the optimal network paths. SIMRAND has been used in several economic-potential studies at NASA's Jet Propulsion Laboratory, involving solar-dish power systems and the construction of photovoltaic arrays. However, any project having tasks that can be reduced to equations and related by measures of preference can be modeled.

SIMRAND analysis consists of three phases: (1) reduction, (2) simulation, and (3) evaluation. In the reduction phase, analytical techniques from probability theory as well as simulation techniques are used to reduce the complexity of the alternative networks. In the simulation phase, a Monte Carlo simulation is used to derive statistics on the variables of interest for each alternative network path. In the evaluation phase, the simulation statistics are compared, and the networks are ranked in preference by a selected decision rule. The user must supply information on project subsystems in terms of equations based on variables (for example, parallel and series assembly-line tasks in terms of the number of items, cost factors, time limits, and the like). The associated cumulative distribution functions and utility functions for each variable must also be provided (for example, allowable upper and lower limits and group-decision factors).

SIMRAND is written in Microsoft FORTRAN 77 for batch execution and has been implemented on an IBM PC-series computer operating under DOS. This program was developed in 1986.

This program was written by Ralph F. Miles of Caltech for **NASA's Jet Propulsion Laboratory**. *NPO-16937 /TN*

FOR ADDITIONAL INFORMATION *CONTACT:*

COSMIC®
112 Barrow Hall
University of Georgia
Athens, GA 30602
(404) 542-3265

Electrotechnology

456 Million-Fold Improvement in Superconductor Resistance

457 High Gain Crossed Field Amplifiers Projects Completed

458 Tool Effectively Bends Pins on Printed Circuit Board Connectors

459 Dual-Bank Microstrip Antenna with Reactive Loading — An effective but bulky coaxial stub is replaced.

460 Blanket Gate Would Address Blocks of Memory — Circuit-chip area would be used more efficiently. (Licensing Opportunity)

461 Designing a Microwave Band-Stop Filter — Lumped-circuit design techniques are applied to iris-coupled cavities.

462 Lightweight Video-Camera Head — A separate optical assembly weighs only 80 grams.

463 Programmable Synaptic Arrays for Electronic Neural Networks — High resistances prevent hotspots in parallel input and output operation. (Licensing Opportunity)

464 Public-Facilities Locator for the Blind — An optoelectronic system would enable blind people to find key places without assistance.

465 Three-Waveguide Beam and Polarization Splitter — Different modes are guided to different output ports.

Testing & Instrumentation

466 Remote Sensor and Cable Identifier

467 Dual Pilot-Tone Calibration Technique — The signal-to-noise ratio would be increased.

Other Items of Interest

543 Variable-Reluctance Motor for Electric Vehicles — A scaled-down motor performed as expected.

NBS technology update

National Bureau of Standards
U.S. Department of Commerce
Gaithersburg, MD 20899

Million-Fold Improvement in Superconductor Resistance

In further developments on the high-temperature superconductor front, NBS and Westinghouse have lowered contact resistivity to a million times less than indium-solder contacts. This is a hundred- to a thousand-fold improvement over the earlier reported results of Ekin (NBS), Panson and Blankenship (both of Westinghouse) who developed the basic technique. The newest results are obtained by annealing the sputter-deposited silver contact pads on the superconductor in oxygen at temperatures up to 500 °C for an hour. (The previously reported technique involved temperatures up to 150 °C, but no oxygen annealing.) Where the intermediate (500 °C) temperatures can be tolerated, the annealing technique yields resistivities of about 10^{-8} ohm-cm^2 at 76 K for bulk sintered samples of $YBa_2Cu_3O_7$. This resistivity was measured for current densities of up to 100 A/cm^2. The voltage-current characteristic was non-linear, having the character of a superconducting proximity effect; at lower current densities, below 30 A/cm^2, the resistivity was unmeasurably low. These results were presented at the Materials Research Society meeting in Boston on Nov. 30 - Dec. 4, 1987. (Similar results have been observed by a group at Auburn University under Y. Tzeng, but using evaporative deposition and annealing for 5 hours at 500 °C.)

FOR ADDITIONAL INFORMATION: For technical details, contact Jack Ekin, Div. 724.05, National Bureau of Standards, Boulder, Colo. 80303; (303) 497-5448.

High Gain Crossed Field Amplifiers Projects Completed

Two Manufacturing Technology (MT) Projects, DNE 107 and DNE 240, were recently completed that will significantly reduce the cost and improve the quality of crossed field amplifiers (CFA). The need for development of low cost production processes first became evident when design changes were made to CFA's to increase the gain of these devices. This design change reduced the size, weight and complexity of the CFA and permitted the elimination of a portion of the electronics in the associated radar. Inherent in this new design were very costly precise manufacturing processes, extremely fine adjustments and extensive testing. Only limited attention was given to optimizing these costly production processes prior to the initiation of two Navy projects to develop the needed manufacturing technology.

Precision tooling, jigs and assembly procedures were developed to closely control the intricate fabrication and assembly processes. As an example, a special multiple rotary support system was developed for use in the process to sputter-deposit coatings on the cathode interface. This system reduced the cost of coating the cathode by 85%. Automated test and control methods were established that have greatly enhanced the evaluation testing and adjustment of the cathode/anode rf circuit interrelationships. As an added bonus, the assembly of light-weight magnets in the tubes reduced the weight of the CFA from 28 to 21 pounds.

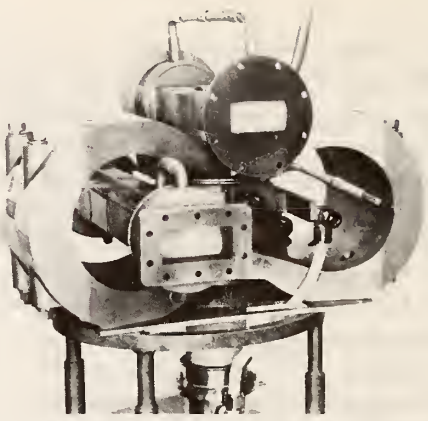

S-BAND CROSSED FIELD AMPLIFIER

The combined accomplishments of these two MT projects will result in reduced production costs that will exceed $5 million in total savings over the first five years of production.

For more information on these programs, please contact:
Commander,
Naval Ocean Systems Center
Attn: Mr. Richard Gamble (Code 9302)
San Diego, CA 92152-5000
Telephone: (619) 225-6457.

For Additional Information:

To discuss the effort further, contact:
AMRF Project
Building 220 —Room B-111
National Bureau of Standards
Gaithersburg, MD 20899
Joan Wellington (documentaion)
(301) 975-3416
Bill Rippey
(301) 975-3417 (user inferface project)

Tool Effectively Bends Pins on Printed Circuit Board Connectors

A tool for bending rows of connector pins in connectors that hold printed circuit boards to a mother board configuration has been developed by the Naval Ocean Systems Center.

The connectors provide electrical contact between the printed circuit boards and the remainder of the electrical circuit configuration. The tool consists of an anvil plate that is fitted at opposite edges with trunions that provide two axes of rotation at those edges. Holding brackets for holding the connector in a predetermined manner are attached at each trunion.

The holding brackets with their appropriate jigs are capable of holding a connector in a manner wherein the connector may be rotated about the trunion axes, causing either the first or second rows of the connector pins to be bent to a predetermined angle relative to an original plane of orientation. By this method the connector with bent pins may be fastened to a mother board at an angle of installation which allows for more dense packaging of printed circuit boards when installed at this angle.

The pin bending tool provides a means for quickly and effectively bending the pins on a connector for printed circuit boards at a predetermined angle to allow the connectors to be mounted on a mother board in a manner that the printed circuit cards will then be configured at said angle relative to the plane of the mother board.

This capability allows commercially available, low-cost, reliable printed circuit boards to be used in special electronics packages that require less cross-sectional area than that normally required when the printed circuit boards are mounted perpendicular to the plane of the mother structure.

For Additional Information:

Backup material on this effort is available from:

Navy Domestic Technology Fact Sheet
Reader Reply Service
Code E211
Naval Surface Weapons Center
Dahlgren, VA 22448-5000
(703) 663-8921

Refer to 120802/TN

NASA Tech Brief
National Aeronautics and Space Administration
Lyndon B. Johnson Space Center, Houston, Texas

Dual-Band Microstrip Antenna With Reactive Loading

An effective but bulky coaxial stub is replaced.

A short-circuited microstrip transmission line serves as a reactive loading element for a microstrip antenna. Constructed integrally with the stripline radiating element, the shorted line preserves the low microstrip profile and enables tuning of the antenna for two-band operation: previously, such tuning required a coaxial loading stub, which protruded into the space above the circuit board.

The loading element (see Figure 1) overcomes the inherent narrow bandwidth of the antenna, splitting the resonance into two different frequencies. The change in resonant frequency is affected by the stub length, L; the insert distance, S; the gap width, G; the strip width, W; and the thickness and permeability of the dielectric.

As G is increased, the lower resonant frequency decreases, but the upper resonant frequency is hardly affected. As S is increased, the two resonant frequencies are brought closer together. L is set according to theoretical predictions of the stub lengths that cause dual resonance. Thus, the antenna can be made to resonate at two specified frequencies by a suitable choice of radiator and loading-element dimensions, as shown for example in Figure 2.

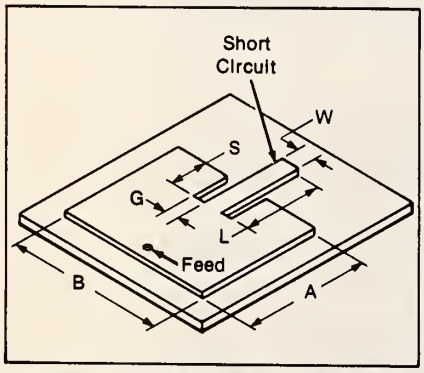

Figure 1. The **Antenna and Loading Element** are made as a unitary microstrip.

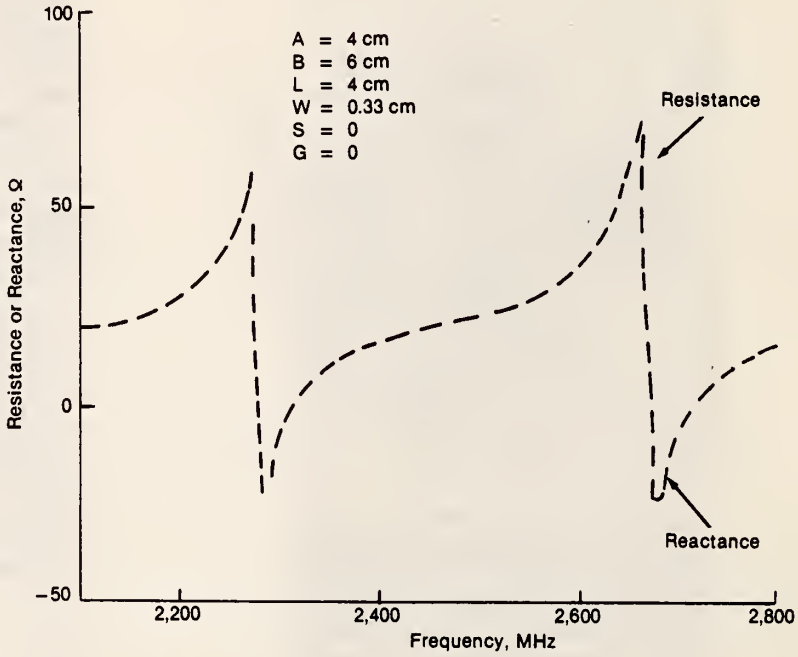

Figure 2. **Two Resonances** are exhibited by a unit like that shown in Figure 1.

This work was done by Shayla E. Davidson of **Johnson Space Center.**
MSC-21118 /TN

FOR ADDITIONAL INFORMATION: *Contact: Director, Technology Transfer Division, P.O. Box 8757, BWI Airport, MD 21240; (301) 621-0100 Ext. 241*
REFER TO THE NUMBER LISTED AT THE END OF THIS ARTICLE

NASA Tech Brief
National Aeronautics and Space Administration
NASA's Jet Propulsion Laboratory, Pasadena, California

Licensing Opportunity

Blanket Gate Would Address Blocks of Memory

Circuit-chip area would be used more efficiently.

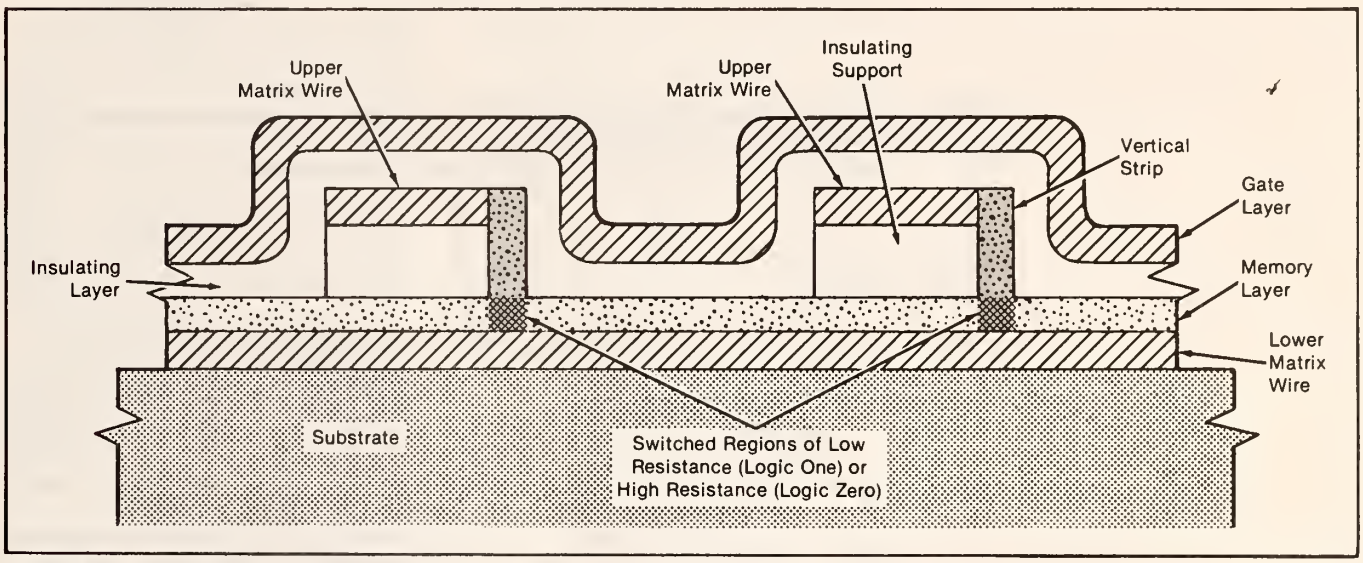

The **Blanket Gate Layer** would overlay the memory cells in a block. (Two cells are shown here.) A voltage on the gate layer would inhibit reading and writing throughout the block. The inhibiting mechanism is much like that in an insulated-gate transistor.

A proposed gate structure would selectively allow and restrict access to blocks of memory in an electronic neural-type network. By breaking the memory into independent blocks, the gate would greatly simplify the problem of reading from and writing to memory. For example, since the blocks would not be used simultaneously, they could share the operational amplifiers that prompt and read information stored in the memory cells. Far fewer operational amplifiers would be needed, and the chip area they occupy would be reduced correspondingly. The cost per bit would drop as a result.

The gate would overlie an array of thin-film amorphous silicon memory cells like those described in the preceding article. Instead of being discrete cells, however, the array of resistors would lie in a single continuous layer in which the extremely high resistivity of the material would isolate the cells from each other. Each block of cells would be provided with its own blanket gate.

Within a blanket gate, memory cells would lie between matrix wires running at right angles to each other in parallel planes (see figure). At each cell, the upper matrix wire would be connected to a vertical strip that makes contact with the memory layer. Like the memory layer, the vertical strips would be made of amorphous hydrogenated silicon or germanium. (The vertical strip replaces both the ballast resistor and the contact described in the preceding article.) A voltage applied between a strip and its lower matrix wire would change the local resistance of the memory film from high to relatively low, thereby switching the memory cell on (changing its logic state from zero to one). The change would be permanent; that is, the memory would be nonvolatile.

The gate structure would include an insulating layer and a conducting gate layer that blankets the cells in a block. A voltage could be applied to the gate layer to deplete the carriers in all the vertical strips in the block. The strips thus could be prevented from conducting pulses fed to them by the upper and lower matrix wires, and both writing and reading of the memory cells would thereby be prevented. The block of memory cells would thus be cut off from the rest of the system. When the blocking voltage on the gate layer is removed, the block would be reconnected to the rest of the system.

Conventional fabrication methods would be used; fine-line lithography would not be necessary. The lower wire matrix would be deposited on a substrate, followed by the amorphous silicon memory layer. Insulating supports would be deposited on each row of cell sites through a mask, and the upper matrix wires would be deposited on the supports. The vertical strips would be deposited on the sides of the supports by evaporation from a silicon source.

In a content-addressable memory, each block of cells would be associated with a class or subclass of contents. For example, a block might be dedicated to data on people whose surnames begin with the letter J. When searching for data on one such person, the controlling and encoding microprocessor would send out a signal to all other blanket gates so that only the J block could be read.

Although the memory array for the blanket gate would not be as densely packed as the discrete-cell memory in the preceding article would be, the bit density would still be quite high — about 10 times that in conventional semiconductor memories. This is because the decrease in cell density

would be more than offset by the elimination of the large circuit-chip area that would otherwise be required for duplicate operational amplifiers.

This work was done by John Lambe, Alexander Moopenn, and Anilkumar P. Thakoor of Caltech for **NASA's Jet Propulsion Laboratory**.

Title to this invention has been waived under the provisions of the National Aeronautics and Space Act [42 U.S.C. 2457(f)], to the Caltech/JPL. Inquiries concerning licenses for its commercial development should be addressed to

Edward Ansell,
Director of Patents and Licensing
Mail Stop 301-6
California Institute of Technology
1207 East California Boulevard
Pasadena, CA 91125.

Refer to NPO-16682, /TN

Jet Propulsion Lab.
4800 Oak Grove Drive
Pasadena CA 91109

Technology Utilization Mgr.: Norman L. Chalfin
Mail Stop 156-211
(818) 354-2240

NASA Resident Technology Utilization Officer: Gordon S. Chapman
Mail Stop 180-801
(818) 354-4849

Patent Counsel: Paul F. McCaul
Mail Code 180-801
(818) 354-2734

FOR ADDITIONAL INFORMATION: *Contact: Director, Technology Transfer Division, P.O. Box 8757, BWI Airport, MD 21240; (301) 621-0100 Ext. 241*

REFER TO THE NUMBER LISTED AT THE END OF THIS ARTICLE

NASA Tech Brief
National Aeronautics and Space Administration
NASA's Jet Propulsion Laboratory, Pasadena, California

Designing a Microwave Band-Stop Filter

Lumped-circuit design techniques are applied to iris-coupled cavities.

A band-stop filter for use with a maser preamplifier in an X-band receiver consists of five resonant cavities coupled through irises to a waveguide (see figure). The design specification calls for the filter to provide 70 dB of rejection at frequencies of 7.145 to 7.235 GHz to protect the maser from a 20-kW transmitted signal, while allowing signals received at 8.4 to 8.5 GHz to pass to the maser with no more than 0.5 dB of insertion loss.

To obtain data to start the design procedure, the return loss and the transmission loss of a one-cavity filter were measured as a function of frequency in and about the stopband for several values of the iris diameter (D_I) and cavity length (L_C). With the help of a computer program, these measurements were fit to the response of an equivalent combination of series and parallel inductances and capacitances representing the cavity/waveguide junctions: it is possible to do this because, over narrow frequency bands, cavity/waveguide filters behave like lumped-element resonant circuits.

From the measurements, curves were obtained to show the variation of the band-stop resonant frequency as a function of D_I and L_C. An infinite number of combinations of D_I and L_C give the same resonant frequency. However, the insertion loss and the transmission loss both increase with D_I. Consequently, the optimum combination of D_I and L_C is the one with the smallest D_I that will still provide the required stop-band transmission loss.

The optimum pair of D_I and L_C was selected by the use of the equivalent inductances and capacitances in a computer program that simulated the characteristics of the five-cavity filter. This program also found the optimum cavity spacing (D_C) for each pair of D_I and L_C. The optimum values for the filter were found to be L_C = 0.82 in. (2.08 cm), D_I = 0.78 in. (1.98 cm), and D_C = 1.58 in. (4.01 cm). These values correspond to a resonant frequency of 7.240 GHz. A tuning screw in each cavity enables fine adjustment of the band-stop resonance frequency to the specified value of 7.190 GHz. A tuning screw at each cavity/waveguide junction is used to adjust the

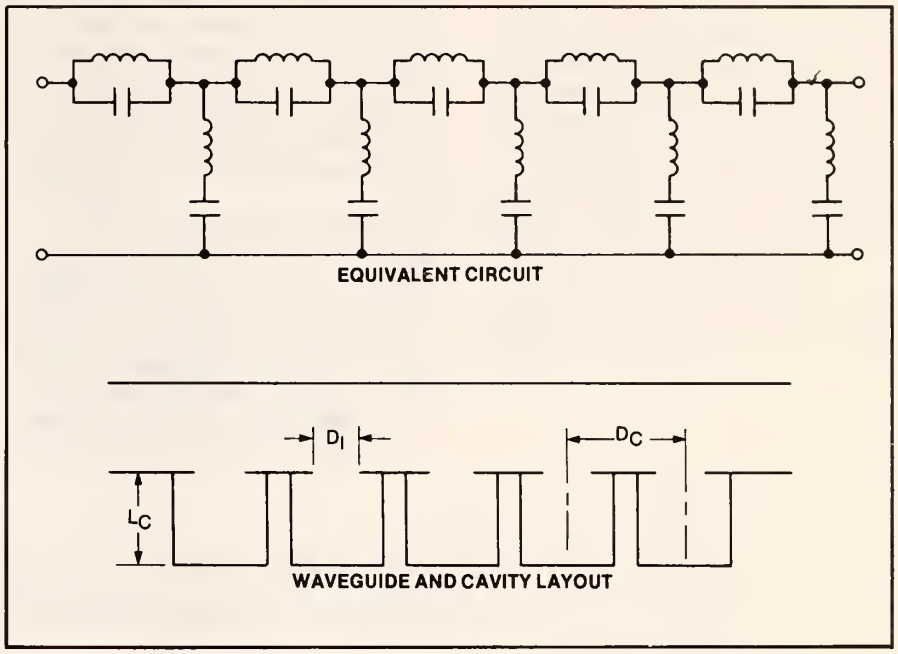

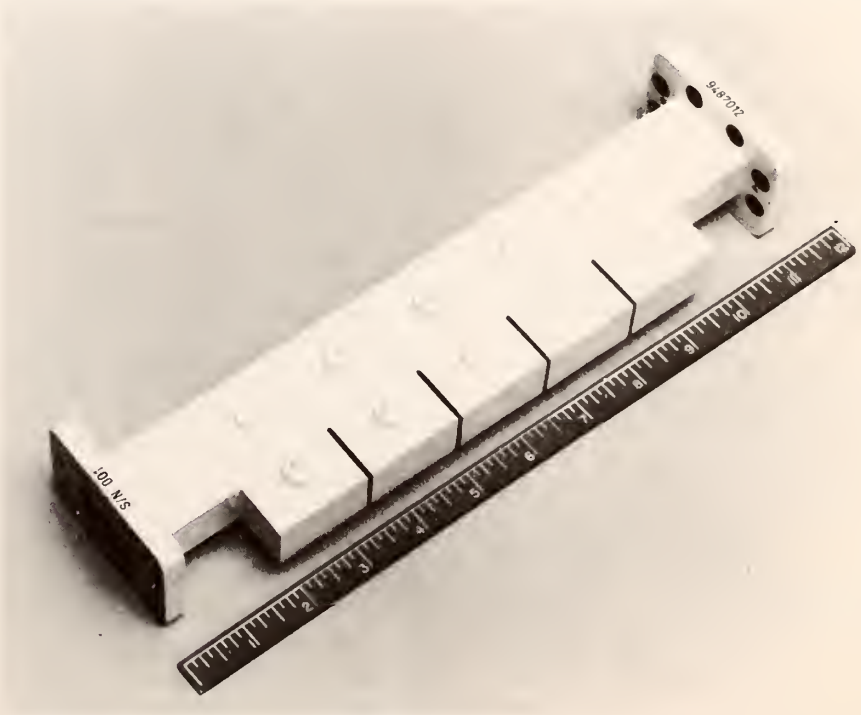

PRODUCTION UNIT

The **Waveguide/Cavity Filter** imitates lumped series and parallel combinations of inductance and capacitance over a narrow stopband centered at 7.190 GHz. The filter is made of standard WR125 waveguide stock.

pass-band voltage standing-wave ratio to no more than the specified maximum of 1.05:1.

This work was done by F. Manshadi of Caltech for **NASA's Jet Propulsion Laboratory**. *NPO-16945 /TN*

FOR ADDITIONAL INFORMATION: *Contact: Director, Technology Transfer Division, P.O. Box 8757, BWI Airport, MD 21240; (301) 621-0100 Ext. 241*

REFER TO THE NUMBER LISTED AT THE END OF THIS ARTICLE

NASA Tech Brief
National Aeronautics and Space Administration
Lyndon B. Johnson Space Center, Houston, Texas

Lightweight Video-Camera Head

A separate optical assembly weighs only 80 grams.

A compact, lightweight video camera head has been constructed by remounting the lens and charge-coupled-device (CCD) image detector from a small commercial video camera in a separate assembly. Such a camera head could be useful in robotics, artificial vision, and vision guidance systems, where minimum size and weight are often important criteria. The camera head was designed to be mounted on the visor of a helmet to monitor the motions of eyes in experiments on vestibulo-ocular reflexes; even the smallest conventional one-piece video camera would have been too massive and bulky for this application.

The camera head measures 41 by 31 by 44 mm and weighs approximately 80 g. The cable that connects the camera head to the camera electronic circuitry is made with a specific wire-bundle twist to reduce line capacitance and to shield against external electromagnetic and radio-frequency interference. The cable can be up to 6 ft (1.8 m) long.

The main camera body and video-synchronization-separator circuit boards are mounted on a 127-by 102-mm mother board. The main camera body contains a power unit and video interface. The genlock and video-synchronization circuits make it easy to connect the camera to existing external television circuitry. The camera requires 12 Vdc at 425 mA.

The CCD image detector is sensitive to radiation from the visible to the near infrared and provides good image contrast. The detector sensitivity peaks at a wavelength of 920 nm. In the visible spectrum, the camera requires a minimum light intensity of 3 lux. A ring-shaped light source that surrounds the lens has been developed to provide uniform infrared and visible illumination over a circular region.

This work was done by David R. Proctor of Technology Inc. for **Johnson Space Center**. *MSC-21246 /TN*

FOR ADDITIONAL INFORMATION: *Contact: Director, Technology Transfer Division, P.O. Box 8757, BWI Airport, MD. 21240; (301) 621-0100 Ext. 241*
REFER TO THE NUMBER LISTED AT THE END OF THE ARTICLE

NASA Tech Brief

National Aeronautics and Space Administration

NASA's Jet Propulsion Laboratory, Pasadena, California

Licensing Opportunity

Programmable Synaptic Arrays for Electronic Neural Networks

High resistances prevent hotspots in parallel input and output operation.

A nonvolatile computer memory combines ultrahigh storage density with extremely-low power dissipation. It can accommodate about 1 billion bits in a square centimeter of surface area. A bit can be written with an expenditure of less than 1 nanojoule of energy and can be read with even lower energy.

The memory was developed for parallel input and output operation such as that in the Hopfield neural network, which is patterned after biological memories. In a neural-network memory, the memorized data do not reside in assigned locations but are widely distributed. The information is found by content rather than by address. Thus, many adjoining memory cells dissipate heat simultaneously as they are read from, and written to, in parallel. Hotspots of excessive dissipation would ordinarily result.

In the new memory, however, the energy released is so small that temperatures stay low even though the cells are densely packed. The cells are thin-film switching elements, the ON resistances of which are high — about 1 MΩ — and the OFF resistances of which are even larger — about 1 GΩ. These extremely high resistances keep current and energy dissipation low when the elements change state.

A cell contains a film of hydrogenated amorphous silicon (or germanium) about 0.2 μm thick sandwiched between a pair of crossed thin-film conducting lines of nickel or indium tin oxide (see figure). A 1-μs voltage pulse applied through the contact changes the resistance of the portion of the film under the contact from $2\times10^9\,\Omega$ to $2\times10^4\,\Omega$, thereby turning ON the portion of the element under the contact.

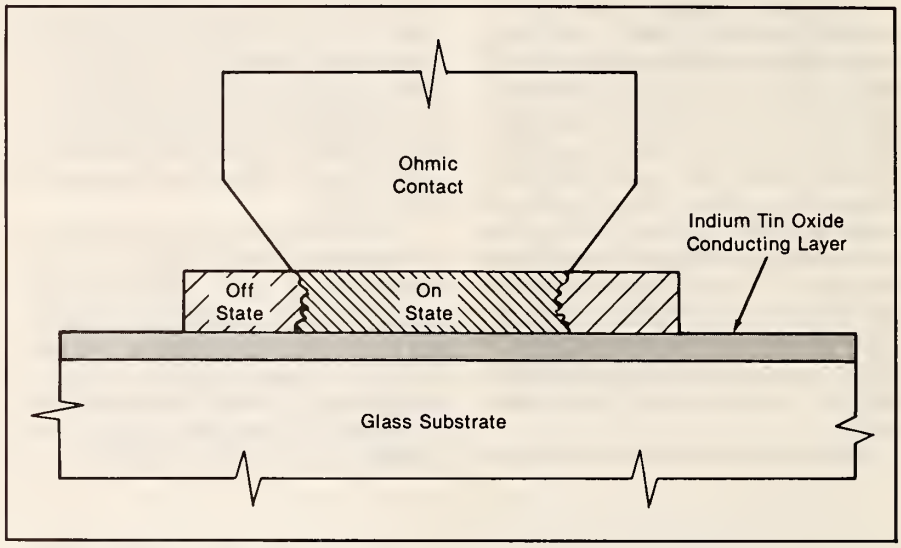

A **Memory Cell** includes an amorphous semiconductor film on a conducting thin-film wire on a glass substrate. An electrical lead makes contact with an area about 1 μm wide on the surface of the amorphous semiconductor film. The thickness of the conducting layer is 0.2 μm.

A large, stable, 1-MΩ thin-film ballast resistor connected in series with each microswitch (synapse) limits the reading and writing current. The resistor ensures that the energy delivered to the semiconductor cell is well controlled and prevents destructive runaway effects.

This work was done by Anilkumar P. Thakoor and John Lambe of Caltech for **NASA's Jet Propulsion Laboratory**.

Title to this invention has been waived under the provisions of the National Aeronautics and Space Act [42 U.S.C. 2457(f)], to the Caltech/JPL. Inquiries concerning licenses for its commercial development should be addressed to

Edward Ansell,
Director of Patents and Licensing
Mail Stop 301-6
California Institute of Technology
1207 East California Boulevard
Pasadena, CA 91125.

Refer to NPO-16674,

Jet Propulsion Lab.
4800 Oak Grove Drive
Pasadena CA 91109

Technology Utilization Mgr.: Norman L. Chaffin
Mail Stop 156-211
(818) 354-2240

NASA Resident Technology Utilization Officer: Gordon S. Chapman
Mail Stop 180-801
(818) 354-4849

Patent Counsel: Paul F. McCaul
Mail Code 180-801
(818) 354-2734

FOR ADDITIONAL INFORMATION: *Contact: Director, Technology Transfer Division, P.O. Box 8757, BWI Airport, MD 21240; (301) 621-0100 Ext. 241*

REFER TO THE NUMBER LISTED AT THE END OF THIS ARTICLE

NASA Tech Brief
National Aeronautics and Space Administration
Lyndon B. Johnson Space Center, Houston, Texas

Public-Facilities Locator for the Blind

An optoelectronic system would enable blind people to find key places without assistance.

A proposed optoelectronic system (see figure) would guide blind people to important locations in public buildings. With the system, a sightless person could easily determine the directions and distances of restrooms, water fountains, stairways, emergency exits, and elevators, for example.

The concept calls for a wall-mounted infrared-pulse transmitter at each of the important locations. A compact circuit worn by the user would receive the infrared signals and convert them to synthetic-voice announcements. The sequence of infrared pulses would be unique for each type of location. The receiver could thus translate a sequence into a specific message in the user's earphone. The loudness of the announcement would increase with the received infrared power, so that the closer the user would come to the location, the louder the announcement would grow.

A 4-bit binary gray code has been tentatively selected for pulse-code-modulating the infrared signal. In this code, three consecutive zeros never occur. The code is easy to implement, and encoding and decoding can each be done by a single silicon integrated-circuit chip.

A transmitter would give out two identifying bursts in rapid sequence — for example, "men's room, men's room" — and would repeat the sequence continually at an even cadence. The repetition rate would be timed so that a person moving at 1 m/s would not miss an announcement when walking through the infrared beam.

In the receiver, codes would be detected by an infrared photodiode and separated by a synchronizing circuit. After decoding, a signal would pass to a shift register having serial input and parallel output. A latching circuit would hold the parallel decoded data briefly before transferring them to a sequence-address read-only memory (ROM).

The ROM would release appropriate phoneme signals to a voice synthesizer. The volume of the amplified synthesizer output would be controlled by an automatic gain controller according to the intensity of the received infrared signal and would thus increase in magnitude with a decrease in the distance to the transmitter. Finally, the synthetic-voice signal would be applied to headphones.

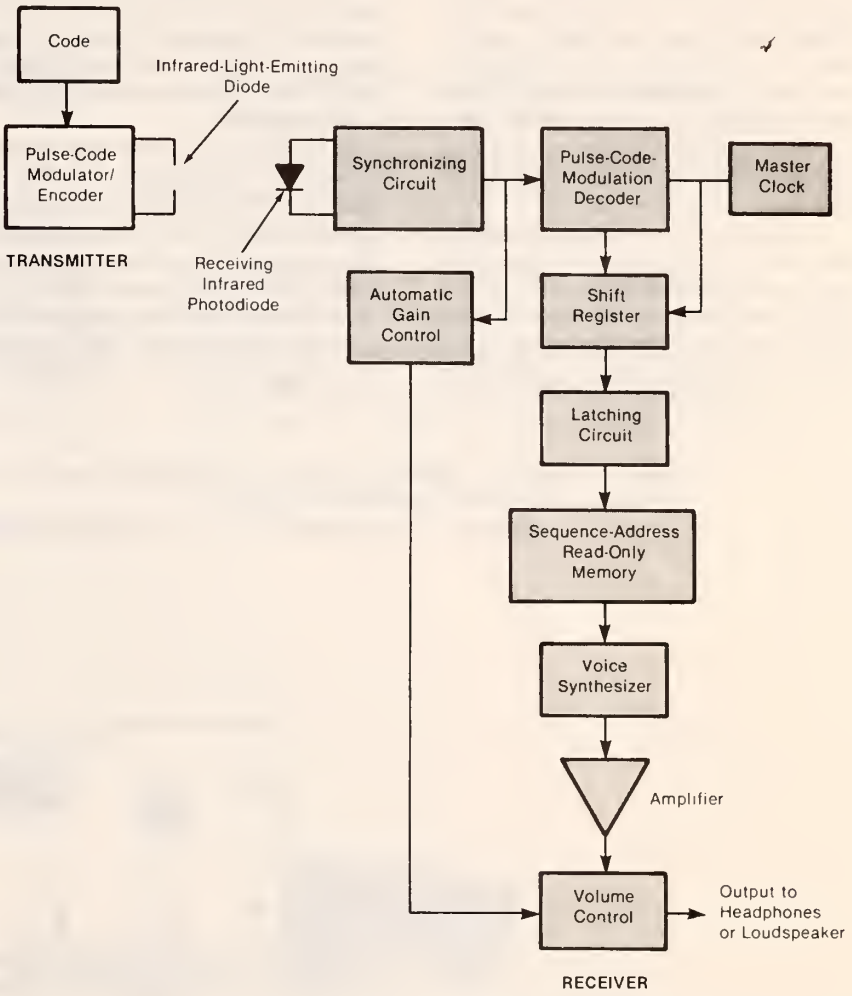

The Circuitry Is Uncomplicated and Inexpensive, in both the transmitter and the receiver. Readily-available light-emitting diodes, photodiodes, and integrated-circuit chips would be used to build the locator aid for the blind.

Infrared is preferable to radio-frequency energy as the transmission medium for several reasons: It does not interfere with other electronic equipment, it fades faster with increasing distance and thus gives a better indication of distance, and it is less subject to noise and errors.

This work was done by Kevin D. Moore of Lockheed Engineering & Management Services Co., Inc., for **Johnson Space Center**. *MSC-21197 /TN*

FOR ADDITIONAL INFORMATION: *Contact: Director, Technology Transfer Division, P.O. Box 8757, BWI Airport, MD. 21240; (301) 621-0100 Ext. 241*
REFER TO THE NUMBER LISTED AT THE END OF THE ARTICLE

NASA Tech Brief
National Aeronautics and Space Administration
NASA's Jet Propulsion Laboratory, Pasadena, California

Three-Waveguide Beam and Polarization Splitter

Different modes are guided to different output ports.

A monolithic ensemble of three waveguides splits an input signal beam into three output beams according to the polarization components. The waveguides are made of titanium diffused in lithium niobate. Before the diffusion step, the titanium is deposited to form an inner (middle) waveguide and outer waveguides on both sides of the inner one.

The gap between each outer waveguide and the inner waveguide is made very small over a predetermined part of the total length. The length of this region of proximity and the size of the gap are selected in conjunction with the diffusion conditions to be used, with a view toward obtaining the desired beam- and polarization-splitting functions. A field plate is placed over each waveguide along at least the portion of its length in the region of proximity to the adjacent waveguide.

In operation, the plates over the outer waveguides are energized with like voltages, while the plate over the inner waveguide is energized with a different voltage. If a signal that has transverse electric and transverse magnetic components is fed into one end of the middle waveguide, then a pure transverse electric signal emerges from the other end of the middle waveguide, while equal transverse magnetic signals emerge from the other ends of the outer waveguides.

This work was done by Gail A. Bogert of AT&T Technologies, Inc., for **NASA's Jet Propulsion Laboratory**.

NPO-16986 /TN

FOR ADDITIONAL INFORMATION: *Contact: Director, Technology Transfer Division, P.O. Box 8757, BWI Airport, MD 21240; (301) 621-0100 Ext. 241*

REFER TO THE NUMBER LISTED AT THE END OF THIS ARTICLE

Oak Ridge National Laboratory

REMOTE SENSOR AND CABLE IDENTIFIER

Key words: Remote sensor; electrical cables; wiring; passive circuits

Large-scale facilities such as nuclear power plants, manufacturing plants, ships, and aircraft are managed by complex electrical control systems. Identifying and connecting the electrical leads in these systems and verifying that the connections are correct are labor-intensive and time-consuming tasks. Typically, a multitude of drawings are required for electricians installing the leads that connect the control room to sensors and actuators throughout the system.

Researchers in the Instrumentation and Controls Division at ORNL have developed a family of small, inexpensive, passive circuits that can be incorporated into sensors, actuators, cable connectors, and other control components (Fig. 1). These circuits provide a means of remote

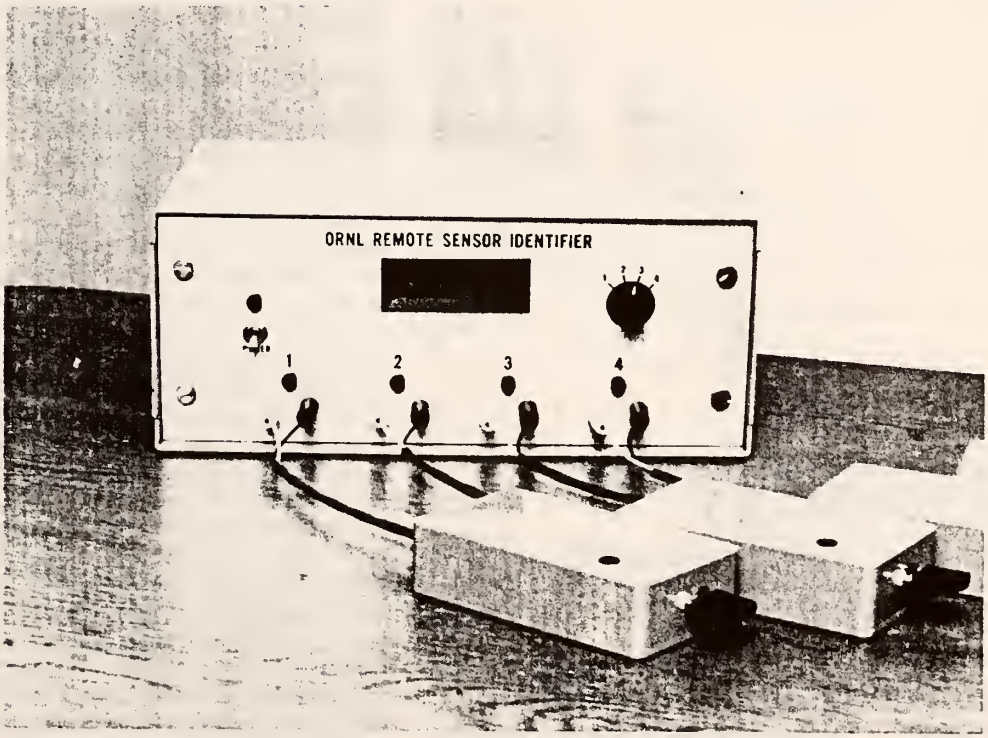

Fig. 1. The remote sensor and cable identifier.

identification of components from a central location. Upon interrogation by the control system, each circuit responds with an identification code unique to the component, and the control system configures itself in response to the existing wiring. After the initialization procedure, the control system can generate its own wiring diagrams, if needed.

The details of these circuits can take several forms and could be designed as an entirely digital integrated-circuit chip. All these circuits include a power converter activated by the interrogating signal, which provides power to the clock, shift register, and electrically alterable read-only memory (EROM). When the converter is powered up by the interrogating signal and when the identifier receives the command to transmit, the identifying bit pattern stored in the EROM is sent from the delay circuit back to the controller.

These unique circuits have several important features.

- They are passive, requiring no internal power supply.
- They can be put on a single large-scale integrated-circuit chip small enough to be incorporated into a component connector.
- They will be inexpensive once the custom chip is designed.
- They can be retrofitted into existing systems cheaply by replacing connectors.
- They can eliminate expensive wiring diagrams.
- They can eliminate wiring errors.

Additional information:

Office of Technology Applications
Information Service
Martin Marietta Energy Systems, Inc.
P.O. Box X
Oak Ridge, TN 37831
Telephone: (615) 574-4192; FTS 624-4192

NASA Tech Brief
National Aeronautics and Space Administration
NASA's Jet Propulsion Laboratory, Pasadena, California

Dual Pilot-Tone Calibration Technique

The signal-to-noise ratio would be increased.

A proposed phase-shift-keying scheme for the radio transmission of digital signals would include two pilot tones, one near each edge of the frequency band (see Figure 1). As in other pilot-tone techniques, the pilot tones would be used to compensate for the effects of multipath fading on the amplitude and phase of the received signal.

The tone-calibration techniques rely on the assumption that the pilot-tone and data components of the transmitted signal are both degraded in the same way by fading. In practice, this is assured by setting the pilot-tone frequencies as close as possible to the data frequency band. After suitable processing, the pilot tones would be used as coherent references in a synchronous data detector to remove the fading phase component and to normalize the fading amplitude component.

By the placement of the pilot tones near the band edges, the dual pilot-tone technique eliminates the guard bands on both sides of a single carrier-frequency pilot tone. Consequently, the data bandwidth and the overall bandwidth can be reduced somewhat. However, near the band edges the pilot tones are more sensitive to frequency shifts and more susceptible to adjacent-channel interference.

A dual-pilot-tone-calibrated receiver is illustrated in Figure 2. The incoming signal is filtered through a bandpass filter. Part of the initially filtered signal z(t), where t = time, is sent to the synchronous detector and part to each of two filters with narrow passbands at the pilot frequencies. The outputs $C_+(t)$ and $C_-(t)$, of the upper and lower tone-frequency filters, respectively, are multiplied to obtain a signal C′(t). This signal includes components at the sum of the two pilot-tone frequencies (which equal twice the carrier frequency f_o) and at the difference between the two pilot-tone frequencies (which equals twice the frequency difference f_p between either pilot tone and the carrier).

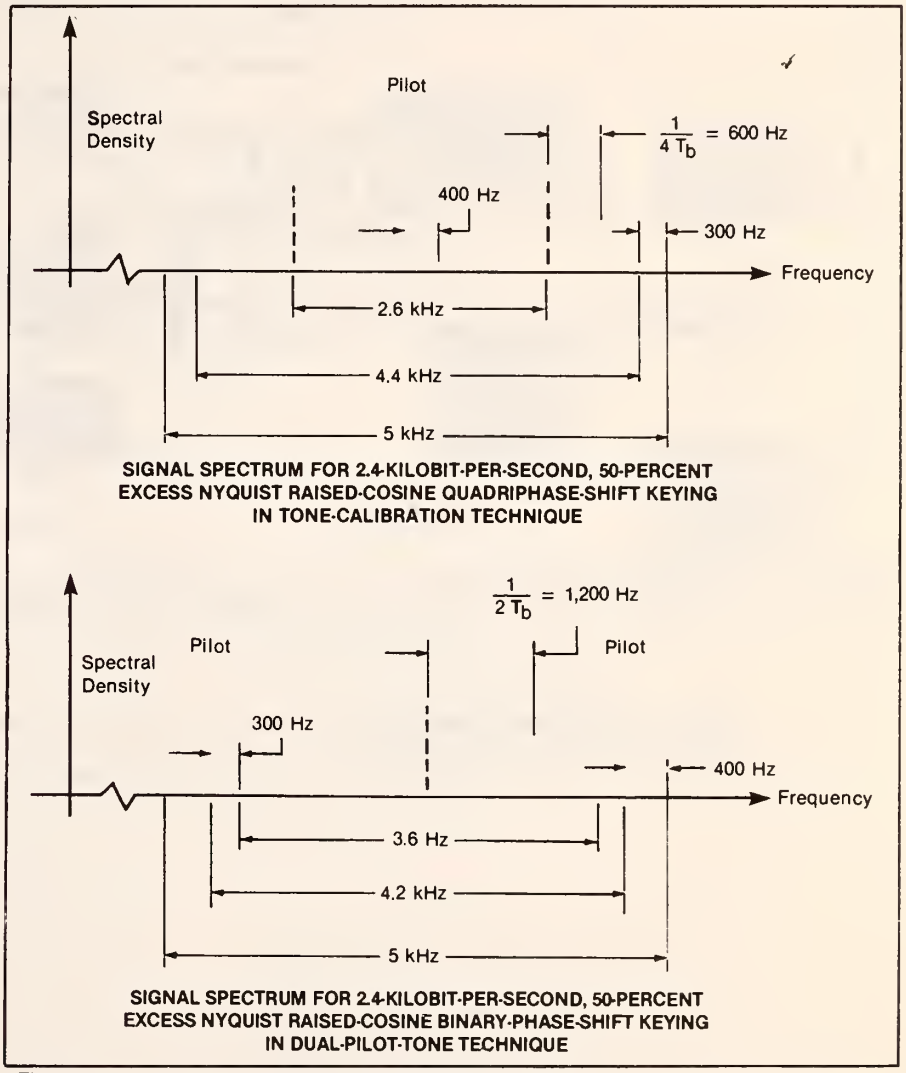

Figure 1. In the **Dual Pilot-Tone Calibration Technique**, two pilot tones are located just outside the sidebands, whereas in an older single-tone method, the pilot tone lies between the sidebands. The bandwidths shown here are typical and for comparison only.

C′(t) is filtered to obtain the $2f_o$ component, which is used in the calibration subsystem, and the $2f_p$ component, which is used in a bit synchronizer. In the calibration subsystem, C′(t) is divided by a squared, low-pass-filtered version of itself to obtain a signal $C_o'(t)$ that has the phase of C′(t) and an amplitude inversely proportional to that of C′(t). $C_o'(t)$ is halved in frequency to obtain $C_o(t)$, which is used to demodulate coher-

ently the bandpass-filtered input.

The dual-pilot-tone technique has been evaluated for various phase-shift keying schemes in terms of the average bit-error probability as a function of the ratio of bit energy to noise spectral density. The calculations show an effective 3-dB improvement in the signal-to-noise ratio, which is likely to overshadow the disadvantages of adjacent-channel interference and frequency offsets.

This work was done by Marvin K. Simon of Caltech for **NASA's Jet Propulsion Laboratory**. *NPO-16930 /TN*

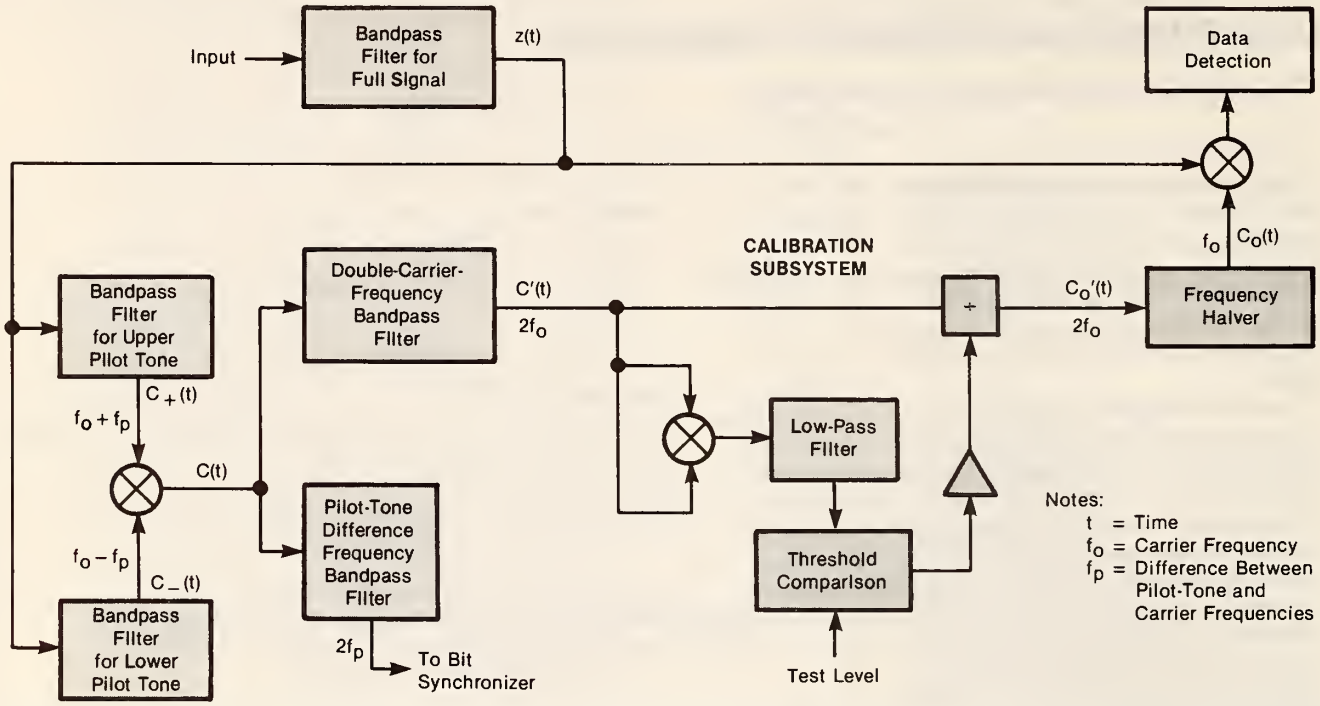

Figure 2. A **Carrier Frequency Is Synthesized** from the two pilot-tone frequencies in the dual-pilot-tone-calibrated receiver. An effective composite carrier signal derived from the pilot tones is used to demodulate coherently the data portion of the received signal.

FOR ADDITIONAL INFORMATION: *Contact: Director, Technology Transfer Division, P.O. Box 8757, BWI Airport, MD. 21240; (301) 621-0100 Ext. 241*

REFER TO THE NUMBER LISTED AT THE END OF THE ARTICLE

Energy

468 Determination of Effects of Atmospheric Contamination on Photovoltaic Cells in Concentrating Systems

469 Monitoring of Residential Groundwater-Source Heat Pumps in the Northeast

470 Vortex Pyrolysis Reactor

471 Molybdenum Resistance Heater

472 Coatings Boost Solar-Cell Outputs — Efficiencies are increased by more-complete utilization of incident light.

473 Long-Life Electrolyte for Nickel/Hydrogen Cells — Decreased initial capacity is more than compensated by increased cycle life.

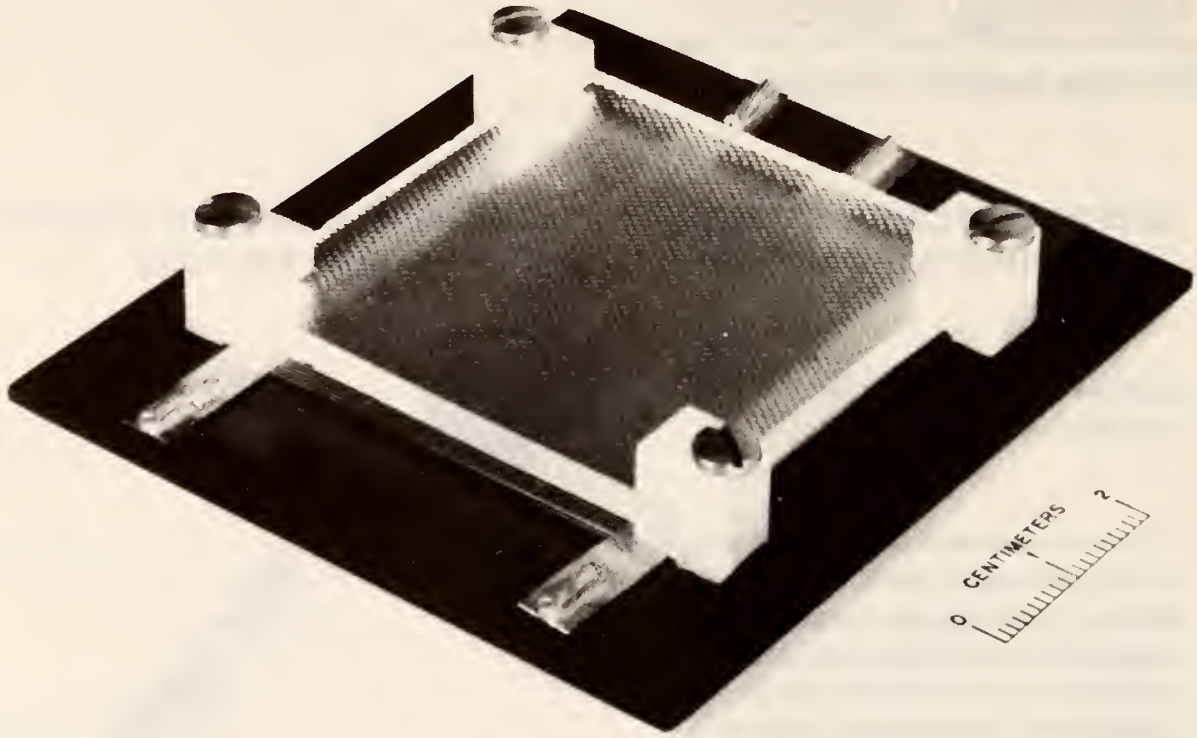

Fig. 2. Cell assembly with cover glass. Spacers created an air gap between the glass and cell assembly.

Additional information:

Office of Technology Applications
Information Service
Martin Marietta Energy Systems, Inc.
P.O. Box X
Oak Ridge, TN 37831
Telephone (615) 574-4192; FTS 624-4192

S. I. Kaplan, *Determination of Effects of Atmospheric Contamination on Photovoltaic Cells in Concentrating Systems,* ORNL/TM-10201, Oak Ridge National Laboratory (December 1986).

Department of Energy

Technology Application

Oak Ridge National Laboratory

MONITORING OF RESIDENTIAL GROUNDWATER-SOURCE HEAT PUMPS IN THE NORTHEAST

Key words: Groundwater; heat pump; residential heating; cooling

Many consumers in the northeastern United States, particularly in rural areas, are considering air-source and groundwater-source heat pumps as alternatives to oil for residential heating. Because both air- and water-source heat pumps are electrically powered, they may be more dependable than oil heating, which relies upon an unpredictable fuel supply. Groundwater-source heat pumps have a further advantage over air-source heat pumps: unlike the air, groundwater retains a constant temperature in all seasons. As space-heating load increases with decreasing outside air temperature, the capacity and efficiency of groundwater-source heat pumps should remain relatively constant.

The report, *Monitoring of Residential Groundwater-Source Heat Pumps in the Northeast: Final Report,* describes a 2-year test of groundwater-source heat pumps for residential heating in the northeastern United States. As part of the DOE/ORNL Building Equipment Research Program, the University of Pittsburgh instrumented and monitored two groundwater-source heat pump systems in central Pennsylvania. These systems were installed and operated by the Allegheny Electric Cooperative, Inc., on a cost-shared basis with the Electric Power Research Institute.

The project team retrofitted these systems into two single-family residences in a rural area of central Pennsylvania that has a 6000-heating-degree-day climate. On-site wells supplied water to the systems at a year-round temperature of about 12°C (54°F). One heat pump was reversible and supplied heating and air-conditioning (Fig. 1); the other was nonreversible and supplied heating only, with a water-to-air heat exchanger added for cooling (Fig. 2). Both systems were monitored to determine their seasonal efficiency and their impact on utility load shapes and to compare their costs with those of other heating systems.

The results of testing these systems indicate that with care in selection and installation, such heat pumps are feasible and highly competitive with oil space heat. Neither system required significant supplemental resistance heat, which indicates that groundwater-source heat pumps are more likely to have a positive influence on winter peak demand and utility load profile than are air-source heat pumps. An adequate water supply is needed, and an appropriate means of water disposition must be provided; well-drilling or water-disposition costs would affect the overall feasibility of using these systems.

Additional information:

For a copy of the report contact:

Office of Technology Applications
Information Service
Martin Marietta Energy Systems, Inc.
P.O. Box X
Oak Ridge, TN 37831
Telephone: (615) 574-4192; FTS 624-4192

R. S. Dougall et al., *Monitoring of Residential Groundwater-Source Heat Pumps in the Northeast: Final Report,* ORNL/Sub/80-7985/1, Oak Ridge National Laboratory (March 1986).

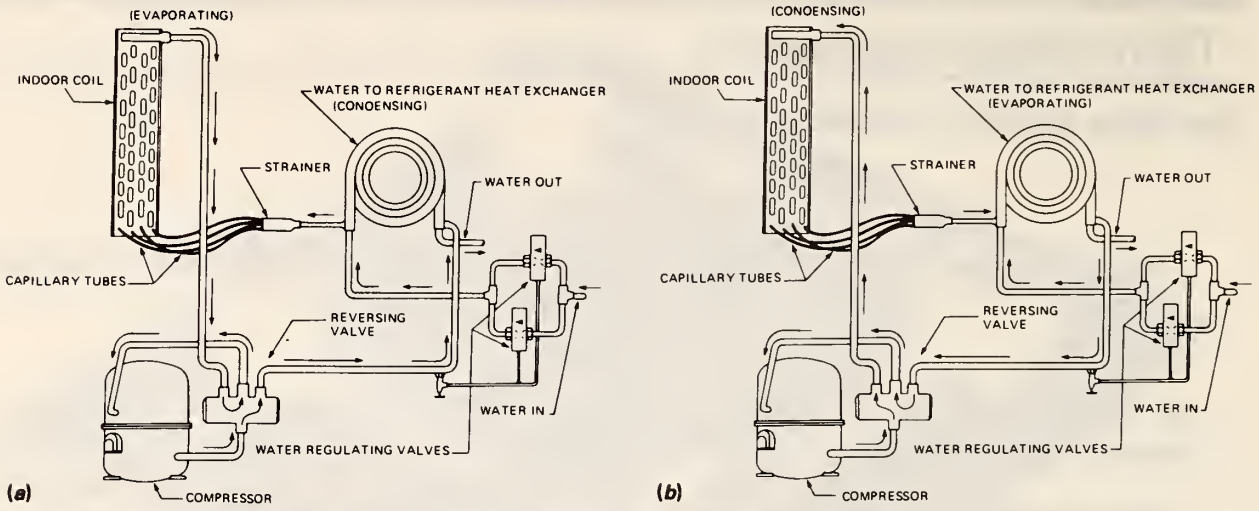

Fig. 1. Reversible groundwater-source heat pump. (*a*) Cooling cycle. (*b*) Heating cycle.

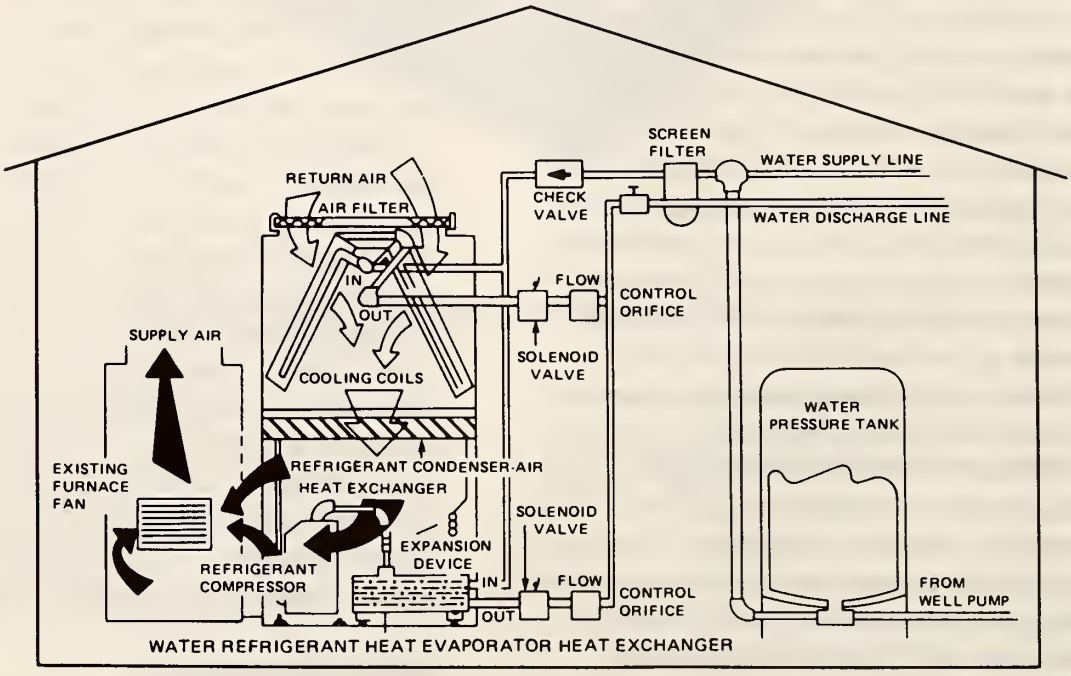

Fig. 2. Heating-only groundwater-source heat pump with direct well-water air-conditioning.

For more information about the research, contact:

R. S. Dougall
School of Engineering
University of Pittsburgh
Pittsburgh, PA 15261

Technology Application

Solar Energy Research Institute

Vortex Pyrolysis Reactor

Background

Organic materials such as agricultural crops and wood represent stored solar energy that can be converted into more convenient fuels. If a practical and economical method for conversion can be developed, these biofuels might supply as much as 20% of current U.S. energy needs.

Thermochemical conversion of biomass into fuel can be accomplished by gasification, liquefaction, or fast pyrolysis. Fast pyrolysis offers an advantage in its rapid production of liquid fuels. In this process, complex molecules are broken into smaller ones by heat in the absence of oxygen. The resulting primary vapors can be condensed into oils with a variety of potential commercial uses.

Conventional fast pyrolysis systems use temperatures as high as 900°C. These high temperatures tend to crack the delicate primary vapors into lower value gases. In addition, high temperatures may cause vapor molecules to rearrange, resulting in pyrolysis tars that are difficult to upgrade into higher value fuels or chemicals. Conventional fast pyrolysis systems therefore may have limited commercial feasibility.

Accomplishments

Researchers at the Solar Energy Research Institute (SERI) have developed an efficient reactor for the rapid conversion of biomass into pyrolysis oils. SERI's unique vortex reactor is ideally suited for fast pyrolysis at low temperatures and short residence times, yielding about 70% oxygenated primary oil vapors by difference (based on elemental balances). Unlike some conventional pyrolysis designs, the SERI reactor can process chipped, granulated, or powdered biomass with little change in operation or yield.

SERI's pyrolysis reactor system achieves short residence times by accelerating biomass particles to high velocities. A gas stream is preheated to temperatures of 400°-750°C at pressures of 0.5-1 MPa; the gas is then accelerated to supersonic velocities by passing it through a small rocket nozzle and expanding it to just above atmospheric pressure. Biomass particles are metered into the gas stream and rapidly accelerated, entering the vortex tube reactor at speeds in excess of 100 m/s.

The gas stream with its

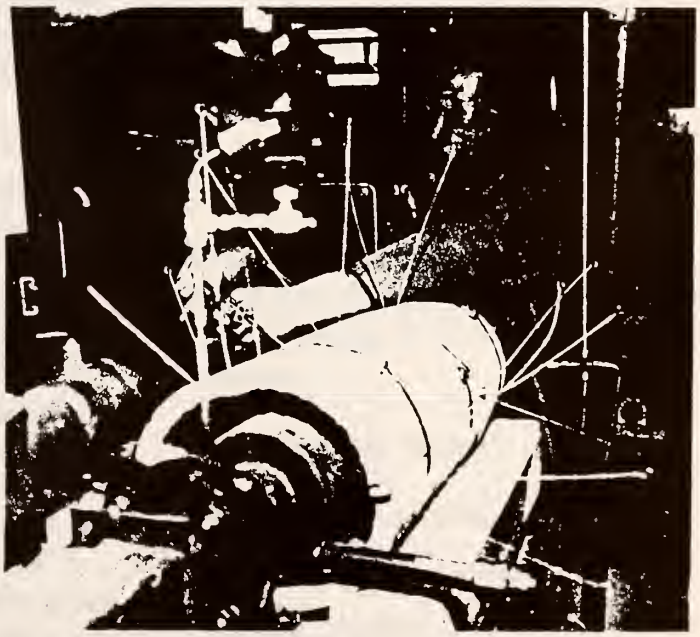

SERI's vortex pyrolysis reactor can process sawdust at a rate of 20 kg/hr; scaled-up reactors may be able to process 250 tons of biomass per day. The Pyrotech Corporation is now developing a prototype commercial reactor system.

entrained biomass enters the specially designed vortex tube through a tangential opening resulting in a cyclonic effect that keeps the fast-moving biomass particles sliding on the heated cylindrical wall. Walls of the tube are heated to 625°C and have a raised helical rib that forces the stream into an unusually tight helical path. Pyrolysis occurs as the particles receive heat fluxes of up to 1000 W/cm².

After passage through the vortex tube, unreacted biomass and large char particles are recycled to the reactor entrance by an internal loop. Recycling continues until particles are reduced to less than 50 μm in size. The entraining gas and vapors then sweep the fine char out of the vortex system and into a hot cyclone separator. At this point, the char is removed and the vapors continue on for collection or further processing prior to condensation.

Researchers have used both hardwood and softwood sawdust in the vortex pyrolysis reactor to produce high oil yields. SERI research is continuing with the pyrolysis of tree bark and the lignocellulosic and plastics portion of municipal solid waste, as well as with the upgrading of sawdust derived oils.

Applications

SERI's vortex pyrolysis reactor may become a practical and economical means to convert biomass into liquid or gaseous fuels. The unique heat transfer mechanism and patented constant-speed feed system may produce high-quality pyrolysis oils at an estimated commercial cost of 5¢/lb. These oils have 75% of the heating value of petroleum on a volumetric basis.

The U.S. Department of Energy is funding SERI studies of three applications of the vortex reactor technology. For the Biofuels and Municipal Waste Division, SERI is investigating the production of high-octane aromatic gasoline from the pyrolysis of wood biomass. For the Energy From Municipal Waste Program, SERI is evaluating the operation of the reactor with feedstock from municipal waste.

In addition, the Office of Industrial Programs is funding both SERI and Colorado State University to develop fast-curing thermosetting adhesives from a phenolics-rich fraction of the pyrolysis oils. Such adhesives have the commercial potential to replace petroleum-derived phenolic resins and expensive resorcinol-based resins currently used in the wood products industry.

Benefits

SERI's vortex reactor achieves its heat transfer rate due to high heat transfer coefficients rather than high temperatures, producing greater quantities of higher quality oils. This process may open the door to large-scale thermoconversion of biomass into high-value liquid fuels.

The resulting vapors take a shorter, faster path through the reactor than the solids do. The shorter exposure of the vapors to a relatively low temperature helps prevent over-cracking and the formation of pyrolysis tars.

Additional Information

Publications

Chum, H.L., et al. (1987). Biomass Pyrolysis Oil Feedstocks for Phenolic Adhesives. *Proceedings of the 194th National Meeting of the American Chemical Society*. New Orleans, Held in August 1987.

Diebold, J., and Scahill, J. (1987). Production of Primary Pyrolysis Oils in a Vortex Reactor. *Preprints of Papers of the Division of Fuel Chemistry, The American Chemical Society*. Vol. 32, No. 2, pp. 21-28.

Diebold, J., and Scahill, J. (1987). Conversion of Wood to Aromatic Gasoline with Zeolite Catalysts. *Proceedings of the Annual AIChE Meeting*. Houston, TX. Held in March 1987.

Patent

Diebold, J., and Scahill, J., Inventors (November 1986). Fluidizing Device for Particulates. U.S. Patent No. 4,620,795. Assignee: U.S. DOE.

Contacts

Business Information: SERI Industry Affairs, (303) 231-7115
Technical Information: SERI Technical Inquiry Service, (303) 231-7303

SERI/SP-260-2734/B-10

Department of Energy

Technology Application

Oak Ridge National Laboratory

MOLYBDENUM RESISTANCE HEATER

Key words: Heater; resistance heater; molybdenum

An inexpensive and expendable molybdenum (Mo) heater can be used as a direct replacement for much more expensive heaters in the smaller commercial resistance-heated furnaces. Normally, such furnaces use tungsten heaters and heat shields to attain temperatures approaching 3000 K (2727°C). The heat shields were replaced with either low-density zirconium oxide block or carbon (C) felt (materials that are commercially available or easy to fabricate with hand tools).

Molybdenum sheeting was used for the resistance heater shown in Fig. 1. Fabrication time for each heater is about 1 h, and each heater costs about 3% of the commercial version. Some experimentation will be needed to adapt the current heater to larger furnaces, mainly in finding the thickness of the molybdenum necessary to provide sufficient current-carrying capacity. In the present version, the temperature difference between the top and bottom of the hot zone was less than 10 K at temperatures up to 2100 K (1827°C). The maximum temperature in the presence of carbon was held at less than the 2483 K (2210°C) eutectic (lowest possible constant melting point) in the molybdenum-carbon (Mo-C) system. The Mo-C interaction at operating temperatures

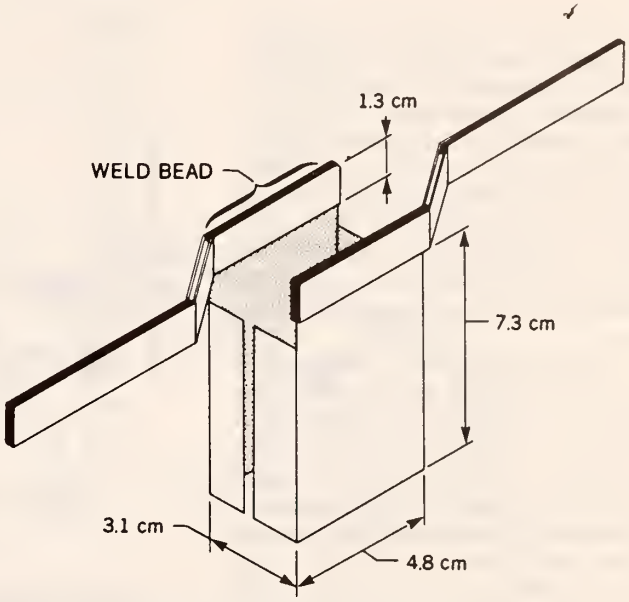

Fig. 1. Molybdenum resistance heating element.

resulted in room-temperature embrittlement, but more than one run was often attained with careful handling of the furnace during sample changes.

Additional information:

Office of Technology Applications
Information Service
Martin Marietta Energy Systems, Inc.
P.O. Box X
Oak Ridge, TN 37831
Telephone: (615) 574-4192; FTS 624-4192

T. B. Lindemer, "Molybdenum Resistance Heater," *Rev. Sci. Instrum.* **58**(8), 1533 (August 1987).

NASA Tech Brief
National Aeronautics and Space Administration
NASA's Jet Propulsion Laboratory, Pasadena, California

Coatings Boost Solar-Cell Outputs

Efficiencies are increased by more-complete utilization of incident light.

The electrical outputs of thin solar photovoltaic cells made of dendritic-web silicon are increased by a combination of front-surface, antireflective coatings and back-surface, reflective coatings. Although the use of such coatings is well established, improvements have been achieved recently through theoretical and experimental studies of ways to optimize the coatings for the particular wavelengths of incident light, cell thicknesses, and cell materials.

If the thickness of the cell is less than or comparable to the photon-absorption length, then an appreciable fraction of the incident light reaches the back surface unused. For example, at wavelengths greater than 0.9 μm, a 125-μm-thick dendritic-web-silicon cell absorbs only 93 percent of the usable photons. In that case, a back-surface reflective coating sends unused light back into the cell, enabling more of it to be converted to electrical energy on the second pass.

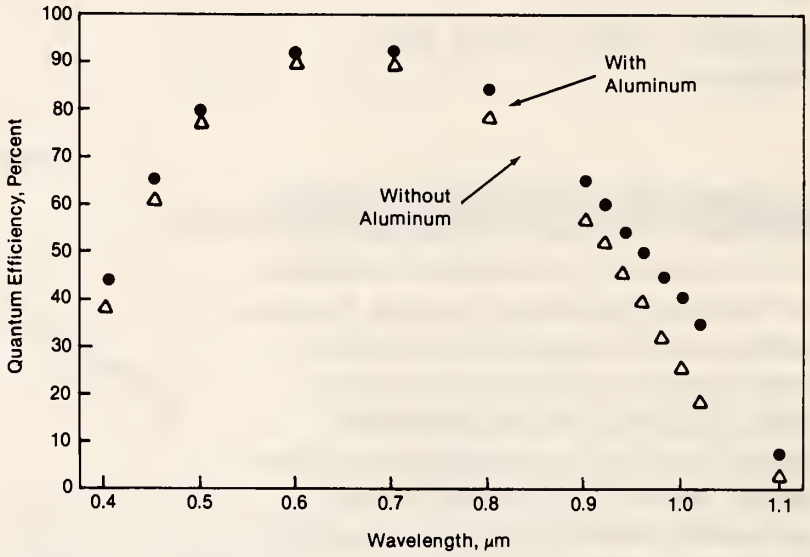

The **Internal Quantum Efficiency** of a photovoltaic cell is increased by the use of a more-reflective back-surface contact made with aluminum.

The Ti/Pd/Ag back metal ordinarily used on solar cells is a poor reflector of photons with wavelengths greater than 0.9 μm. However, aluminum reflects 90 to 95 percent at these wavelengths, and a reflective back-surface contact can be made of Al/Ti/Pd/Ag. Measurements of the output of a cell at visible and near-infrared wavelengths showed that the inclusion of aluminum in the back-surface coating produces a small increase in efficiency (see figure).

The front antireflection coating increases the cell output further by enabling more light to enter the cell. According to calculations, an improved antireflection coating can be made by thermally evaporating a 548-Å layer of ZnSe, followed by a 1,040-Å layer of MgF_2, on the bare silicon surface. If the cell has a passivating surface layer of silicon dioxide, then the layer thicknesses must be changed to 398 Å and 1,080 Å, respectively. With these thicknesses, the predicted increase in short-circuit cell current is 51.7 percent. Experiments with coated cells showed increases of as much as 50 percent. The discrepancy between the prediction and the measurements is probably due to absorption in the ZnSe film.

This work was done by Ajeet Rohatgi, Robert B. Campbell, T. W. O'Keefe, Posenjit Rai-Choudbury, and Richard A. Hoffman of Westinghouse Electric Corp. for **NASA's Jet Propulsion Laboratory**. *NPO-16819 /TN*

FOR ADDITIONAL INFORMATION: *Contact: Director, Technology Transfer Division, P.O. Box 8757, BWI Airport, MD 21240; (301) 621-0100 Ext. 241*

REFER TO THE NUMBER LISTED AT THE END OF THIS ARTICLE

NASA Tech Brief
National Aeronautics and Space Administration
Lewis Research Center, Cleveland, Ohio

Long-Life Electrolyte for Nickel/Hydrogen Cells

Decreased initial capacity is more than compensated by increased cycle life.

State-of-the-art nickel/hydrogen cells use electrolytes containing 31 percent KOH. It is known that the cell capacity decreases as the concentration is decreased from this value and increases as the concentration is increased. Because of this observation, the recommendation had been to increase the electrolyte concentration in the cell.

However, experiments have shown a surprisingly substantial increase of cycle life of nickel/hydrogen cells when the KOH concentration in the electrolytes was decreased from the industry standard of 31 percent, while the life was decreased when the concentration was increased. This discovery is particularly important in view of the prior recommendation to increase the concentration to increase the cell capacity. The benefit of the increase of the cycle life as the concentration is decreased is expected to outweigh the reduction of the capacity at the beginning of life.

Life tests were carried out at 23 °C, using nickel/hydrogen boilerplate cells containing flight-type nickel electrodes and electrolyte of various KOH concentrations (21, 26, 31, and 36 percent). The regime of the life test was a continuous cycling by 17.5-min discharge at the 2.74-C rate and 27.5-min recharge at the 1.92-C rate, resulting in a charge/discharge ratio of 1.10 and a depth of discharge of 80 percent of the rated capaci-

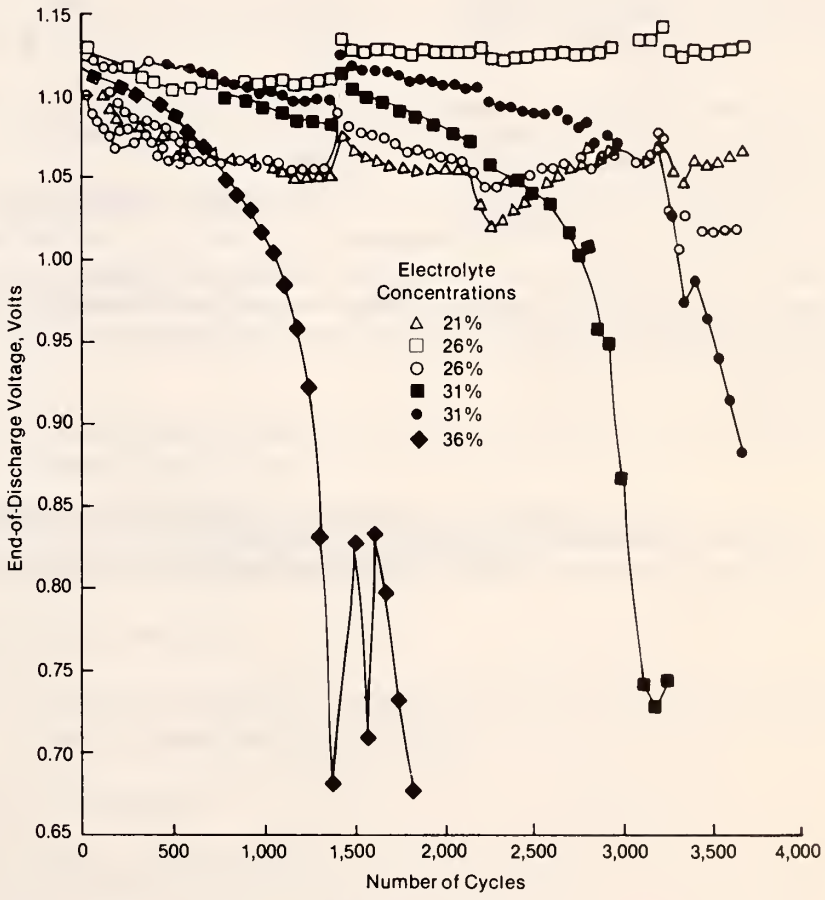

Figure 1. The **End-of-Discharge Voltages** were measured after repeated charge/discharge

ty. The results of this life test to date are summarized in Figures 1 and 2.

The test cells with 36 and 31 percent KOH failed by low end-of-discharge voltage of 0.9 V after 1,300 and 3,300 cycles on the average, respectively, as shown in Figure 1, while the cells with lower KOH concentrations exceeded those lifetimes. The cell capacities at various life cycles are shown in Figure 2. The initial capacity decreased as the KOH concentration was decreased. However, the capacity change (decrease) with cycling was also reduced as the KOH concentration was decreased. This benefit appears to outweigh the initial capacity loss in many applications.

High cycle life is critically important for nickel/hydrogen cells, especially for a low-Earth-orbit satellite application where 6,000 cycles are typically required per year. The high cycle life can also be traded into low battery weight by operating the battery at an increased depth of discharge. High cycle life is also important for such terrestrial applications as electrical vehicles and aircraft.

This work was done by H. S. Lim and S. A. Verzwyvelt of Hughes Aircraft Co. for **Lewis Research Center**. *Further information may be found in A86-24802, "KOH Concentration Effect on the Cycle Life of Nickel-Hydrogen Cells."*

Copies may be purchased from AIAA Technical Information Service Library 555 West 57th Street, New York, New York 10019 Telephone No. (212) 247-6500.
LEW-14301 /TN

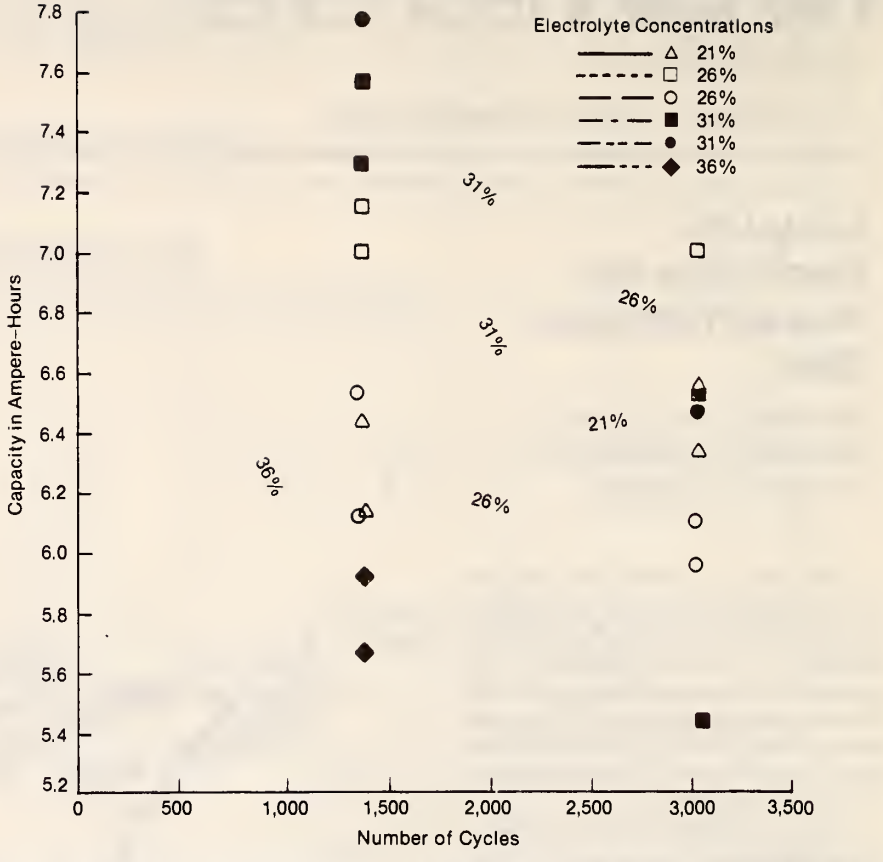

Figure 2. The **Charge Capacities** of cells were measured after repeated charge/discharge cycles. The electrolyte concentrations are the same as those of Figure 1.

FOR ADDITIONAL INFORMATION: *Contact: Director, Technology Transfer Division, P.O. Box 8757, BWI Airport, MD 21240; (301) 621-0100 Ext. 241*
REFER TO THE NUMBER LISTED AT THE END OF THIS ARTICLE

Engineering

474 Rototicon: Real-Time Control for an Autonomous Mobile Robot

475 Snail Cryopump

476 Advanced Numerical Methods for Ship Hydrodynamic Design

477 Lightweight Glass-Reinforced Plastic Deckhouse Panel Concept Developed

478 Computer-Aided Design of Turbine Blades and Vanes — Analysis and design procedures lead quickly to an efficient and strong final design.

479 Cover for Duct Expansion Joint — The size ad shape fo the cover reduces stress and increases strength. (Licensing Opportunity)

480 Estimating the Crack-Extension-Resistance Curve — The curve can not be obtained from residual strength data alone.

481 Failure-Time Distribution of an *m*-Out-of-*n* System — Formulas for reliability are extended to more general cases.

482 Stiffness Properties of Laminated Graphite/Epoxy Cylinders — The dominant constituent property is the longitudinal Young's Modulus of the fibers.

483 Wet-Atmosphere Generator — The water content in a gas is controlled. (Licensing Opportunity)

484 "Thumball" Auxiliary Data-Input Device — A track-ball-type device is mounted on a joystick operated by a thumb. (Licensing Opportunity)

Testing & Instrumentation

485 Sensor-Failure Simulator — Outputs of defective sensors are simulated or studies of reliability of control systems.

Other Items of Interest

470 Vortex Pyrolysis Reactor

Department of Energy

Technology Application

Oak Ridge National Laboratory

ARTIFICIAL INTELLIGENCE, ROBOTICS, AND MANUFACTURING PROCESSES

ROBOTICON: REAL-TIME CONTROL FOR AN AUTONOMOUS MOBILE ROBOT

Key words: Robotics; expert system; control

The research team at ORNL's Center for Engineering Systems Advanced Research (CESAR) has developed an expert system for the control of an autonomous mobile robot. This expert system, called ROBOTICON, was developed for use with the HERMIES-IIB, which is being tested for use in surveillance, diagnosis, and repair work in hazardous environments (Fig. 1).

ROBOTICON controls the actions of the HERMIES-IIB in real time and with a set of user-specified rules that are conveniently entered into the program with the help of a menu-driven graphics interface. Most other commercially available expert systems do not work in real time. The data bases of most standard commercial expert systems are static. Existing systems have not been used to control processes but have operated in an advisory mode only. ROBOTICON contains a dynamic data base and actually controls the robot's actions.

Industry and research laboratories in several countries are developing autonomous robots that will have an enormous impact on industry as well as on other human endeavors, such as space exploration and the exploitation of underwater resources. Autonomous robots have the potential to reduce the risk associated with work in dangerous environments and to eliminate human error and fatigue. The ROBOTICON expert system

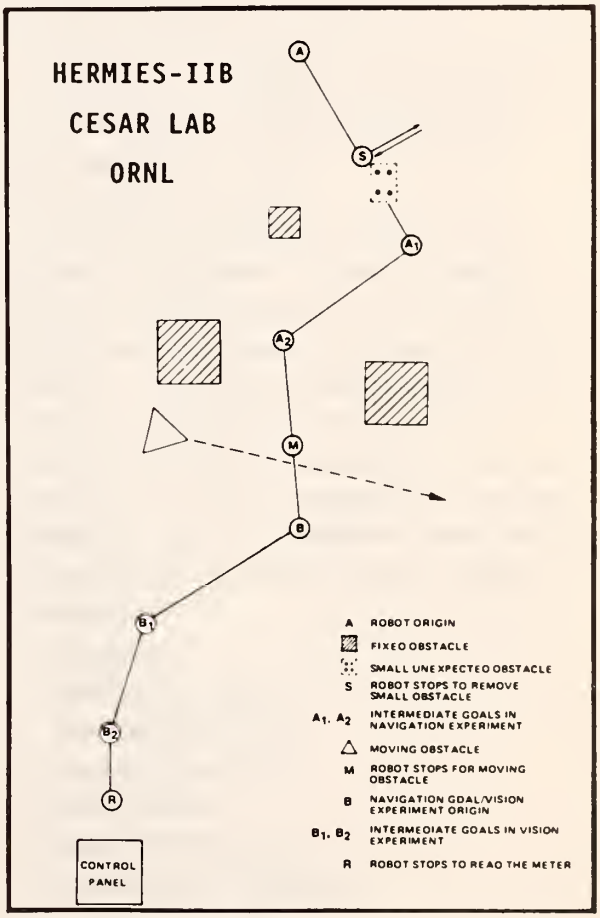

Fig. 1. Layout of the experimental area for HERMIES-IIB. The robot navigates from point A to point B, stopping at intermediate goals A_1 and A_2, and responding to dynamic obstacles at points S and M. The robot moves from point B to the control panel, stopping at intermediate goals B_1 and B_2. At point R the robot is close enough to read a meter on the control panel.

provides an excellent human-machine interface for enabling humans to understand and control autonomous robots because it allows the robot to explain what it is doing and why. It also provides a convenient tool for the robot to learn a better way to do its tasks.

This system could be used for the real-time control of any autonomous system, such as an automated vehicle or industrial plant, provided the sensors and effectors of that system are compatible with the ROBOTICON software.

Additional information:

Office of Technology Applications
Information Service
Martin Marietta Energy Systems, Inc.
P.O. Box X
Oak Ridge, TN 37831
Telephone: (615) 574-4192; FTS 624-4192

Charles Weisbin, Gerard de Saussure, and David Kammer, "Self-Controlled: A Real-Time Expert System for an Autonomous Mobile Robot," *Computers in Mechanical Engineering* **5**(2), 12-19 (September 1986).

B. L. Burks et al., "Autonomous Navigation, Exploration, and Recognition Using the HERMIES-IIB Robot," *IEEE Expert: Intelligent Systems and Their Applications* **2**(4), 18-27 (Winter 1987).

Department of Energy

Technology Application

Oak Ridge National Laboratory

SNAIL CRYOPUMP

Key words: Cryopump; continuous regeneration; semiconductor processing; sputtering; plasma ion etching; molecular beam epitaxy; ion-beam lithography; optical coating; plasma metalizing; chemical-vapor deposition; fusion energy; cryosorption

Many scientific and industrial processes require a controlled vacuum environment that must be free of contaminants and must be flushed continuously with a working gas. In many instances, these gases may be highly corrosive or radioactive. Vacuum pumps are used to evacuate such chambers and to maintain a low pressure during the working process. Cryopumps, which freeze out the process gases, are desirable because they can pump at high rates of speed and because they do not introduce contaminants into the working gases. Typically, however, a cryopump cannot be run continuously at high throughput because the gases rapidly form a thick frost layer on the pump's walls. A regeneration cycle is necessary to remove these solid deposits.

The snail cryopump, a clean, all-metal dry vacuum pump, can operate continuously at high pumping speeds (1600 L/s) and at a sustained high inlet pressure (up to 1 Torr). The "snail" is a cleansing device that resides within the pump and, like its namesake, clears deposits from the walls over which it passes (Fig. 1) while the pump is in full operation. The snail is a motor-driven regenerator that follows a helical path over the cylindrical wall of the cryopump. The snail has two designs: one is a mechanical scraper; the other is heated to melt the deposits that it encounters. Each is held against the wall of the pump by a heated, spring-loaded bellows, which is attached to a forepump that evacuates the loosened deposits. Because of the snail, this cryopump design does not require chronic shutdown for defrosting.

The snail cryopump was designed by the Fusion Energy Division at ORNL for pumping deuterium and hydrogen gas in the cryogenic pellet-fueling gun used to refuel tokamak fusion reactors. It is also a significant addition to the entire vacuum industry, which depends on cryopumps for clean, high-speed pumping. For example, the following semiconductor thin-film processes require the cleanliness, speed, and high throughput that the snail cryopump provides continuously:

- sputtering,
- plasma ion etching,
- molecular beam epitaxy,
- ion-beam lithography,
- optical coating,
- plasma metalizing, and
- chemical-vapor deposition.

The snail concept can be further developed to regenerate cryosorption-type cryopumps. For example, it could continuously form and regenerate cryosorption surfaces of condensed gases (a technique used to pump helium)

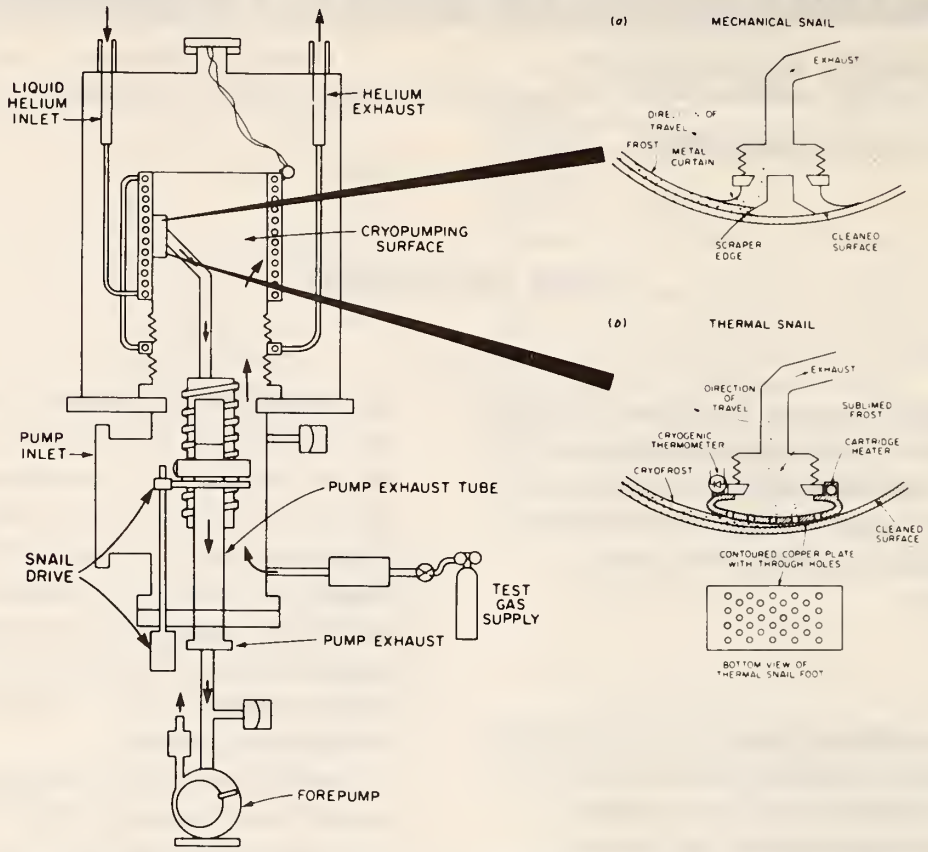

Fig. 1. The snail cryopump and two optional snail designs, *(a)* the mechanical snail and *(b)* the thermal snail.

Additional information:

Office of Technology Applications
Information Service
Martin Marietta Energy Systems, Inc.
P.O. Box X
Oak Ridge, TN 37831-6257
Telephone (615) 574-4192; FTS 624-4192

C. A. Foster, "High-Throughput Continuous Cryopump," *J. Vac. Sci. Technol. A* **5**, 2558-62 (July/August 1987).

Advanced Numerical Methods for Ship Hydrodynamic Design

In recent years, the David Taylor Naval Ship R&D Center has focused on the development of mathematical and numerical methods for the solution of the equations describing the flow about a ship as it moves through the water.

Traditionally, these equations could be solved only approximately because of their formidable nature. As a result, analytical techniques could play only a minor role in the design process. Many of the challenges which had to be overcome originated in the complicated nature of many naval geometrics and flows, including the need to deal with the difficult mathematical boundary condition at the water surface. The new methods developed, including efficient algorithms for making use of the latest supercomputer power, have successfully met many of the challenges and allow the economical computation of such quantities as water velocities, wave elevations, and pressure values at thousands of points on and near ship hulls. This capability now allows both ship designers and ship hydrodynamics researchers to use a complimentary approach involving computations as well as model tests.

One excellent example of a product of this research which has already made an impact on ship design is the XYZ Free Surface (XYZFS) Program. This program can compute the wave resistance and three-dimensional flow field of realistic ship hulls. Since 1977, XYZFS has been used to analyze more than 100 ships ranging from a low-speed tanker to high-speed destroyers.

For Additional Information:

Backup material on this effort is available from:

Navy Domestic Technology Fact Sheet
Reader Reply Service
Code E211
Naval Surface Weapons Center
Dahlgren, VA 22448-5000
(703) 663-8921

Refer to 120803/TN

Lightweight Glass-reinforced Plastic Deckhouse Panel Concept Developed

In recent years, the David Taylor Research Center has focused on the development of glass-reinforced plastic (GRP) concepts for ship deckhouse applications. The Use of GRP has a number of advantages: a weight reduction of approximately 40 percent relative to conventional steel deckhouses; reduced lifecycle maintenance costs through improved fatigue reliability; and the potential for enhanced survivability.

To realize these advantages, a lightweight GRP deckhouse panel concept has been developed and evaluated. The hat-stiffened GRP panel concept, including panel-to-panel joint details, evolved from in-house analytical and experimental investigations of a series of panel geometries.

The panel, manufactured by Brunswick Corporation, was manually laid-up from E-glass and flame-retardant isophthalic polyester resin, and autoclave-cured. The autoclave cure was intended to simulate future low-cost, high-quality automatic production processes. This process resulted in GRP panel strength properties more than twice those attainable with the traditional, room temperature cure/boat building processes.

The GRP panel with joint details was structurally tested in May 1987 at White Sands Missile Range. During this test, the all-GRP 8-ft x 15-ft deckhouse panel was blast-tested side by side with a heavier GRP/steel panel. Both panels behaved well.

For Additional Information:

Backup material on this effort is available from:

Navy Domestic Technology Fact Sheet
Reader Reply Service
Code E211
Naval Surface Weapons Center
Dahlgren, VA 22448-5000
(703) 663-8921

Refer to 121003/TN

NASA Tech Brief
National Aeronautics and Space Administration
Marshall Space Flight Center, Alabama

Computer-Aided Design of Turbine Blades and Vanes

Analysis and design procedures lead quickly to an efficient and strong final design.

A quasi-three-dimensional method for determining the aerothermodynamic configuration of a turbine uses computer-interactive analysis and design and computer-interactive graphics. The design procedure can be executed rapidly so that the designer can easily repeat it to arrive at the best performance, size, structural integrity, and engine life.

The engine-balance calculation establishes the overall turbine specifications, which are fed to a two-dimensional gas-path program for preliminary evaluation (see figure). This interactive program enables the designer to alter various design parameters iteratively while adhering to constraints imposed by the operating conditions of the common-shaft pump. Such parasitic losses as those of incidence, diffusion, leakage, and tip clearance are evaluated, and the overall turbine efficiency is predicted.

The designer uses the two-dimensional configuration from the gas-path program in a quasi-three-dimensional program to analyze the streamline-curvature flow field. This program establishes the meridional stream-surface locations and the characteristics of the associated velocity and pressure fields. At first, the designer enters only the inlet and outlet data for the rotor blades and stator vanes — such data as flow angles and edge thicknesses and locations — and the distributions of efficiencies or loss coefficients for the blades and vanes. The initial run gives an overall picture of the approximate flow field.

In succeeding trials, the designer enters the estimated blade-thickness distribution, axial chord, and other blade-profile parameters; the blade-stacking angles; the flow angles; the end-wall contours; and the axial locations of blades and vanes. The designer analyzes the reactions, radial loading distributions, and secondary flow effects

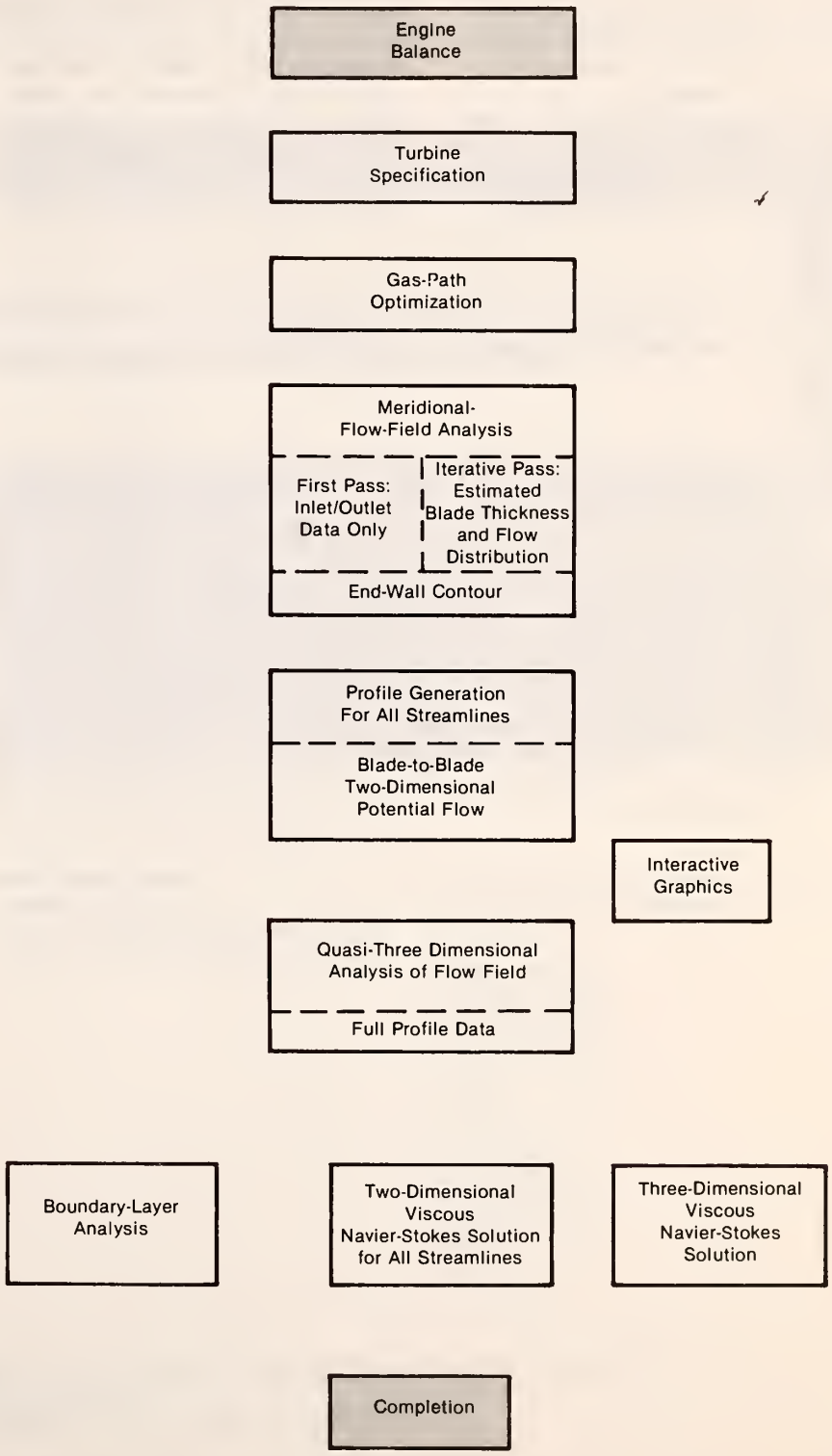

The **Sequence of Events in Aerothermodynamic Analysis and Design** starts with the engine-balance equations and ends with boundary-layer analysis and viscous-flow calculations. The analysis-and-design procedure is interactive and iterative throughout.

and eventually finds a preliminary optimized meridional configuration.

The next task is to generate the final blade profiles on various streamlines. The designer uses a program that determines the velocity and pressure distributions over the full blade profile along a streamline. By variation of the blade-coordinate distribution from the inlet to the outlet, the load distribution can be adjusted to achieve an optimum design. The results are displayed on a screen so that the designer can examine them immediately.

When all the profiles show acceptable loading characteristics, the profile data are transferred to a program for hub-to-tip analysis and another program for blade-to-blade analysis. The two programs interact to provide the quasi-three-dimensional analysis of the flow field. The blade-profile-generation and flow-field-analysis steps are repeated as many times as necessary to achieve the required blade characteristics.

Meanwhile, the designer can evaluate the blade and vane stackings with three-dimensional interactive graphics. The designer considers various stacking options and reviews the continuity of blade and vane surfaces, streamline-surface cross sections, and three-dimensional perspective views. (A stress-analysis engineer should become involved at this point to guide the choices of stacking, lean angles, and profile-thickness distribution to achieve a suitable stress distribution.)

Finally, a boundary-layer-analysis program is executed on the streamline profiles to ensure that flow is stable throughout the turbine, and viscous Navier-Stokes equations are solved — a time-consuming procedure carried out only when the design is close to completion.

This work was done by Wayne Q. Hsu of Rockwell International Corp. for **Marshall Space Flight Center**. *MFS-29265 /TN*

FOR ADDITIONAL INFORMATION: *Contact: Director, Technology Transfer Division, P.O. Box 8757, BWI Airport, MD 21240; (301) 621-0100 Ext. 241*

REFER TO THE NUMBER LISTED AT THE END OF THIS ARTICLE

NASA Tech Brief
National Aeronautics and Space Administration
Marshall Space Flight Center, Alabama

Licensing Opportunity

Cover for Duct Expansion Joint

The size and shape of the cover reduces stress and increases strength.

A cover for expansion joints on ductwork seals tightly while accommodating the movement of a joint. The cover provides ample bonding area on both members of a joint.

The cover (see figure) is molded from silicone resin in an omega-shaped cross section. The resin is reinforced with glass fibers or, preferably, with Kevlar (or equivalent) aromatic polyamid. The cross section allows the cover to flex readily with the contraction or expansion of the joint, without applying a peeling stress to the bonded edges — a stress mode in which the silicone adhesive is weakest.

The molding die is circular, with radius equal to that of the duct on which the cover will be installed. This ensures that the cover edges will lie flat on the duct.

The cover was developed as a replacement for a flat, glass-reinforced cover for a cryogenic fuel duct on the Space Shuttle. The tape tended to apply a peel stress to the adhesive when the joint contracted. Moreover, the tape provided a bond area only ½ in. (1.3 cm) wide on each element of the joint. The new cover not only reduces peeling stresses but provides a ¾-in. (1.9-cm) bond width on each edge.

This work was done by A. R. Brown of Rockwell International Corp. for **Marshall Space Flight Center**. *No further documentation is available.*

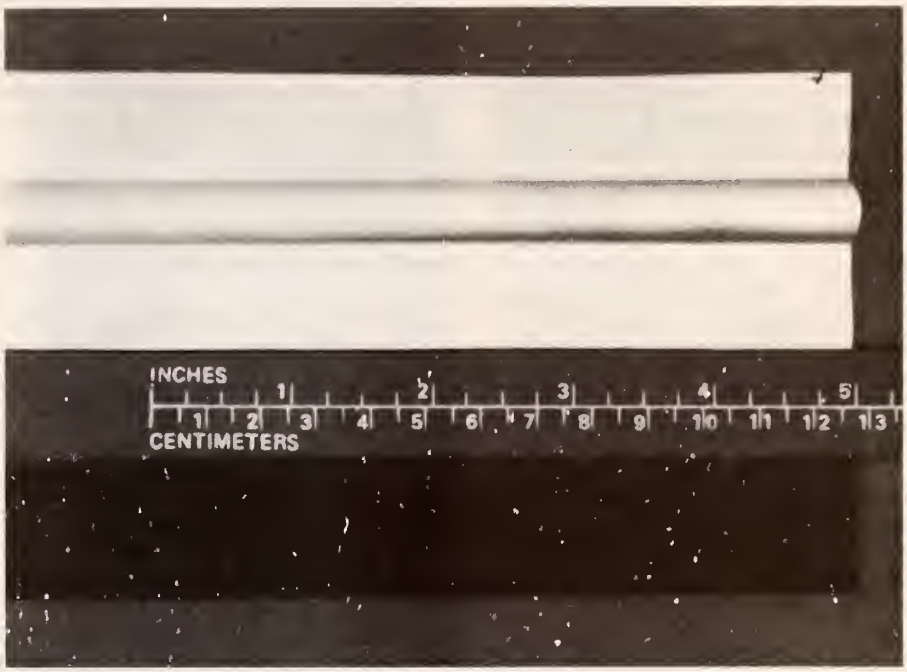

The **Edges of an Omega-Shaped Cover** fit on the opposing members of an expansion joint. The arch of the omega takes up expansion and contraction without unduly stressing the adhesive bonds on the joint members.

Inquiries concerning rights for the commercial use of this invention should be addressed to the Patent Counsel, Marshall Space Flight Center Refer to MFS-29189 /TN

George C. Marshall Space Flight Center
Technology Utilization Officer: Ismail Akbay
Code AT01
Marshall Space Flight Center,
AL 35812
(205) 544-2223
Patent Counsel:
Leon D. Wofford, Jr
Mail Code CC01
Marshall Space Flight Center,
AL 35812
(205) 544-0024

FOR ADDITIONAL INFORMATION: *Contact: Director, Technology Transfer Division, P.O. Box 8757, BWI Airport, MD 21240; (301) 621-0100 Ext. 241*
REFER TO THE NUMBER LISTED AT THE END OF THIS ARTICLE

NASA Tech Brief
National Aeronautics and Space Administration

Estimating the Crack-Extension-Resistance Curve

The curve can now be obtained from residual-strength data alone.

A new analytical method enhances the capability to determine the crack-extension curve or "R-curve" of a sample. One of the most powerful techniques available to an analyst of fractures of materials, the "R-curve" can be used to predict failure loads for any initial crack size in any specimen or structure for which a stress-intensity analysis is available. For accurately predicting failure loads for stiffened-skin aircraft panels and bulkhead components, an accurate determination of the "R-curve" is necessary.

To determine the "R-curve," precracked specimens are tested with special displacements continually measured to failure. In the past, however, often the only data taken (and reported) were the initial crack length and the maximum load. New tests are required to accurately determine the "R-curve" accurately even though many residual-strength data are available in company files.

In the new analytical method, the "R-curve" can be estimated from residual-strength data alone, provided that the quantity and quality of data are sufficient to permit numerical differentiation with confidence. For some applications, the estimation may suffice. For others, the estimation will help set up an efficient "R-curve" test plan. The method has been verified by using data from the literature and by participation in a predictive blind round-robin program.

This work was done by Thomas W. Orange of **Lewis Research Center**. *Further information may be found in NASA TM-87182 [N86-18750/NSP], "Estimating the R-Curve from Residual Strength Data." [A03]*

Copies may be purchased [prepayment required] from the National Technical Information Service, Springfield, Virginia 22161, Telephone No. (703) 487-4650. Rush orders may be placed for an extra fee by calling (800) 336-4700.
LEW-14509 /TN

FOR ADDITIONAL INFORMATION: *Contact: Director, Technology Transfer Division, P.O. Box 8757, BWI Airport, MD 21240; (301) 621-0100 Ext. 241*
REFER TO THE NUMBER LISTED AT THE END OF THIS ARTICLE

NASA Tech Brief
National Aeronautics and Space Administration
NASA's Jet Propulsion Laboratory, Pasadena, California

Failure-Time Distribution of an *m*-Out-of-*n* System

Formulas for reliability are extended to more general cases.

Formulas have been derived for the probabilities of failure and survival and for the probability distribution of the time to failure of $n+1-m$ components of a system that initially contains n good components. The formulas should be useful in analyses of the reliabilities of practical systems and structures, especially of redundant systems of identical components, among which operating loads may be distributed equally.

The theory applies to a system that survives as long as at least m components survive and for which the failure rate of each of the $1-i$ components that remain at a given time is λ_i. Because increased stress is often placed on the surviving components, the failure rates tend to increase with each component failure; that is, $\lambda_0 \leqslant \lambda_1 \leqslant \ldots \leqslant \lambda^{n-m}$. However, the theory is valid even where this inequality does not hold.

The problem is to find the probability distribution of the time T to failure of the system, assuming that the intervals between the $n-m+1$ component failures in the sequence leading to system failure are independent and exponentially distributed with overall failure rates $\alpha_i = (n+1-i)\lambda_i$. The probability distribution can then be used to calculate the system reliability function $R(t)$, which is the probability of survival to time t; that is, the probability that T will exceed t.

Previous workers had developed probability distributions for the case in which all the α_i have the same value α, and for the case in which all the α_i are different. In the first case, T has a gamma distribution with shape parameter $n-m+1$ and scale parameter α. In the second case, the formula for $R(t)$ requires an individual, exponentially distributed term for each α_i. This study adapts the previous formulas to the intermediate case in which there are some equalities among the α_i. In this case, T can be expressed as the sum of independent gamma-distributed variables, one for each distinct overall failure rate β_i. The result is that

$$R(t) = \left\{ B \sum_{k=1}^{a} \sum_{\ell=1}^{r_k} [\Phi_{k\ell}(-\beta_k)]/(\ell-1)!\beta^{r_k-\ell+1} \sum_{j=0}^{r_k-\ell} [(\beta_k t)^j \exp(-\beta_k t)]/j! \right\}$$

where $B = \prod_{j=1}^{a} \beta_j{}^{r_j}$,

$$\Phi_{k\ell}(t) = \frac{d^{\ell-1}}{dt^{\ell-1}} \prod_{\substack{j=1 \\ j\neq i}}^{a} (\beta_j + t)^{-r_j},$$

r_j is the number of overall failure rates having the same distinct value β_j, and a is the number of such rates.

This work was done by Ernest M. Scheuer of Caltech for **NASA's Jet Propulsion Laboratory**. *NPO-17069 /TN*

FOR ADDITIONAL INFORMATION: *Contact: Director, Technology Transfer Division, P.O. Box 8757, BWI Airport, MD 21240; (301) 621-0100 Ext. 241*
REFER TO THE NUMBER LISTED AT THE END OF THIS ARTICLE

NASA Tech Brief
National Aeronautics and Space Administration

Stiffness Properties of Laminated Graphite/ Epoxy Cylinders

The dominant constituent property is the longitudinal Young's modulus of the fibers.

A report discusses the stiffnesses of cylindrical shells formed from composite graphite/epoxy laminates, as calculated from traditional composite-lamination theory. Such shells are being evaluated for use as cases for solid-fuel rocket motors. The stiffness results were compared with quasi-experimental stiffnesses developed from pressure tests of cylindrical bottles. The sensitivities of stiffnesses to variations in the constituent materials and in geometric parameters were examined with the help of two computer programs, which are included in an appendix to the report.

The macromechanics of laminated cylinders are described by a matrix constitutive equation for cylinder walls that was developed from classical lamination theory. The column matrix of the force and moment vectors is expressed in terms of the extensional-stiffness matrix, the coupling-stiffness matrix, the bending matrix, and the column matrix of the midplane strains and plate curvatures.

The properties of the graphite-fiber constituent of the composite that were varied include the longitudinal and transverse Young's moduli, E_1 and E_2, respectively, the shear modulus G_{12}, and the primary Poisson's ratio ν_{12}. Also varied were the Young's modulus, the shear modulus, and the Poisson's ratio of the epoxy matrix. The effect of variations in the helical winding angle was also studied; in forming the cylinders, the fibers in each lamination are parallel to each other but may be at different angles in different layers.

Expressions based on the rule of mixtures are used to estimate E_1 and ν_{12} of the composite from the values of the corresponding properties of the graphite fiber and the epoxy matrix. Empirical equations are used to estimate E_2 and G_{12}.

In general, it was found that the longitudinal Young's modulus of the fibers was the dominant contributor to the stiffness of the laminate. With the exception of the Poisson's ratio, the general stiffness parameters of the laminate change 82 percent of the proportion of a small change in the longitudinal Young's modulus of the fibers. On the other hand, the stiffness of the laminate is insensitive to large changes in the Poisson's ratio of either the fiber or the matrix, even though changes in these ratios cause the Poisson's ratio of the laminate to vary widely. The largest contributions of the transverse Young's and the shear moduli of the fiber to any laminate stiffness term were 8.7 and 10 percent, respectively. The contributions of the same moduli to the Poisson's ratio of the laminate were 3.4 and 15 percent, respectively.

In the simplified case of micromechanical theory of plane stress in laminates, which is adequate for thin cylinders, only the four elastic constants E_1, E_2, ν_{12}, and G_{12} are required. These can be measured experimentally by using standard laboratory tests or by a combination of micromechanical theory and pressure testing of tubes.

This work was done by R. Noel Tolbert of Tennessee Technical University for **Marshall Space Flight Center**.
"Stiffness Properties for Dynamic Modeling of Composite Graphite - Epoxy Cylindrical Orthotropic Shells," MFS-27157 /TN

FOR ADDITIONAL INFORMATION: *Contact: Director, Technology Transfer Division, P.O. Box 8757, BWI Airport, MD 21240; (301) 621-0100 Ext. 241*
REFER TO THE NUMBER LISTED AT THE END OF THIS ARTICLE

NASA Tech Brief
National Aeronautics and Space Administration
Marshall Space Flight Center, Alabama

Licensing Opportunity

Wet-Atmosphere Generator

The water content in a gas is controlled.

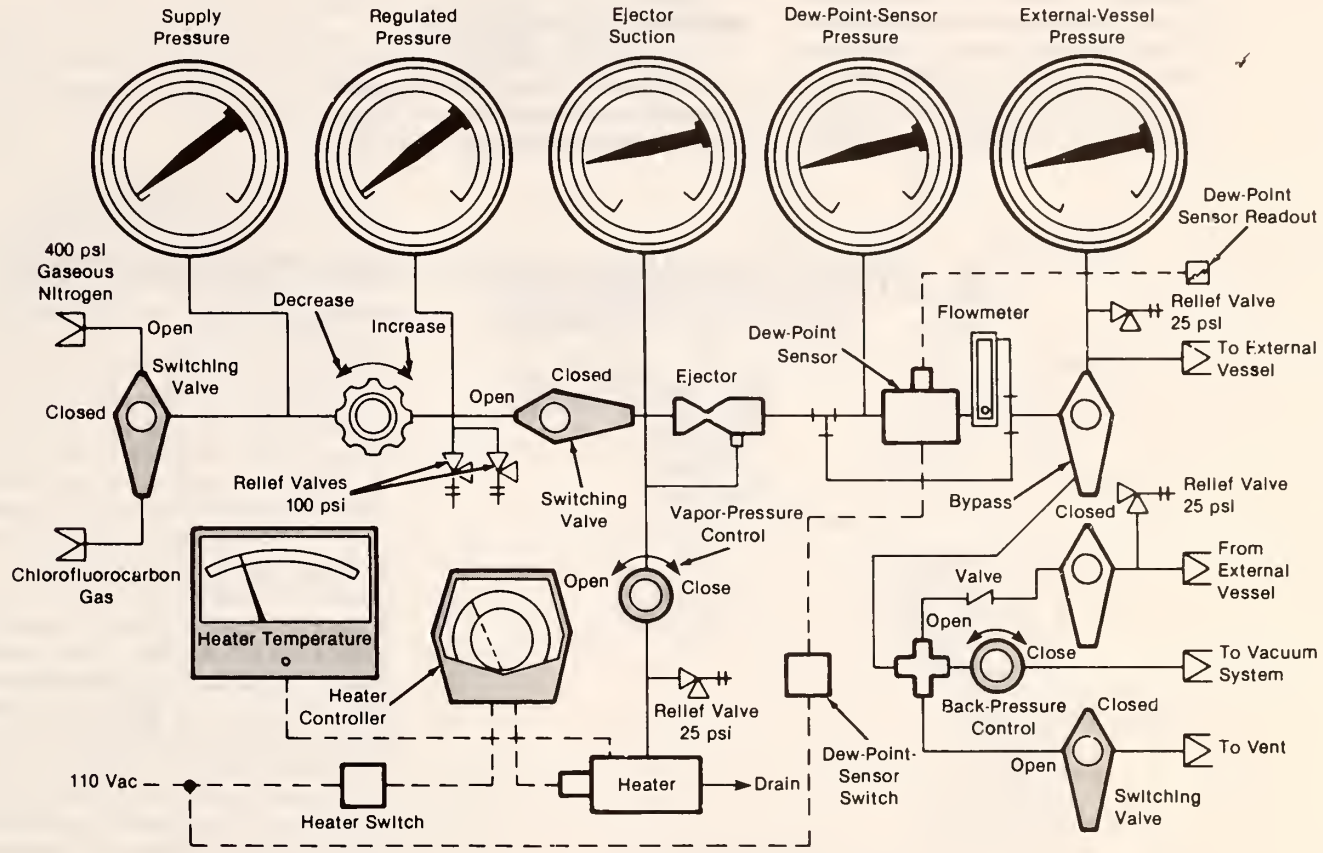

Gas-Flow Conditions in the nitrogen, water vapor, and nitrogen/vapor mixture can be set by the operator with the help of these valves, gauges, and electrical controls.

A portable flow-control system generates a nitrogen/water atmosphere having a range of dew points and pressures. One use of the system is to provide wet nitrogen for the canister of a wide-field camera that requires this special atmosphere. The system can also be used to inject trace gases other than water vapor for the leak testing of large vessels. Mixtures of gases can be used as carriers for the moisture. Potential applications are in photography, hospitals, and calibration laboratories.

The system uses pressurized nitrogen to power an ejector — essentially a venturi tube with a line from a water-vapor supply tapped into the low-pressure region (see figure). The low pressure draws the vapor into the venturi, where the vapor mixes with the main flow.

Liquid water for the vapor is held in a 1-gallon (3.8-liter) bottle in the suitcaselike system housing. The line from the bottle to the ejector passes through a regulating valve that mechanically controls the flow by throttling. The pressure in the bottle is regulated by a heater; an operator sets the heater temperature to a value that yields a saturation pressure greater than the suction of the ejector.

Once mixed in the ejector, the water vapor and nitrogen are directed to an external vessel or to a vent by regulator valves. Valves may also be set to admit vacuum or return flow from the vessel to the system.

A sample line is tapped from the main flow line and sent to a dew-point sensor. The pressure at the sensor is regulated so that it is the same as that in the external vessel; this ensures an accurate reading because the dew point is a function of the pressure. If necessary, the operator ad-

justs the dew point by adjusting the flow of water vapor or nitrogen to the ejector.

The sensor is an automatically controlled optical device. A condensate-detector mirror is illuminated with an intense beam from a light-emitting diode. A photodetector monitors the light reflected from the mirror. The detector is fully illuminated when the mirror is clear but sees less light when dew forms on the mirror, scattering light out of the path to the detector.

The photodetector is part of a bridge circuit that produces a large output current when the mirror is dry. The bridge output is amplified and applied to a thermoelectric cooler, which reduces the temperature of the mirror. As dew begins to form on the mirror, the light to the photodetector starts to decrease, the bridge output current drops, and the thermoelectric cooling is reduced. A feedback loop in the sensor quickly stabilizes the thermoelectric cooling control so that a thin dew layer is maintained on the mirror. A precise thermometer embedded in the mirror monitors the dew-point temperature of the layer.

The sensor can reduce the temperature of the gas/vapor mixture by as much as 45 °C. This means, for example, that, with the system at a temperature of 25 °C, dew-points between 25 and −20 °C can be measured.

This work was done by Richard M. Hammer and Janice K. McGuire of Teledyne Brown Engineering Corp. for **Marshall Space Flight Center**.

Inquiries concerning rights for the commercial use of this invention should be addressed to the Patent Counsel, Marshall Space Flight Center Refer to MFS-28177/TN

George C. Marshall Space Flight Center
Technology Utilization Officer: Ismail Akbay
Code AT01
Marshall Space Flight Center,
AL 35812
(205) 544-2223
Patent Counsel: Leon D Wofford, Jr
Mail Code CC01
Marshall Space Flight Center,
AL 35812
(205) 544-0024

FOR ADDITIONAL INFORMATION: *Contact: Director, Technology Transfer Division, P.O. Box 8757, BWI Airport, MD 21240; (301) 621-0100 Ext. 241*

REFER TO THE NUMBER LISTED AT THE END OF THIS ARTICLE

NASA Tech Brief
National Aeronautics and Space Administration
Langley Research Center, Hampton, Virginia

Licensing Opportunity

"Thumball" Auxiliary Data-Input Device

A track-ball-type device is mounted on a joystick and operated by a thumb.

The Thumball is designed to enable the precise input of data about two different axes to an autopilot, avionics computer, or other electronic device without the need for the operator to remove his or her hands from the joystick or other vehicle control levers.

The Thumball mechanism (see figure) includes a ball retained in a socket in the end of the control handle in such a way that it is free to rotate. Two rollers are pressed by spring-loaded bearings against the ball at points 90° apart about its circumference. As the ball is turned by the operator's thumb, friction drives the two rollers and their respective disks through angles proportional to the rotation of the ball about its x and y axes. This well-known mechanism, called a spherical integrator, simply resolves the motion of the ball into its components about the x and y axes.

The two disks are made of transparent material and have a pattern of dark and transparent sectors printed on their surfaces. A pair of light sources and a pair of photodetectors are mounted on opposite sides of each disk in such a way that, as the disk rotates, light is alternately transmitted to and cut off from the photodetectors. As the disk rotates, the outputs of its two photodetectors produce two square waves, displaced from each other by 90°. The direction of the displacement is an indication of the direction of rotation of the disk, and the number of pulses produced is a measure of the amount of rotation of the disk. The square waves are passed through suitable decoding logic that converts them into a series of clockwise or counterclockwise pulses that can be fed directly to the autopilot or avionics computer to effect a change in heading and/or pitch trim, to reposition a cursor on the screen of a cathode-ray tube, or to make any other precise adjustment required.

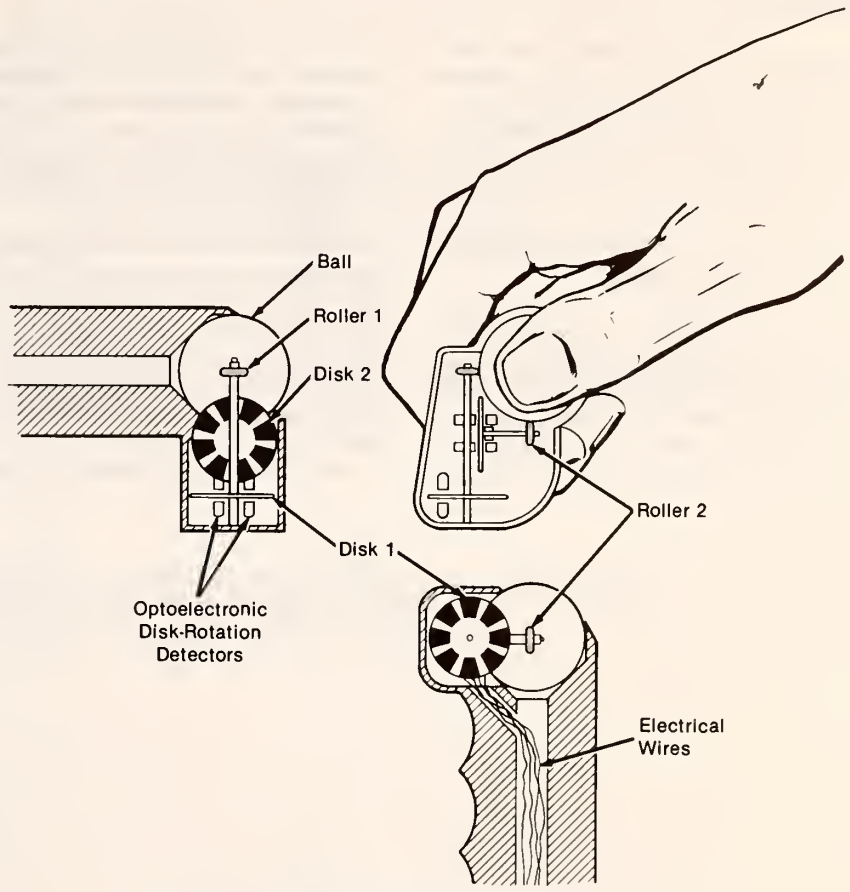

The **Thumball Mechanism** is mounted on the end of a joystick.

This work was done by H. Douglas Garner, Anthony M. Busquets, Thomas W. Hogge, and Russell V. Parrish of **Langley Research Center**.

This invention is owned by NASA, and a patent application has been filed. Inquiries concerning nonexclusive or exclusive license for its commercial development should be addressed to the Patent Counsel, Langley Research Center Refer to LAR-13626. /TN

Langley Research Ctr.
Technology Utilization Officer: John Samos
Mail Stop 139A
Hampton, VA 23665
(804) 865-3281

Patent Counsel. George F. Helfrich
Mail Code 279
Hampton, VA 23665
(804) 865-3725

FOR ADDITIONAL INFORMATION: *Contact: Director, Technology Transfer Division, P.O. Box 8757, BWI Airport, MD 21240; (301) 621-0100 Ext. 241*
REFER TO THE NUMBER LISTED AT THE END OF THIS ARTICLE

NASA Tech Brief
National Aeronautics and Space Administration

Sensor-Failure Simulator

Outputs of defective sensors are simulated for studies of reliability of control systems.

A real-time sensor-failure simulator (SFS) was designed and built for use with the Advance Detection, Isolation, and Accommodation (ADIA) program. The equipment consists of an IBM PC/XT computer and associated analog circuitry. The user defines failure scenarios to determine which sensor signals fail and the method(s) used to simulate failure.

The user interface is entirely menu-driven and allows one to define, save, retrieve, and edit failure scenarios. The analog circuitry has five separate signal paths, with independent digital-to-analog conversion (D/A) equipment for each path. The D/A equipment, controlled by the computer, modifies the analog signals to simulate failures of sensors. The SFS was designed to be programmable, reliable, flexible, and to provide for repeatable failure scenarios. Given these characteristics, it can be used for efficient evaluation and demonstration of sensor-failure-detection logic.

The SFS has been tested in a closed loop with a controls interface and monitoring unit, the ADIA control, and a real-time hybrid simulation of the F100 engine. As a first application, the SFS will be used to simulate sensor failures of a full-scale F100 engine in conjunction with the ADIA test program.

This work was done by Kevin J. Melcher, John C. Delaat, Walter C. Merrill, Lawrence G. Oberle, and Gerald G. Sadler of **Lewis Research Center** *and Joseph H. Schaefer of the U.S. Army. Further information may be found in NASA TM-87271 [N86-31792/NSP], "A Sensor Failure Simulator for Control System Reliability Studies." [A03]*

Copies may be purchased [prepayment required] from the National Technical Information Service, Springfield, Virginia 22161, Telephone No. (703) 487-4650. Rush orders may be placed for an extra fee by calling (800) 336-4700.
LEW-14533 /TN

FOR ADDITIONAL INFORMATION: *Contact: Director, Technology Transfer Division, P.O. Box 8757, BWI Airport, MD 21240; (301) 621-0100 Ext. 241*
REFER TO THE NUMBER LISTED AT THE END OF THIS ARTICLE

Environmental Science & Technology

486 Design, Construction, and Maintenance of Cover Systems for Hazardous Waste: An Engineering Guidance Document

487 Guidance Manual for Selection and Use of Sorbents for liquid Hazardous Substance Releases

Testing & Instrumentation

488 Field Dispersant Effectiveness Test

489 Environmental "Frozen Assets" Described in Videotape

Other Items of Interest

468 Determination of Effects of Atmospheric Contamination on Photovoltaic Cells in Concentrating Systems

United States
Environmental Protection
Agency

Hazardous Waste Engineering
Research Laboratory
Cincinnati OH 45268

Research and Development

EPA

Project Summary

Design, Construction, and Maintenance of Cover Systems for Hazardous Waste: An Engineering Guidance Document

Introduction

Regulations for the management of hazardous waste disposal facilities have been promulgated by the Environmental Protection Agency (EPA) as directed by the Resource Conservation and Recovery Act (RCRA). New hazardous waste disposal facilities must meet the requirements of Title 40, Code of Federal Regulations, Part 264 (40 CFR 264) in order to receive a permit. RCRA also dictates actions for correcting old sites presenting endangerment. As a part of its response to RCRA, the EPA has issued technical documents to assist in the complex and important task of planning adequate disposal facilities.

The full document of this project provides technical guidance on design, construction, and maintenance of cover for hazardous waste facilities based largely on waste management practice, concepts in soil construction, and innovations to encourage new designs and practice developed by creative and competent engineers within the limits of RCRA regulations. Suitable designs are ultimately translated into construction therefore, and some of the guidance is formulated directly as specifications.

Basis of Technical Design

The physical characteristics of the site and the configuration of its surface are among the most important factors upon which cover design is based. Sometimes, site characteristics directly influence design of the entire disposal unit or the assemblage of disposal units; for example, it is necessary to limit the size of disposal units or waste cells in hilly terrain, and their orientation and arrangement may also be restricted by operational considerations. Broad, flat sites present fewer restrictions on size, orientation, and arrangement of the disposal units.

The character of the waste can have long-term impacts on the cover and its performance in relation to subsidence, differential offset, and soil particle migration. It is even helpful conceptually to regard the disposal unit as the lower component or foundation of the cover with a transition to the backfill soil within the waste cells Influences follow either from the voids and other physical condition of the waste at the time of burial or from chemical-related changes that take place over a long period. Characterizing the waste focuses attention on unfavorable eventualities that in some cases may be avoidable. Certain worthwhile limitations on waste character and form as well as placement procedures may be incorporated in the plan of operations.

The chemical constitution and the reactivity of bulk and containerized waste always deserve careful consideration in cover design and the design of the disposal unit. A listing of wastes to go into each cell is already required in Subpart B, 40 CFR 270. In large disposal facilities, this undertaking may be complicated or simplified by any operational plan to segregate wastes into subcells according to waste type. The eventual deterioration and breakdown of initially rigid elements such as steel barrels, bale straps, and boxes will have to be evaluated as to their expected histories and the ultimate effects. Although it is frequently found that metals and sometimes even paper are little affected by burial in the short term (e.g., at the Savannah River Plant), the long-term effects over tens of years and to the design life of the facility must be addressed to the highest degree available with state-of-the-art knowledge and practice.

The potential for generation of gases or liberation of volatiles should also be considered in cover and disposal unit design. It may be necessary to provide diversions and vents for gases blocked from their upward pathways by the cover. Vents to the atmosphere may be adequate for toxic components of low concentration that will be quickly dispersed in the air to acceptable levels. In extreme cases where the gas or volatile component may reach a harmful concentration, it may be necessary to provide on line or contingency features for absorption filters or other means of

reducing concentration of toxic components. General categories of reactive wastes that can conceivably affect the performance of cover are volatile organic chemicals, inorganic acids, materials capable of reacting with others in the waste cell, materials capable of undergoing volume change, and saturated materials.

The hydrological environment of a disposal site constitutes the most influential combination of related external factors in cover design and maintenance. The several aspects of climate, particularly the precipitation regime have direct impacts on the performance of the cover in blocking percolation into the waste cell. Besides being foremost among general constraints to cover design, the climate enters into detailed analysis and evaluation of proposed cover designs.

The importance of the hydrological system can be illustrated by considering two extreme cases. It is believed that most of the low rainfall of a typical year at the arid Hanford and Richland, Washington, LLRW disposal facilities penetrates no more than a few meters of depth. Since the ground water is at much greater depth, most radionuclides carried downward by percolating water stop well above the water table. Thus, these facilities and another hazardous waste facility to the south near Arlington, Oregon, benefit directly from the dry regime. On the other hand, uncontrolled waste sites in the relatively damp midwestern and eastern United States frequently exhibit ground-water contamination plumes of serious dimensions and concentrations despite the presence of cover over the waste in some cases. Major storm events must also be considered, since even an arid region can be subjected to infrequent but major storms that cause anomalous ground saturation and percolation to a depth ordinarily not reached. Accordingly, a rather complete review of expectable storm events and their frequencies should be required in preparing the background on the hydrological system.

Other aspects of the hydrological system that need to be reviewed are the evapotranspiration history, the water-retention characteristics of the near-surface soil, and surface runoff parameters as well as available measurements at gaging stations. In the broader sense of hydrology, the ground-water system constitutes an important part. Familiarization with ground-water configuration, flow directions, and velocities is essential, if for no other reason than to plan and to anticipate contingencies for unexpected performance or even failure of the containment system.

General Design Concepts

Once the functions of the cover have been established or constrained by regulation or standard or by clearcut technical objectives such as reduction of percolation to insignificant levels, elements of the design are defined and integrated using conventional design methods.

A key task of cover design is the selection of suitable materials. The cover usually will include a synthetic membrane and a large volume of soil or soil-like material, but other materials are sometimes included also: i.e., Portland cement, bituminous concrete, seal coats, and geotextiles. Guidance on suitability of various types of soil for performing cover functions and for general long-term service ranking for various engineering functions has been developed based on considerable experience in the Bureau of Reclamation, Corps of Engineers, and other construction and engineering organizations. Classification is according to the Unified Soil Classification System (USCS).

Emphasis on the best soil for the cover will occasionally be unfeasible, since the soils available at or near the site will be chosen for reasons of economy. The strategy of cover design targets the most effective use of those available materials, usually in a layered construction. The availability of material may extend off-site. Fly ash available in the near vicinity continues to be an attractive possibility for use because of its relatively fine grain size which, by careful compaction or addition of reactive chemicals, can be brought to a strength and permeability that may be suitable for fulfilling cover functions.

Example Designs

The appendix in the full report provides guidance on preparing specifications for four example designs. The preparation of plans and specifications demands careful attention to detail, and sometimes the choice of wording can have costly legal ramifications. Therefore, the specifications in the appendix as well as the designs themselves are intended for guidance rather than for direct application at any facility.

Richard J. Lutton is with the U.S. Army Engineering Waterways Experiment Station, Vicksburg, MS 39180
Robert P. Hartley is the EPA Project Officer (see below)
The complete report entitled "Design, Construction, and Maintenance of Cover Systems for Hazardous Waste: An Engineering Guidance Document," (Order No. PB 87-191 656/AS; Cost: $18.95, subject to change) will be available only from
National Technical Information Service
5285 Port Royal Road
Springfield, VA 22161
Telephone: 703-487-4650
The EPA Project Officer can be contacted at
Hazardous Waste Engineering Research Laboratory
U.S. Environmental Protection Agency
Cincinnati, OH 45268

United States
Environmental Protection
Agency

Hazardous Waste Engineering
Research Laboratory
Cincinnati OH 45268

Research and Development

EPA

Project Summary

Guidance Manual for Selection and use of Sorbents for Liquid Hazardous Substance Releases

The document described herein is a guidance manual developed to provide information for the selection and use of sorbents for cleanup or control of liquid hazardous substances. Literature reviews, sorbent manufacturer data and experiences of Federal On-Scene Coordinators were reviewed in conjunction with laboratory studies to determine the compatibility and sorption capacity of selected representative hazardous liquid-sorbent pairs. The combined experimental and literature data were used to prepare the manual. On-scene coordinators and their technical support personnel are the primary target audience for the manual.

Before utilizing the manual, the user must first identify the spilled liquid. If it is one of the 212 liquid hazardous substances addressed in the manual, a reference is provided to one of 26 ''Sorbent Selection and Use Guides.'' Each of the guides enables the user to rapidly identify the generic sorbent classes, physical forms, and methods for application and collection that are most suitable for each of three different chemical release-control scenarios: (1) a spill onto land; (2) a floating release into water; and (3) immobilization for landfilling.

The manual contains ''Sorbent Data Sheets'' for 13 generic classes of sorbents other than activated carbon. These data sheets contain information on manufacturers, acquisition costs, bulk density and sorbent limitations. The sorption capacity of 190 sorbent-chemical pairs was determined and recorded in the manual. The manual also includes cost estimation procedures, test methods, hazardous liquid physical properties, and a description of the rationale for the relase-control scenarios.

Introduction

Spills and releases of liquid hazardous substances can pose a severe threat to the public and the environment. Such substances may be released at fixed sites or during transportation accidents. Sorbents are potentially effective materials for cleaning up and controlling many such releases. The guidance manual is designed to facilitate the selection and use of appropriate sorbents for treating releases of hazardous liquids. While the manual is targeted primarily to Federal On-Scene Coordinators (OSC) and their technical support staffs, it is also meant to assist personnel who respond to releases of hazardous liquids and immobilize such substances prior to disposal, or who engage in emergency response for cleanup or control of industrial spills.

Development of the manual involved a review of the literature, sorbent manufacturers' data, OSC experiences, and laboratory studies. The laboratory studies determined the compatibility and sorption capacity of selected hazardous liquid-sorbent pairs. To establish a framework for the manual, three liquid release-control scenarios were studied: (1) a spill onto land; (2) a floating release onto water; and (3) immobilization for landfilling. "Sorbent Selection and Use Guides'' were developed which list sorbents for each release-control scenario. Sorbent Data Sheets were also prepared for each of 13 classes of sorbents. The manual also provides information on sorbent application, collection and disposal, cost estimation procedures, test methods, hazardous liquid physical properties, and a narrative to enable selection of appropriate sorbents. The manual is designed to provide information for both rapid decision making and for conducting thorough evaluations of alternative sorbent-use strategies.

Conclusions

A Guidance Manual for the Selection and Use of Sorbents for Liquid Hazardous Substance Releases provides a concise compilation of information and data pertaining to the selection, acquisition, application, collection, regeneration, and disposal of sorbents. The inclusion of a chemcial index (by chemical name and DOT number), which is cross-referenced to Sorbent Selection and Use Guides and Sorbent Data Sheets, enables the user to quickly locate pertinent sorbent information for the liquid hazardous substances addressed in the manual. The manual includes 190 sorption capacity measurements taken as part of the project and which were unavailable in the literature prior to this effort. The availability of a condensed source of information on sorbents promotes their efficient use by assisting decision-makers to estimate and compare the effectiveness and cost of various sorbent-use strategies. Although the primary target audience for the manual is Federal On-Scene Coordinators and their technical support staffs, the manual is also applicable to the needs of spill clean-up managers representing State and local agencies as well as the private sector.

R. Melvold and S. Gibson are with Environmental Monitoring and Services, Newbury Park, CA 91320, and R. Scarberry is with JRB Associates, McLean, VA 22102
Michael Royer is the EPA Project Officer (see below)
The complete report entitled "A Guidance Manual for the Selection and Use of Sorbents for Liquid Hazardous Substance Releases," (Order No. PB 87-208 765/AS, Cost: $18.95, subject to change) will be available only from
National Technical Information Service
5285 Port Royal Road
Springfield, VA 22161
Telephone: 703-487-4650
The EPA Project Officer can be contacted at
Releases Control Branch
Hazardous Waste Engineering Research Laboratory—Cincinnati
U.S. Environmental Protection Agency
Edison, NJ 08837

United States
Environmental Protection
Agency

Hazardous Waste Engineering
Research Laboratory
Cincinnati OH 45268

Research and Development

EPA

Project Summary

Field Dispersant Effectiveness Test

Introduction

This project was conducted to develop a Field Dispersant Effectiveness Test (FDET) and determine the dispersibility of various commonly transported oils (mostly crude). The test is required to be economical, simple enough for use in the field, and able to provide realistic results. In addition, the test was used to generate a data base that has much of the information necessary to determine the feasibility of dispersing a specific spilled oil and the chemical agent(s) best suited for the job.

Initial steps in this study included evaluating the theoretical implications of shaking a sealed container to generate the desired oil droplets. The primary constraint was to make the droplets small enough (i.e., 10-20 μm) to approach the values encountered with ocean induced dispersion. Various methods were considered for the mixing process and demonstrated that moving the mixture of oil, dispersant and water in a sealed tube along its longitudinal axis at a set frequency, stroke length and time would provide the necessary energy level to produce an acceptable dispersion.

The practical constraints of time saving and simplicity were met by utilizing an apparatus that was readily available from any hardware store or laboratory (see Figure 1). A standard half-inch test tube was used for mixing the dispersant, oil and water, and a flashlight, ruler, and stopwatch, for determining the separation of the oil from the water. The height of the clear water space under the dispersed oil layer provided the basis for calculating the Percent Dispersion. The entire test procedure requires less than fifteen minutes.

Finally, the FDET was used to evaluate various oils and dispersants and to develop a data base of oil dispersibility. Eighteen commonly transported crude oils and six dispersants were selected for the test (see Table 1). Nine of the oils were also sparged and six were emulsified with water to make them comparable to the oil at a spill site. Three different dispersant-to-oil ratios were used to determine the best combination and each test was performed in triplicate to meet data quality objectives. The results were put into a dBase III program for future reference.

Results and Conclusions

It is possible to obtain a rapid evaluation of oil dispersibility, at the site of an oil spill, using readily available hardware from the laboratory and proper application of dispersants. A person responding to an oil spill would only need a copy of the FDET method, some dispersant, a couple of droppers, a ruler, and a test tube to determine the dispersibility of the oil. The test could be performed on a beach or a rolling ship without prior training and provide a report of good, fair, or poor dispersion that is comparable to laboratory test results.

The FDET relies on mixing variables that have been selected as a practical extension of the turbulence theory to generate droplet sizes that closely resemble the dispersion of oil occuring at sea. This study determined that a stroke length of 4 inches, a frequency of 120 cpm, and a shake time of one minute permitted adequate dispersion of the oil. A faster or longer stroke raised the stability of the dispersion, but made the test physically exhausting. A shorter or slower shake time made a less stable dispersion. The shake selected makes the test easier to perform, more precise and a better representation of dispersion at sea.

The settling time also affects the determination of the dispersion. Measurements after settling for 5 and 15 minutes do not allow differentiation between a good and a poor dispersion. The 5-minute measurement demonstrates insufficient equilibration of the droplet motion. The 15-minute measurement suffers from the restriction imposed by the height of the test tube. The tests showed that only the 10-minute measurement provides a clear differentiation between good and poor dispersion.

The FDET results obtained compare well with the results obtained with the

EPA Revised Standard Dispersant Effectiveness Test (see Figure 2). Prudhoe Bay oil was tested with fifteen dispersants using both methods and the effectiveness values overlapped for eleven out of the fifteen cases. Both methods agreed in classification of a good dispersion (60-100%), fair dispersion (20-59%) and poor dispersion (<20%).

All of the oils tested dispersed with four out of six dispersants considered. Eighteen oils were tested for dispersibility using up to six dispersants. Most of the oils dispersed more than 70% by volume with a good dispersant but failed to disperse by more than 40% with a poor dispersant. Removal of the most volatile components of the oil and emulsification with up to 30% water did not change the dispersibility of the oil.

The FDET has been used to establish a data base of information on oil dispersibility and dispersant effectiveness. The dBase III file covers the physical properties of the 18 oils tested and their dispersibility using up to 6 different dispersants. The data in this file will facilitate proper selection and application of dispersants in the field.

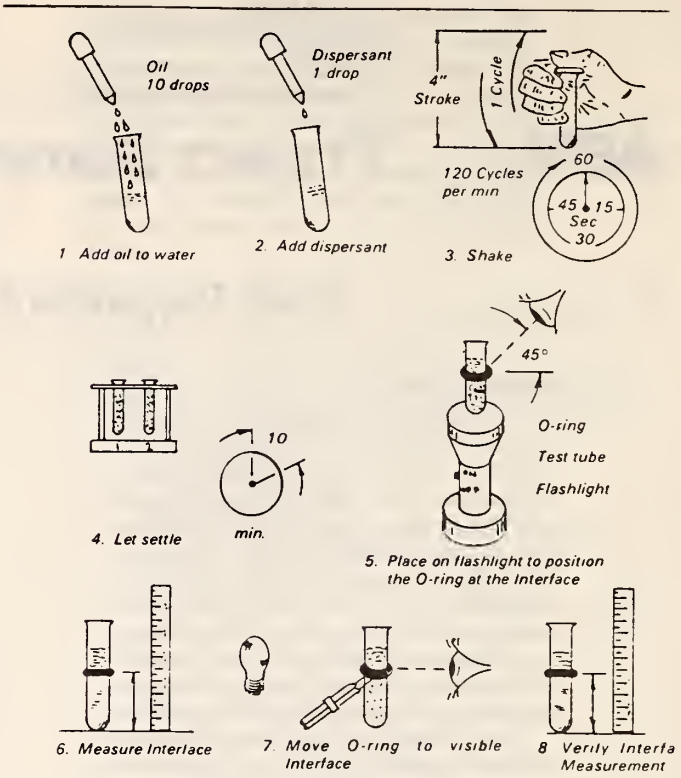

Figure 1. The FDET Procedure.

Table 1. *List of Test Fluids*

Oils	Source
Arabian Light	API/EPA SROP
Prudhoe Bay	API/EPA SROP
South Louisiana	API/EPA SROP
No. 2 Fuel	API/EPA SROP
Bunker C	API/EPA SROP
Bunker C	API
Bachequero	API — Exxon
Lagunillas	API — Exxon
Mississippi Heavy	API — Texaco
BCF-17	API — Texaco
Topped Lago Medio	API — Texaco
Minas Crude	API — Texaco
Murban	OHMSETT stock
La Rosa	OHMSETT stock
Gabon	OHMSETT stock
Hybernia	OHMSETT stock
Amauligak	OHMSETT stock
Alberta	OHMSETT stock
DFM	OHMSETT stock

Dispersants	Source
D — 609	Arco Chemical Co.
1100WD	British Petroleum
1100X	British Petroleum
Corexit 9527	Exxon Chemical Co.
Magnotox	Magnus Maritec Int'l, Inc.
ECO Atlantol AT7	ASPRA, Inc.

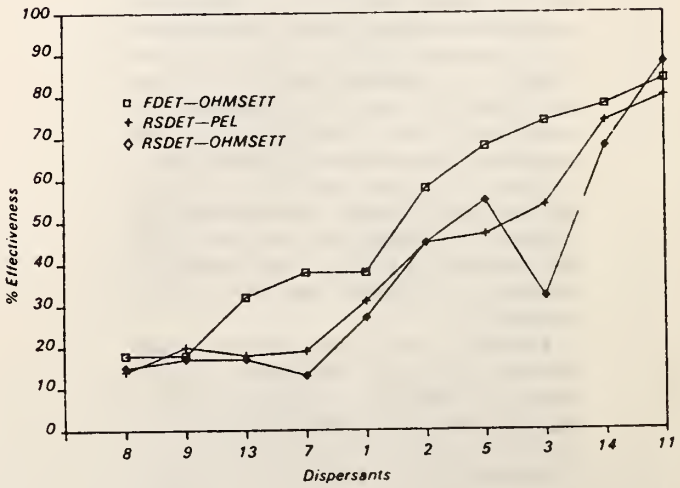

Figure 2. Comparison of dispersibility of Prudhoe Bay crude oil effectiveness by FDET and RSDET.

NBS technology update

National Bureau of Standards
U.S. Department of Commerce
Gaithersburg, MD 20899

Environmental "Frozen Assets" Described In Videotape

A project that is using frozen environmental samples to monitor pollution trends acros the country is described in an 8-1/2-minute videotape now available from NBS. The tape examines the National Biomonitoring Specimen Bank, which is a storage facility and clean laboratory for samples such as human livers and marine specimens (fish, mussels, mammal tissue, and sediment) as well as food products. These kinds of samples are banked because they are excellent indicators of pollution contamination at a particular time and location. Human livers, for example, are collected because they act as "sponges" in which toxic chemicals accumulate. Project researchers store samples at liquid nitrogen temperatures and can withdraw these materials at any time for reliable analysis. By periodically analyzing banked samples, scientists can examine pollution trends.

FOR ADDITIONAL INFORMATION:

For more information about obtaining the videotape, or for details about the National Biomonitoring Specimen Bank project, contact Dr. Stephen Wise, A113 Chemistry Bldg., National Bureau of Standards, Gaithersburg, MD 20899; (301) 975-3112. The specimen bank is a cooperative venture among NBS, the Environmental Protection Agency, and the National Oceanic and Atmospheric Administration, with support from other organizations.

Manufacturing, Machinery, & Tools

490 Welding of Nickel Aluminide and Nickel-Iron Aluminides

491 Novel Vapor-Deposited Lubricants for Metal-Forming Processes

492 Fixture for Polishing Optical-Fiber Ends — Wedged and beveled ends are lapped with precision for laser applications. (Licensing Opportunity)

493 Grinding Inside a Toroidal Cavity — Weld lines can be ground smooth within about 0.001 in. (0.025 mm). (Licensing Opportunity)

494 Inflatable Probe Would Manipulate Delicate Parts — Delicate parts would be grasped gently. (Licensing Opportunity)

495 Locating Residual Wax in Coolant Channels — Neutron inspection finds deposits and defects invisible to x-rays.

496 Tool Protects Internal Threads During Rework — A simple device covers some areas but exposes other areas for grinding.

Software

497 COMMIX Code for Metal Casting — Teaching an old code new tricks.

498 Advanced Software for the Efficient Manufacture of Complex Industrial Castings

499 Allocating Spare Parts in Complicated Systems — Assortments are analyzed for cost effectiveness and effects on system functionality.

Welding of Nickel Aluminide and Nickel-Iron Aluminides

Because welding is often used during the fabrication of structural components, one of the key issues in the development of nickel aluminides and nickel-iron aluminides for engineering applications is their weldability. The goals of this study at Oak Ridge National Laboratory were to characterize weldment microstructures and to identify some of the factors controlling weldability of ductile Ni_3Al alloys.

Ni_3Al is an ordered intermetallic compound having a face-centered-cubic (FCC) crystal structure below about 1395 C and, unlike many other intermetallic compounds, exists over a relatively large range of composition, being stable from about 72 to 78.5 atomic percent nickel at temperatures below 1150 C. This range of stoichiometry means that Ni_3Al can be extensively alloyed.

A major impediment to the use of Ni_3Al as an engineering material has been its brittleness in polycrystalline form. The low ductility of polycrystalline Ni_3Al results from grain boundary weakness, which causes fracture to occur intergranularly with little or no deformation within individual grains. Microalloying with boron can have a substantial beneficial effect on the ductility of this compound by controlling the chemistry of grain boundaries. Macroalloying is used to control phase stability and bulk properties. Some of the more promising alloys are based on the Ni_3Al-Fe_3Al pseudo-binary system. Iron dissolves in Ni_3Al up to about 15 atomic percent without disturbing the crystal structure or causing the stabilization of second phases at low temperatures and appears to improve fabricability.

The nominal compositions of the alloys used in this study are listed in Table 4. Ingots (500 g) of the alloys were prepared from pure charge materials and a Ni-18 atomic percent B master alloy by vacuum arc melting and drop casting. Weldments were made by the autogenous bead-on-plate technique with either the electron beam (EB) or gas tungsten arc (GTA) process. The parameters for each process were adjusted to produce full-penetration welds at various travel speeds. EB welds were made in a 6 kW machine at welding speeds from 0.9 to 64 mm/s. Beam voltages were 60 to 100 kV, and beam currents were 1 to 6 mA. GTA welds were made with a 1.6-mm-diameter thoriated tungsten electrode and argon shielding gas. The GTA welding parameters were 12 to 14 V and 12 to 35 A at welding speeds ranging from 0.9 to 15.4 mm/s.

Table 4. Alloy Compositions

Alloy	Composition, atomic percent				
	Ni	Al	Fe	B	Others
IC-15	75.8	24.0	–	0.24 (500 wppm)	–
IC-25	69.9	18.9	10.0	0.24 (500 wppm)	0.5 Ti + 0.5 Mn
IC-103	70.0	18.9	10.0	0.10 (200 wppm)	0.5 Ti + 0.5 Mn

A transmission electron microscopy investigation of the fusion zone and the microstructures of alloy IC-25 revealed the presence of antiphase domain boundaries (APBs) and confirmed the formation of a martensitic β' phase. The β' phase formed in both the FZ and heat-affected zone (HAZ), but more extensively in the former. In the HAZ, β' in the form of platelets was observed exclusively on grain boundaries. It originated from the heating of material in the HAZ close to the fusion zone to temperatures above the β solvus.

The results of a previous study showed that boron and iron concentrations as well as welding speed were all important factors in determining the weldability of Ni_3Al alloys.

The boron-doped Ni_3Al (alloy IC-15) was EB and GTA welded at 0.9, 1.7, and 3.4 mm/s with no preheating, and at 3.4 mm/s with a 400 C preheat. All of these weldments contained visible cracks on their as-welded surfaces. Cracks were generally located in both the FZ and the HAZ and were mainly intergranular. When HAZ cracks were examined on polished and etched sections, they did not appear to have formed by liquation at grain boundaries or second phases. The authors suggest that greater localization of stresses and more rapidly changing stress distributions with time at higher welding speeds result in HAZ cracking due to grain boundary weakening at elevated temperatures.

Cracking frequency versus EB welding speed is plotted in Figure 1 for IC-25 and IC-103. The nickel-iron aluminide alloy IC-25 was very susceptible to cracking at welding speeds exceeding about 13 mm/s. On the other hand, sound crack-free welds were made in alloy IC-103, which had a lower boron content than IC-25, at speeds up to 50.8 mm/s. In IC-25, most of the cracks were confined to the HAZ, although a few were observed in the FZ. All crack paths were intergranular, and HAZ cracks tended to extend in a direction normal to the welding direction. For both alloys, the primary phase in the FZ had the same ordered structure as the annealed base metal. The second phase, distributed interdendritically, was martensitic β', which forms from the aluminum-rich β phase. The volume fraction of β' in the FZ varied from 0.09 to 0.12 and increased with welding speed. The β' phase also formed on the HAZ grain boundaries in both alloys, particularly at welding speeds below about 13 mm/s. The presence of grain boundary β' in the HAZ did not appear to be a major factor in HAZ cracking. For instance, IC-103 welds did not crack at low speeds when HAZ β' was present or at high speeds when it was not. No other microstructural differences between these alloys were found by optical metallography.

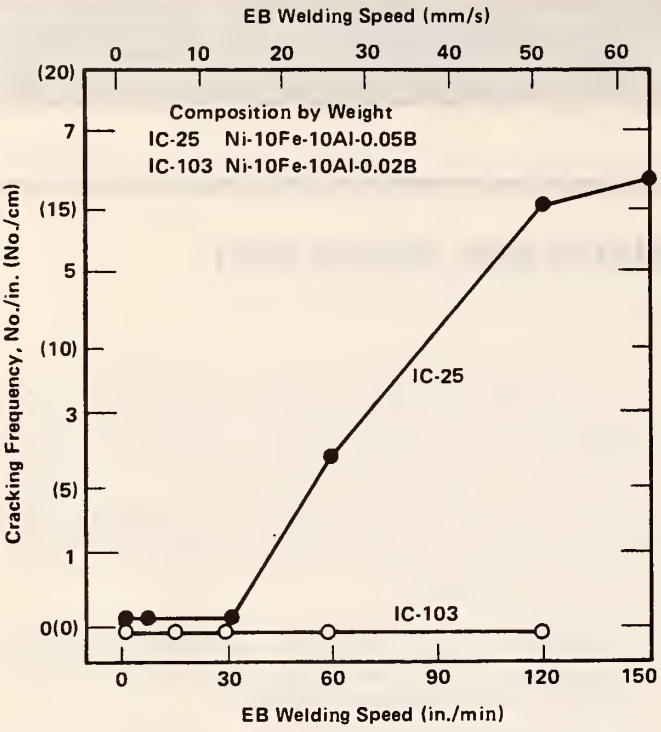

Figure 1. Cracking Frequency as a Function of Welding Speed for the Iron-Containing Ni_3Al Alloys

SEM examination of fracture surfaces of EB welds made at 33.9 mm/s and fractured at room temperature showed that IC-25 broke across existing HAZ cracks in a brittle intergranular mode. There was no evidence of liquid films on the crack surface, indicating that HAZ cracking occurred after passage of the molten weld pool, i.e., at some temperature below the solidus. A solidification structure was evident in the FZ, and the base metal showed the typical ductile intergranular failure mode. Room temperature tensile test results for defect-free EB weldments of IC-25 made at a welding speed of 4.2 mm/s are given in Table 5. Two specimens were tested in each orientation. Both specimens of parallel orientation fractured across the pinhole of one of the grip ends, so the true ultimate tensile strength and elongation values would be higher than those recorded. These results show that sound weldments in nickel-iron aluminides can display excellent strength and ductility at room temperature.

Table 5. Tensile Test Results for IC-25 EB Welds

Specimen Location	Yield Strength, MPa	Ultimate Tensile Strength, GPa	Elongation, percent
Weldment, ⊥ axis	341.2	1.290	41.5
Weldment, ∥ axis	398.5	>1.205[a]	>26.5[a]
Base material	386.1	1.214	45

(a) Specimens fractured across pinhole.

The type of defect found most frequently in GTA welds in IC-25 was crater cracks, although HAZ cracks were also found as welding speed increased. The crater cracking was related to impurities in the shielding gas; small additions of oxygen or hydrogen to the shielding gas resulted in cracking.

FOR ADDITIONAL INFORMATION: A copy of the report is available from NTIS, Springfield, VA 22161; (703) 487-4600.
NTIS order number: DE85-018168/NAC
Price code: A03

United States
Environmental Protection
Agency

Air and Energy Engineering
Research Laboratory
Research Triangle Park NC 27711

Research and Development

EPA

Project Summary

Novel Vapor-Deposited Lubricants for Metal-Forming Processes

This report gives results of a laboratory study of the feasibility of using vapor-phase lubrication to lubricate industrial metal forging dies. It gives results of six tasks conducted during the study and discusses the potential production and environmental impact of the process. If a vapor lubrication system can be developed for general industrial use it can significantly reduce the volume of forging lubricants required by present industrial forging operations. The laboratory results indicate that it may be possible to reduce potential air pollution emissions from forging using vapor lubrication by as much as 85%. This would be accomplished by using 85% less lubricant volume during metal forging.

Introduction

The forging and shaping of metal parts is one of many metal fabricating processes that may generate emissions of volatile organic compounds (VOCs) and hydrocarbons. In typical metal forming operations hot metal is squeezed in dies to produce metal shapes in the form of the die cavity. This process may require many intermediate forming and shaping steps using successively more accurate dies to reach the finished product. A key aspect of these shaping steps is the lubrication of the dies and metal parts to allow easy release of the part from the die. The used lubricants frequently result in emissions containing VOCs and potentially toxic metal to the atmosphere.

This report presents the results of a Phase I study that investigated the feasibility of using vapor-phase lubrication for industrial metal forging dies. It presents the results of six tasks conducted during the study and discusses the potential production and environmental impact of the effectiveness of the process. A vapor lubrication system developed for general industrial use could significantly reduce the volume of forging lubricants required by present industrial forging operations.

The project proposes to use a vapor-phase polymer film to lubricate forging dies in their closed position. An injection device allows lubricant vapor to be applied automatically through passages in the flange areas of the die. This eliminates large volumes of liquid die lubricants and the resulting emissions typically generated during this operation.

Project Plan

Six tasks were performed during the project. Each was designed to produce vital elements and data for a future pilot scale unit. The six tasks were to:

- Establish a fully operational, laboratory scale vapor-phase lubricant delivery system (LDS).
- Formulate lubricants and evaluate the lubricity of the vapor-deposited polymers using the ring compression test.
- Forge parts using conventional lubricants to provide baseline data.
- Modify the forging die to permit vapor-phase lubrication.
- Forge five parts using vapor-phase lubrication in a modified die.
- Quantitatively compare the emissions from vapor-deposited lubrication with those from the conventional oil-based lubrication system.

Emission Results

The volume of lubricant used during each experiment was determined qualitatively by the metal flow and release properties exhibited by each technique. Metal flow is defined by the interface friction factor (m value) which is a measure of metal flow within the die. Release properties are defined by the relative ease with which the part can be removed from the die. It was assumed that all lubricant used during each experiment was volatilized to the atmosphere. This represents the worst case scenario for the process. Table 1 summarizes the results.

Conclusion

Although this project included a limited number of experiments, it did show that vapor-phase lubrication is feasible for metal forging. It can also result in a significant reduction of potential emissions to the atmosphere. The process could reduce emissions from forging and casting operations by as much as 85%.

The project represents only the first step, laboratory feasibility, of the development program for vapor-phase lubrication. Significant research and development still remains, including die lubrication system design and lubricant formulation development.

Table 1. *Average Emissions and Forging Parameters*

	Conventional Lubrication	Vapor-Phase Lubrication
Average block and finish per part, ml	76	11.3
Average forging force, ton (kN)	75 (667)	75 (667)
Average forging time, sec	60	60

J. J. Mills is with Martin Marietta Laboratories, Baltimore, MD 21227
Charles H. Darvin is the EPA Project Officer (see below)
The complete report, entitled "Novel Vapor Deposited Lubricants for Metal-Forming Processes," (Order No. PB 87-227 351/AS; Cost: $11.95, subject to change) will be available only from
National Technical Information Service
5285 Port Royal Road
Springfield, VA 22161
Telephone: 703 487-4650
The EPA Officer can be contacted at:
Air and Energy Engineering Research Laboratory
U.S. Environmental Protection Agency
Research Triangle Park, NC 27711

NASA Tech Brief
National Aeronautics and Space Administration
Langley Research Center, Hampton, Virginia

Licensing Opportunity

Fixture for Polishing Optical-Fiber Ends

Wedged and beveled ends are lapped with precision for laser applications.

When an injected laser is coupled into an optical fiber, emission instabilities arise because of optical feedback losses from the fiber into the laser. However, high coupling efficiency and feedback suppression can be achieved by shaping the input end of a multimode fiber into a wedge and by beveling the output end at a suitable angle [see "Wedge Fibers Suppress Feedback of Laser Beam" (LAR-13074), pages 94 and 95, *NASA Tech Briefs*, Vol. 9, No. 4 (Winter 1985)]. A fixture that has been designed for the precise cutting of end-polished fibers into specific depths and angles provides accurate repeatability during the polishing process.

Each end-polished fiber requires an obtuse-angled wedge or roof configuration at one end and a bevel at the other. These requirements posed problems in ensuring accuracy of the angles, repeatability of the angles (both from one side of the obtuse angle to the other and from fiber to fiber), and precise splitting of the core [0.001 in. (0.025 mm) or less] in the center of the fiber [0.005 in. (0.13 mm)] for the obtuse-angled wedge. A fixture allows the operator to overcome all of these problems and to accomplish precise work. This fixture holds the fiber accurately, adjusts to the correct angle, controls the amount of stock removed from one side of the fiber to the other, supports the fiber as the angle is polished, controls the finish on the fiber, and allows the fiber to be removed for inspection and to be accurately repositioned to continue polishing.

The holding block (see figure) is grooved to hold the fiber in the exact position required for polishing. The fiber is locked in position with a retaining strap and cannot rotate or slide back during polishing. A base fixture for the holding block has an adjustable angle stop, which is set at the desired angle, and a micrometer feed that allows the operator control over the inward pressure on the fiber. The holding block is set on the base fixture and aligned with the angle stop. Anchored to the side of the block is the fiber support. Once the fiber is in position for polishing, the fiber support is slid out from its holder and locked into position near the tip of the fiber. This component supports the fiber, not allowing it to bend or bow under pressure during polishing and thus change the angle. The fiber is slowly moved into position using the micrometer feed and accurately beveled to the proper angle. This fixture also has a stop adjustment that allows the operator to remove the holding block for inspection of the fiber and to replace it accurately.

The ends that require the obtuse-angled wedge require two polishing steps. The first step is similar to the beveled-edge

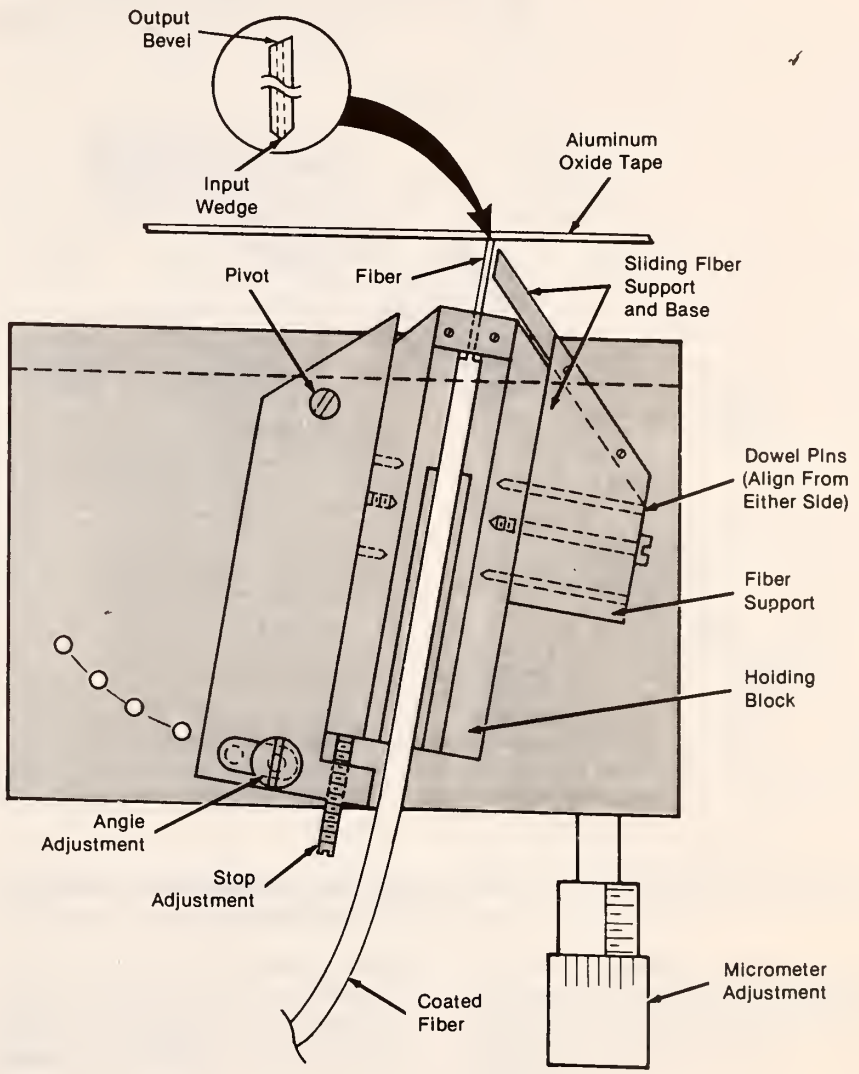

For an Obtuse-Angled Wedge End, both sides of the fiber are polished similarly. After one side of the fiber is lapped, the fiber support is removed. The holding block with the fiber is turned over, and the fiber support is replaced. The second side of the fiber is then lapped.

polishing, except that the angle is polished only half way through the fiber, then the holding block is removed. The fiber support is removed from the polished side of the holding block and placed on the opposite side. The holding block then is turned over and accurately replaced on the base fixture. The second half of the fiber is polished to obtain the proper obtuse-angled wedge.

This work was done by Leroy H. Barlow and Vincent A. Pirone of RCA Corp. for **Langley Research Center**. *No further documentation is available.*

Inquiries concerning rights for the commercial use of this invention should be addressed to the Patent Counsel. Langley Research Center Refer to LAR-13510 /TN

Langley Research Ctr.
Technology Utilization Officer: John Samos
Mail Stop 139A
Hampton, VA 23665
(804) 865-3281
Patent Counsel: George F. Helfrich
Mail Code 279
Hampton, VA 23665
(804) 865-3725

FOR ADDITIONAL INFORMATION: *Contact: Director, Technology Transfer Division, P.O. Box 8757, BWI Airport, MD 21240; (301) 621-0100 Ext. 241*
REFER TO THE NUMBER LISTED AT THE END OF THIS ARTICLE

NASA Tech Brief
National Aeronautics and Space Administration
Marshall Space Flight Center, Alabama

Licensing Opportunity

Grinding Inside a Toroidal Cavity

Weld Lines can be ground smooth within about 0.001 in. (0.025 mm).

A grinding tool for smoothing longitudinal weld lines inside a toroidal cavity includes a curved tunnel jig to guide a grinding "mouse" along the weld line (see figure). The curvature of the tunnel jig is matched to the shape of the toroid so that the grinding ball in the mouse can follow a circular arc of the correct radius as the mouse is pushed along the tunnel. The tool enables precise control of grindout shape, yet is easy to use.

Weld-free areas of the toroid serve as position references for the alignment of the tunnel jig with the toroid. During grinding, the tunnel jig is clamped against the inner wall of the toroid by an air-driven piston. (Screw clamps could be used instead.) The depth of the grind is controlled by adjusting the distance by which the grinding ball protrudes from the mouse.

Shims are placed along the inner sides of the tunnel jig to control the lateral position of the mouse on each grinding pass. The steps between passes can be made small enough so that the ridge between adjacent grind paths is 0.001 in. (0.025 mm) or less. The ground surface can then be polished to achieve a smoother finish if desired.

A flexible driving cable connects an external air-powered or electric motor to the grinding ball in the mouse. The handle used by the operator to slide the mouse through the tunnel is attached to the mouse by a curved rod. The perpendicular force of the grinding ball against the surface to be ground is provided by a small air-powered cylinder on the side of the mouse opposite that of the grinding ball.

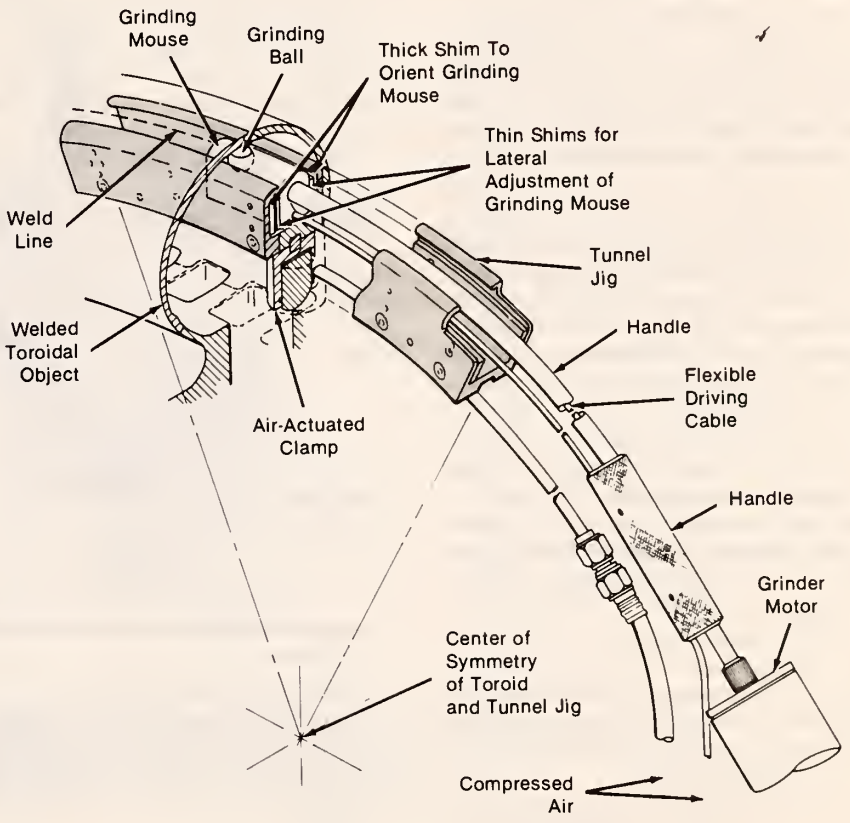

The **Grinding Tool** smoothes out protruding material along weld lines inside a toroidal chamber. The curved tunnel jig guides the grinding mouse.

This work was done by Walter Mayer, James F. Adams, and Richard K. Burley of Rockwell International Corp. for **Marshall Space Flight Center**. *No further documentation is available.*

Inquiries concerning rights for the commercial use of this invention should be addressed to the Patent Counsel, Marshall Space Flight Center Refer to /TN MFS-29249

George C. Marshall Space Flight Center
Marshall Space Flight Center, AL 35812
Technology Utilization Officer: Ismail Akbay
Code AT01
(205) 544-2223
Patent Counsel:
Leon D. Wofford, Jr.
Mail Code CC01
(205) 544-0024

FOR ADDITIONAL INFORMATION: *Contact: Director, Technology Transfer Division, P.O. Box 8757, BWI Airport, MD 21240; (301) 621-0100 Ext. 241*
REFER TO THE NUMBER LISTED AT THE END OF THIS ARTICLE

NASA Tech Brief
National Aeronautics and Space Administration
Marshall Space Flight Center, Alabama

Licensing Opportunity

Inflatable Probe Would Manipulate Delicate Parts

Delicate parts would be grasped gently.

A proposed inflatable probe would grasp parts gently. Unlike many existing robotic end effectors with hard grasping fingers, the proposed mechanism would not apply high contact pressures and is therefore less likely to damage delicate parts.

The rigid probe would be surrounded by a bladder (see figure). The probe would be inserted in a hole of slightly larger diameter in the part to grasped. The depth of insertion would be limited by three resilient bumpers, which could serve as stops to control the position and orientation of the part if necessary.

Once the probe was inserted, the bladder would be inflated to a preset maximum pressure, expanding against the inside of the hole in the part to grasp it firmly but gently. After moving the part to the desired position, the bladder would be deflated and the probe withdrawn.

The principal disadvantage of the concept is the need to provide a hole of the specified diameter in every part to be handled. However, this may be offset by the advantages of simplicity and reliability of the inflatable bladder.

This work was done by Carter K. Lord of Olis Engineering for **Marshall Space Flight Center**. *For further information, Circle 2 on the TSP Request Card.*

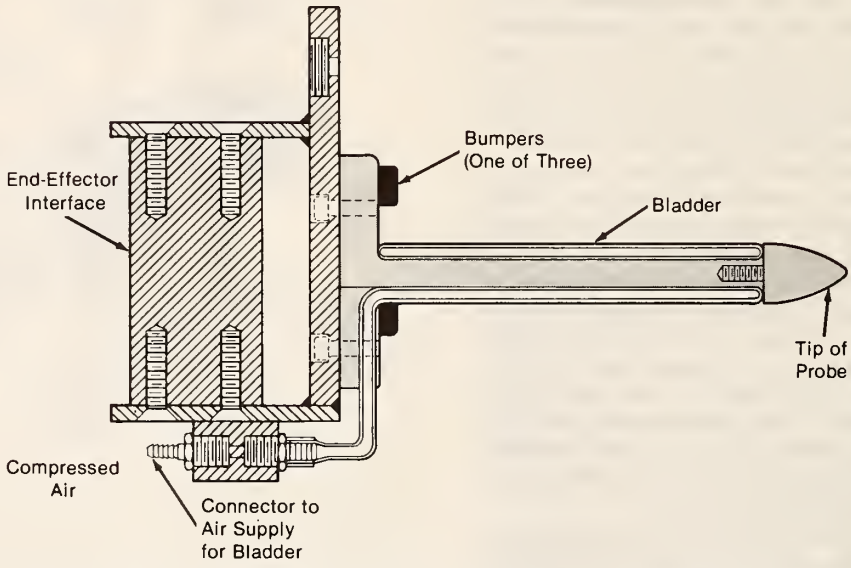

A **Cylindrical Bladder Would Be Inflated** against the inner wall of surrounding hole in the part to be grasped.

In accordance with Public Law 96-517, the contractor has elected to retain title to this invention. Inquiries concerning rights for its commercial use should be addressed to

Carter K. Lord
Olis Engineering
Olis Enterprises, Inc.
P.O. Box 408#D
Sedalia, CO 80135

Refer to MFS-26045, /TN

George C. Marshall Space Flight Center
Marshall Space Flight Center, AL 35812
Technology Utilization Officer: Ismail Akbay
Code AT01
(205) 544-2223
Patent Counsel:
Leon D. Wofford, Jr.
Mail Code CC01
(205) 544-0024

FOR ADDITIONAL INFORMATION: *Contact: Director, Technology Transfer Division, P.O. Box 8757, BWI Airport, MD 21240; (301) 621-0100 Ext. 241*
REFER TO THE NUMBER LISTED AT THE END OF THIS ARTICLE

NASA Tech Brief
National Aeronautics and Space Administration
Marshall Space Flight Center, Alabama

Locating Residual Wax in Coolant Channels

Neutron inspection finds deposits and defects invisible to x rays.

Residues of machining or plating wax that block internal channels in heat exchangers or other metal parts are readily detected by neutron radiography. The technique has been used to inspect the coolant channels in the Space Shuttle main combustion chamber. However, it is also useful for finding such other hidden nonmetallic deposits as core material in turbine-blade coolant passages, braze "stop-off" in injector orifices, internal voids in rubber parts, flaws in metal-to-polymer seals, and voids in encapsulating compounds surrounding cables or electronic components. Such defects are usually not revealed by conventional x-ray inspection.

Previously, residual wax in hidden channels was detected by infrared chemical analyses of samples of effluent perchloroethylene, which had dissolved small amounts of the wax during passage through the channels. The method depended on operator skill in doing the test and processing the sample and often gave incorrect or uncertain results. Another infrared technique — one that measures relative heat-transfer rates by image analysis — is of little use because it does not give the exact locations of channel restrictions.

Unlike x-radiography, neutron radiography readily detects many low-density materials even when they are surrounded by larger quantities of denser materials. Materials with similar properties and densities often appear quite different when viewed by neutron radiography.

A beam of low-energy neutrons, produced by fission in a nuclear reactor, is directed at the part to be inspected. Some neutrons pass through the part unaffected, whereas others are deflected or absorbed by nuclei, depending on the nature of the local material. Those that pass through produce short-term radioactivity in a scintillator screen that is used to expose photographic film.

The technique gives a comprehensive view of the hidden channels. Several film exposures are made from different points of view, so that triangulation can be used to determine the locations of residual wax deposits. From densitometer readings and parallax exposures, partially blocked channels can be distinguished from completely blocked ones. Machining wax in channels 0.1 in. (2.5 mm) thick can be easily detected even when shielded by 0.5 in. (1.3 cm) of Inconel* nickel/iron alloy, with no significant damage to the metal part.

*Inconel is a registered trademark of the Inco family of companies.

This work was done by Douglas M. Guthrie of Rockwell International Corp. for **Marshall Space Flight Center**. *No further documentation is available.*
MFS-29212 /TN

FOR ADDITIONAL INFORMATION: *Contact: Director, Technology Transfer Division, P.O. Box 8757, BWI Airport, MD. 21240; (301) 621-0100 Ext. 241*
REFER TO THE NUMBER LISTED AT THE END OF THE ARTICLE

NASA Tech Brief
National Aeronautics and Space Administration
Marshall Space Flight Center, Alabama

Tool Protects Internal Threads During Rework

A simple device covers some areas but exposes other areas for grinding.

A tool protects part of an internal thread from damage while an adjacent surface is ground or machined. The tool also collects machining debris so that they do not contaminate the part.

The tool is a flanged cylinder with a window (see figure). Grinding and other operations can be done through the window while the tool masks the threaded surface to be protected. The flange positions the window precisely in the hole to be reworked. The cylinder can be rotated so that the window exposes the full circumference for machining.

The tool was developed to remove the portion of a thread that had been extended to too great a depth in a hole. With the tool, the thread extending below a depth of 0.87 ± 0.06 in. (2.21 ± 0.15 cm) could be ground away without damage to the thread above that depth. The grinding chips and dust fell to the bottom of the tool and were removed with the tool at the completion of grinding.

This work was done by Gary E. Deese of Rockwell International Corp. for **Marshall Space Flight Center**. *No further documentation is available.*
MFS-29234 /TN

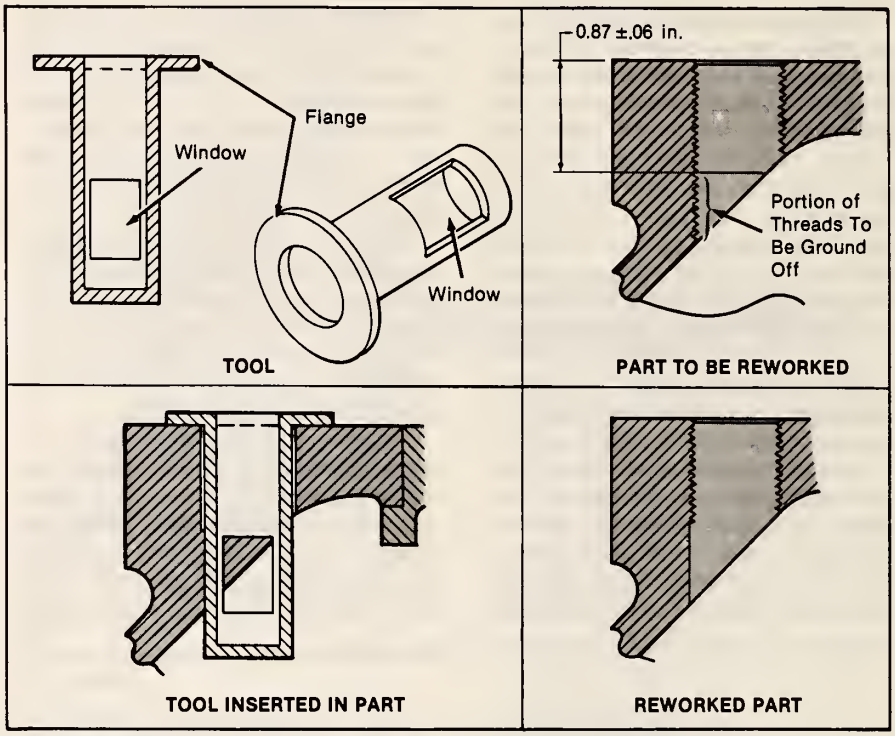

The **Protective Tool** fits into a threaded hole. The wall of the hole can be machined through the window without damage to the portion of the thread hidden by the tool.

FOR ADDITIONAL INFORMATION: *Contact: Director, Technology Transfer Division, P.O. Box 8757, BWI Airport, MD 21240; (301) 621-0100 Ext. 241*
REFER TO THE NUMBER LISTED AT THE END OF THIS ARTICLE

04-02-0188

COMMIX Code for Metal Casting

Teaching an old code new tricks

Casting is one of the most direct methods of producing industrial parts in a desired shape. It permits economical fabrication of intricate parts that often are subjected to high stresses and strains--for example, gasoline and diesel engine cylinder blocks. Because casting provides design flexibility, metallurgical versatility, and economic benefits, each year many millions of cast shapes are produced, ranging in size and weight from a fraction of an inch to many feet and from a few ounces to over 250 tons.

Although the casting process is one of the oldest known metallurgical techniques, it involves a host of complex phenomena that are still not thoroughly understood--phenomena that control the quality of the final product. Often the desired casting shape is highly irregular, so the casting mold is complicated. Furthermore, flow into the mold is complex, and the metal changes from liquid to solid. Air and other gases may be trapped within the molten material, forming a multicomponent flow mixture. Nonuniform heat transfer, coupled with large temperature differences and other factors, can produce currents in molten regions. All these factors rule out a purely analytical analysis of the process. But now, with the development of advanced computer technology and sophisticated numerical methods, the phenomena that affect the casting process can be characterized and better understood, leading to the development of

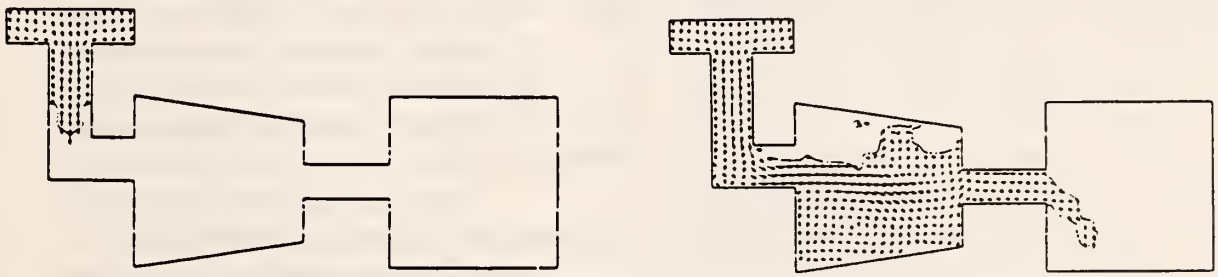

COMMIX can track the gas/liquid interface during the filling of a casting mold.

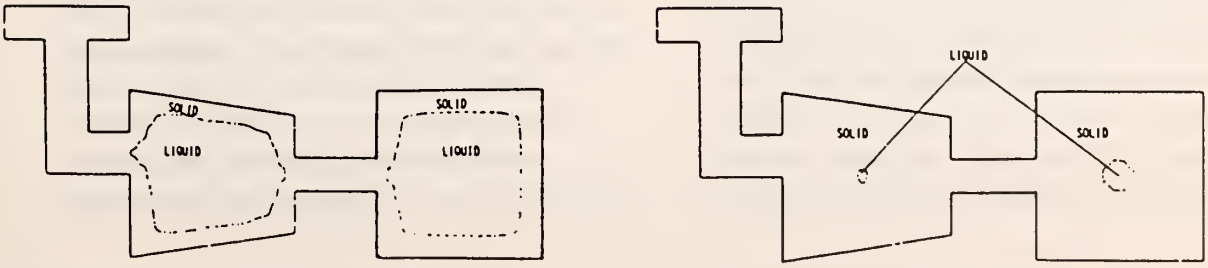

The modeling results can show the solidification front in a casting mold.

computer-aided design and the fabrication of near net-shape products.

Argonne National Laboratory has developed a state-of-the-art computer program called COMMIX that can model complex fluid flow and heat transfer--the primary phenomena involved in casting. COMMIX was developed with funding from the U.S. Nuclear Regulatory Commission, U.S. Department of Energy, and Electric Power Research Institute over the past ten years to describe fluid flow and heat transfer in reactor cooling systems. The cumulative cost for the development and validation is approximatley ten million dollars. COMMIX was developed to analyze nuclear reactor systems, but is a general-purpose, well-tested code that can be used to analyze a wide variety of heat transfer and fluid flow phenomena in other complex industrial systems. It is currently used by more than 50 industrial and research organizations.

COMMIX can readily be applied to model the complex shapes inherent in casting. It can be used for any material to produce any shape or size of casting. The modifications needed to describe stages of the casting process can be done relatively easily, quickly, and inexpensively. The basic formulation of COMMIX is better suited to complex geometrical shapes than are other finite-volume fluid-flow/heat transfer codes.

Argonne is working in partnership with Lester B. Knight and the Department of Energy to form a consortium to develop COMMIX as a design tool for the casting industry. Briefings have been given to a number of major casting firms with the proposal to jointly fund a two-year program to develop a generic code. A Phase III program will involve a series of proprietary studies with individual firms to tailor the code to their specific needs.

Additional Information

Key Words: metal casting, manufacturing processes, multicomponent flow, fluid flow, heat transfer

Patent Status: There is no patent on the application of COMMIX to metal casting at this stage of development.

Potential Applications/Spinoffs: None.

Literature Fluid and Heat Transfer Modeling for Castings. H. M. Domanus, Y. Y. Liu, and W. T. Sha. Proc. of Modeling and Control of Casting and Welding Processes, Santa Barbara, CA, Jan. 12-17, 1986.

For More Information: Contact the Technology Transfer Center, Argonne National Laboratory, 9700 S. Cass Ave., Argonne, IL 60439 (312/972-7694).

Department of Energy

Technology Application

Oak Ridge National Laboratory

Computer Software

ADVANCED SOFTWARE FOR THE EFFICIENT MANUFACTURE OF COMPLEX INDUSTRIAL CASTINGS

Key words: Casting; software; coordinate measuring machine; high-precision measurement; numerically controlled machining

Specialized computer programs developed at Martin Marietta Energy Systems, Inc., extend the capabilities of coordinate measuring machines (CMMs), casting technology, and numerically controlled machine tools. These programs were developed and applied during the construction of the Advanced Toroidal Facility torsatron, a new fusion plasma device. They were first used in the production of near net-shape castings of complex, massive stainless steel parts (Fig. 1). They have also been used to machine these parts on a five-axis milling machine, which has greatly reduced setup and machining times.

A three-dimensional surface can be measured with a CMM, but telling whether a part is acceptable poses a challenge when the part has no reference surfaces and no parts that are exactly correct. These programs compare data from measured parts with an ideal shape defined in the computer using mathematical "springs" (the spring force law). These springs are placed between the data from the measured part and the ideal part, and the coordinates of the measured part are rotated and translated until the energy in the springs is minimized. This comparison reveals whether the ideal shape can be found within the actual measured casting. The methods developed to apply these programs consist of three basic parts.

First, a program was developed to allow the CMM to automatically measure a complicated part so that exact placement of the part is not critical. Second, in the computer, the measured data were compared to the shape of an ideal part to establish the best fit for that part. This knowledge allowed modification of the moulds for the castings, as well as biasing the fit of the part to emphasize certain properties. For example, the parts in Fig. 1, cast to within the required tolerance of $\pm \frac{1}{8}$ in., required no surface machining. However, because of a design change, more room was required. The part's shape was repositioned in the computer to suit the design change.

Third, for machining, each part was approximately positioned in a five-axis milling machine. The concept of "floating datum," as embodied in a set of tooling balls affixed to the part, was used to position the part so that it fit and so that the machine itself measured the location of the tooling balls. A new computer tape was made with these data. The new tape quickly supplied revised milling instructions and

eliminated the need for long setup time. Tolerances of 1 mil were achieved over the 7-ft parts in this way.

Applications for these techniques are numerous:

- precision casting of large parts,
- accurate measurement of castings and other parts lacking reference sufaces,
- precision machining of difficult parts, and
- automatic measurement with CMMs.

Additional information:

Office of Technology Applications
Information Service
Martin Marietta Energy Systems, Inc.
P.O. Box X
Oak Ridge, TN 37831
Telephone: (615) 574-4192; FTS 624-4192

Fig. 1. Stainless steel support Ts for the Advanced Toroidal Facility torsatron. During machining, most of the metal was removed from the "nose" of each T to suit a design change. The actual surfaces of the Ts were barely skimmed by the cutter. Each piece was machined in 4 h.

NASA Tech Brief
National Aeronautics and Space Administration

Allocating Spare Parts in Complicated Systems

Assortments are analyzed for cost effectiveness and effects on system functionality.

The Eisenberger-Maiocco algorithm (EMA) is an efficient Markov algorithm to aid in the provision of spare parts. Two calculations are performed by EMA: (1) forecasting the availability of a system with a given pool of spare parts and (2) determining the most cost-effective assortment of spares. EMA was used in NASA's Deep Space Network project to calculate the probability that a system would continue to function with the spares available at each location.

The system to be analyzed is defined in terms of modules, which are any pieces of equipment that may fail, be repaired, or be replaced. A module can be in one of three states: (1) working, (2) spare, or (3) failed and waiting for repair. For each module type in the system configuration, there is an actual number in use by the system and a minimum number for the system to function. A module type is considered "down" (that is, failed) when there are fewer than the required minimum number working, and there are no spares in the stockpile.

The input to EMA includes such module data as the mean time between failures, the mean time to repair, the number of spares, and the cost of each item. EMA determines the overall system availability, or uptime ratio, as the probability that the system will function during a given time. EMA can also calculate the most cost-effective assortment of spares for a given range of uptime ratios.

EMA is written in interpreter PC-BASIC and is for interactive execution. It has been implemented on an IBM PC-series computer operating under DOS 2.0 with a central-memory requirement of approximately 64K of 8-bit bytes. This program was developed in 1978.

This program was written by I. Eisenberger, G. Lorden, Fredric Kajikawa, F. Maiocco, Jodie Gunn, and Ethel Kameyama of Caltech for **NASA's Jet Propulsion Laboratory**. *NPO-16973 /TN*

FOR ADDITIONAL INFORMATION *CONTACT:*

COSMIC®
112 Barrow Hall
University of Georgia
Athens, GA 30602
(404) 542-3265

Materials

500 Cellulose III Cotton Fiber Resists Abrasive Wear (Licensing Opportunity)

501 Superplasticity in Aluminum-Base Alloys

502 Data Management System for Materials Sciences

503 Corrosion Data on Cable Shielding Published

504 Testing Long-Term Exposure to Vacuum — A laboratory facility enables storage of materials under controlled vacuum conditions.

505 Numerical Simulation of Silicon-Ribbon Growth — A mathematical model includes nonlinear effects.

506 Determination of Grain-Size Distributions — Images of microstructures are analyzed by transform methods.

507 Effects of Radiation on Insulators — Data have been compiled on a variety of thermosetting and thermoplastic polymers.

508 Temperature, Humidity, and Polymer Aging — A theoretical basis is found for an empirical equation.

509 Galvanic Corrosion in (Graphite/Epoxy)/Alloy Couples — Some alloys need protection against corrosion in salt water.

510 Optimization of Processing of Si_3N_4 — Process changes are iterated under the guidance of x-radiography.

511 Lubrication Handbook for the Space Industry — Properties and application data are given for over 500 solid and liquid lubricants.

512 Microstructure and Weld Cracking in Inconel 718* — Theories on the relationship between metallurgy and microfissuring are confirmed.

513 Polyarylene Ethers with Improved Properties — Ease of processability and mechanical properties generally exceed those of commercial materials. (Licensing Opportunity)

514 Stronger Fire-Resistant Epoxies — A new curing agent improves mechanical properties and works at a lower temperature. (Licensing Opportunity)

Testing & Instrumentation

515 Laser Sensors Used to Detect Material Vibration — Vibrations of Less Than One Micron are Measured

Other Items of Interest

491 Novel Vapor-Deposited Lubricants for Metal-Forming Processes

528 Alternative Refrigerants

542 Field Repair of Thermoplastic Windows and Canopies — A hand-held induction heater makes quick and easy repairs.

United States Department of Agriculture

Research Technology
Agricultural Research Service

Cellulose III Cotton Fiber Resists Abrasive Wear

The quest to improve on nature has led scientists to such well-known innovations as durable-press, fire-resistant, and stain-release finishes for cotton textiles. One of the latest fibers developed in the laboratory is a rare crystalline form of cellulose that promises to improve durable-press cotton's resistance to wear. The fiber, derived from native cotton and termed Cellulose III, also affords good permeability to dyes, pigments, and other textile chemicals, a help in dyeing and processing.

The fiber begins as plain cotton cellulose, selected from fiber, yarn, or fabric. It is treated with ammonia vapors at high temperature and pressure until its crystalline structure changes. Interatomic distances within the fiber are altered, converting the original Cellulose I into a new, highly stable crystalline form of Cellulose III. The changes in geometric configuration can be observed by X-ray diffraction.

Crystalline Cellulose III can itself be immersed in ethylenediamine and then boiled in dimethylformamide. This will convert it to Cellulose IV, yet another crystalline configuration of interest to scientists; it is stable for only a short period of time before reverting to its original form.

Although laboratory methods for producing these crystalline substances are too costly for manufacturers, less expensive ways to mass produce the substance are being sought. Since Cellulose III can add strength to durable-press cottons, it may be a component of tomorrow's cotton durable-press fabrics.

For technical information, contact Timothy A. Calamari or Lawrence Yatsu, USDA-ARS, Southern Regional Research Center, 1100 Robert E. Lee Blvd., P.O. Box 19687, New Orleans, LA 70179. Phone (504) 286-4265. *Patent Application Serial No. 07/063,357, "Stable Crystalline Cellulose III Polymorphs."*

For inquiries concerning rights for the commercial use of this invention should be addressed to

Office of Federal Patent Licensing
Center for the Utilization of Federal Technology
Room 13R, NTIS
Springfield, VA 22161; (703) 487-4738

Refer to Patent Application 7-063,357/TN

Superplasticity in Aluminum-Base Alloys

An investigation of superplasticity in advanced aluminum-base alloys is in progress at the University of California. A recent report on this study, which is being supported by the Air Force Office of Scientific Research, presents a brief summary of current results as well as an outline of future work plans.(2)

The superplastic behavior in an Al-2.6Cu-2.4Li-0.2Zr-0.07Fe alloy has been determined as a preliminary step in determining the effects of hydrostatic pressure on cavitation and enhanced plasticity. The results of tests conducted at atmospheric pressure are shown in Figure 1a in which tensile elongation at 840 F is plotted as a function of strain rate. Maximum elongation was measured at a strain rate between 10^{-3} and 10^{-4} per second. Examination of these specimens indicated that both grain boundary sliding and grain rotation had occurred.

The superplastic behavior of mechanically alloyed 1N91211 is shown in Figure 1b. This alloy showed enhanced plasticity at much higher strain rates than observed in the Al-Li alloy. Similar behavior was also observed in a 2124 powder metallurgy alloy containing a dispersion of SiC whiskers. Future work on these two alloys will consist of additional measurements of plasticity at strain rates between 10^{-3} and 10^{2} per second, load relaxation studies, and measurements of creep behavior. Microstructural studies will be conducted to determine the contribution of cavitation and dislocation motion to enhanced plasticity.

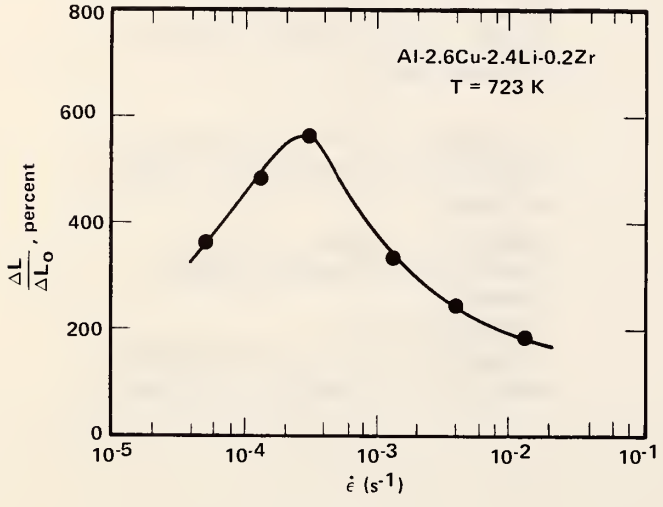

a. Aluminum-lithium alloy

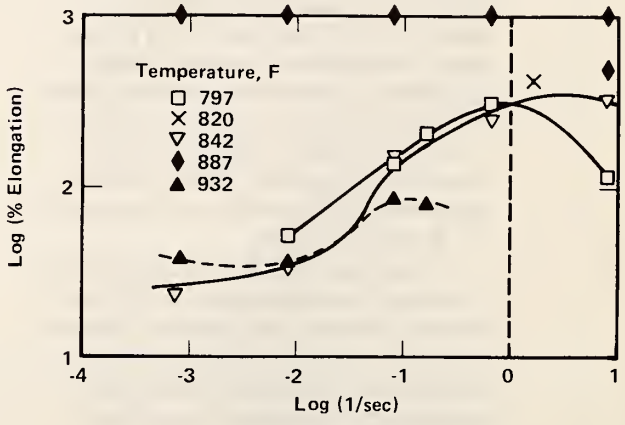

b. Mechanically alloyed IN90211

Figure 1. Tensile Elongation as a Function of Strain Rate for Two Aluminum Alloys

FOR ADDITIONAL INFORMATION:

A full description of this activity is contained in a backup report which may be purchased from NTIS, Springfield, VA 22161; (703) 487-4650.

NTIS order number: AD-A179651/NAC
Price code: A03

Lawrence Berkeley Laboratory

Data Management System for Materials Sciences

A prototype computerized information system that improves accessibility to scientific data on material properties has been designed by scientists with the Lawrence Berkeley Laboratory.

Called MIST -- Materials Information for Science and Technology -- the prototype system provides easy access to the most up-to-date data on the properties of metallic alloys. Designed by researchers in LBL's Information and Computing Sciences Division, MIST demonstrates what could be done for other scientific disciplines too.

The development of MIST is part of a joint effort by the U.S. Department of Energy and the National Bureau of Standards to increase scientific and engineering productivity in this country through better dissemination of research data. Leading the work at LBL is computer scientist John McCarthy.

"Major strides have been made during the past three decades to help scientists and engineers keep up with the data explosion," says McCarthy. "Certain fields, such as chemistry, have developed sophisticated systems of retrieving computerized information, and other fields, such as molecular biology, have developed mechanisms for shared access to experimental data. In many scientific disciplines, however, data is piling up and we don't know how to store and index it to make it available to a broad community of scholars.

McCarthy and his colleagues began the designing of MIST by surveying scientists and engineers from several of DOE's national laboratories to determine user needs.

"We also looked into features that would be useful to other areas of science as well," he says.

A big problem they found was diversity -- in nomenclature (dozens of different names for any one thing), in the form in which existing data has been recorded, and in the level of computer expertise among the system's potential users.

Two other major issues that needed to be addressed involved "meta-data," descriptions which help users and computer programs understand and manipulate the data being described, and "decentralization," means by which data can be entered into the system from a number of sources but still be standardized.

In meeting these challenges, the LBL computer scientists designed into MIST an active thesaurus and glossary to handle the diverse nomenclature; standardized representation of data and meta-data; automatic conversion of units of measurement; and multiple interfaces, including terse commands for experts and menus that lead beginners through the system step-by-step.

MIST offers many other desired features as well. For example, users can search for data by different material designations, property names, and independent variable specifications. Retrieved data can be displayed or down-

loaded in a variety of formats -- including facsimiles of published tables or graphs as they appear in scientific handbooks. Users also have access to the thesaurus and glossary at all times, for definitions of terms and cross-references. Flexibility has also been built into the system to permit the data base to evolve and expand.

A number of national and international organizations input the data now contained in MIST. To coordinate this far-flung effort, LBL's computer scientists provided an ongoing electronic mail-based computer conference. On the agenda for MIST's future is the establishment of regular mechanisms by which any of the different groups around the country that gather this sort of information can enter data as it comes in so that MIST will contain the most recent experimental results.

MIST was implemented on SPIRES, a database management system, developed at Stanford, which runs on IBM mainframes. McCarthy and Benson are now designing an advanced workstation interface to MIST using Apple Macintosh computers. Initiated and supported in part by Sandia National Laboratory, this work should open the way for MIST to be interfaced with other computer workstations in the future.

FOR ADDITIONAL INFORMATION:

Public Information Department, Lawrence Berkeley Laboratory, 1 Cyclotron Road, Berkeley, CA, 94720; (415) 486-5771.

NBS technology update

National Bureau of Standards
U.S. Department of Commerce
Gaithersburg, MD 20899

Corrosion Data on Cable Shielding Published

The increase of underground telephone cable installations has created a demand for information on the corrosion of shielding materials. Corrosion Evaluation of Underground Telephone Cable Shielding Materials (NBSIR 87-3546) reports on the performance of various underground cable systems after exposure for up to 7 years. For the study by NBS and the Rural Electrification Administration, 48 different shielding systems, incorporating either metal or plastic-coated metals, were placed in six soil environments. Some specimens were prepared with portions of the outer jackets damaged to simulate what could occur in actual field installations. Others were electrically coupled to copper strips to create a galvanic cell between the copper and noncopper shield materials. The data show that for specimens buried up to 7 years, few were resistant to corrosion in all of the soils.

FOR ADDITIONAL INFORMATION:

A full description of this activity is contained in a backup report which may be purchased from NTIS, Springfield, VA 22161; (703) 487-4650.

NTIS order number: PB88-153788/NAC
Price Code: A06

NASA Tech Brief
National Aeronautics and Space Administration

Testing Long-Term Exposure to Vacuum

A laboratory facility enables storage of materials under controlled vacuum conditions.

A facility for studying the long-term effects of vacuum on materials is described in a report. The facility was built for testing specimens of materials used in solid-rocket motors, including propellants, casings, insulators, and liners.

The vacuum storage system maintains specimens at constant temperature and high vacuum. It enables the specimens to be removed easily and safely for analysis. It includes six canisters connected to a vacuum manifold. Samples of outgassing products from the specimens are collected on salt plates cooled to 50 °F (10 °C).

A nitrogen storage system maintains specimens at 77 °F (25 °C) in pure, dry nitrogen gas under a gauge pressure of 2 to 4 psi (14 to 28 kPa). It enables the comparison of control specimens with specimens exposed to the vacuum. It, too, consists of a set of canisters.

The canisters are maintained at the constant temperature of 77 ± 5 °F (25 ± 3 °C) by circulating heated water that flows through jackets on the canisters. An instrumentation-and-control system measures and records the operating parameters and generates control signals and alarm indications as necessary.

This work was done by D. L. Clark, Charles E. Forsyth, Thomas L. Rerucha, and William J. Arbegast, Jr., of Martin Marietta Corp. for **NASA's Jet Propulsion Laboratory**. *To obtain a copy of the report, "In-Situ Vacuum Effects Testing of Solid Rocket Motor Materials," NPO-16944 /TN*

FOR ADDITIONAL INFORMATION: *Contact: Director, Technology Transfer Division, P.O. Box 8757, BWI Airport, MD 21240; (301) 621-0100 Ext. 241*

REFER TO THE NUMBER LISTED AT THE END OF THIS ARTICLE

NASA Tech Brief
National Aeronautics and Space Administration
NASA's Jet Propulsion Laboratory, Pasadena, California

Numerical Simulation of Silicon-Ribbon Growth

A mathematical model includes nonlinear effects.

A mathematical model in development will simulate the growth of a silicon ribbon from a melt. Unlike previous models, this one takes account of the entire temperature and stress history of the ribbon. The material history is important because it strongly affects the achievable quality and growth rate of the product. Numerical simulations performed with the new model will help in the search for the temperature distribution, pulling speed, and other conditions that favor the growth of wide, flat, relatively defect-free silicon ribbons for solar photovoltaic cells at economically attractive, high production rates. The model is also applicable to materials other than silicon.

Silicon ribbons can be grown in widths of up to 2 cm and at speeds of up to 1 cm/s. At greater widths or speeds, ribbon growth tends to become unstable at the ribbon/melt interface, ribbons tend to buckle transversely to the direction of growth, and residual stresses cause both shattering during cutting and dislocations in crystal structure that degrade electrical efficiency. For realistic numerical simulations, the model takes account of the accumulation of thermal and mechanical changes that cause these deleterious effects.

The ribbon is treated as a plane membrane so that the problem can be simplified to two dimensions. The two-dimensional stress/strain equations include the effects of elastic, plastic, and creep strains; total displacements; thermal expansion; and gravitation (see figure). In practice, the gravitational stress is negligible. The thermal components of strain are expressed in terms of the temperature distribution and the coefficients of thermal expansion. The tendency toward buckling is evaluated in the usual way, by seeking the solution for ribbon bending in the presence of in-plane stresses only.

To simulate the highly nonlinear effects of plasticity, the model must include the following:

- A criterion to determine whether the material has yielded;
- A flow rule to compute the incremental plastic strain;
- A hardening rule to follow the stress-included changes of the yield surface;
- A rule for the temperature dependence of the yield stress (see figure) to follow the changes of the yield surface with temperature; and
- A rule for the annealing mechanism to compute the dissipation of accumulated plastic strains.

The creep loading is related to the viscous behavior of silicon at high temperatures. The simulation incorporates the Sumino model of silicon viscosity, which expresses the creep rate in terms of the temperature, the dislocation density, and other parameters dependent on the material.

The combined equations for the stresses, strains, displacements, and temperature distribution are placed in finite-spatial-element form, with spatial and temporal thermal boundary conditions. At each time step, the position of the ribbon (and consequently the boundary and solution domain) is incremented to simulate the ribbon motion, and the spatial solutions are obtained. For the history-dependent quantities, the increments at each time step are accumulated.

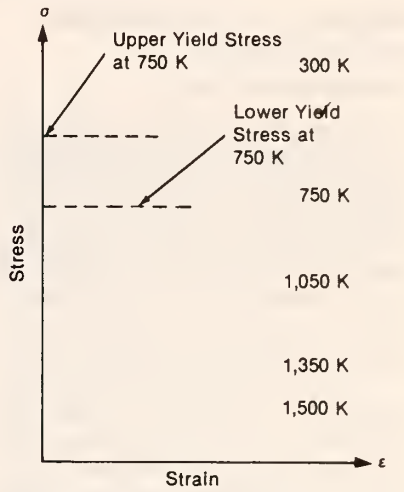

The **Stress-vs.-Strain** relationship of silicon is highly nonlinear and temperature-dependent in the high-temperature, plastic-flow region.

This work was done by Ben K. Woda, Chin-Po Kuo, Senol Utku, and Sujit Kumar Ray of Caltech for **NASA's Jet Propulsion Laboratory**. *NPO-16805 /TN*

FOR ADDITIONAL INFORMATION: *Contact: Director, Technology Transfer Division, P.O. Box 8757, BWI Airport, MD 21240; (301) 621-0100 Ext. 241*
REFER TO THE NUMBER LISTED AT THE END OF THIS ARTICLE

NASA Tech Brief
National Aeronautics and Space Administration

Determination of Grain-Size Distributions

Images of microstructures are analyzed by transform methods.

A report discusses the determination of the distributions of grain sizes by the analysis of images of microstructures. Such material properties as tensile strength, hardness, yield stress, fracture stress, and resistance to impact are influenced by grain-size distributions. Thus, analyses of material properties can benefit from detailed knowledge of grain-size distributions.

The shapes of grains are generally so complex that determination of grain-size distributions by current techniques are crude and imprecise. Estimates of the mean or average grain diameter can be determined from the grain-size distribution.

A theory is developed to relate the density of frequency components to the density of length components. The density of length components corresponds directly to the grain-size distribution function, from which the mean shape, size, and orientation of the grains can be obtained.

The two-dimensional gradient of a microstructure is tone-pulse encoded. The encoded image is subsequently Fourier transformed to determine the density of frequency components $F(s,\phi)$. The spatial density of length components $P(r,\phi)$ (grain-size distribution) can be determined directly from the density of frequency components $F(s,\phi)$ using the relation

$$|P(r',\phi)| = |F(s,\phi)|s$$

where ϕ is the angle of a point in polar coordinates; $s = 1/r'$; $r' = (x^2 \times y^2)^{1/2}$; and x and y are the horizontal and vertical coordinates, respectively.

Once $P(r',\phi)$ is determined, the mean grain size, shape, and orientation are obtainable from

$$D(\phi) \equiv \sum_{r'} |P(r',\phi)| r' / \sum_{r'} |P(r',\phi)|$$

Extensions of this work are continuing to examine porosity-size distributions in ceramics and fiber-spacing distributions in composites. The results of these studies may prove useful in the automotive, aerospace, aeronautical, nuclear, and construction industries.

This work was done by Edward R. Generazio of **Lewis Research Center.** *Further information may by found in NASA TM-88790 [N86-31065/NSP], "Determination of Grain Size Distribution Function Using Two-Dimensional Fourier Transforms of Tone Pulse Encoded Images."*

Copies may be purchased from the National Technical Information Service, Springfield, Virginia 22161, [A02] LEW-14508./TN

FOR ADDITIONAL INFORMATION: *Contact: Director, Technology Transfer Division, P.O. Box 8757, BWI Airport, MD. 21240; (301) 621-0100 Ext. 241*
REFER TO THE NUMBER LISTED AT THE END OF THE ARTICLE

NASA Tech Brief
National Aeronautics and Space Administration

Effects of Radiation on Insulators

Data have been compiled on a variety of thermosetting and thermoplastic polymers.

A report presents data on the responses of electrically insulating thermosetting and thermoplastic polymers to radiation. The lowest-threshold-dose (LTD) levels and the 25-percent-change levels are presented for such properties as tensile strength and electrical resistivity. Data on radiation-induced outgassing are also given.

The author notes that microscopic changes in insulators are indicated by changes in the macroscopic physical properties and that the LTD is an important indicator of the dose level at which the changes start to occur. For comparisons of the sensitivities of different materials to radiation, a consistent LTD should be used. The author proposes that the LTD be defined as that which produces a 1-percent change in the physical property of interest.

The tensile strengths of some insulators increase initially, even after the LTD is reached. The material becomes stronger because of cross-linking. In such cases, an "engineering-threshold-dose" can be used in comparing materials for design purposes. The author defines the engineering threshold dose as the dose that causes the property in question to decrease to a value 1 percent below the value before irradiation. LTD's sometimes vary with temperature or other condition of the insulating material.

Such effects as outgassing are known to be nonlinear even in the absence of radiation. This suggests that the LTD's for outgassing are probably nonlinear too.

This work was done by Frank L. Bouquet of Caltech for **NASA's Jet Propulsion Laboratory**. *To obtain a copy of the report, "Thresholds of Radiation Effects on Insulators," NPO-17032 /TN*

FOR ADDITIONAL INFORMATION: *Contact: Director, Technology Transfer Division, P.O. Box 8757, BWI Airport, MD. 21240; (301) 621-0100 Ext. 241*
REFER TO THE NUMBER LISTED AT THE END OF THE ARTICLE

NASA Tech Brief
National Aeronautics and Space Administration

Temperature, Humidity, and Polymer Aging

A theoretical basis is found for an empirical equation.

A report presents an analysis of experimental data on the electrical resistivity of a polymer (polyvinyl butyral) as a function of temperature and relative humidity. The resulting theoretical expression for the electrical resistivity (or its reciprocal, conductivity) resembles a generally accepted empirical law for the corrosion rate (or its reciprocal, lifetime).

The author begins by noting that experimentally the electrical resistivity at zero relative humidity obeys an Arrhenius relationship with an activation energy of 11.243 kcal/mole. Semilog plots of resistivity versus temperature at other values of relative humidity are found to be nearly parallel, and prompt an examination of the hygroscopic properties of the material in question. When replotted, the data show that at a given temperature the logarithm of resistivity decreases linearly with the relative humidity, suggesting that the electrical resistivity decreases with increased water absorption.

The concentration of water absorbed in the polymer is assumed to be proportional to the vapor pressure of water in the air and to an Arrhenius temperature-dependence factor characterized by an activation energy for water-vapor absorption. Plots of resistivity versus water-vapor pressure at fixed temperatures have temperature-dependent slopes that can be fit by least squares to such an Arrhenius factor with an activation energy of 9.23 kcal/mole.

Next, the vapor pressure is expressed as the product of the relative humidity and the saturation vapor pressure, which is governed by yet another Arrhenius equation and the parameters of which are well known from previous measurements. This relationship is inserted in the equation that describes the plot of electrical resistivity versus water-vapor pressure. After a Taylor-series expansion about the absolute temperature of 273 K (0 °C) and neglect of small higher-order terms, the equation has the form

$$\ln \rho(t,\text{R.H.}) = A - k_1 t - k_2 (\text{R.H.})$$

where ρ = electrical resistivity, t = temperature in °C, R.H. = relative humidity, and A, k_1, and k_2 are constants.

The form of this equation is the same as that of the empirical equation for the corrosion lifetime. The author points out that this suggests a relationship between leakage currents and corrosion in insulating materials. It may be possible to define the corrosion lifetime as the time during which a specified amount of charge is transferred through leakage. In that case, the equation would be experimentally associated with the correlation among lifetime, relative humidity, and temperature.

This program was written by Edward F. Cuddihy of Caltech for **NASA's Jet Propulsion Laboratory**. *To obtain a copy of the report, "Aging Correlation Between Corrosion Lifetime and Relative Humidity and Temperature,"*
NPO-16908 /TN

FOR ADDITIONAL INFORMATION: *Contact: Director, Technology Transfer Division, P.O. Box 8757, BWI Airport, MD. 21240; (301) 621-0100 Ext. 241*
REFER TO THE NUMBER LISTED AT THE END OF THE ARTICLE

NASA Tech Brief
National Aeronautics and Space Administration

Galvanic Corrosion in (Graphite/Epoxy)/Alloy Couples

Some alloys need protection against corrosion in salt water.

The effects of a galvanic coupling between graphite/epoxy composite material (G/E) and D6AC steel, 6061-T6 aluminum, and Inconel* 718 nickel alloy in salt water are described in a report. An introductory section of the report summarizes previous corrosion studies of G/E with other alloys. The details of sample preparation are presented along with photographs of the samples before and after immersion.

The tests were conducted in aqueous 3.5-percent NaCl solutions at 22 °C. In the experiments requiring electrical contact between the G/E and the alloy, bolts of a stainless steel previously found to be compatible with G/E were used to hold the G/E and metal specimens in contact.

The corrosion potentials of the alloys were measured with respect to a saturated calomel electrode. Galvanic currents were measured with a corrosion-measurement console. The corrosion rates of the alloy specimens were calculated from the weight losses and immersion times.

The measurements show that the steel and aluminum alloys require protection against corrosion when they are galvanically coupled to G/E in salt water, while the nickel alloy is relatively unaffected and is compatible with G/E. The study also shows that the aluminum alloy is effective as a sacrificial anode, providing cathodic protection to the steel when both are galvanically coupled to G/E.

The report also describes six tests of methods of protecting the steel and aluminum alloys against galvanic corrosion. When the G/E is completely coated with paint or a paint/polyurethane resin combination, the steel is adequately protected by either a zinc-rich primer with a final coat of grease or by a primer/topcoat combination with a final coat of grease. The aluminum is protected by epoxy chromate primer/epoxy paint, with a final coat of grease. However, the grease may not be necessary in the case of the aluminum.

*Inconel is a registered trademark of the Inco family of companies.

This work was done by Merlin D. Danford and Ralph H. Higgins of **Marshall Space Flight Center**. *Further information may be found in NASA TP-2236 [N84-13263/NSP], "Galvanic Coupling Between D6AC Steel, 6061-T6 Aluminum, Inconel 718, and Graphite-Epoxy Composite Material: Corrosion Occurrence and Prevention."*

Copies may be purchased from the National Technical Information Service, Springfield, Virginia 22161, [A02]
The report is also available on microfiche at no charge. MFS-27055 /TN

FOR ADDITIONAL INFORMATION: *Contact: Director, Technology Transfer Division, P.O. Box 8757, BWI Airport, MD. 21240; (301) 621-0100 Ext. 241*
REFER TO THE NUMBER LISTED AT THE END OF THE ARTICLE

NASA Tech Brief
National Aeronautics and Space Administration

Optimization of Processing of Si_3N_4

Process changes are iterated under the guidance of x-radiography.

Silicon nitride is a prime candidate for heat-engine applications because of its resistance to oxidation and thermal shock and its strength at room and high temperatures. However, scatter in mechanical properties is a great disadvantage for design and reliability. This scatter is attributed to defects and inhomogeneities that occur during the processing of Si_3N_4 powder compositions or during the fabrication of silicon nitride parts.

In recent work at NASA Lewis Research Center, density gradients in sintered silicon nitride, characterized by x-radiography, were identified and appeared strongly dependent upon powder-processing and sintering conditions. A NASA technical memorandum describes a systematic investigation, based upon this preliminary work, of density-gradient/flexural-strength relationships as affected by processing.

The results of this program showed that a sintered Si_3N_4 composition containing approximately 6 weight percent each of Y_2O_3 and SiO_2, developed by NASA and designated NASA 6Y, was significantly improved. The improvement over baseline material was accomplished by the iterative utilization of conventional x-radiography to characterize structural (density) uniformity as affected by systematic changes in powder processing and high-pressure, nitrogen sintering parameters. A dense-case/less-dense-core structure, revealed by x-radiography of the baseline material, was eliminated by incorporating wet sieving of powders and increasing powder-grinding time and by increasing sintering time, minimizing BN (boron nitride) setter contact, and adjusting the sintering height in the furnace.

Four-point flexural strengths of 125,000, 79,000 and 67,000 psi (860, 540, and 460 MPa, respectively) at room temperature, 2,200 °F (1,200 °C) and 2,500 °F (1,370 °C), respectively, represent improvements of 56, 38, and 21 percent over baseline NASA 6Y properties. Improved material uniformity and reliability were demonstrated by a threefold reduction in the standard deviation and a fourfold increase in the Weibull modulus at room temperature. Accompanying the improvement in strength was a change in the type of flaw causing failure, from a more strength-limiting flaw to a less strength-limiting columnar β-Si_3N_4 grain.

This work was done by William A. Sanders and George Y. Baaklini of **Lewis Research Center**. *Further information may be found in NASA TM-87251 [N86-31729/NSP], "Correlation of Processing and Sintering Variables with the Strength and Radiography of Silicon Nitride."*

Copies may be purchased from the National Technical Information Service, Springfield, Virginia 22161, [A03]
LEW-14456 /TN

FOR ADDITIONAL INFORMATION: *Contact: Director, Technology Transfer Division, P.O. Box 8757, BWI Airport, MD. 21240; (301) 621-0100 Ext. 241*
REFER TO THE NUMBER LISTED AT THE END OF THE ARTICLE

NASA Tech Brief
National Aeronautics and Space Administration

Lubrication Handbook for the Space Industry

Properties and application data are given for over 500 solid and liquid lubricants.

A 458-page handbook covers many of the solid and liquid lubricants used in the space industry. It will also be a useful reference in industrial and military applications of lubricants. Part A of the handbook is a compilation of data on the chemical and physical properties of over 250 solid lubricants, including bonded solid lubricants, dispersions, and composites. Similarly, part B covers over 250 liquid lubricants, greases, oils, compounds, and fluids.

Each part includes an introduction that describes the general characteristics of the various types of lubricants covered, a glossary, and tabulations of standard specifications (e.g., MIL, NASA, or ASTM specifications) and other test procedures. Part B also includes appendixes containing viscosity-conversion data, the international system of units, and conversion factors.

Lubricants and lubricant properties are arranged systematically so that designers, engineers, and maintenance personnel can conveniently locate data needed for their work. Cross-reference tables provide access to the data by types of lubricants, by applications, by product names, by manufacturers, and by specifications.

For each solid lubricant, the basic properties tabulated include compositions; suggested uses; compatibility with jet and other hydrocarbon fuels, solvents, liquid oxygen, and rocket fuels; and notes on such matters as usable temperature ranges, curing conditions, and tensile strengths. Also provided for many solid lubricants are data on methods of application, on resistance to radiation, on outgassing properties, on load capacity, on wear life, on coefficients of static and dynamic friction in air and vacuum, on electrical conductivities, on resistance to corrosion, and on weight losses in vacuum.

The properties listed for liquid lubricants vary from type to type. For lubricating oils, the properties listed generally include compositions (including additives), viscosities, specific gravities, flash points, fire points, pour points, stabilities under corrosion and oxidation, humidity-test results, neutralization numbers, evaporation percentages, carbon-residue percentages, colors, and precipitation numbers.

This work was done by Ernest L. McMurtrey of **Marshall Space Flight Center**.

in NASA TM-86556 [N86-31730/NSP], "Lubrication Handbook for the Space Industry."

Copies may be purchased from the National Technical Information Service, Springfield, Virginia 22161, [A19]

The report is also available on microfiche at no charge.

To obtain a microfiche copy, Circle 17 on the TSP Request Card.

MFS-27169 /TN

FOR ADDITIONAL INFORMATION: *Contact: Director, Technology Transfer Division, P.O. Box 8757, BWI Airport, MD. 21240; (301) 621-0100 Ext. 241*

REFER TO THE NUMBER LISTED AT THE END OF THE ARTICLE

NASA Tech Brief
National Aeronautics and Space Administration

Microstructure and Weld Cracking in Inconel 718*

Theories on the relationship between metallurgy and microfissuring are confirmed.

A report describes research on the effects of the microstructure on the cracking of heat-affected zones of welds in Inconel 718* alloy. In experimental studies, specimens were subjected to various combinations of time-varying thermal and mechanical stresses to simulate welding conditions and to identify the physical and chemical effects that cause microfissuring.

The report details specific correlations between microfissuring and grain size, Ni_3Nb (δ phase), hardness, $Ni_3(Al, Ti)$ (γ' phase), Ni_3Nb (γ'' phase), solution annealing heat treatment, and age-hardening heat treatment. Indirect correlations between microfissuring and impurity segregation are also presented.

The combined experimental results of this investigation and previous investigations appear to support a generalized theory of carbide liquation that explains the susceptibility to microfissuring. According to the theory, at sufficiently high temperature (but below the melting point of the alloy), liquid NbC forms along grain boundaries. The liquid NbC feeds Nb to the Ni-rich matrix, causing eutectic melting. Displaced by the additional molten material, the NbC spreads further along the grain boundaries, causing further melting. Under the strain imposed by welding, microfissures open to the liquid. When the alloy cools, Laves phases precipitate from the liquid along the microfissures.

The intergranular liquid distribution is controlled by the elements absorbed by the liquid from the grain-boundary region during the liquation and wetting process. Thus, the chemical composition of the grain-boundary region just before welding affects the susceptibility to microfissuring during welding. In particular, impurities appear to contribute to microfissuring. The susceptibility increases with the grain size because there is less grain-boundary area over which to spread the liquid, and the effect of the liquid is therefore magnified.

The chemical and microstructural alloy properties are determined by manufacturing processes and heat treatments. As a result of this research, the susceptibility to microfissuring of an alloy part to be welded can now be evaluated on the basis of its metallurgical properties and process history. Because an intergranular-liquid mechanism also appears to cause hot cracking in the Nb-bearing 347 stainless steel, the generalized theory may be important to all Nb-bearing Ni or Fe alloys.

*Inconel is a registered trademark of the Inco family of companies.

This work was done by R. G. Thompson of the University of Alabama for **Marshall Space Flight Center.** *To obtain a copy of the report, "Effect of Microstructure on Weld HAZ Cracking of Inconel 718," MFS-27121 /TN*

FOR ADDITIONAL INFORMATION: *Contact: Director, Technology Transfer Division, P.O. Box 8757, BWI Airport, MD. 21240; (301) 621-0100 Ext. 241*
REFER TO THE NUMBER LISTED AT THE END OF THE ARTICLE

NASA Tech Brief
National Aeronautics and Space Administration
Langley Research Center, Hampton, Virginia

Licensing Opportunity

Polyarylene Ethers With Improved Properties

Ease of processability and mechanical properties generally exceed those of commercial materials.

As part of an effort to develop improved composite matrices for potential use on aerospace vehicles, a series of new polyarylene ethers (PAE's) were prepared from the reaction of activated dihalo compounds with various bisphenols. These compounds exhibit excellent processability by compression molding, plus good mechanical properties.

The linear PAE's prepared are the polycondensation products from the reaction of either 1,3-bis(4-chloro or fluorobenzoyl) benzene or 1,4-bis(4-chloro or fluorobenzoyl) benzene with any one of the following bisphenolic compounds: bis(3-hydroxyphenyl) methane; bis(4-hydroxyphenyl) methane; 1,1-dimethyl-bis(4-hydroxyphenyl) methane; or 9,9-bis(4-hydroxyphenyl) fluorene. Measured number-average molecular weights for the PAE's range from 13,500 to 39,400 g/mole, and glass-transition temperatures vary from 114 to 243 °C. Ethynyl-terminated polyarylene ethers (ETPAE's) also were prepared by end-capping hydroxy-terminated PAE's with 4-ethynylbenzoyl chloride.

Composites, films, moldings, and adhesives were prepared. The physical and mechanical properties of the polymers were compared with those of commercially available PAE's. Some of the new PAE's exhibit high levels of thermoplastic flow and shear thinning and have use-temperature ranges that exceed those of commercially available materials. The fracture toughnesses of some PAE's are significantly higher than those of commercial materials. Some of the PAE's prepared are also insensitive to aggressive solvents and some have levels of crystallinity that should afford low coefficients of thermal expansion. The cured ETPAE's also exhibit excellent processability, high adhesive properties, and good resistance to hydraulic fluids.

All of the PAE's prepared are suitable for use as adhesives, coatings, films, membranes, and composite matrices. These materials show properties that make them potentially useful for both spacecraft and aircraft applications. The low coefficients of thermal expansion of some of the new PAE's should lead to improved dimensional stability for space structures, and their fracture toughnesses and excellent processability make them ideally suited for aircraft composites.

This work was done by Paul M. Hergenrother and Brian J. Jensen of **Langley Research Center** *and Stephen J. Havens of PRC Kentron, Inc.*

This invention is owned by NASA, and a patent application has been filed. Inquiries concerning nonexclusive or exclusive license for its commercial development should be addressed to the Patent Counsel, Langley Research Center Refer to LAR-13555./TN

Langley Research Ctr.
Hampton, VA 23665
Technology Utilization Officer: John Samos
Mail Stop 139A
(804) 865-3281
Patent Counsel:
George F. Helfrich
Mail Code 279
(804) 865-3725

FOR ADDITIONAL INFORMATION: *Contact: Director, Technology Transfer Division, P.O. Box 8757, BWI Airport, MD. 21240; (301) 621-0100 Ext. 241*
REFER TO THE NUMBER LISTED AT THE END OF THE ARTICLE

NASA Tech Brief
National Aeronautics and Space Administration
Ames Research Center, Moffett Field, California

Licensing Opportunity

Stronger Fire-Resistant Epoxies

A new curing agent improves mechanical properties and works at a lower temperature.

The use of aminophenoxycyclotriphosphazene curing agents yields stronger, more heat- and fire-resistant epoxy resins. Because the epoxies can be cured without solvents, the formation of voids is suppressed. However, the new curing agents can be used with solvent if necessary; for example, for coating fabrics or casting films.

Curing proceeds in stages at temperatures of 120 to 125 °C and 175 to 180 °C, followed by postcuring at 225 °C. A tough, brown polymer results. The curing reaction has been monitored by Fourier-transform infrared spectrometry and by differential scanning calorimetry and is well understood (see figure).

The cured resins are thermally stable up to about 350 °C. When burned, the cured resins yield usually high amounts of char, which is highly desirable for fire-resistant applications. The char yields in nitrogen at 800 °C range from 42 to 55 percent; in air at 700 °C they range from 32 to 40 percent.

Graphite-fiber-reinforced epoxy resins cured with the new agents have properties superior to those cured with such conventional agents as diaminodiphenylsulfone. For example, a laminate made with one of the improved formulations exhibited a tensile strength of 72,080 psi (497 MPa), whereas a similar laminate made with a commercial resin cured by diaminodiphenylsulfone had a tensile strength of 51,639 psi (356 MPa).

This work was done by George M. Fohlen and John A. Parker of **Ames Research Center** *and Devendra Kumar of the National Research Council.*

Inquiries concerning rights for the commercial use of this invention should be addressed to the Patent Counsel, Ames Research Center Refer to ARC-11548/TN

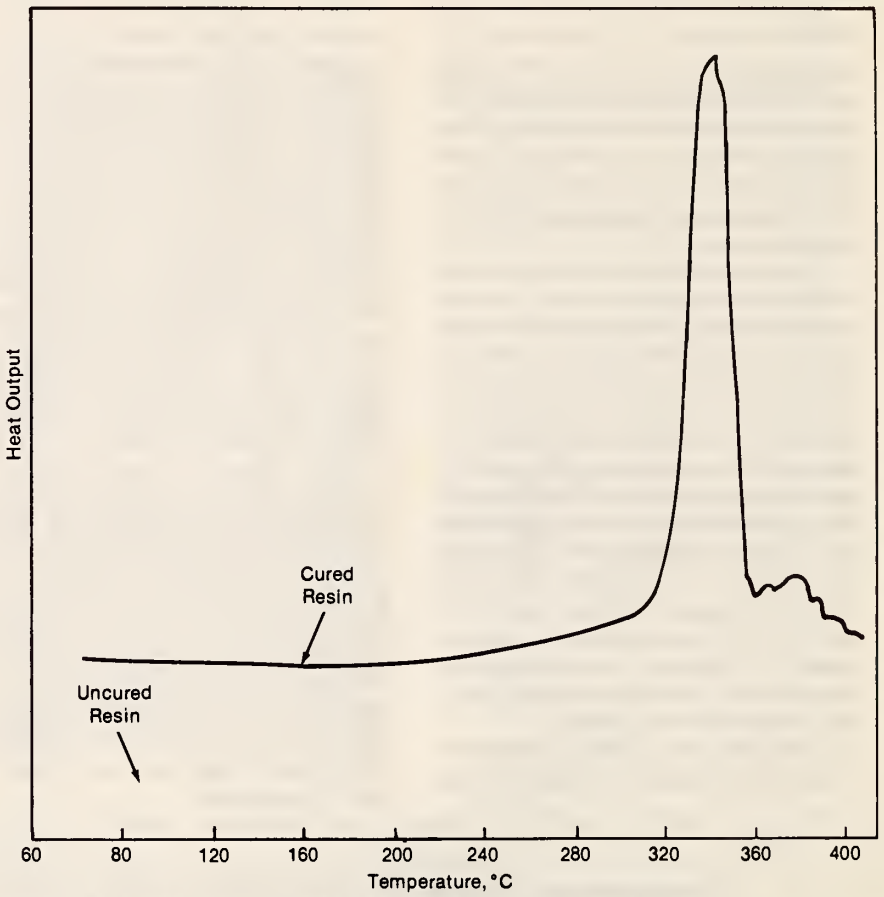

Thermograms Made by Differential Scanning Calorimetry show one exothermic peak for the cured and two exothermic peaks for uncured epoxy resin containing the new curing agent. The peak at 163 °C indicates the polymerization reaction (that is, curing) whereas the peak at 330 °C indicates decomposition. The polymerization takes place at a lower temperature than it does with other curing agents.

Ames Research Ctr.
Moffett Field, CA 94035
Technology Utilization Officer: Laurance Milov
Mail Code 223-3
(415) 694-6370
Patent Counsel:
Darrell G. Brekke
Mail Code 200-11
(415) 694-5104

FOR ADDITIONAL INFORMATION: *Contact: Director, Technology Transfer Division, P.O. Box 8757, BWI Airport, MD. 21240; (301) 621-0100 Ext. 241*
REFER TO THE NUMBER LISTED AT THE END OF THE ARTICLE

Laser Sensors Used to Detect Material Vibration

Vibrations of Less Than One Micron Measured

Scientists have demonstrated the potential for using acoustic vibration patterns to inspect thermal protection tiles used on space shuttle orbiters.

The research was conducted for NASA to develop an inspection technology for examining tiles following space shuttle flights to identify loose or damaged tiles. Initial research was focused on development of a technique using non-contacting laser sensors for detection of the tiles' vibrational response to acoustic signals. INEL laboratory studies to date have demonstrated that a laser sensor can be used to detect vibrational response and that loose or damaged tiles vibrate with different patterns than tiles without bonding defects or other damage.

The non-contacting laser technique involves the use of acoustic waves to cause small vibrations on a tile. These vibrations are sensed with a laser beam that is focused on the tile surface. The very small amount of light that is reflected from the tile is used to derive a signal that follows any surface displacement. A portable computer work station then collects and analyzes these signals to detect variations in the vibrational response of the tile to identify any abnormal conditions.

Using the technique, vibrations of less than one micron (one-millionth of a meter) in wavelength can be detected. The technique is especially suited for non-contacting field inspection of materials with dark rough surfaces such as the orbiter tiles. The laser sensors have other potential applications, particularly for inspecting complex materials used in the aerospace industry.

With the initial success of the project, NASA will fund additional work for theoretical studies and development of a portable sensor to demonstrate the feasibility of field inspections.

The ultimate goal of the project is to develop a practical field inspection system for NASA using non-contacting laser sensors. Because of the complex nature of the tiles and because inspection requires a non-contacting technique, conventional nondestructive examination (NDE) techniques haven't proven feasible, Barna says.

FOR ADDITIONAL INFORMATION:

Dr. Jane M. Welch, Manager, ORTA, Idaho National Engineering Laboratory, P.O. Box 1625, Idaho Falls, ID 83415; (208) 562-8318. Refer to DOE/INEL-029/TN.

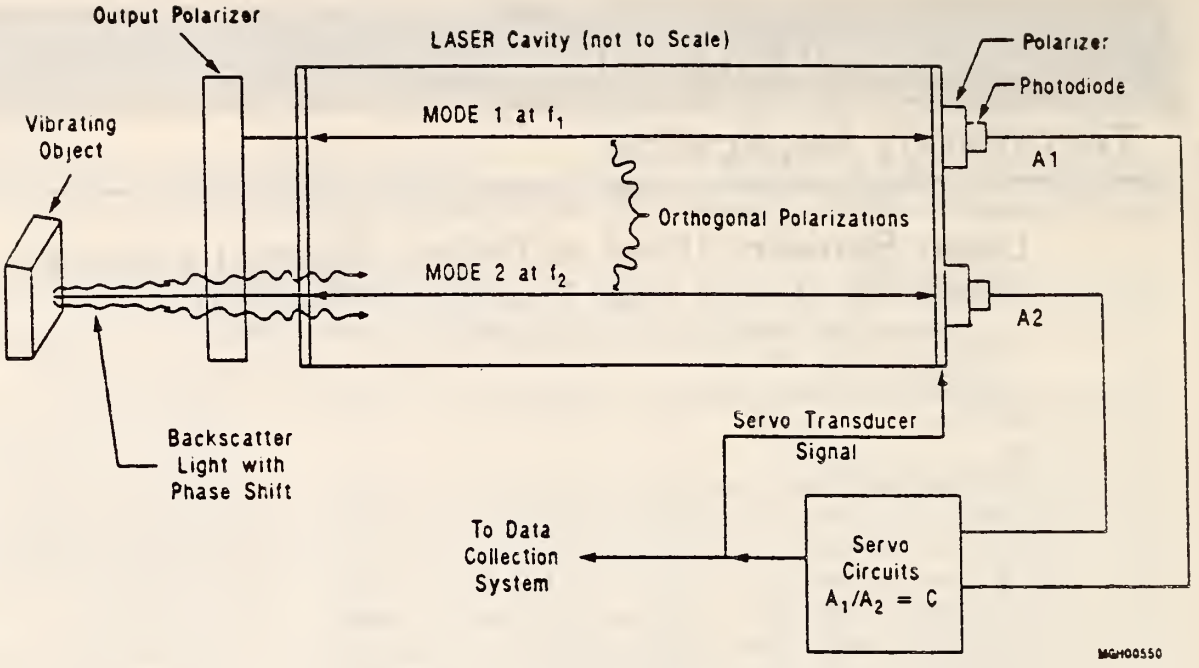

Stabilized laser--concept of operation.

Medicine & Biology

516 Three-Dimensional Electron Microscopy of Biologically Active Macromolecules

517 Arm-Powered Bicycle for the Disabled

518 Automatic Decomposition of the Electromyogram

519 Human Movement Monitoring System to Study Posture, Walking, and Jumping

520 Handbook on Animal Models Available

521 Powered Lift for Paraplegics — People with paralyzed legs ca transfer themselves to and from wheelchairs. (Licensing Opportunity)

Testing & Instrumentation

522 Fiber-Optics Flouroimmuno-Sensor

523 Biomolecular Interaction Analysis System (BIAS) — Using a microcomputer to extend chromatography techniques.

524 Holter Monitoring Predicts Effectiveness of Antiarrhythmia Treatment

525 Low Voltage Scanning Electron Microscope

Other Items of Interest

464 Public-Facilities Locator for the Blind — An optoelectronic system would enable blind people to find key places without assistance.

NIH
Research & Technology

Federal
Technology
Resource

U.S. Department of Health and Human Services Public Health Service National Institutes of Health

Three-Dimensional Electron Microscopy of Biologically Active Macromolecules

A newly developed, more powerful transmission electron microscope (400 kilovolts) -- in conjunction with a scanning microdensitometer for digitization of the information in the electron micrographs, a computer for data processing, and a graphics facility for interactive processing and map interpretation — is being used to explore the three-dimensional structure of biological macromolecules like interferon at levels approaching that of the atom. Identification of this structure is a critical step in understanding how these molecules attach and interact with other molecules, how they actually function within living organisms.

The medium high-voltage electron microscope and its ancillary equipment are being installed at the department of molecular and cellular biology and the department of biochemistry of the University of Arizona in Tucson.

The microscope resource is supported by the Biomedical Research Technology Resources Program of the NIH Division of Research Resources, as is a TV video image intensifier system and part of the cost of the computer system.

Two kinds of investigations are being undertaken with the new microscope. The first is high-resolution studies that focus on thin protein crystals, says Dr. Wah Chiu, associate professor of molecular and cellular biology and of biochemistry at the University of Arizona and principal investigator for the microscope project.

Many kinds of proteins cannot yet be made to form large crystals suitable for x-ray crystallography. These proteins are more amenable to examination with the electron microscope, which offers unique opportunities to obtain multiple high-resolution images that can be integrated by computer processing into a picture of the entire three-dimensional structure.

This research can be done with transmission electron microscopes at conventional voltages (up to 100 kilovolts). Under certain conditions, such as when the specimen is relatively thick, and particularly when it is tilted past a certain angle on the microscope stage, the assumptions of image contrast theory used to interpret the high resolution data collected at 100 kilovolts break down and the three-dimensional picture obtained is no longer reliable. Dr. Chiu notes that the 400-kilovolt instrument will enable researchers to obtain 3.5 angstrom data from specimens thinner than 300 angstroms that can be interpreted directly with existing image contrast theory

This means that the new microscope will have the capacity to resolve at a level of 3.5 angstroms the three-dimensional structure of proteins such as crotoxin, a neurotoxin that is one constituent in the venom of the Brazilian rattlesnake. At this level of resolution, the backbone of the protein molecule can be traced. Further resolution of the structure, to a level at which each atom can be identified (1.5 angstroms), can be done through the imaging process because this microscope has that resolving power.

Medium-resolution studies (10-50 angstroms) on larger biological materials such as viruses, chromatin fibers, and muscle filaments comprise the second type of research conducted with the microscope. Some of these specimens have a thickness close to 1,000 angstroms or more. This kind of investigation can be performed with conventional, lower-voltage transmission electron microscopes. However, the medium high-voltage electron microscope provides better contrast when imaging thick specimens because the higher energy electrons produce less chromatic aberration in the electron images.

An integral aspect of exploring the possibilities -- and limitations — of the medium high-voltage electron microscope is the development of special laboratory techniques for the preparation of specimens, along with several modifications to the conventional setup of the microscope to enhance the retrieval of high-resolution images and preserve the specimen in a chemical environment that is close to its natural state.

In line with the goal of keeping samples as close to their natural state as possible, Dr. Chiu works with unstained and unfixed specimens. The preparation technique involves quick freezing of the biological specimen in liquid ethane. The frozen specimen is then transferred with a specially built transfer device into the electron microscope, which is equipped with a cold stage. The frozen specimen embedded in a thin layer of amorphous ice is kept below – 150 degrees Celsius while it is studied in the electron microscope.

Dr. Chiu and his associate Dr. Tzyy-Wen Jeng built a high-resolution (3.5 angstroms) cold stage operated at – 150°C and an effective anticontaminator for their conventional (100 kilovolt) electron microscope, so this procedure has been used routinely in their laboratory. A high-resolution cold stage is being developed and will be added to the basic configuration of the 400 kilovolt electron microscope.

Photo courtesy of Dr. Wah Chiu

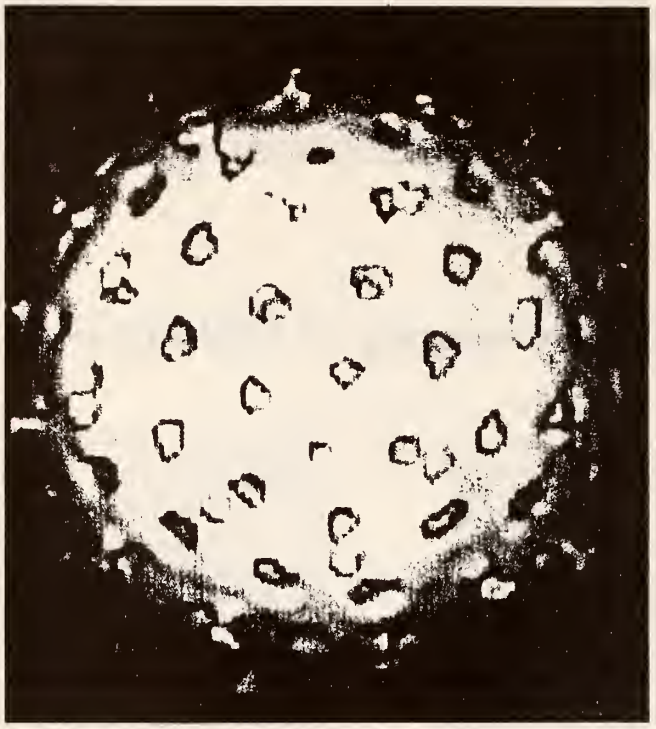

Photo courtesy of Dr. Wah Chiu and the *Journal of Virology*

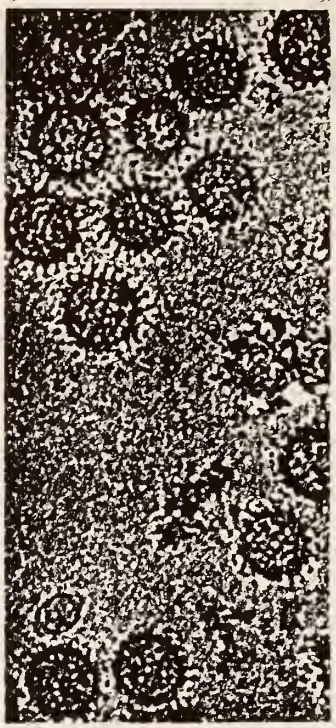

This electron image of frozen hydrated La Crosse virions, recorded by Dr. Y. Talmon and Ms. G. J. Wang in Dr. Chiu's laboratory at the University of Arizona, reveals details of the structure of this virus, which causes encephalitis in humans.

Dr. Chiu and Dr. B. V. V. Prasad have reconstructed the three-dimensional structure of simian rotavirus from multiple images of frozen, hydrated rotavirions in different orientations.

The three-dimensional data for most specimens are obtained by tilting the microscope stage at different angles. In some specimens, such as virus particles that possess helical or icosahedral symmetry, no tilting is necessary. Images of different views can be combined to produce the three-dimensional structure. Dr. Chiu and his associates Drs. M. F. Schmid and D. G. Morgan are developing a new strategy for computer processing of electron micrographs for retrieving phase information necessary for the three-dimensional reconstruction of crystalline and semicrystalline objects at high resolution. To assist in the work of interpretation and display, Dr. Chiu's lab also has a color raster monitor and a vector graphic display system, he says.

Crotoxin complex, an early focus for high-resolution research with the medium high-voltage microscope, consists of two proteins, one acidic (crotoxin A) and one basic (crotoxin B). Crotoxin B is an enzyme, a phospholipase that digests the lipids in cell membranes and is therefore capable of rupturing red blood cells. Crotoxin B also is toxic to the nerve cells that connect to voluntary muscle. Only when the two venom proteins are combined is the full toxic effect of crotoxin expressed.

As yet, no one knows the precise mechanism underlying the synergy between the neurotoxic and phospholipase actions of the crotoxin components. But it is known that crotoxin B binds at two tissue sites, one before (presynaptic) and one after (postsynaptic) the junction between the muscle cell and the adjacent nerve fiber.

Dr. Chiu comments that it is this capacity of crotoxin to interact with both presynaptic and postsynaptic membranes that makes it a desirable system for investigating the relationship between protein structure and function. Learning more about this relationship will mean substantial progress toward the goal of unraveling the mechanism that underlies neurotoxicity.

Intermediate-resolution studies are aimed at learning more about macromolecular assemblies like the La Crosse virus and the rotavirus. The La Crosse virus (*Bunyaviridae*) causes encephalitis in humans. Rotaviruses (*Reoviridae*) are the major pathogens of infantile gastroenteritis in humans and animals. These viruses account for more than a million human deaths every year in developing countries. Being able to do the kind of analyses made possible by this resource will provide useful information leading to a better understanding of the basic mechanism of viral infectivity and will give clues for the rational design of antiviral drugs.

Dr. Chiu notes that the clinical applicability of the intermediate-resolution methods extends far beyond viruses to include structures like mammalian cell membranes such as that of the red blood cell in sickle cell anemia, and protein-DNA aggregates, especially those involved in DNA repair and replication, and aggregates of actin with the associated proteins essential for muscle contractility.

For more information on using the resource for high-resolution studies of biological structures, electron crystallography, or related projects, contact:
Dr. Wah Chiu
Department of Biochemistry
Biological Sciences West Building
University of Arizona
Tucson, Arizona 85721
Telephone: (602) 621-5566

The studies described in this article have been supported by the Biomedical Research Technology Program of the NIH Division of Research Resources, the National Institute of General Medical Sciences, and the Department of Defense

Arm-Powered Bicycle for the Disabled

PROBLEM: Once the basic living needs are attended to, mobility and recreation become paramount to the complete rehabilitation and societal integration of an individual with a lower limb disability. Whether for recreation, sport, therapy or self-powered transportation, bicycling is a popular activity providing many physical, psychological and social benefits. Bicycling is potentially as natural and revitalizing an activity for the physically challenged as it is for the able-bodied. The major obstacle has simply been the design and availability of a suitable arm-powered bicycle.

SIGNIFICANCE: The availability of an arm-powered bicycle will extend mobility and exercise beyond wheelchairs to offer the dignity, the control, and the exhilarating freedom through movement associated with balancing and riding a bicycle. Besides the direct individual benefits, an arm-powered bicycle will also enhance integration and public awareness of the physically challenged.

BACKGROUND: Arm-powered tricycles have been around for at least 50 years. Currently, several companies market tricycles for children and adults, including an attachment which converts a wheelchair into a tricycle.

The first arm-powered bicycle began as a VA sponsored student project in the Stanford University Mechanical Engineering Design Division during the 1979/80 school year. Development of several successive prototypes continued at the RR&D Center, culminating in an initial production of three distinct models: adult (Fig. 1), child (Fig. 2), and touring/racing (Fig. 3).

The arm-powered bicycle features drive, steering and power input at the hand cranks. Adjustable side casters smoothly touch down at the desired lean, and also fasten down for four-wheel maneuverability indoors. An optional folding crank tower facilitates transfer to and from wheelchairs.

HYPOTHESIS: The technology to develop arm-powered bicycles with features responding to special physical needs may be drawn from recent advances in arm-powered tricycle, human-powered vehicle and sport wheelchair design. A suitable arm-powered bicycle design will improve the quality of life for the many physically challenged individuals who are eager to ride a bicycle.

Fig. 1. Adult version of *Handbike*.

Fig. 2. Child version of *Handbike*.

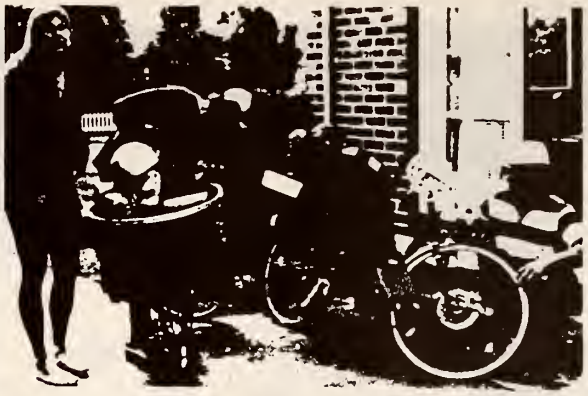

Fig. 3. Touring/racing version of *Handbike*.

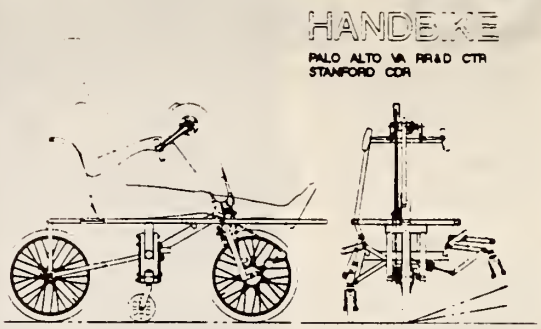

Fig. 4. CAD drawing of *Handbike*.

APPROACH: The approach has been to design, build and test successive prototypes, incorporate improvements, evaluate alternative configurations, and enhance the manufacturability of the design.

STATUS: The fourth version of the arm-powered bicycle, a pre-production prototype called the *Para-Bike*, was completed in Autumn, 1982. In Spring, 1983, a company named Recreational Mobility, located near Eugene, OR, was incorporated to begin production of the *Para-Bike*. Renamed the *Handbike*. three improved design versions were marketed (Figs. 1–3). Although Recreational Mobility is no longer producing the *Handbike*, a *Technology Transfer Manual* is currently being prepared at the RR&D Center to facilitate production of the *Handbike* by other potential manufacturers. Layout and detail drawings near completion (Fig. 4), using computer-aided design facilities at the Stanford Center for Design Research, will be included in the *Technology Transfer Manual*. A Request for Evaluation proposal has been submitted to the VA Rehabilitation R & D Evaluation Unit for performance and mechanical evaluations of the *Handbike*.

For Additional Information:

To discuss this effort further, contact:

Dr. Larry Leifer
Rehabilitation Research and Development Center
Veterans Administration, 3801 Miranda Avenue 640/153, Palo Alto, CA 94304; (415) 858-3991

Automatic Decomposition of the Electromyogram

PROBLEM: The electromyographic (EMG) examination plays an important role in the diagnostic evaluation of many neuromuscular disorders. It involves recording an electrical signal from a contracting muscle using a needle electrode. In current practice most neurologists assess EMG signals in a way that is qualitative and subjective—by listening to their sound and by watching their pattern as they flash across an oscilloscope screen in real time.

SIGNIFICANCE: There is a widely felt need for a quantitative method for analyzing EMG signals that would be more objective, more reproducible, and, hopefully, more diagnostically sensitive than the subjective methods in current use.

BACKGROUND: There have been two major approaches to quantitative EMG analysis. The first approach has been to decompose the signal into its component motor-unit action potentials (MUAPs). This approach has proven to be diagnostically sensitive, but it is limited to weak contractions because of the difficulty of decomposing high-force EMG signals—commonly called "interference patterns" because of their resemblance to random noise. The second approach has been to try to characterize high-force interference patterns statistically, for example by their power spectral density. This approach has proven to be insensitive and unreliable. At present, no method of quantitative EMG analysis has gained wide acceptance.

HYPOTHESIS: We hypothesize that advanced signal-processing techniques can be employed to efficiently and accurately decompose moderately complex EMG interference patterns into their component MUAPs.

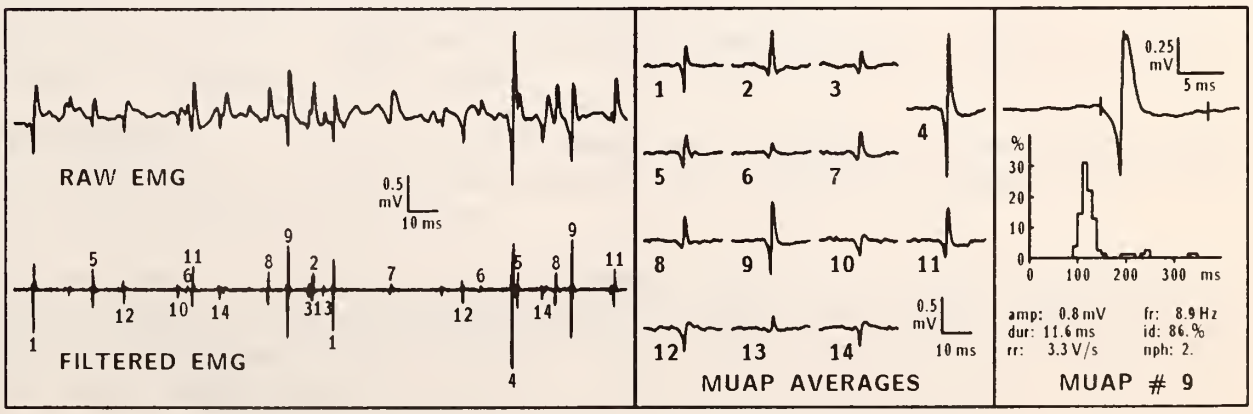

Fig. 1. Example of typical decomposition obtained using the ADEMG method. (Left) The uppermost trace shows a segment of the raw EMG signal, the lower trace shows the signal after filtering with the identfied spikes numbered. (Center) Waveforms of the 14 different MUAPs identified. (Right) Magnification of MUAP #9, along with histogram of interspike intervals and table of measured properties.

APPROACH: We have written a computer program (ADEMG for Automatic Decomposition Electromyography) for extracting MUAPs from EMG signals recorded during conventional EMG examinations (Fig. 1). The program achieves greater speed and accuracy than existing EMG analysis methods through the use of four innovative signal-processing techniques: (1) a fast digital filter for transforming MUAPs into sharp spikes which can be easily detected and accurately identified; (2) an efficient algorithm for aligning and comparing spikes which achieves high temporal resolution at a low sampling rate; (3) a method for verifying or rejecting tentatively identified MUAP trains based on the regularity of their interspike intervals; and (4) a new noise-reducing algorithm for back-averaging the MUAP waveforms from the raw signal using their identified spikes as triggers. The program can analyze a 10-second EMG signal in ninety seconds of computation time and is able to decompose signals containing as many as 15 MUAP trains.

STATUS: We have used ADEMG as implemented on a PDP-11/34 minicomputer to collect normative MUAP properties for the biceps muscle, and are continuing to collect a data base of properties from other muscles and from patients with known neuromuscular disorders. Tests of the ADEMG method's accuracy and diagnostic sensitivity involving computer simulations and a comparative study with other quantitative EMG techniques on groups of patients with selected neuromuscular disorders are underway. ADEMG is also being implemented on a commercial electromyograph in order to make it more widely available to neuromuscular electrodiagnosticians.

PUBLICATIONS:

- McGill, K.C., A method for quantitating the clinical electromyogram, *Ph.D. dissertation*, Stanford University, 1985.
- McGill, K.C., Cummins, K.L., and Dorfman, L.J., Automatic decomposition of the clinical electromyogram, *IEEE Trans Biomed Eng.*, BME-32: 470–477, 1985.
- McGill, K.C., and Dorfman, L.J., Automatic decomposition electromyography (ADEMG): validation and normative data in brachial biceps, *Electroenceph. Clin. Neurophysiol.*, 61: 453-461, 1985.

For Additional Information:

To discuss this effort further, contact:

Dr. Kevin McGill
Rehabilitation Research and Development Center
Veterans Administration, 3801 Miranda Avenue 640/153, Palo Alto, CA 94304; (415) 858-3991

Human Movement Monitoring System to Study Posture, Walking and Jumping

PROBLEM: In order to assess musculoskeletal disabilities associated with posture and gait, it is necessary to record simultaneously kinematic, electromyographic, and kinetic data from each patient.

SIGNIFICANCE: By developing an experimental framework that allows simultaneous monitoring of three-dimensional kinematics, muscle activity, and kinetics during movement, it will be possible to more completely analyze complex motor tasks. This will allow us to accurately record the exact sequence of kinesiological events in these motor tasks.

BACKGROUND: The Selspot system, a three-dimensional monitoring system manufactured by Selcom Selective Electronic Inc., is used to digitize and record traces of motion. It has proved to be a useful tool for recording experimental kinematics. However, the software supplied by Selcom for controlling the Selspot system took up the full resources of our PDP-11/34 computer, so that data collected from other sources during an experiment had to be recorded off-line on an analog tape recorder. Synchronizing this data with the Selspot data was difficult and increased experimental errors by a significant amount. In order to record kinetic, electromyographical and kinematic data simultaneously with a single computing system, we needed to modify the Selspot software and the memory configuration of the computer.

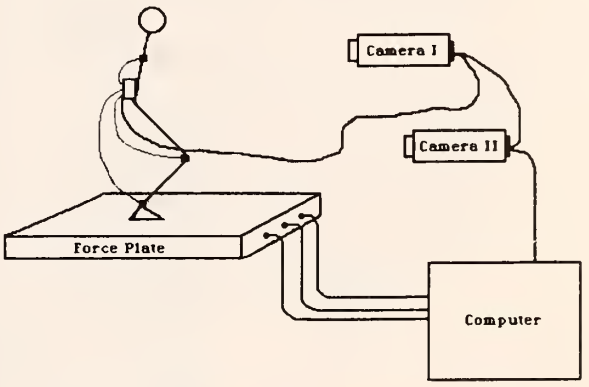

Fig. 1. Movement monitoring system.

HYPOTHESIS: A single computer system can be configured to simultaneously record kinetic, electromyographical, and three-dimensional position data, thus providing a means to time code data with a high degree of accuracy.

APPROACH: Existing computer programs allowed us to collect and store thirty-two channels of kinetic and electromyographic data. By modifying the memory configuration of a Digital PDP-11/34 and the Selcom software, we were able to record kinematic and kinetic data with a single computer system.

STATUS: Currently it is possible, with a single computing system, to simultaneously record data from twenty peripheral channels and the Selspot system for a period of five seconds. We are in the process of writing programs that will initialize and start both systems with a minimum amount of input from the user. Steps are also being taken to allow the data to be displayed as it is collected to confirm data acquisition.

For Additional Information:

To discuss this effort further, contact:

Dr. Felix Zajac
Rehabilitation Research and Development Center
Veterans Administration, 3801 Miranda Avenue 640/153, Palo Alto, CA 94304; (415) 858-3991

NIH
Research & Technology
U.S. Department of Health and Human Services Public Health Service National Institutes of Health

Handbook on Animal Models Available

Information on 16 new animal model studies is now available as the 16th fascicle to the *Handbook: Animal Models of Human Disease* and can be obtained from the Registry of Comparative Pathology at the Armed Forces Institute of Pathology.

The volume contains information compiled from the *American Journal of Pathology and the Comparative Pathology Bulletin*, four supplemental updates to models published earlier, a cumulative index to subjects in all 16 publications, and an author's index. The 16 fascicles of the *Handbook* now contain a total of 351 illustrated studies.

The *Handbook* is published with support from the NIH Division of Research Resources under the auspices of Universities Associated for Research and Education in Pathology, Inc. (UAREP).

The 16th fascicle can be purchased in a three-ring binder that holds three fascicles for $10 or unbound for $7. Copies of fascicles 1 through 15 can be ordered for $5 each. A folder with the contents of each fascicle and an order blank is available without charge.

Researchers interested in obtaining this publication or the other fascicles must prepay with a check or money order payable to UAREP sent to the Registry of Comparative Pathology, Armed Forces Institute of Pathology, Washington, D.C. 20306.

NASA Tech Brief
National Aeronautics and Space Administration
Ames Research Center, Moffett Field, California

Licensing Opportunity

Powered Lift for Paraplegics

People with paralyzed legs can transfer themselves to and from wheelchairs.

A battery-operated lift is designed to aid paraplegics in moving about locally. It can raise or lower a paraplegic from or to a bed, toilet, or wheelchair, for example. The paraplegic controls the operation of the lift with a toggle switch and a joystick.

A prototype (see figure) has been constructed, and further refinements are expected. The lift includes a rolling frame with a body support that is raised and lowered on a column by a pair of drivescrews. The user positions the wheelchair within the frame and places his arms over a pair of curved, padded armpit hooks. The user flips the toggle switch so that the hooks rise on the column. As they rise, the user's weight bears down on them, and the weight is transferred through a cam that causes a pair of padded leg supports to move inward, just behind his knees. The user's body is thus supported at four points.

When the supports reach the desired height, the user flips the toggle switch to stop the upward motion and uses the joystick to move the lift forward, backward, left, or right, as necessary. The joystick controls two independent dc motors, enabling the lift to be positioned precisely and rotated. The motors and a rechargeable battery are in a compact enclosure at the base of the column.

To return to a wheelchair, the user simply reverses the procedure. He uses the joystick to position himself over the chair and operates the toggle in the reverse direction to lower himself into the seat.

This work was done by of Ben Aubert of **Ames Research Center**. *No further documentation is available.*

Inquiries concerning rights for the commercial use of this invention should be addressed to the Patent Counsel, Ames Research Center Refer to ARC-11638 /TN

Ames Research Ctr.
Moffett Field, CA 94035
Technology Utilization Officer: Laurance Milov
Mail Code 223-3
(415) 694-6370
Patent Counsel: Darrell G. Brekke
Mail Code 200-11
(415) 694-5104

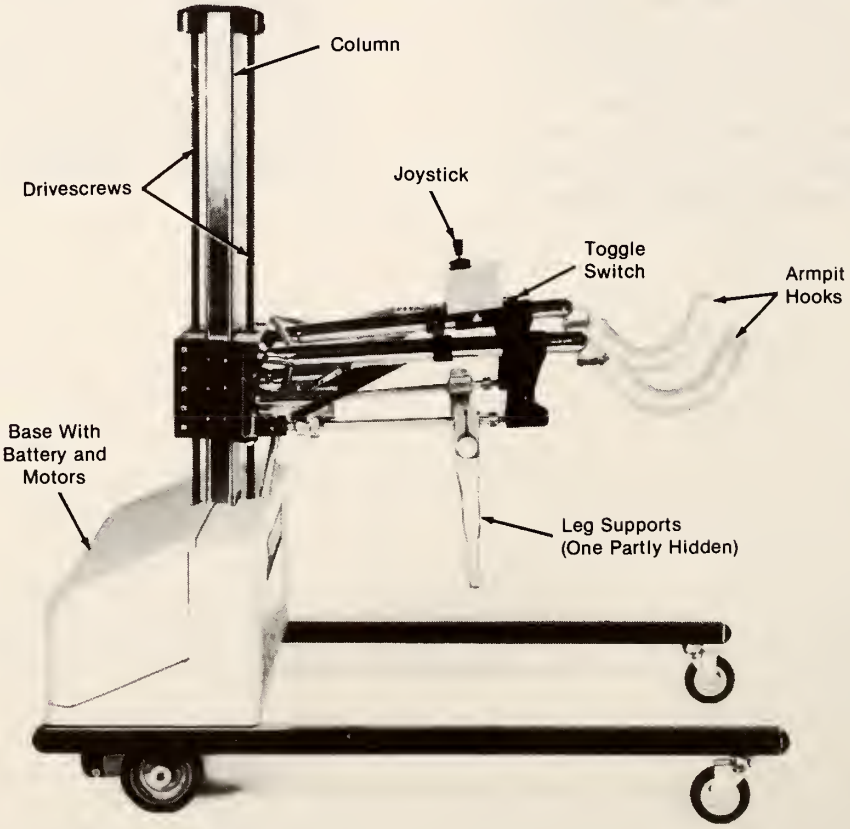

The **Prototype of the Paraplegic Lift** is operated by a toggle switch and a joystick. The lift can be plugged into a household electrical outlet for recharging when it is not in use.

FOR ADDITIONAL INFORMATION: *Contact: Director, Technology Transfer Division, P.O. Box 8757, BWI Airport, MD 21240; (301) 621-0100 Ext. 241*

REFER TO THE NUMBER LISTED AT THE END OF THIS ARTICLE

Oak Ridge National Laboratory

FIBER-OPTICS FLUOROIMMUNO-SENSOR

Key words: Fiber-optics sensor; antibody; antigen; immunofluorescence; carcinogen; immunoassay

The Fiber-Optics Fluoroimmuno-Sensor (FIS), developed by researchers from ORNL and The University of Tennessee, Knoxville, is a portable system that detects specific materials in complex samples. The FIS can identify trace amounts of chemical and biological materials, either in vitro or in vivo. This device, which combines fiber-optics laser technology with immunofluorescence spectroscopy, derives its selectivity from the specificity of antibody-antigen reactions.

Antibodies, covalently bonded to the end of a fiber-optics microprobe, are used for real-time monitoring by the FIS [Fig. 1(*a*)]. Targeted antigens in a sample attach to the bound antibodies [Fig. 1(*b*)]. Laser excitation through a fiber-optics waveguide causes the antigens to fluoresce, and this fluorescence is measured by a sensitive optical technique [Fig. 1(*c*)].

The FIS is an improvement on conventional, laboratory-oriented immunoassay techniques. Features unique to the FIS are its portability, versatility, and speed. Nonfluorescent compounds can also be monitored using fluorotagging and competitive binding techniques. No elaborate reagent setup is necessary, and data can be collected in real time. FIS technology avoids the use of radioactive reagents and the expensive detection equipment that radioimmunoassays

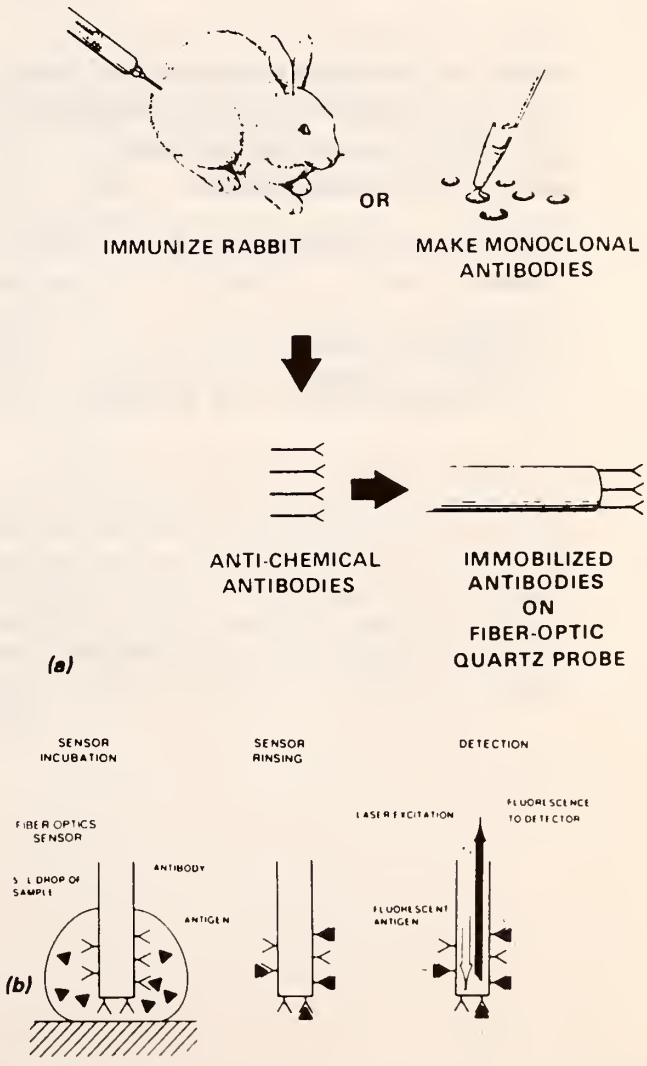

Fig. 1. The FIS. *(a)* Antibodies are produced and covalently bonded to a fiber-optic microprobe. *(b)* Antigens bind to the microprobe and receive laser illumination; An optical detector identifies the antigen by its laser-induced fluorescence.

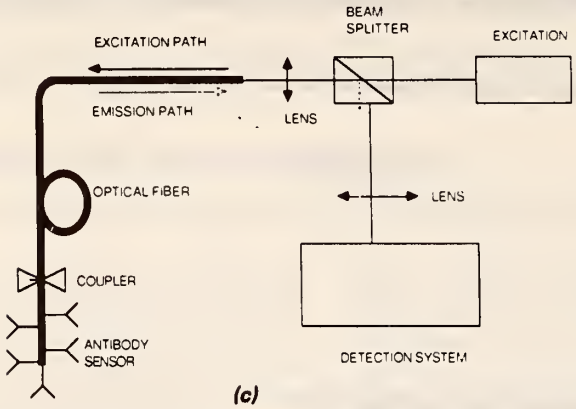

Fig. 1. *(c)* Schematic diagram of a prototype FIS instrument.

require. The fiber-optics microprobe itself opens the way for development of a new generation of smart catheters/sensors with a variety of applications to complex systems:

- detecting viral infections such as the AIDS virus,
- screening for cancer,
- monitoring response to drug therapy,
- assessing human exposure to toxic chemicals, and
- monitoring the environment.

Additional information:

Office of Technology Applications
Information Service
Martin Marietta Energy Systems, Inc.
P.O. Box X
Oak Ridge, TN 37831
Telephone (615) 574-4192; FTS 624-4192

T. Vo-Dinh et al., "Antibody-Based Fiberoptics Biosensor for the Carcinogen Benzo(a)pyrene," *Appl. Spectrosc.* **41** 735-38 (1987).

T. Vo-Dinh et al., "A Portable Fiberoptic Monitor for Fluorimetric Bioassays," *Appl. Spectrosc.* **40**, 696-700 (1986).

T. Vo-Dinh et al., "Fiberoptics-Based Immunofluorescence Spectrosopy for Monitoring Exposure to Polynuclear Aromatic Compounds," *Proceedings of the 10th International Symposium on Polycyclic Aromatic Hydrocarbons, October 21-23, 1985, Battelle Laboratories, Columbus Ohio*, Battelle Laboratories, Columbus Ohio, 1985.

8. J. Tromberg et al., "Fiberoptic Chemical Sensors for Competitive Binding Fluoroimmunoassay," *Anal. Chem.* **59**, 1226-30 (1987).

08-01-0188

Biomolecular Interaction Analysis System (BIAS)
Using a microcomputer to extend chromatography techniques

Immunodiagnostic assays are used medically to evaluate trace levels of numerous hormones and physiologically important proteins; all units of blood used in transfusions are screened immunologically for hepatitis and other virally transmitted diseases. Immunotherapy is a recently developed field in which well-defined monoclonal antibodies will be used to transport clinical agents, drugs, or radioligands to pathologically abnormal cells or tissues. A system Argonne has developed will be a useful tool for evaulation of these biologically produced reagents. The system extends high performance liquid chromatography (HPLC) techniques familiar to biotechnology and pharmaceutical industries to the quality control and development of the reagents used in immunodiagnostics and immunotherapy.

The noncovalent association of two protein molecules or a protein and a molecule of DNA results in the formation of a complex that, during size-exclusion liquid chromatography, migrates more rapidly than the individual consitituents would. Therefore, if the elution profile of a mixture of two interacting macromolecules is compared with a synthetic profile formed by the summation of the two individual chromatograms for each of the two macromolecules, the result is a measure of the interaction.

To permit this quantitative analysis, a microcomputer has been interfaced to a miniscale size-exclusion liquid chromatography system. Data are stored on magnetic disks for subsequent analysis. The interaction chromatograms are interpreted by reference to computer-generated simulated elution profiles. Analytical runs can be completed in as little as 15 minutes, making possible routine and systematic evaluation and quality control of interactive biological macromolecules.

The analytical system currently is being used to biophysically characterize the kinetics and specificity of interactions between antibodies and their antigens. This capability has diverse applications for the development and quality control of macromolecular reagents used in biotechnologies that involve monoclonal antibodies, genetic engineering, and protein engineering. The system can also be used to conduct basic research into the biophysical basis of macromolecular interactions and into the characterization of biomedically important interactions.

Specific applications include (1) determination of specificity and avidity of polyclonal antisera and monoclonal antibodies used for immunodiagnostics and immunotherapy, (2) mapping of spatial locations of determinants on antibody (receptor) surface during development of synthetic vaccines, and (3) evaluation of specific and nonspecific binding of proteins to nucleic acids.

(over)

Additional Information

Key Words: antibodies, biomolecular interaction, immunodiagnostics, immunotherapy, size exclusion liquid chromatography, macromolecular reagents, antibodies

Patent Status: Patent pending.

Potential Applications/Spinoffs: Upon extension of chromatography models and computer simulations, this system of interaction analysis will permit the systematic evaluation of interaction kinetics of various forms of antibodies specific for macromolecular antigens.

Literature: Size-Exclusion HPLC Analysis of Epitopes. Fred J. Stevens, William E. Carperos, William J. Monato, and Neil J. Greenspan. Journal of Immunological Methods (in press, 1988). Macromomolecular Interactions: Application of Microcomputer-Controlled, High Speed Size-Exclusion Chromatography. Fred J. Stevens, Donald A. LeBuis, William J. Eisler, and Clinton F. Ainsworth. LCGC--Magazine of Liquid and Gas Chromatography 4:340-348 (1986). Analysis of Protein-Protein Interaction by Simulation of Small-Zone Size-Exclusion Chromatography: Application of an Antibody-Antigen Association. Fred J. Stevens. Biochemistry 25:981-993 (1986).

For More Information on This Technology: Contact the Technology Transfer Center, 9700 S. Cass Ave., Argonne, IL 60439 (312/972-7694).

NIH
Research & Technology

U.S. Department of Health and Human Services Public Health Service National Institutes of Health

Holter Monitoring Predicts Effectiveness of Antiarrhythmia Treatment

Holter monitoring can predict the long-term clinical efficacy of the antiarrhythmic agent amiodarone in patients with ventricular tachycardia researchers in Baltimore, Maryland, report.

Holter monitoring is a technique for ambulatory, long-term, continuous recording of electrocardiographic signals on magnetic tape and replaying the recording at rapid speed for scanning and selection of significant but fleeting changes that might otherwise escape notice.

"Our prospective study showed that Holter monitoring can be used in the early stage of treatment with amiodarone to accurately predict its long-term effectiveness in suppressing ventricular tachycardia in high-risk heart patients," says Dr. Enrico P. Veltri, assistant professor of medicine at The Johns Hopkins Medical Institutions and director of the sudden death prevention program at Sinai Hospital in Baltimore.

Amiodarone was originally used as an antianginal drug in Europe in the 1960's and then approved by the Food and Drug Administration in 1985 as a treatment for life-threatening arrhythmias. Investigators at the Sinai and Johns Hopkins divisions of cardiology have studied more than 500 patients who were referred for amiodarone treatment. The prospective study was designed to confirm results of an earlier retrospective study in which they found Holter monitoring to be a useful guide for evaluating the efficacy of amiodarone.

In the prospective study Dr. Veltri and his associates studied 52 high-risk patients with recurrent ventricular tachycardia who were hospitalized in the Johns Hopkins General Clinical Research Center. Most of the patients had severe coronary artery disease, defined as greater than 70 percent coronary artery narrowing, and a low ejection fraction, which is a measure of the heart's pumping ability. All the patients had a history of sustained ventricular tachycardia manifested either by transient loss of consciousness, lightheadedness, or cardiac arrest requiring cardiopulmonary resuscitation or defibrillation.

At the beginning of the study the patients all had nonsustained ventricular tachycardia, defined as three or more repetitive ventricular beats during a period of less than 30 seconds on a single baseline Holter monitor. All had failed to respond to up to three different antiarrhythmic drugs and had not been treated with amiodarone. Dr. Veltri explains that the patients were referred because they were at extremely high risk for sudden death caused by fatal disruption of the heart rhythm.

The study results showed that amiodarone was very effective in suppressing ventricular tachycardia and that 72 hours of Holter monitoring done in the first 10 days of treatment with amiodarone could accurately predict the long-term efficacy of the drug.

"We found that Holter monitoring had an 85 percent overall predictive accuracy in assessing the patients' long-term response to amiodarone," Dr. Veltri says. "If the patient responded to the drug early in the treatment there was an excellent outlook over the long-term treatment. But patients who did not respond in the early phases of treatment remained at high risk," he adds.

Amiodarone completely suppressed nonsustained ventricular tachycardia in 34 of the patients within the first 10 days of treatment. Only 3 of these 34 (9 percent) developed episodes of ventricular tachycardia in the follow-up phase.

Additional reading:

1. Denes, P., Santarelli, P., Masson, M., and Uretz, E., Prevalence of late potentials in patients undergoing Holter monitoring. *American Heart Journal* 113:33–36, 1987.

2. Pratt, C. M., Theroux, P., Slyman, D., Riordan-Bennett, A., Morisette, D., Galloway, A., Seals, A. A., and Hallstrom, A., Spontaneous variability of ventricular arrhythmias in patients at increased risk for sudden death after acute myocardial infarction: Consecutive ambulatory electrocardiographic recordings of 88 patients. *American Journal of Cardiology* 59:278–83, 1987.

3. Veltri, E. P., Griffith, L. S. C., Platia, E. V., Guarnieri, T., and Reid, P. R., The use of ambulatory monitoring in the prognostic evaluation of patients with sustained ventricular tachycardia

Dr. Enrico Veltri and Mr. Rod Graham of the cardiology department at Sinai Hospital of Baltimore show how the leads for the Holter monitor are attached.

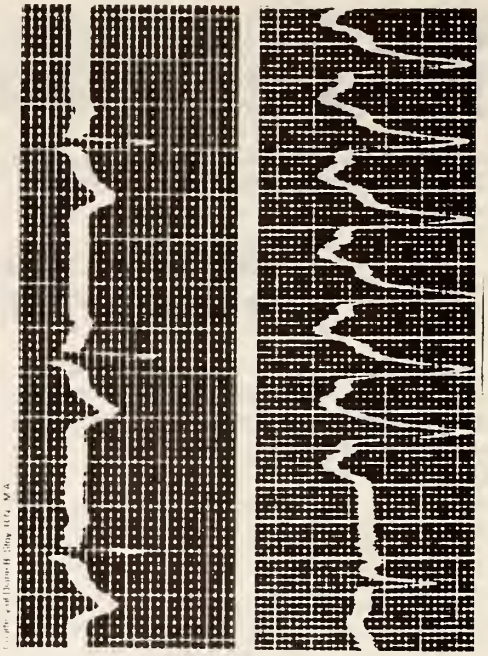

The electrocardiogram strip on the left was made during normal heart rhythm. The strip on the right shows ventricular tachycardia followed by the resumption of normal sinus rhythm.

treated with amiodarone. *Circulation* 74:1054–1060 1986

4. Nademanee, K., Singh, B. N., Callahan, B., Hendrickson, J., and Hershman, J. M., Amiodarone, thyroid hormone indexes, and altered thyroid function: Long-term serial effects in patients with cardiac arrhythmias. *American Journal of Cardiology* 58:981–6. 1986.

5. Ingerslev, J. and Bjerregaard, K., Prevalence and prognostic significance of cardiac arrhythmias detected by ambulatory electrocardiography in subjects 85 years of age. *European Heart Journal* 7:570–75, 1986.

6. Veltri, E. P., Reid, P. R., Platia, E. V., and Griffith, L. S. Amiodarone in the treatment of life-threatening ventricular tachycardia: The role of Holter monitoring in predicting long-term clinical efficacy. *Journal of American College of Cardiology* 6:806. 1985.

7. Vlay, S. C., Kallman, C. H., and Reid, P. R., Prognostic assessment of survivors of ventricular tachycardia and ventricular fibrillation with ambulatory monitoring *American Journal of Cardiology* 54:87, 1984.

8 Miroski, M., Reid, P. R., Winkle, R. A., Mower, M. M., Watkins, L., Jr., Stinson, E. B., Griffith, L. S Kallman, C. H., and Weisfeldt, M. L., Mortality in patients with implanted automatic defibrillators. *Annals of Internal Medicine* 98:585–588. 1983.

For Additional Information:

To locate information or professional contacts on this effort, contact:

Research Resources
Information Center,
1601 Research Blvd.,
Rockville, MD 20850
(301) 984-2870

Refer to item XII, No. 01/TN

Research on the treatment of ventricular tachycardia discussed in this article was supported in part by the General Clinical Research Centers Program of the NIH Division of Research Resources and by the National Heart, Lung, and Blood Institute

NIH Research & Technology

Federal Technology Resource

U.S. Department of Health and Human Services Public Health Service National Institutes of Health

Low Voltage Scanning Electron Microscope

A new type of scanning electron microscope at the Integrated Microscopy Resource (IMR) for Biomedical Research at the University of Wisconsin in Madison is providing biologists with the most accurate images of cell surfaces ever achieved, says Dr. Gerald Schatten, director of the IMR.

The half-million dollar microscope uses a low voltage electron beam that produces images with unprecedented contrast and resolution without the need to coat specimens with thick layers of heavy metal. The instrument is the first Hitachi S-900 to be installed anywhere and the only one specially modified for low-voltage operation in biological research, Dr. Schatten notes.

Dr. James Pawley, associate professor of zoology at the University of Wisconsin-Madison and physicist-in-charge of the selection and modification of the new low voltage scanning electron microscope (LVSEM) at the IMR, hopes that it will now be possible to directly image antibodies, cell receptors, viruses, and other molecules larger than 30 to 50 angstroms that are attached to cell surfaces. With other scanning electron microscopes (SEM), 100 angstroms is about the limit of useful resolution.

"This opens up research opportunities in hematology, immunology, cellular and molecular biology, and probably much more. We can look in detail at cell surface structure. We can follow interactions between cells and viruses or between cells and proteins such as antibodies. We can identify individual surface antigens or cell surface receptors, to name just a few," says Dr. Ralph Albrecht, associate professor of veterinary science and pediatrics at the University of Wisconsin-Madison. He is using the new microscope to study cell receptors on platelets and their relationship to internal cell structures.

LVSEM technology was initially developed for microchip manufacturers, who needed a low voltage electron beam of 1 to 5 kilovolts to check their chips for faults. The higher voltage beams used in conventional SEM destroy the electrical properties of the chips.

But the LVSEM's produced for the microchip industry only provide 50 nm resolution at 1 kilovolt for a useful magnification of up to about 10,000 times. This is adequate for examining microchips, but far below the requirements of many biological researchers who use magnifications of up to 200,000 times to study cell structures, antibodies, or viruses. The LVSEM at the Integrated Microscopy Resource for the first time combines a 3 nm beam diameter with the increased contrast of 1 kilovolt operation.

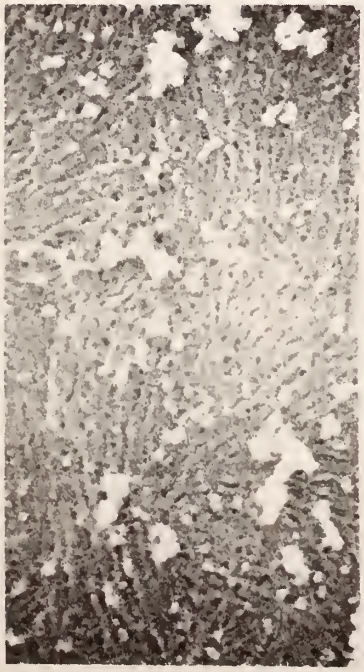

Photo courtesy of Dr. James B. Pawley; sample by Dr. Stanley Erlandsen

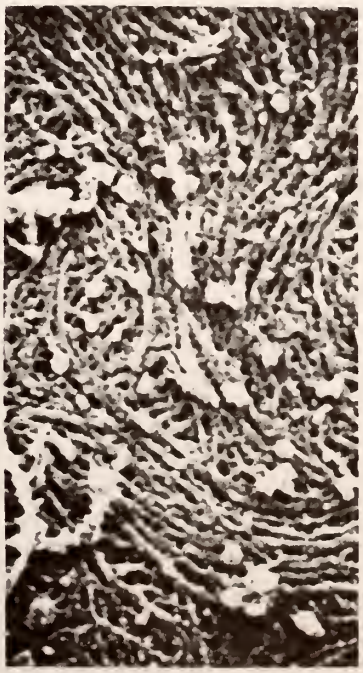

The mat of fibrils that make up the cell wall of a Giardia cyst is magnified 50,000 times in both images. The image on the left was taken with a 20 kilovolt beam, that on the right with 1 kilovolt. At the higher voltage undue prominence is given to the fibrils extending from the surface, while the shape of the fiber mat is not well conveyed. The 1 kilovolt image gives a more accurate impression of the actual sample topography. The field width is 1.8 micrometers.

To avoid subsurface backscattering and produce an image of just the surface, researchers working with conventional SEM must coat specimen cells with a relatively thick layer of dense conductive metal—usually gold or platinum—about 100 to 200 angstroms thick. Because the density of the metal is about 100 times that of the dried tissue, the metal coating substantially reduces beam penetration. This makes surface images appear clearer, but the coating also obscures fine details of the cell's contours.

Taken together, the advantages of less beam penetration and thinner coatings add up to an important advance in the study of cells. Researchers will now be able to see viruses and other particles and watch their interactions with cell surfaces, where the viruses attack, how many attack, and what changes occur in the cell at that moment. This, in turn, may help explain why some viruses attack only certain cells. Interferon and interleukin receptors may also be observed directly. Most of these objects are beyond the 100 angstrom resolution threshold of conventional SEM, but within the limits of LVSEM.

Since the need for coatings is decreased, LVSEM should also permit biologists to move more freely between different microscopes. The IMR provides facilities for biologists to use a three-step approach to study the relationship between interactions at the cell surface and their effects on internal cell components. First, the cell is imaged while alive using video-enhanced light microscopy. Then the cell is fixed and dried and its internal ultrastructure revealed by a high-voltage electron microscope, which uses a beam of about a million volts to penetrate through the specimen. Finally it is coated with metal to investigate its surface.

The LVSEM and other instruments at the IMR are available for use by qualified biomedical researchers. Contact:

Dr. Gerald Schatten
Director, Integrated Microscopy Resource
1675 Observatory Drive
Madison, Wisconsin 53706
Telephone (608) 263-3147

Additional reading:

1. Albrecht, R. M., Olorundare, O. E., Bielich, H. W., and Simmons, S. R., Correlative video enhanced DIC-LM, HVEM, and low-voltage high-resolution SEM in the study of surface and internal ultrastructure. *Proceedings of the 45th Annual Meeting of the Electron Microscopy Society of America*, pp. 556–559. 1987.
2. Pawley, J. B. and Scala, W. R., Low-voltage SEM update. *Proceedings of the 44th Annual Meeting of the Electron Microscopy Society of America*, pp. 654–657, 1986.
3. Pawley, J., Low voltage scanning electron microscopy. *Journal of Microscopy* 136:45–67, 1984.

Natural Resources Technology & Engineering

526 Diffusion of Contaminants in the Atmosphere Studied

527 Calculating Atmospheric Effects in Satellite Imagery: Part 2 — Practical computational techniques are developed.

NAVY
Domestic Technology Transfer Fact Sheet

Diffusion of Contaminants in the Atmosphere Studied

The study of atmospheric diffusion can be simply defined as the investigation of the diluting effects of the atmosphere on a released contaminant. The atmosphere is most often in a turbulent state implying that its motions can be predicted only in a stochastic sense.

Since virtually all gaseous pollutants and most airborne particulates very quickly become well mixed on the molecular level in the troposphere, diffusion of those materials can be described in a similar probabilistic manner. Introducing statistics automatically requires the user to consider the variations of those statistics in time and space. As an example of the latter, a predicted crosswind concentration distribution represents only a first-order approximation to the actual distribution, which will often show significant variations from that prediction. The study of those fluctuations is presently only beginning.

A study recently conducted by the Naval Postgraduate School (NPS), under the sponsorship of the Naval Environmental Prediction Research Facility, focuses on the time variations of diffusion statistics, specifically, the standard deviation of the crosswind concentration distribution. In a previous study, NPS researchers found that overwater releases of material will diffuse in the crosswind direction with two scales of motion. On one scale, material will disperse about the centerline of the plume or cloud due to turbulence of length scales close to the plume or cloud size. This scale of dispersion is referred to as *relative diffusion*, implying that the statistics can be observed by the motions of parcels relative to each other in a moving frame of reference. On the second and much larger scale, the plume or puff will disperse relative to a fixed axis, usually chosen to be mean wind direction. Turbulence acts on the instantaneous plume or puff as if it were a single entity and is referred to as *single-particle diffusion*.

Previous studies have implicitly considered the combined diffusion properties of both components when hourly averaged plume parameterizations were derived from tracer experiments. In this study, however, the two components are separated in order to supply more information on the nature of the diffusion processes and resultantly more knowledge of potential hazard from a contaminant release.

Most descriptions of plume parameters rely on empirical formulae and/or major assumptions about the physical behavior of the atmosphere. Verification of these parameterizations therefore should utilize data gathered under a wide variety of atmospheric conditions and geographical locations.

For Additional Information:

Backup material on this effort is available from:

Navy Domestic Technology Fact Sheet
Reader Reply Service
Code E211
Naval Surface Weapons Center
Dahlgren, VA 22448-5000
(703) 663-8921

Refer to 121002/TN

NASA Tech Brief
National Aeronautics and Space Administration

Calculating Atmospheric Effects in Satellite Imagery: Part 2

Practical computational techniques are developed.

A report discusses the practical considerations of the calculation of three-dimensional radiative transfer. It is an extension of the earlier theoretical developments described in "Calculating Atmospheric Effects in Satellite Imagery" (NPO-16373), page 82, *NASA Tech Briefs*, Vol. 9, No. 3 (Fall 1985).

The report begins with a review of the previous work. The theory is based on a model that includes a vertically inhomogeneous atmosphere bounded by a non-uniform, non-Lambertian surface. The theory takes account of the influence of atmospheric absorption and scattering on remote surface sensing. It includes the adjacency effect, in which photons originating in neighboring regions are scattered into the line of sight.

The calculation entails the separation of the total intensity field into a diffuse and direct component. The radiative-transfer equation for the diffuse field is solved by performing a two-dimensional spatial Fourier transform and solving the resulting one-dimensional equations for each of the Fourier components. The spatial-domain diffuse field is then reconstructed with the inverse transform, from which the direct field can then be obtained.

The calculations described in the present report rely on a FORTRAN radiative-transfer computer program, 'RTRAN.3D', that calculates the Fourier components of the three-dimensional diffuse intensity field. Programs were also developed for this research to specify the model atmosphere and surface parameters. Another newly developed program reconstructs the spatial-domain field from the Fourier components calculated by 'RTRAN.3D'.

The report discusses some of the practical aspects of the implementation of these algorithms on a minicomputer. Some symmetries and approximations are invoked to increase the computational efficiency.

Several model calculations are performed, and numerical results are presented. Of particular interest is the albedo-step-function problem, in which two adjoining expanses of ground have different reflectivities. The results suggest that the calculation method as a whole is practical, accurate, and versatile. The atmospheric and surface phase functions can be arbitrarily complex, and solutions are not restricted to nadir observation only. Furthermore, both internal intensity fields and radiation escaping from the top and bottom of the atmosphere can be calculated.

This work was done by David J. Diner and John V. Martonchik of Caltech for **NASA's Jet Propulsion Laboratory**. *To obtain a copy of the report, "Atmospheric Transfer of Radiation Above an Inhomogeneous Non-Lambertian Reflective Ground: Part II: Computational Considerations and Results," NPO-16371 /TN*

FOR ADDITIONAL INFORMATION: *Contact: Director, Technology Transfer Division, P.O. Box 8757, BWI Airport, MD 21240; (301) 621-0100 Ext. 241*
REFER TO THE NUMBER LISTED AT THE END OF THIS ARTICLE

Physical Sciences

528 Alternative Refrigerants

529 New Diffraction and Crystal Databases Available

530 Thermodynamic Refrigerant Mixture Charts now Available

531 New Use for High-Transition (HT) Superconductors Demonstrated

532 Hybrid Electrostatic/Acoustic Levitator — Particles and drops can be rotated and vibrated.

Software

533 Computer Program for Linear Algebra — A collection of routines is provided for basic vector operations.

534 Fast-Polynomial-Transform Program — A modular approach saves computational resources.

535 Mathematical Routines for Engineers and Scientists — Programs for frequently-used mathematical procedures save time.

Testing & Instrumentation

536 "Signatures" Help Researchers Trace Artifact Origins

537 Modulated-Voltage Metastable-Ionization Detector — The range of measurable gas concentrations is extended. (Licensing Opportunity)

538 Ultrasonic Scanner Evaluated

539 Three-Axis Superconducting Gravity Gradiometer — Gravity Gradients can be measured even on accelerating platforms. (Licensing Opportunity)

Other Items of Interest

456 Million-Fold Improvement in Superconductor Resistance

NBS technology update

National Bureau of Standards
U.S. Department of Commerce
Gaithersburg, MD 20899

Alternative Refrigerants

Refrigerants, chlorofluorocarbon (CFC) compounds in particular, have come under intense scrutiny because of the concern that they could ultimately deplete the ozone layer which protects the Earth against harmful levels of ultraviolet radiation from the sun. An international agreement has been proposed to limit production of some CFCs. But information on new refrigerants or refrigerant compounds is sketchy. In the December 1987 issue of ASHRAE Journal, NBS researchers David A. Didion and Mark O. McLinden discuss the problem and present a systematic approach to help find viable alternatives from the thousands of possible combinations of chemical elements. Using their appraoch, the NBS researchers isolated a range of CFCs that should be environmentally acceptable as well as retaining desired properties of proper boiling point, nonflammability, low toxicity, and acceptable atmospheric lifetime. Didion and McLinden conclude that while some CFCs are no longer acceptable, alternative refrigerants will probably come from the same class of compounds. This research is part of a long-term program at NBS to develop fundamental data, mathematical models, and power measurement techniques for using refrigerant mixtures in refrigeration and power machinery.

FOR ADDITIONAL INFORMATION
Dr. David Didion
Bldg. Research Room B122
National Bureau of Standards
Gaithersburg, MD 20899
(301) 975-5881

NBS technology update

National Bureau of Standards
U.S. Department of Commerce
Gaithersburg, MD 20899

New Diffraction and Crystal Databases Available

Analytical chemists in industry, universities, and government will be interested in two new computerized standard reference databases for use in identifying the structures in materials. The NBS/Sandia/ICDD Electron Diffraction Database, developed by the bureau, Sandia National Laboratory, and the International Centre for Diffraction Data (ICDD), contains evaluated data for more than 70,000 inorganic substances. It is an important analytical tool for researchers using electron microscopes to identify unknown substances. The NBS Crystal Database contains complete crystallographic and chemical data on more than 120,000 compounds. In addition to its use in identifying unknown crystalline materials, the software program permits chemical data to be combined with crystal structure information to solve many chemistry problems.

FOR ADDITIONAL INFORMATION:

Both databases are available for lease in a variety of formats, including tapes and disks, from the International Centre for Diffraction Data, 1601 Park Lane, Swarthmore, PA 19081; (215) 328-9400. For information on the NBS Standard Reference Data Program, write or call: Office of Standard Reference Data, A323 Physics Bldg., National Bureau of Standards, Gaithersburg, MD 20899; (301) 975-2208.

NBS technology update

National Bureau of Standards
U.S. Department of Commerce
Gaithersburg, MD 20899

Thermodynamic Refrigerant Mixture Charts now Available

A series of 13 large-scale thermodynamic charts indicating the properties of refrigerants and refrigerant mixtures has been developed by researchers in the NBS Centers for Building Technology and Chemical Engineering as part of a larger study of refrigerant properties. The charts, aimed at heating, cooling, and refrigeration industries, are computer-generated and available in hard-copy form to interested persons. NBS envisions several applications for the charts such as helping pinpoint new combinations of refrigerants with properties that will improve the efficiency of heat pumps. Bureau researchers also hope the charts will help industries discover alternatives to refrigerants such as R-12, a chlorofluorocarbon-containing material used in automobile air conditioners as well as in home and industrial refrigerators.

FOR ADDITIONAL INFORMATION: The charts are available free of charge from Dr. David A. Didion, B122 Building Research, National Bureau of Standards, Gaithersburg, MD 20899; (301) 975-5881.

New Use for High-Transition (HT) Superconductors Demonstrated

A team of scientists from the Naval Research Laboratory (NRL) reports a breakthrough in the first known demonstration of the development and use of high-transition temperature superconductors as sensors of infrared radiation.

The team states that this development may have profound implications on the ultimate use of these materials in future Navy and Department of Defense systems that require sensitive detection of electromagnetic radiation in the optical and infrared portion of the spectrum. Conventional radiation detectors used in various space systems today must be kept in a very low-temperature environment to operate efficiently. NRL's high-transition temperature superconducting detectors of the future, to be based on the NRL development, should eliminate these problems.

The NRL team reports that the sensors were made by evaporating films of the Yttrium, barium, copper, and oxygen (Y-BA-CU-O) materials in a state-of-the-art molecular beam epitaxy unit in a composition that made the films granular, that is, superconducting grains imbedded in a nonsuperconducting matrix.

The films were then patterned, and an evaporative technique was used to produce very low-resistance contacts to the films. The granular nature of these films made them particularly sensitive to the radiation, as previously demonstrated by the same team on the more conventional superconductors (niobium nitride in a matrix of boron nitride). The sensitivity to radiation was determined by shining a pulsed infrared laser on the surface of the film and detecting the voltage developed across the current biased film. The response time was about 10^{-8} seconds.

For Additional Information:

Backup material on this effort is available from:

Navy Domestic Technology Fact Sheet
Reader Reply Service
Code E211
Naval Surface Weapons Center
Dahlgren, VA 22448-5000
(703) 663-8921

Refer to 121102/TN

NASA Tech Brief
National Aeronautics and Space Administration
NASA's Jet Propulsion Laboratory, Pasadena, California

Hybrid Electrostatic/Acoustic Levitator

Particles and drops can be rotated and vibrated.

A levitator for liquid drops and small particles includes both electrostatic and acoustic components for versatility in the manipulation of samples. The sample is levitated electrostatically and rotated or vibrated acoustically. Because the electrostatic and acoustic forces are independent of each other, the hybrid levitator is especially suitable for studies of drop dynamics. Like all-acoustic or all-electrostatic systems, it can also be used in studies of containerless material processing.

The levitator (see Figure 1) includes two dish-shaped electrodes that generate the levitating electrostatic field. A liquid-injection nozzle enters the levitation chamber through a hole in the center of the lower electrode. An acoustic transducer is attached to each of two orthogonal vertical faces to produce orthogonal acoustic standing waves in the chamber.

To facilitate the adjustment and stabilization of the vertical position of the sample, the electrostatic portion of the levitator is controlled by a digital feedback system. The acoustic transducers are locked to each other in frequency and phase. To apply an acoustic torque to rotate the sample, a phase difference of 90° is imposed. The torque is varied by adjusting the amplitude of the sound.

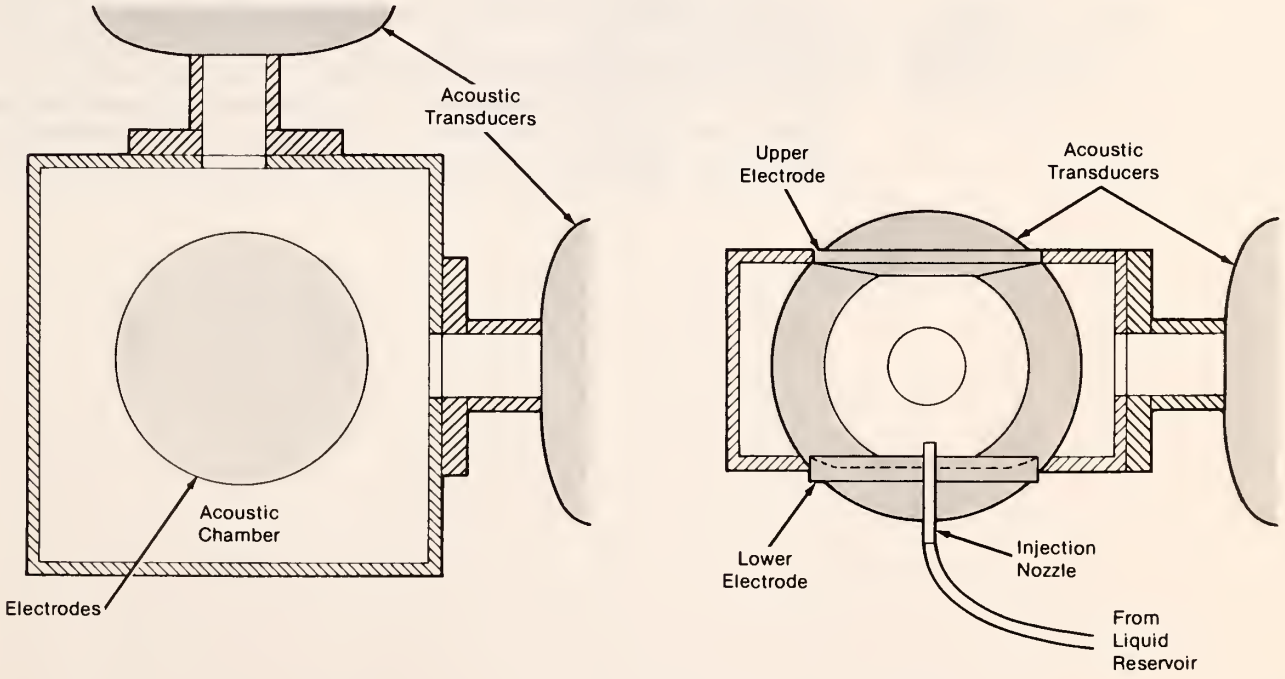

Figure 1. The **Vertical Levitating Force** is applied to the sample by the upper and lower electrodes. Torques or vibrational forces in the horizontal plane are applied by the acoustic transducers.

A nonrotating sample can be made to vibrate by fixing the phase difference at zero and sinusoidally modulating the amplitude. Both a nonzero phase difference and amplitude modulation can be used to produce rotation and vibration. If the sample is a liquid drop, it can be rotated until it breaks in two (see Figure 2). The levitator can also manipulate aluminum shells, glass shells, and wooden spheres.

This work was done by Won K. Rhim, Eugene H. Trinh, Sang K. Chung, and Daniel D. Elleman of Caltech for **NASA's Jet Propulsion Laboratory**.

NPO-16834 /TN

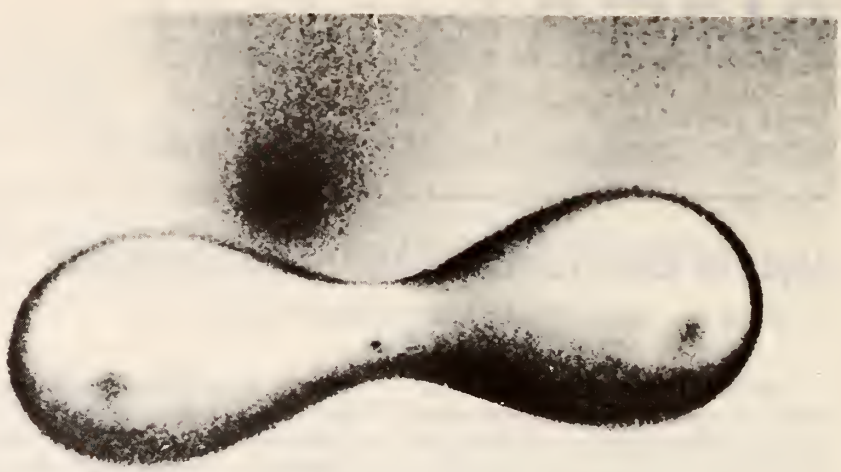

Figure 2. An **Electrically Charged Water Drop** about 4 mm in diameter was levitated electrostatically and rotated acoustically until it assumed a dumbbell shape and broke apart.

FOR ADDITIONAL INFORMATION: *Contact: Director, Technology Transfer Division, P.O. Box 8757, BWI Airport, MD 21240; (301) 621-0100 Ext. 241*

REFER TO THE NUMBER LISTED AT THE END OF THIS ARTICLE

Computer Program for Linear Algebra

A collection of routines is provided for basic vector operations.

The Basic Linear Algebra Subprogram (BLAS) library is a collection of FORTRAN-callable routines for employing standard techniques to perform the basic operations of numerical linear algebra. The BLAS library was developed to provide a portable and efficient source of basic operations for designers of programs involving linear-algebraic computations. The subprograms available in the library cover the operations of dot product, multiplication of a scalar and a vector, vector plus a scalar times a vector, Givens transformation, modified Givens transformation, copy, swap, Euclidean norm, sum of magnitudes, and location of the element of largest magnitude. Since these subprograms are to be used in an ANSI FORTRAN context, provisions are made for the case of single precision, double precision, and complex data. All of the subprograms have been thoroughly tested and produce consistent results even when transported from machine to machine.

The BLAS library is supplied as a machine-independent ANSI FORTRAN-77 version and assembler-code versions. The assembler versions offer extra efficiency in operations involving large vectors. The mainframe BLAS has been implemented on IBM-370, UNIVAC-1100, and CDC-6000 series computers. The PC BLAS FORTRAN version requires one of the following compilers: Lahey F77L, IBM-PC Professional FORTRAN, or Microsoft FORTRAN. The PC BLAS assembler version requires the Microsoft Macro assembler and a math coprocessor. The PC implementation allows individual arrays of over 64K. The BLAS library was developed in 1979, and the PC version was made available in 1986.

This program was written by F. T. Krogh and R. J. Hanson of Caltech for **NASA's Jet Propulsion Laboratory**.

NPO-17121 /TN

FOR ADDITIONAL INFORMATION *CONTACT:*

COSMIC®
112 Barrow Hall
University of Georgia
Athens, GA 30602
(404) 542-3265

Fast-Polynomial-Transform Program

A modular approach saves computational resources.

A computer program uses a fast-polynomial-transformation (FPT) algorithm applicable to two-dimensional mathematical convolutions. Two-dimensional convolutions have many applications, particularly in image processing. Two-dimensional cyclic convolutions can be converted to one-dimensional convolutions in polynomial rings. Traditional FPT methods decompose one-dimensional cyclic polynomials into polynomial convolutions of different lengths. This program decomposes cyclic polynomials into polynomial convolutions of the same length. Thus, only FPT's and fast Fourier transforms of the same length are required. This modular approach can save computational resources. To enhance its appeal further, the program is written in the transportable C language.

The five steps in the algorithm are the following:

1. Formulate the modulus-reduction equations.
2. Calculate the polynomial transforms.
3. Multiply the transforms by use of a generalized fast Fourier transformation.
4. Compute the inverse polynomial transforms.
5. Reconstruct the final matrices by use of the Chinese remainder theorem.

The input to this program comprises the row and column dimensions and the initial two matrices. The matrices are printed out at all steps, ending with the final reconstruction.

This program is written in C for batch execution and has been implemented on the IBM PC series of computers under DOS with a central-memory requirement of approximately 18K of 8-bit bytes. The program was developed in 1986.

This program was written by T. K. Truong, I. S. Hsu, and Y. F. Chu of Caltech for **NASA's Jet Propulsion Laboratory.**

NPO-17030 /TN

FOR ADDITIONAL INFORMATION *CONTACT:*

COSMIC®
112 Barrow Hall
University of Georgia
Athens, GA 30602
(404) 542-3265

Mathematical Routines for Engineers and Scientists

Programs for frequently-used mathematical procedures save time.

A package of computer programs provides the scientific and engineering community with the means to perform routine mathematical manipulations. This collection will enable scientists to concentrate on their work without having to write their own programs to solve common problems, thus saving considerable amounts of time.

The package contains 16 subroutines. Each is separately documented with descriptions of the invoking subroutine call, its required parameters, and a sample test program. The functions available include the following:

- Maximums, minimums, and sorting of vectors;
- Factorials;
- The generation of random numbers with uniform or Gaussian distribution;
- Complementary error function;
- Fast Fourier transformation;
- Integration by Simpson's rule;
- Determinants and inverses of matrices;
- Bessel function for any order and modified Bessel function for zero order;
- Roots of a polynomial;
- Roots of a nonlinear equation; and
- The solution of first-order ordinary differential equations using Hamming's predictor-corrector method.

There is also a subroutine for using a dot-matrix printer to plot a given set of *y* values for a uniformly-increasing *x* value.

This package is written in FORTRAN 77 (Super Soft Small System FORTRAN compiler) for batch execution and has been implemented on the IBM PC series under MS-DOS with a central-memory requirement of approximately 28K of 8-bit bytes for all subroutines. The program was developed in 1986.

This program was written by A. V. Kantak and F. Davarian of Caltech for **NASA's Jet Propulsion Laboratory**.

NPO-17165 /TN

FOR ADDITIONAL INFORMATION *CONTACT:*

COSMIC®
112 Barrow Hall
University of Georgia
Athens, GA 30602
(404) 542-3265

NBS technology update

National Bureau of Standards
U.S. Department of Commerce
Gaithersburg, MD 20899

"Signatures" Help Researchers Trace Artifact Origins

NBS scientists are collaborating with researchers from the Smithsonian Institution and The Corning Museum of Glass on several projects that aim to trace the origins of a variety of precious historical artifacts. They are using lead isotope ratio analysis, a method that can help locate where paints, glazes, metal alloys, and other lead-based raw materials came from that make up many art objects. Researchers measure the inherent ratio of three isotopes-- lead 206, 207, and 208--to a fourth stable isotope, lead 204. This produces a "signature" characteristic of a particular lead deposit or mine location and in many cases allows the lead to be traced to its source. Currently, researchers are examining lead glazes in excavated pottery from Caribbean sites in an effort to link the objects to early Spanish explorers or later New World sources. Another project in the works is a study of metal ingots and fishing weights--which contain lead--from a shipwreck found off the southern coast of Turkey that is believed to be over 3,000 years old. Data from this work will help historians map ancient trade routes. Other uses of lead isotope ratio analysis are in NBS studies such as determining human exposure to lead poisoning cases.

FOR ADDITIONAL INFORMATION
Dr. Lynus Barnes
Physics, A23
National Bureau of Standards
Gaithersburg, MD 20899
(301) 975-4100

NASA Tech Brief
National Aeronautics and Space Administration
Ames Research Center, Moffett Field, California

Licensing Opportunity

Modulated-Voltage Metastable-Ionization Detector

The range of measurable gas concentrations is extended.

A voltage-control feedback circuit extends the range of sample concentrations that can be measured by a metastable-ionization detector coupled to a gas chromatograph. A conventional detector measures concentrations from parts per billion to parts per million but saturates at higher values. The new detector retains the sensitivity of conventional ones but automatically reduces its voltage to prevent current saturation at higher values, thereby enabling the quantitative determination of relative concentrations approaching 100 percent.

In a metastable-ionization detector, the chromatography carrier gas (usually helium) is exposed to an electric field and energetic electrons from a radioactive source. This combination raises the carrier-gas atoms to a metastable state, which, in helium, has an ionization potential of 19.8 eV. Sample constituents having lower ionization potentials are ionized and collected at the electrodes that form the electric field.

At low concentrations, the collected current, less the background current due to the radioactive source, is proportional to the concentration of the sample constituents in the carrier gas. At high concentrations, an arc discharge forms, and the detector current saturates at a current limited by a protective resistor.

To prevent saturation, the improved detector (see Figure 1) includes a voltage modulator controlled by the detector output current. In the modulator circuit, the detector-current signal from the electrometer is fed to a differential amplifier, offset by an amount that compensates for the background, and then fed to a modulation amplifier. When the modulation-amplifier input exceeds the preset value corresponding to the threshold current, the

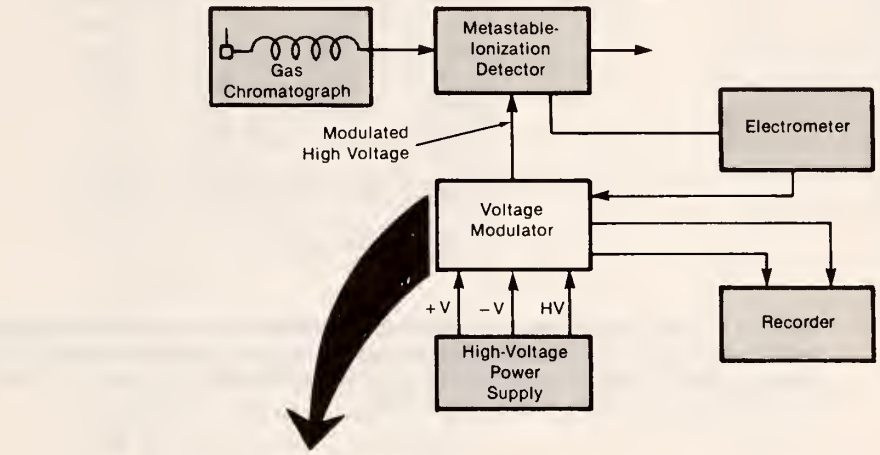

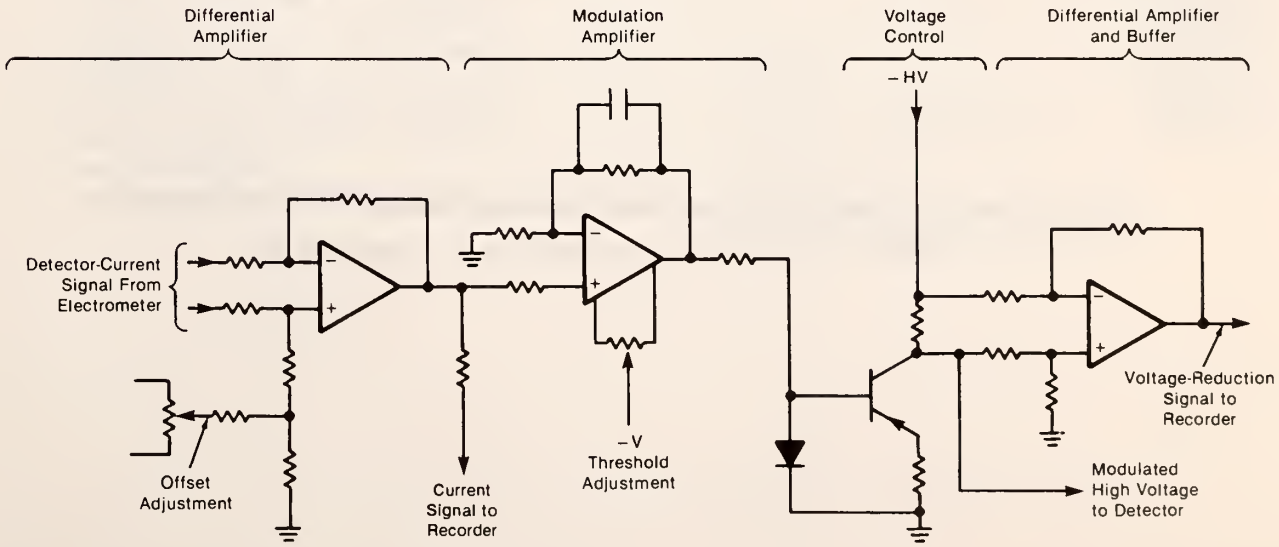

Figure 1. The **Modulated-Voltage Metastable-Ionization Detector** includes feedback circuitry to prevent current saturation. When the detector current begins to exceed a threshold, the detector high voltage is reduced to keep the current from rising much more.

modulation-amplifier output turns on the transistor in the transistor/resistor voltage-control amplifier.

The amplifier gains are chosen so that the high voltage is reduced by the amount needed to keep the detector current from rising significantly above the threshold. At sample concentrations above the threshold, the reduction in voltage is used as the measure of concentration. This voltage reduction is detected by a differential buffer amplifier and fed to the recorder. The relationship between the voltage reduction and the concentration is not linear; a calibration curve must be obtained empirically for each sample constituent.

Figure 2 shows an example of recorder output from a gas chromatograph fed with a helium carrier containing four sample gases at various concentrations. The nitrogen current peak just exceeds the threshold and is therefore followed quickly by a small voltage-reduction peak. The argon current peak greatly exceeds the threshold and so is quickly followed by a large voltage-reduction peak. The methane and krypton current peaks are below the threshold and cause no voltage reduction.

This work was done by Glenn C. Carle, Daniel R. Kojiro, and Donald E. Humphry of **Ames Research Center**.

This invention is owned by NASA, and a patent application has been filed. Inquiries concerning nonexclusive or exclusive license for its commercial development should be addressed to the Patent Counsel, Ames Research Center
Refer to ARC-11503 /TN

Ames Research Ctr.
Moffett Field, CA 94035
Technology Utilization Officer: Laurance Milov
Mail Code 223-3
(415) 694-6370
Patent Counsel:
Darrell G. Brekke
Mail Code 200-11
(415) 694-5104

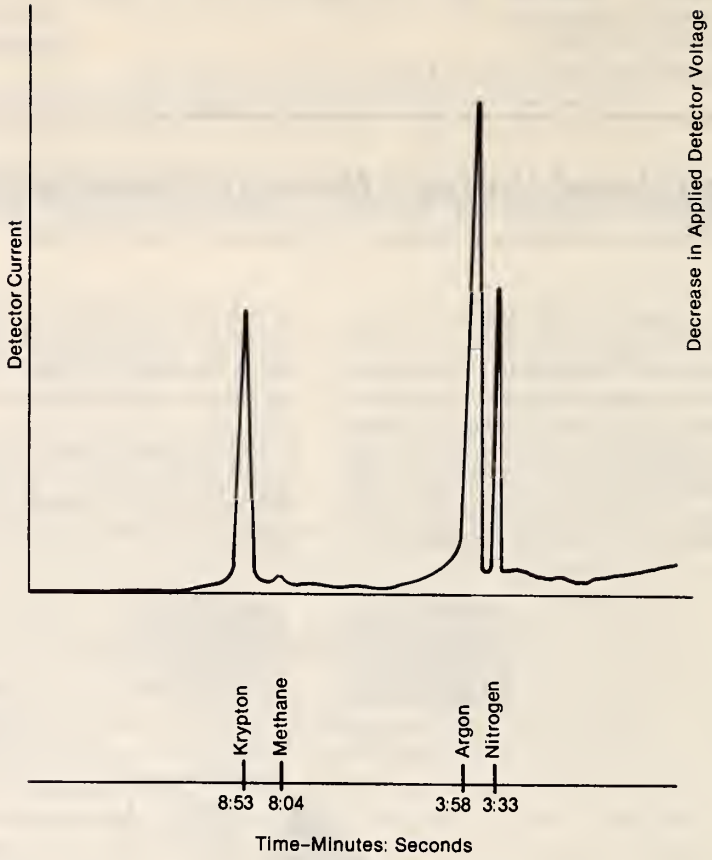

Figure 2. This **Recorder Output** shows the detector-current and voltage-reduction signals from a gas mixture with constituents both above and below the threshold concentration. Those above the threshold cause both current and voltage-reduction peaks. Those below the threshold give rise to current peaks only.

FOR ADDITIONAL INFORMATION: *Contact: Director, Technology Transfer Division, P.O. Box 8757, BWI Airport, MD. 21240; (301) 621-0100 Ext. 241*
REFER TO THE NUMBER LISTED AT THE END OF THE ARTICLE

NAVY
Domestic Technology Transfer Fact Sheet

Ultrasonic Scanner Evaluated

The David Taylor Naval Research Center (DTNRC) is evaluating an ultrasonic Time-of-Flight Diffraction (TOFD) scanner that incorporates a Synthetic Aperture Focusing Technique (SAFT) for weld defect depth and length measurements with an accuracy goal of ± 1 millimeter. The initial evaluation of the sys-tem was performed with three naval alloy plates (HY-80, HY-100, and HSLA-80) containing electric discharge machined (EDM) notches of various depths. The performance trials indicate that controlled, linear scanning is feasible using the mechanics employed.

The probe-holder easily follows the surface of the plate, without the necessity for the plane of the plate to be closely parallel with the plane of the x-y scanner. Scanning can be controlled by using a low-cost personal computer; the same low-cost computer can easily be programmed to collect, process and display ultrasonic data in various formats.

The speed of the scanning depends on the nature of the data being collected, the amount of averaging being carried out, etc. For example, in the evaluation where ten averages are made on each A-scan collected, the linear speed is 0.005 inch/second. The scattered signals produced by EDM notches in the depth range from 6 to 20 millimeters are clearly distinguished against the background of grain-scatter from the parent plate; the TOFD/SAFT system measured the EDM notches, both depth and length location and sizing, to the accuracy of ± 1 millimeter.

For Additional Information:

Backup material on this effort is available from:

Navy Domestic Technology Fact Sheet
Reader Reply Service
Code E211
Naval Surface Weapons Center
Dahlgren, VA 22448-5000
(703) 663-8921

Refer to 121103/TN

NASA Tech Brief
National Aeronautics and Space Administration

Licensing Opportunity

Three-Axis Superconducting Gravity Gradiometer

Gravity gradients can be measured even on accelerating platforms.

A three-axis superconducting gravity gradiometer is based on flux quantization and the Meissner effect in superconductors and employs a superconducting quantum interference device as an amplifier. It incorporates several magnetically levitated proof masses, as described in the preceeding article, "Six-Axis Superconducting Accelerometer" (MFS-26040). The gradiometer design integrates the accelerometers for operation in a differential mode. The principal use is expected to be in commercial instruments for the measurement of Earth-gravity gradients in geophysical surveying and exploration for oil.

In the gravity gradiometer, the signals representing common-mode acceleration (due to motions of the instrument platform) are balanced out, leaving an apparent differential-acceleration reading for each axis proportional to the distance between two acceleration detectors along that axis and to the projection of the gravity gradient along that axis.

The gravity bias of the Earth is nulled by stable magnetic levitation using superconducting persistent currents. The levitation coils for the two proof masses for each axis are connected in series to stiffen the suspension springs against common-mode accelerations while keeping the differential-mode compliance unchanged. The common-mode resonance is damped by eddy-current dissipation; this improves the common-mode rejection. The stable magnetic field arising from persistent currents creates the effect of a negative spring, which increases the compliance of the differential mode and thereby increases the sensivity to gravity gradients.

Piezoelectric crystals are employed to align precisely the sensitive axes of the component accelerometers. This suppresses both the instrument errors associated with coupling to the cross-component linear accelerations and the modulation of the Earth-gravity bias caused by angular motions.

As in the accelerometer, force-rebalance feedback currents are applied to the proof masses for both the common and differential modes. In addition, cold damping feedback is applied to damp actively the differential mode. This reduces the nonlinearity error of the instrument and improves its dynamic range.

The instrument simultaneously reads out three in-line component gradients and three common-mode linear accelerations. The common-mode signals can be used to stabilize the platform, to compensate for errors, and to obtain the precise position of the instrument during a survey. The three gradient signals provide valuable cross-checks of the gravity data. The sum of these gradient signals reflects the attitude rate of the instrument and provides a cross-check of platform gyroscope readings.

A room-temperature gravity gradiometer developed by the Navy has a sensitivity limited to about 10 $s^{-3/2}$. The new superconducting gravity gradiometer has a sensitivity of $\sim 10^{-1}$ to $\sim 10^{-4}$ $s^{-3/2}$ and greater stability as well. The only serious limitation is the need for liquid helium to maintain the instrument at a temperature of ~2 to ~5 K.

This work was done by Ho Jung Paik of the University of Maryland for **Marshall Space Flight Center**. *No further documentation is available.*

In accordance with Public Law 96-517, the contractor has elected to retain title to this invention. Inquiries concerning rights for its commercial use should be addressed to

Ho Jun Paik
Department of Physics and Astronomy
University of Maryland
College Park, MD 20742

Refer to MFS-26041, /TN

George C. Marshall Space Flight Center
Marshall Space Flight Center, AL 35812
Technology Utilization Officer: Ismail Akbay
Code AT01
(205) 544-2223
Patent Counsel:
Leon D. Wofford, Jr.
Mail Code CC01
(205) 544-0024

FOR ADDITIONAL INFORMATION: *Contact: Director, Technology Transfer Division, P.O. Box 8757, BWI Airport, MD 21240; (301) 621-0100 Ext. 241*
REFER TO THE NUMBER LISTED AT THE END OF THIS ARTICLE

Transportation & Components

540 Airplane Wings for Faster Climbing and Slower Landing — Reshaped airfoils improve performance. (Licensing Opportunity)

541 Computer Scheduling of Airplane Arrivals — Controllers would be assisted in the coordination of many simultaneous flights. (Licensing Opportunity)

542 Field Repair of Thermoplastic Windows and Canopies — A hand-held induction heater makes quick and easy repairs.

543 Variable-Reluctance Motor for Electric Vehicles — A scaled-down motor performed as expected.

Other Items of Interest

484 "Thumball" Auxiliary Data-Input Device — A track-ball-type device is mounted on a joystick operated by a thumb. (Licensing Opportunity)

NASA Tech Brief
National Aeronautics and Space Administration
Ames Research Center, Moffett Field, California

Licensing Opportunity

Airplane Wings for Faster Climbing and Slower Landing

Reshaped airfoils improve performance.

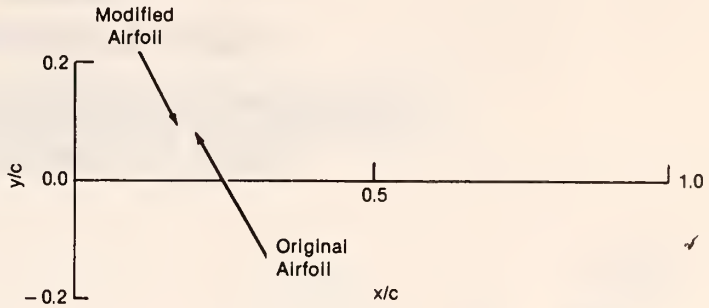

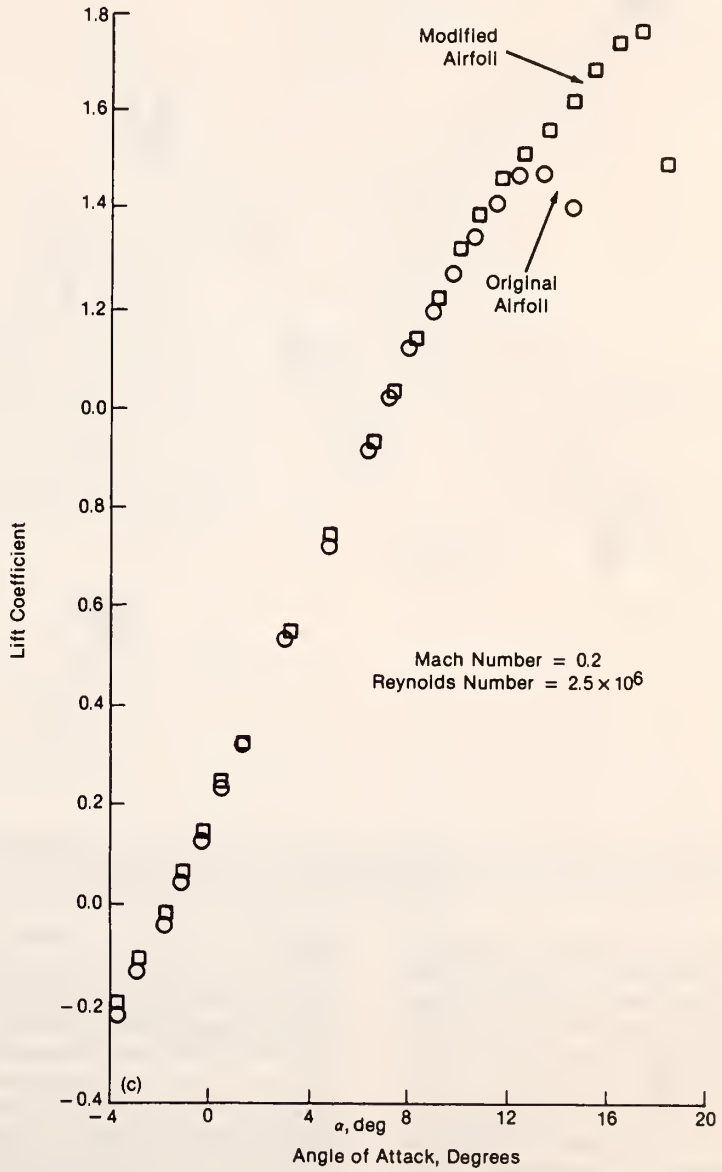

The **New Shape** of a NACA 63-215 airfoil (above) increases the maximum coefficient of lift and angle of attack (below). The ratios y/c and x/c represent the thickness and chordwise dimensions, respectively, of a wing normalized to the chord, c.

The performances of general-aviation airplanes can be improved by modifying airfoil shapes. An equation is used to determine a new contour for each type of wing. The calculations are straightforward enough to be done on a hand calculator; a computer is not necessary.

The equation applies to National Advisory Committee for Aeronautics (NACA) 63-, 64-, and 65-series airfoils with lift coefficients between 0 and 1 and maximum thickness-to-chord ratios between 0.06 and 0.18. These airfoils are used on a variety of general-aviation aircraft, including single-engine, propeller-driven airplanes and small passenger jet airplanes. The calculations determine new shapes for the upper surfaces of cambered airfoils or for both surfaces of uncambered airfoils.

The modification of an airfoil increases the bluntness of the leading edge and adds forward camber. It does so without introducing discontinuities in curvature anywhere, not even in the region where the modified shape blends with the original shape.

The increase in the forward thickness of the airfoil reduces the adverse pressure gradient near the leading edge of the upper surface at high angles of attack and results in a larger maximum coefficient of lift. Stalling characteristics are thereby improved, shorter and slower landings are possible, and the rate of climb is increased.

When it was used to modify a NACA 63-215 airfoil shape (see figure), the equation yielded a shape that gives approximately a 20-percent increase in the maximum lift coefficient. It also substantially increased the allowable angle of attack. The equation can be used to design new high-performance airfoils and to modify existing designs.

This work was done by Susan Cliff-Hovey of **Ames Research Center.** *No fur-*

ther documentation is available.

Inquiries concerning rights for the commercial use of this invention should be addressed to the Patent Counsel, Ames Research Center Refer to ARC-11598 /TN

Ames Research Ctr.
Moffett Field, CA 94035
Technology Utilization Officer: Laurance Milov
Mail Code 223-3
(415) 694-6370
Patent Counsel:
Darrell G. Brekke
Mail Code 200-11
(415) 694-5104

FOR ADDITIONAL INFORMATION: *Contact: Director, Technology Transfer Division, P.O. Box 8757, BWI Airport, MD 21240; (301) 621-0100 Ext. 241*

REFER TO THE NUMBER LISTED AT THE END OF THIS ARTICLE

NASA Tech Brief
National Aeronautics and Space Administration
Ames Research Center, Moffett Field, California

Licensing Opportunity

Computer Scheduling of Airplane Arrivals

Controllers would be assisted in the coordination of many simultaneous flights.

A prototype computer-based system has been developed to assist air-traffic controllers in scheduling the arrivals of many airplanes at an airport and at designated points along the approaches to the airport. The system is an evolving product of efforts to relieve the human controllers of routine tasks by incorporating as much as possible of their expertise into expert systems of computer programs. In recognition of the overriding requirement to promote safety, the system relies on the proved ability of human controllers to solve unforeseen problems and is therefore designed to be highly interactive: it explains its actions to the controllers, offers menus of commands, accepts modifications of flight plans, and incorporates special or temporary operating rules that the controllers may have to impose in specific situations.

The prototype system is designed to follow as many as 100 airplanes within a radius of 150 nautical miles (278 kilometers) of Denver, Colorado. Conventional jet-airplane traffic enters this Denver terminal area at four points called "feeder fixes" (see figure). For each new arrival, the system develops an admissible flight plan. As each airplane progresses through the terminal area, the system monitors the deviation of the airplane from its flight plan and provides advisory notices to return it to its assigned schedule. In cases of such disruptions as missed approaches and closed runways, the system revises the flight plans of all the aircraft in the terminal area.

The arrival time assigned to each airplane is based partly on the speed range of the airplane in standard flightpath calculations. The system also takes account of such requirements as the minimum allowable distances between consecutive airplanes on the same route, the different minimum-distance requirements for different classes of airplanes, and the prevention of conflicts with previously scheduled airplanes. For example, if none of these requirements can be satisfied for an entering airplane, the system will advise that it fly in a holding pattern at the feeder fix until the next available entry time.

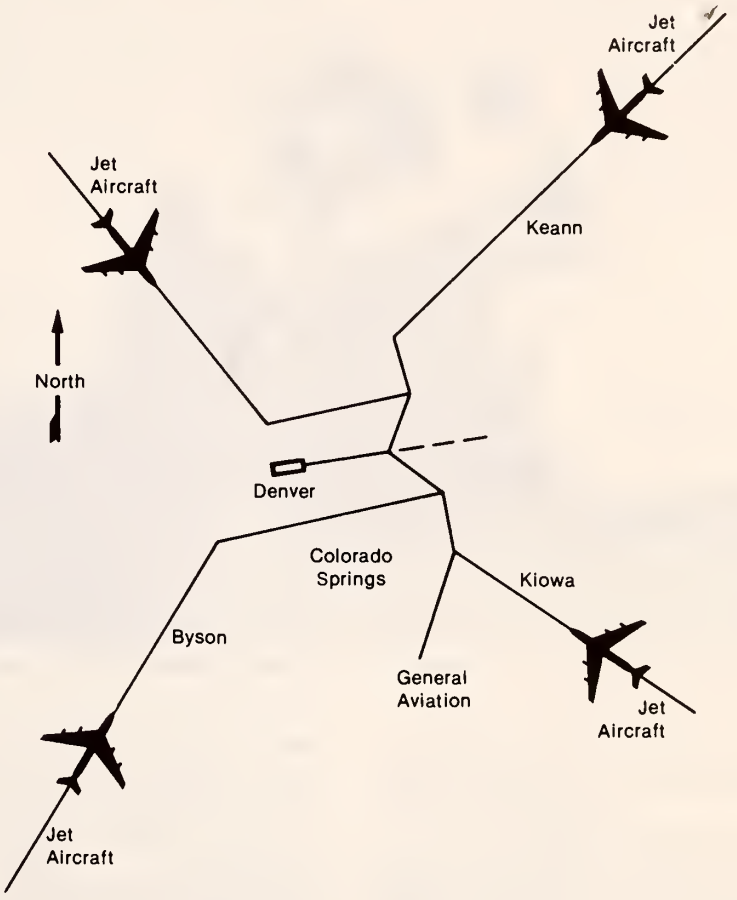

Air Traffic Heading Toward Denver along four routes is scheduled by the prototype system. All airplanes are assumed to be on instrument flight rules, and all landings are assumed to take place at Denver Stapleton Airport on runway 26L.

The system operates on a Symbolics 3600 computer. The software is written in the Symbolics Zetalisp language, which accommodates component programs in compatible versions of the MRS, FORTRAN, and Lisp languages. The Lisp functions call FORTRAN programs to run when numerical subroutines are needed. MRS (Meta-level Reasoning System) is a logic-programming language used to treat facts, rules, backtracks in the search for alternative solutions, and other elements of planning.

The further development of the system is likely to require the acquisition of more expertise from the air-traffic controllers, research through simulation and field tests, and the incorporation of flight regulations. Issues that need to be addressed include the optimization of flightpaths (for example, for fuel-efficient descents), procedures to minimize deviations from schedules, and strategies to increase the capacities of airports.

This work was done by L. Tobias and J.

L. Scoggins of **Ames Research Center**. *Further information may be found in NASA TM-88234 [N86-28068/NSP], "Time-Based Air Traffic Management Using Expert Systems."*

Copies may be purchased from the National Technical Information Service, Springfield, Virginia 22161, [A04]

Inquiries concerning rights for the commercial use of this invention should be addressed to the Patent Counsel. Ames Research Center Refer to ARC-11742./TN

Ames Research Ctr.
Moffett Field, CA 94035
Technology Utilization Officer: Laurance Milov
Mail Code 223-3
(415) 694-6370
Patent Counsel:
Darrell G. Brekke
Mail Code 200-11
(415) 694-5104

FOR ADDITIONAL INFORMATION: *Contact: Director, Technology Transfer Division, P.O. Box 8757, BWI Airport, MD. 21240; (301) 621-0100 Ext. 241*
REFER TO THE NUMBER LISTED AT THE END OF THE ARTICLE

NASA Tech Brief
National Aeronautics and Space Administration
Langley Research Center, Hampton, Virginia

Field Repair of Thermoplastic Windows and Canopies

A hand-held induction heater makes quick and easy repairs.

Aircraft maintenance is currently the most challenging area of battlefield repair. When repairing aircraft windscreens, skins, or mainframes, structural integrity and high quality of repair are difficult to achieve under the constraints of battlefield operations. Repair under these conditions must be simple, quick, and durable. The repairs must be possible under severe weather conditions and in primitive shelters. Repair materials must remain stable and manageable at temperatures from 32 to 120 °F (0 to 49 °C). The use of induction-heating techniques and toroid bonding equipment developed at Langley Research Center has made these repairs relatively quick and easy.

Toroid bonding equipment is based on a self-tuning, solid-state power oscillator feeding 30- to 80-kHz power to a ferrite toroid. The toroidal shape introduces a uniform, concentrated magnetic flux into the materials to be bonded, causing eddy currents to flow in a ferromagnetic susceptor and/or paramagnetic adherends. These currents heat only the bond line or its vicinity. The power required to heat a bond area of 1 $in.^2$ (6.5 cm^2) to 800 °F (430 °C) within 1 min is less than 300 W, with most bonding temperatures requiring less than 200 W. Since no large fixtures are heated, the cooling rate is rapid, typically less than 2 min from the bonding temperature to the glass-transition temperature of the bonded material.

These toroid bonding techniques have been further developed to meet typical field-repair requirements. The induction-heating power supply has been engineered into a "ruggedized" solid-state unit, in a 1-ft^3 (0.028-m^3) package weighing 20 lb (9.1 kg). A hand-held bonding gun weighing 3 lb (1.4 kg) plugs into this power supply on a long cord. The maximum power required is 300 W. Lightly loaded repair bonds can be made in several minutes at an average power input of 150 W on metallic, polymeric, or polymer-matrix materials.

On-the-Spot Aircraft-Windscreen Repairs are made easily with a hand-held toroid bonding gun.

Field repairs were made by Langley Research Center personnel at the Hampton Aerospace Park on fighter-aircraft canopies (see photo). The patches were approximately 2 ft^2 (0.19 m^2) each and required 2 h from start to finish. In addition, repairs were made on .45-caliber bullet holes on a helicopter polycarbonate windscreen. Polycarbonate patches applied using the hand-held bonding gun formed effective doubler plates over the cracks emanating from the bullet holes, to restrain crack propagation. Each bond took less than 10 min per hole.

The toroid bonding field-repair technique provides repairs that are faster, simpler, and stronger than those using conventional techniques. The portable, ruggedized equipment and other equipment related to toroid induction are now available commercially as a result of this work.

This work was done by Robert L. Fox and James R. Tyeryar of **Langley Research Center**. *LAR-13525 /TN*

FOR ADDITIONAL INFORMATION: *Contact: Director, Technology Transfer Division, P.O. Box 8757, BWI Airport, MD. 21240; (301) 621-0100 Ext. 241*
REFER TO THE NUMBER LISTED AT THE END OF THE ARTICLE

NASA Tech Brief
National Aeronautics and Space Administration

Variable-Reluctance Motor for Electric Vehicles

A scaled-down motor performed as expected.

A report describes research on a variable-reluctance electric-motor drive for eventual use in electric-vehicle propulsion. The primary design and performance criteria were the torque and power output per unit mass of the motor, the cost (with emphasis on the inverter circuit needed for the motor), and the drive efficiency (with emphasis on the motor). For each criterion, an optimized drive design was developed, and these designs were then unified to yield a single electric-vehicle drive.

The theoretical treatment of variable-reluctance-motor drives led to the design of a 60-kW motor with a mass of 65 kg. To reduce the cost of the inverter, a three-phase system was selected. (Three is the minimum number of phases for a self-starting variable-reluctance motor). There are four rotor poles and six stator poles. An alternating polar alignment of the phase windings (NSNSNS) eliminates the mutual inductance between the phases and maintains flux symmetry in the back iron. The windings are bifilar.

The stator-pole angle is 32°, which is a compromise between a large overlap region and a large winding-slot volume. The rotor-pole angle is 45°. The rotor-pole pitch was designed to allow for a large maximum-inductance region in the phase-inductance profile to provide extra time to remove currents. The radial gap between the rotor and the stator was designed to be the smallest permitted by manufacturing limitations. The number of turns on each stator pole is constrained by the current levels required for operation with a 240-V supply.

Because the inverter circuit includes only three power switches, its cost is lower than that of competitive circuits. The circuit enables independent control of the currents in each phase, thereby enhancing the capability for optimum output and efficiency. The power switches must block a forward electromotive force of 480 V, with a 240-V safety margin. Though the switches could be silicon-controlled rectifiers, gate turn-off thyristors (GTOT's) are preferred because of their simpler commutation requirements. The GTOT's selected have voltage, current-at-turn-off, and root-mean-square-current ratings of 1,300 V, 600 A, and 400 A, respectively. Each GTOT can be commutated with a field-effect transistor at turn-on and with a silicon-controlled rectifier at turnoff.

To test the motor-design concepts, a 3.8-kW version was designed and built by scaling down all the dimensions of the 60-kW unit by a factor of about 2.5. The smaller motor was not thermally designed, however; the scaledown was only magnetic for verification of the mathematical design models. The small motor performed as expected, showing excellent agreement with the predicted scaled-down electromechanical characteristics. Provided that the thermal constraints are satisfied, it thus appears that the 60-kW unit will perform as expected.

This work was done by Jeffrey H. Lang of Massachusetts Institute of Technology for **NASA's Jet Propulsion Laboratory**. *To obtain a copy of the report, "Variable-Reluctance Motor Drives for Electric Vehicle Propulsion," NPO-16993 /TN*

FOR ADDITIONAL INFORMATION: *Contact: Director, Technology Transfer Division, P.O. Box 8757, BWI Airport, MD 21240; (301) 621-0100 Ext. 241*

REFER TO THE NUMBER LISTED AT THE END OF THIS ARTICLE

NTIS Order Form

NTIS Telephone Numbers

To Order Reports
(703) 487-4650

For Subscription Questions
(703) 487-4630

Other Information
(703) 487-4600

Editorial Questions
(703) 487-4805

Postage:
NTIS uses First Class Delivery, or equivalent service, on all shipping. For information about one day RUSH ordering, call (703) 487-4600.

NTIS PRICE CODE SCHEDULE *

This schedule gives the current values to the price codes cited in those Tech Notes having a backup report available from NTIS.

Microfiche	
A01	$6.95
Paper copy	
A02	9.95
A03	12.50
A04 through A05	14.95
A06 through A09	19.95
A10 through A13	25.95
A14 through A17	32.95
A18 through A21	38.95
A22 through A25	44.95
A99	Call for price

Customers in Canada, United States, and Mexico use this schedule. Other addresses should write for the price listing, number PR-360-4.

Prices effective January 1, 1988

Use this form ONLY to order reports designated as available from NTIS

MAIL ORDER TO: National Technical Information Service
U.S. DEPARTMENT OF COMMERCE
5265 Port Royal Road
Springfield, VA 22161

Send me the reports I have selected on this form. I have placed order numbers in appropriate blanks and have indicated the quantity. IF ADDRESS LABEL

Last Name: .....

Title: .....

Company/Organization: .....

Address: .....

.....

City/State/Zip: .....

Telephone Number: .....

METHOD OF PAYMENT

☐ Check enclosed payable to NTIS for $ .....

☐ Charge to my NTIS Deposit Account, No: ....

☐ Purchase order number: .....

Charge to: ☐ American Express ☐ VISA ☐ MasterCard

Card Number: .....

Expation date: .....

Signature: .....
(Required to validate order)

NTIS ORDER NUMBER (Use only for backup reports stated as available from NTIS)

NTIS Order Number	*Price**	*Quantity*	*Total Price*
.....	.....	.....	.....
.....	.....	.....	.....
.....	.....	.....	.....
.....	.....	.....	.....
.....	.....	.....	.....
	Shipping and handling fee		$3.00 .....
	Total		.....

NTIS Order Form

NTIS Telephone Numbers

To Order Reports
(703) 487-4650

For Subscription Questions
(703) 487-4630

Other Information
(703) 487-4600

Editorial Questions
(703) 487-4805

Postage:
NTIS uses First Class Delivery, or equivalent service, on all shipping. For information about one day RUSH ordering, call (703) 487-4600.

NTIS PRICE CODE SCHEDULE *

This schedule gives the current values to the price codes cited in those Tech Notes having a backup report available from NTIS.

Microfiche	
A01	$6.95
Paper copy	
A02	9.95
A03	12.50
A04 through A05	14.95
A06 through A09	19.95
A10 through A13	25.95
A14 through A17	32.95
A18 through A21	38.95
A22 through A25	44.95
A99	Call for price

Customers in Canada, United States, and Mexico use this schedule. Other addresses should write for the price listing, number PR-360-4.

Prices effective January 1, 1988

Use this form ONLY to order reports designated as available from NTIS

MAIL ORDER TO: National Technical Information Service
U.S. DEPARTMENT OF COMMERCE
5265 Port Royal Road
Springfield, VA 22161

Send me the reports I have selected on this form. I have placed order numbers in appropriate blanks and have indicated the quantity. IF ADDRESS LABEL

Last Name: .....

Title: .....

Company/Organization: .....

Address: .....

.....

City/State/Zip: .....

Telephone Number: .....

METHOD OF PAYMENT

☐ Check enclosed payable to NTIS for $ .....

☐ Charge to my NTIS Deposit Account, No: ....-.....

☐ Purchase order number: .....

Charge to: ☐ American Express ☐ VISA ☐ MasterCard

Card Number: .....

Expation date: .....

Signature: .....
(Required to validate order)

NTIS ORDER NUMBER (Use only for backup reports stated as available from NTIS)

NTIS Order Number	*Price**	*Quantity*	*Total Price*
.....	.....	.....	.....
.....	.....	.....	.....
.....	.....	.....	.....
.....	.....	.....	.....
.....	.....	.....	.....
	Shipping and handling fee		$3.00 .....
	Total		.....

- Agriculture & Food
- Computers
- Electrotechnology
- Energy
- Engineering
- Environmental Science & Technology
- Manufacturing, Machinery, & Tools
- Materials
- Medicine & Biology
- Natural Resources Technology & Engineering
- Physical Sciences
- Transportation & Components

Route To:

PENN STATE UNIVERSITY LIBRARIES
A000072009970

PARTMENT OF COMMERCE
l Technical Information Service
1, Va. 22161

BUSINESS
r Private Use, $300

DEPARTMENT OF COMMERCE • UNITED STATES •
Stimulating America's Progress
1913-1988

AN EQUAL OPPORTUNITY EMPLOYER

BULK RATE
POSTAGE & FEES PAID
NTIS
Permit No. G-292